

**ASSESSMENT OF THE EFFECTS OF CLAY DIAGENESIS ON SOME
PETROPHYSICAL PROPERTIES OF LOWER CRETACEOUS
SANDSTONES, BLOCK 3A, OFFSHORE ORANGE BASIN.SOUTH AFRICA.**

A Thesis In Applied Geology (Petroleum Unit)



**UNIVERSITY of the
WESTERN CAPE**

BY

**UNIVERSITY of the
Chris Adesola Samakinde
WESTERN CAPE**

**Submitted in Fulfilment of the Requirements for the Degree of Magister
Scientiae in the Department of Earth Sciences, University
of the Western Cape, Cape Town, South Africa**

**Supervisor: Dr Mimonitu Opuwari
Co Supervisor: Prof. Jan Van Bever Donker**

July, 2013.

ABSTRACT

Clay diagenesis phenomenon and their effects on some petrophysical properties of lower cretaceous siliciclastic sandstones, offshore Orange basin have been established. Previous studies on Orange basin revealed that chlorite and quartz cements have significantly compromised the reservoir quality in this basin but it is expected that the reservoirs shows better improvement basinward, an analogy of this is displayed by tertiary sandstones deposit, offshore Angola. The main goal of this thesis is to perform reservoir quality evaluation by intergrating geological, geochemical and geophysical tools to substantiate the effects of clay minerals distribution and its subsequent diagenesis on the intrinsic properties (porosity, permeability and saturation) of reservoir intervals encountered within three wells in block 3A (deeper waters), offshore Orange basin.

Five lithofacies were identified based on detailed core description from wells KF-1, KH-1 and AU-1 in this block. The facies were grouped based on colour and grain sizes, they are named : A1 (shale), A2 (sandstone), A3 (siltstone), A4 (dark coloured sandstone) and A5 (conglomerates). Depositional environment is predominantly marine, specifically, marine delta front detached bars and deepwater turbiditic sandstone deposit. Geophysical wire line logs of gamma ray, resistivity logs combo and porosity logs were interpreted, parameters and properties such as VCL, porosity, permeability and saturation were estimated from these logs and the values obtained were compared with values from conventional core analysis data, the values agreed well with each other. Detailed petrographic studies (SEM, XRD and thinsection) plus geochemical studies (CEC, EDS, pH, Ec) were carried out on twenty two core samples to establish if these clay minerals and other cements have pervasive effects on the reservoir quality or otherwise.

The reservoir within KF-1 well is thin and has an extreme low permeability value averaging 0.01 md, core porosity of 10 %, sonic log derived porosity of 14.6 % and average gas and water saturation of 18 % and 82% respectively (Simandoux model). AU-1 well reservoir is 6.5 metres thick with estimated values of 10 % for porosity, permeability of 0.015md, VCL of 32 % and water saturation value of 65 %. KH-1 well has reservoir thickness of about 9 m while water saturation estimated from Simandoux saturation model is 50 %. Porosity is low with an average of 8.9 %, VCL

of 30 % also extreme low permeability value of 0.09 md. There were consistent presence of kaolinite, montmorillonite and quartz cement within the reservoirs of the three wells from observations made from SEM, SEM analysis also revealed the presence of chlorite at a deeper depth, chlorite might have been formed from kaolinite due to the presence of Mg and Fe as observed from EDS plus an alkaline pore fluids as interpreted from the porewater pH. SEM also revealed the presence of illite in KH-1 well which is not present in the other two wells (AU-1 and KF-1).

XRD confirms the presence of these minerals as observed from SEM interpretation and specifically the presence of illite in KH-1, it however does not indicate the presence of chlorite. Other cements such as albite, siderite, calcite and halite were also detected from the XRD. Thin section analysis reveals the presence of glauconite in KF-1 well and KH-1 well, this observation implies marine environment influence in the reservoirs, this is further justified by the detection of halite from XRD. The pH of porewaters in all wells range from slightly acidic nature to predominant alkaline pore fluids, specifically from 6.78 - 9.5 while CEC ranges between 27 - 64.5 meq/100g for AU-1 well, 5 - 6.6 meq/100g for KF-1 well, and 7.3 - 80.5 meq/100g for KH-1 well. These values implies the dominance of mixed clay minerals of K-S and S-I layers coupled with the occurrence of chlorite and illite which were formed at a later stage of the paragenetic sequence. Clay minerals occurred as pore coating and pore filling in the reservoirs while the presence of montmorillonite, quartz cements and calcite cements indicates that there have not been great improvements on the reservoir quality in deeper waters.

It was deduced that pervasive cementation of quartz, calcite, montmorillonite, chlorite and illite cements exerted a major effect on the porosity and permeability of lower Cretaceous sandstones in block 3A, Orange basin. Judging by this study, the peculiar Orange basin reservoir quality problems persist and ultra deep waters may be further explored for reservoirs with better quality.

Keywords: Clay minerals, Diagenesis, Petrophysical properties, Cretaceous sandstones and Orange basin.

DECLARATION

I declare that my research work titled; ‘Assessment of the Effects of Clay diagenesis on some Petrophysical Properties of Lower Cretaceous Sandstones, Block 3A, Offshore Orange Basin, South Africa.’ is my own work, that it has not been submitted before for any degree or examination in any other university, and that all sources I have used or quoted have been indicated and acknowledged by means of complete references

Chris .A. SAMAKINDE



July 2013.

.....

Signature

DEDICATION

Dedicated to the memory of my late father Dr Nath. L. Samakinde (1951-2010).



ACKNOWLEDGEMENT

Not by power, nor by might but by his spirit says the Lord of host (Zac;4:6).I thank God for the gift of life and for strengthening me till the completion of this study, his praises will continually be in my mouth.

My gratitude goes to Inkaba ye Africa for granting me the bursary to carry out the analysis necessary for the completion of this study. I am also indebted to the Petroleum agency SA for releasing the data and samples needed to do the research. Special thanks to Leon Koopman for his assistance in taking core samples, also, Dr Remy Butcher of the ITHEMBA labs, Somerset, Capetown. is well appreciated for processing the XRD data .Mention must be made of the people at the electron microscope Lab, department of Physics, University of the Western Cape for helping out with my SEM analysis , also people at the Analytical Laboratory of Stellenbosch University for samples milling, department of chemistry, University of the Western Cape for porewater geochemistry analysis and BEM laboratory for my CEC analysis.

I want to appreciate my good friends (Tope Odeyemi, Gbemi Apantaku, Seun Fadipe, Rotimi Adeniyi, Tomide Fajuyitan Achu Nimuno, Thierry Kamgang, Alfred Onaneye, Toun Akinladenu, Shola Anjoorin, Nehemiah Dominic, Seyi Abegunde and Emmanuel Nformi) for standing by me during the course of my research. The list is endless, I am only human to leave out some names. I will like to also thank Pastor Oduwole of the Redeemed Christian church of God for his spiritual support and all members of Redeem church are appreciated.

I want to thank Dr and Dr (mrs) Fayanju for their immense support in all ramifications, I am lucky to be blessed with people like them and I pray God reward you abundantly for all the support given to me. Mention must be made of the Akinrinlola and Ojo's family for their support at all times, God bless you real good. My great nephews; Samuel and Emmanuel provided a source of happiness and joy during the course of the programme, you guys are the light of the world. To my mother Mrs Janet Samakinde, you are the best thing that has ever happened to me, I can't thank you enough for your moral, financial and spiritual support and I pray that your labour over me would not be in vain.

Without my supervisor, Dr Mimonitu Opuwari, the research would not have been successful. I can't thank you enough for your constructive criticism, proof reading, advise, encouragement and both financial and moral support. Your assistance made my research work more enjoyable, thanks and God bless!! I want to thank Prof. Jan Benver Donker for his fatherly support and for playing a great role and also providing the stability needed to complete the research work.

Lastly, I want to thank my wife, Mrs Mo' Samakinde for showing enormous patience, understanding and encouragement and for putting some pressure which serves as a source of motivation. Thank you and love always.



TABLE OF CONTENTS

TITLE PAGE

ABSTRACT

DECLARATION

DEDICATION

ACKNOWLEDGEMENT

TABLE OF CONTENTS

LIST OF FIGURES

LIST OF TABLES

LIST OF APPENDICES

APPENDIX



UNIVERSITY *of the*
WESTERN CAPE

CHAPTER ONE

1.1 Introduction	1
1.2 Aims and Objectives of study	4
1.3 Scope of Work.....	4
1.4 Study Area.....	5
1.5 Previous Work on Orange Basin.....	11
1.6 Reservoir Studies.....	13

CHAPTER TWO

2.1 Literature Review.....	15
2.2 Clays and Clay Minerals.....	15
2.2.1 Kaolinite Group.....	15
2.2.2 Chlorite Group	17
2.2.3 Illite Group.....	19
2.2.4 Montmorillonite /Smectite Group	21
2.3 Core Description.....	24
2.4 Depositional Environment.....	26
2.5 Petrophysical Properties.....	27
2.5.1 Porosity.....	27
2.5.2 Permeability.....	29
2.5.3 Fluid Saturation.....	31
2.6 Diagenetic Studies.....	32



CHAPTER THREE

3.1 Regional Geology.....	34
3.2 Tectono-Stratigraphy.....	35
3.3 Brief description of Petroleum Systems.....	38
3.3.1 Source Rock.....	38
3.3.2 Reservoir Rock.....	38
3.3.3 Traps.....	39

CHAPTER FOUR

4.1 Materials and Methods.....	40
4.1.1 Wireline logs.....	42
4.1.1.1 Classification based on Principles of usage.....	43
4.1.1.2 Classification based on Operational Principles.....	43
4.1.2 Methods of Wireline logs usage.....	43
4.1.2.1 Gamma Ray log:.....	43
4.1.2.2 Density Log.....	45
4.1.2.2.1 Formation Bulk Density.....	45
4.1.2.3 Neutron Log.....	46
4.1.2.3.1 Compensated neutron log.....	47
4.1.2.3.2 Sidewall Neutron Porosity Log.....	47
4.1.2.4 Resistivity Logs.....	48
4.1.2.4.1 Induction logs.....	48

4.1.2.4.2 Laterolog.....	48
4.1.2.4.3 Micro-Resistivity log.....	48
4.2 Petrophysical Properties Estimation.....	49
4.2.1 Volume of Shale.....	49
4.2.2 Fluid saturation.....	49
4.2.3 Porosity.....	50
4.2.4 Permeability.....	50
4.3 Wireline logs Loading.....	51
4.4 Core Description.....	51
4.5 Scanning Electron Microscopy/EDS (Energy Dispersive Spectrometry).....	52
4.6 XRD.....	55
4.7 Thin sections Analysis.....	55
4.8 Cation Exchange Capacity.....	57
4.9 Porewater Chemistry.....	58



CHAPTER FIVE

5.1	Presentation of Results: Cores, Geophysical logs and Petrophysical properties...	59
5.1.1	Core Description.....	60
5.1.1.1	Core Description of KF-1 Well.....	60
5.1.1.2	Core Description of AU-1 Well.....	63
5.1.1.3	Core Description of KH-1 Well.....	65
5.1.2	Geological Interpretation of Wireline Logs.....	69
5.1.2.1	Geological Interpretation of Wireline Log for KF-1 Well.....	70
5.1.2.2	Geological Interpretation of Wireline Log for KH-1 Well.....	73
5.1.2.3	Geological Interpretation of Wireline Log for AU-1 Well.....	76
5.1.3	Summary of Core Description and Wire line logs.....	79
5.1.3.1	Summary of Core Description.....	79
5.1.3.2	Summary of Wire line Logs Interpretation.....	80

CHAPTER SIX

6.1	Petrography and Geochemistry.....	81
6.1.1	Scanning Electron Microscope Interpretations.....	81
6.1.1.1	Scanning Electron Microscope Interpretation for AU-1 well.....	81
6.1.1.2	EDS Interpretation for AU-1 Well.....	83
6.1.1.3	Scanning Electron Microscopy Interpretation for KF-1 Well.....	86
6.1.1.4	EDS Interpretation for KF-1.....	86
6.1.1.5	Scanning Electron Microscopy Interpretation for KH-1 well.....	89
6.1.1.6	EDS Interpretation of KH-1 well.....	90

6.1.1.7	Summary of SEM and EDS analysis.....	94
6.1.2	XRD Interpretation.....	95
6.1.2.1	XRD Interpretation for AU-1 well.....	95
6.1.2.2	XRD Interpretation for KF-1 well.....	104
6.1.2.3	XRD Interpretation for KH-1 well.....	108
6.1.2.4	Summary of XRD Interpretation.....	118
6.1.3	Thin Section Interpretation.....	119
6.1.3.1	Thin Section Interpretation of AU-1 well.....	119
6.1.3.2	Thin Section Interpretation of KF-1 well.....	121
6.1.3.3	Thin Section Interpretation of KH-I well.....	122
6.1.3.4	Summary of Thin Section Interpretations.....	125
6.1.4	Pore water Chemistry Interpretation.....	126
6.1.4.1	pH and Ec Interpretation for AU-1 Well.....	127
6.1.4.2	pH and Ec Interpretation for KH-1 Well.....	129
6.1.4.3	pH and Ec Interpretation for KF-1 Well.....	131
6.1.5	CEC Interpretation for All Wells.....	133
6.1.5.1	Cation Exchange Capacity Interpretation of KF-1 well.....	134
6.1.5.2	Cation Exchange Capacity Interpretation of AU-1 well.....	138
6.1.5.3	Cation exchange capacity interpretation of KH-1 well.....	144

6.1.5.3 Cation Exchange Capacity Interpretation of KH-1well.....	140
6.1.5.4 Summary of Ph, Ec and CEC Interpretation of All Wells.....	142
6.1.6 Qv Plots Interpretation.....	144

CHAPTER SEVEN

7.1 Discussions	146
7.2 KF-1 Well.	146
7.3 AU-1 Well.....	147
7.4 KH-1 Well.....	149
7.5 Conclusions.....	151

REFERENCES

APPENDIX



LIST OF FIGURES

Figure 1.0: Thesis Framework.....	3
Figure 1.1 Western, eastern and southern offshore zones of South Africa (Petroleum Agency SA brochure, 2003).....	7
Figure 1.2: Location Map Of block 3A offshore Orange basin, (Global Pacific Partners 2011).....	9
Figure 1.3 Locality map of wells in Block 3A, Offshore, Orange Basin.....	10
Figure 2.0: SEM pictures showing different Authigenic Clay minerals in different Basins.....	23
Figure 2.1: Cores layout.....	25
Figure 2.2: Sidewall-Coring Scheme.....	26
Figure 2.3: Porosity identification in various rock samples.....	29
Figure 2.4 Rock permeability ranges.....	31
Figure 2.5: Various diagenetic regimes in reservoir rocks.....	33
Figure 3.0: The rift phase in the Late Jurassic – Lower Valanginian showing the break up of Africa, Madagascar and Antarctica.....	34
Figure 3.1: Chronostratigraphic and sequence stratigraphic diagram of the Orange Basin.....	37
Figure 4.0: Methodology Framework.....	41
Figure 4.1: Gamma ray tool.....	44
Figure 4.1.1: Typical Gamma ray log response to different lithology.....	44
Figure 4.2: Schematic diagram of Compensated neutron tool.....	57
Figure 4.3: Scanning Electron Microscopy Machine/EDS.....	53
Figure 4.4: Scanning and detection system in scanning electron microscope.....	54

Figure 4.5: XRD concept diagram.....	55
Figure 4.6: Typical thin section photomicrograph.....	56
Figure 5.0: Different core photos at various depth for KF-1 Well.....	62
Figure 5.1: Different core Photos taken at various depth for AU-1 well.....	65
Figure 5.2: Different core Photos taken at various depth for KH-1 well	68
Figure 5.3: Suite of Logs interpreted for KF-1 well.....	70
Figure 5.4 : Gamma ray log Histogram for KF-1 well showing values range of clean sands to Shale.....	72
Figure 5.5: Suite of Logs interpreted for KH-1 well.....	76
Figure 5.6: Suite of Logs interpreted for AU-1 well.....	77
Figure 6.0 (A-F): Photomicrographs of SEM and EDS of AU-1 well.....	83
Figure 6.1 (A-C): Photomicrographs of SEM and EDS for KF-1 well.....	87
Figure 6.2(A-F): Photo Micrographs of SEM and EDS for KH-1 well.....	91
Figure 6.3 : XRD Photos of AU-1 well.....	96
Figure 6.4: XRD Photos of KF-1 well.....	108
Figure 6.5: XRD Photos of KH-1 well.....	112
Figure 6.6 : Thin section photos of AU-1 well.....	120
Figure 6.7: Thin section photos of KF-1 well.....	121
Figure 6.8: Thin section photos of KH-1 well.....	122
Figure 6.9: Porewater Chemistry plots of AU-1 well.....	128
Figure 6.10: Porewater Chemistry plots of KH-1 well	130
Figure 6.11: Porewater Chemistry plots of KF-1 well.....	132
Figure 6.12: Cations and Cations exchange plots of KF-1 well.....	136
Figure 6.13: Cations and Cations exchange plot for AU-1 Well.....	139

Figure 6.14.Cations and Cations exchange plot of KH-1 well.....141

Figure 6.15:Histograms plots of CEC For all wells.....143

Figure 6.16:Plots of Qv against Porosity for all wells.....144

Figure 6.17: Idealized Diagenetic Model of Clay Minerals Encountered within Block 3A, Reservoirs, Orange Basin. South Africa.....145



LIST OF TABLES

Table 1.0: Name and Locations of wells studied.....	6
Table 1.1: List of Samples and Wells studied.....	8
Table 4.0: Density values of various rock samples.....	45
Table 4.1 CEC values of different Clay minerals.....	60
Table 5.0; Summary of Core description for KF-1 well	63
Table 5.1: Summary of Core description for AU-1 well	66
Table 5.2: Summary of Core description for KH-1 well.....	68
Table 5.3: Petrophysical properties estimation values for KF-1 well.....	75
Table 5.4: Petrophysical properties estimation values for KH-1 well.....	78
Table 5.5: Petrophysical properties estimation values for AU-1 well.....	81
Table 6.0: Standard table charts for Clay minerals CEC values and grain density...	136
Table 6.1: Estimated values of CEC for all wells.....	137
Table 7.0: Table of different Petrophysical properties of Cretaceous Sandstones estimated from Wireline logs processed on Interactive Petrophysics (IP) software..	

150

1.1 Introduction

The Orange basin is situated at the South western continental margin of South Africa and covers an estimated area of 130,000 km² (Gerrard and Smith, 1982). The basin has been in the spot light recently due to its seeming potential to host significant accumulations of hydrocarbons, and because the successful exploration and discovery of economic accumulations of hydrocarbons in this basin hold huge implications for the growth and development of the South African economy. The basin is often regarded as an underexplored basin (PASA Brochure, 2003), therefore there is a need to continuously search for and expose detailed geological constraints which are limiting the economic viability of the basin.

This study is centred on assessing how distribution and diagenesis of clays affect the basic petrophysical properties (porosity, permeability and saturation) of the lower Cretaceous sandstones encountered within the basin. The importance of examining the effects of clay diagenesis in Block 3A (deeper waters), offshore Orange basin arose from previous work by Jikelo (2000) and Adekola (2010) who observed that lower Cretaceous sandstones in the Orange basin have consistently shown low porosity and permeability due to quartz and clay cements, despite being siliciclastic, however Jikelo (op.cit) suggested the situation would improve basinward (deeper waters) where the depositional environment is more favourable for the formation of rock units with better quality, an analogy of which is displayed by Tertiary channel deposit, offshore Angola. In view of this, it is assumed that these defects (poor porosity and permeability) could be either pervasive or show significant improvement as a result of post depositional alterations of clay minerals in deeper waters, hence, the justification of this study. It should be noted that the continuous appraisal and development of any hydrocarbon field is often based on the values calculated from petrophysical properties.

Clays are regarded as phyllosilicate minerals which are formed on the surface (alterites, soils and sediments) or in some subsurface conditions (diagenesis and hydrothermal) (Bjorkum and Nadeau, 1998). Despite substantial scientific research reports, accurate determination of the petrophysical effects of clay minerals on reservoir quality has been challenging because clay minerals and other sedimentary materials can exist in sandstone reservoirs as a detrital shale component in the form of shale laminae, structural clast and dispersed shale matrix and can also be present as authigenic clays in sandstones (Bjorkum and Nadeau , op.cit).

Different authigenic clay minerals that have been identified include pore filling kaolinite, pore lining chlorite, pore bridging illite and a swelling smectite (Ellis and Singer, 2007). The petrophysical and hydraulic properties of sandstones could be affected by the intrinsic properties of these clay minerals while the pore geometry can also be associated with the occurrence and spatial distribution of clays and clay minerals (Wilson and Pittman, 1977). Worthington (2008), used a petrophysical model to characterize the effects of clay mineralogy on sandstones; the model explains that porosity logs (sonic, density and neutron logs) must be corrected for clay mineral effects before porosity can be evaluated.

Wilson (1977) , highlighted the importance of diagenesis in petroleum exploration and proposed a diagenetic trap as another type of trap in petroleum exploration. In the Brazillian Espirito Santos basin, distribution of clays and its diagenetic effects exert a major influence in promoting the development of very heterogeneous, complex and irregularly-connected pore systems which strongly impact oil recovery from the clastic pre- salt reservoirs, (De Ros et al, 2009). The control of diagenesis on the petrophysical properties of reservoirs is crucial for the construction of a model for characterization and prediction of reservoir quality during exploration and production.

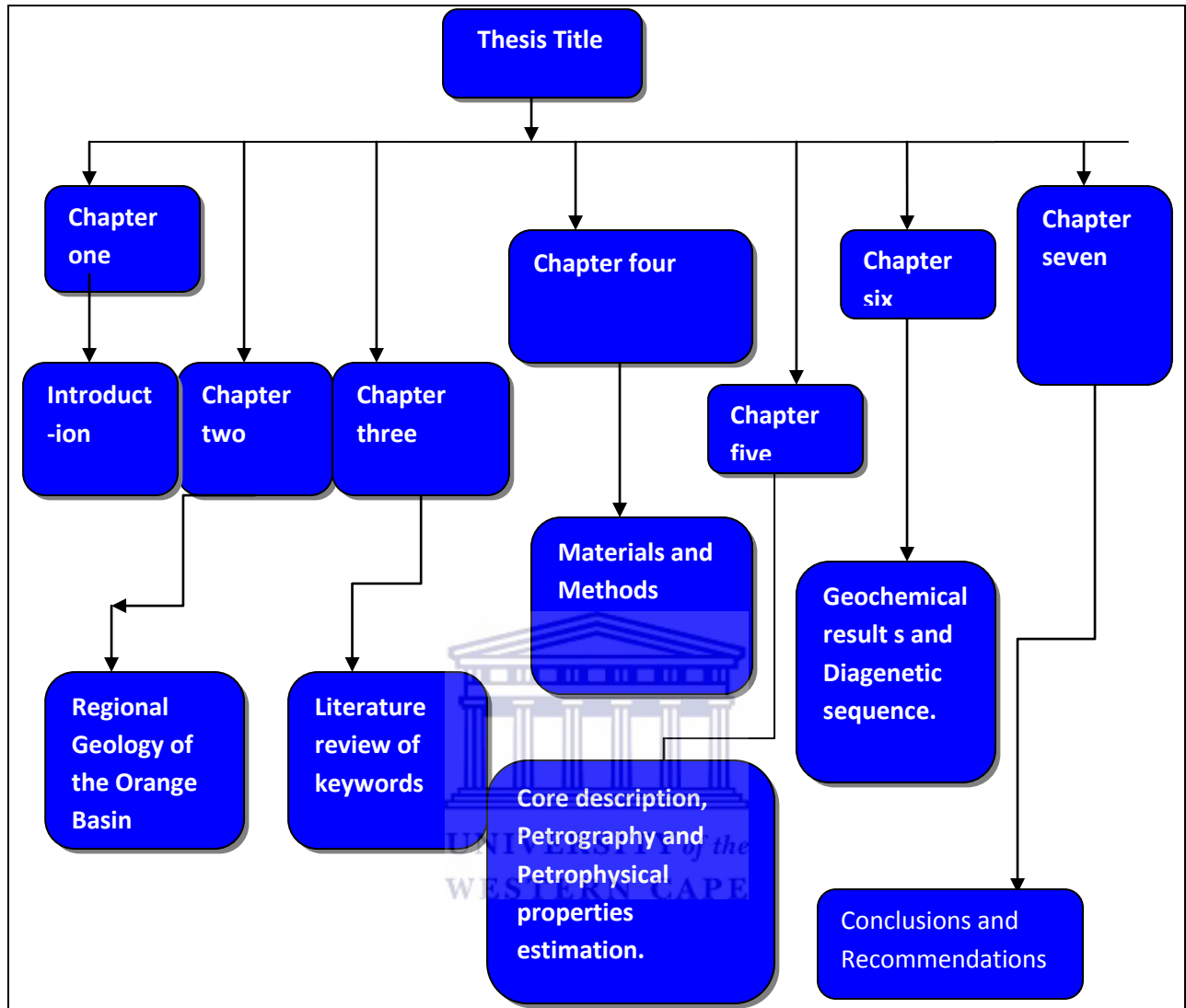


Figure 1.0: Thesis Framework

1.2 Aims and Objectives of study

The aim of this study is to assess the effects and influence of clay diagenesis on reservoir quality of lower Cretaceous sandstones, offshore Orange basin. The assessment will be done by examining, integrating and interpreting results from core descriptions, wire line logs, geochemical analyses and petrographic studies to understand clay diagenetic constraints on basic petrophysical properties of reservoir zones identified from cores and gamma ray logs in three wells. The petrophysical property values (porosity, permeability, saturation) would be estimated from computed petrophysical interpretation (CPI) of geophysical wireline logs using Industry acceptable mathematical formulas suitable for calculating appropriate parameters. Various diagenetic clay minerals and their significant effects will be clearly defined and a diagenetic model will be constructed to illustrate timing of formation and differential distribution of clay minerals in the three wells under study.

The objectives of this study amongst many includes;

- To understand the linkage between clay diagenesis, depositional environments and petrophysical characteristics of the sandstone reservoirs.
- Use this linkage to understand the importance of clay effects on the reservoir quality of the sandstones units.
- To provide, based on analyses carried out, the most qualitative reservoir zones that could be charged by hydrocarbon migration.

1.3 Scope of Work;

The scope of this study is outlined below;

- Delineation and lithological description of reservoir intervals.
- Estimation of basic petrophysical parameters to appraise the reservoir quality.
- Assessment of distribution of clays and their diagenesis to understand the constraints they place on reservoir quality.

- Cation exchange capacity and EDS (Energy Dispersive Spectrometry) analysis of delineated reservoirs to know the exchangeable cations and basic elemental composition of the reservoirs respectively.
- Analysis of interstitial pore waters of the reservoir sands to know the influence of Ec and Ph on clay diagenesis.
- Interpretation of pore systems by identifying clay minerals lining, filling or bridging the reservoir pores through thin section and Scanning Electron Microscopy (SEM).
- Construction of a diagenetic model to show the distribution of clay minerals in the three wells under study.
- X-ray diffraction (XRD) analysis for phase quantification of clay minerals.

1.4 Study Area

The Orange basin, offshore South West Africa is located within the passive continental margin of the South Atlantic between 31⁰ and 35⁰ S. It was developed within a divergent plate setting in response to extensional tectonics of the lithosphere that is related to the divergence of the South American and African plates in the late Jurassic; this was followed by seafloor spreading and opening of the South Atlantic Ocean in the Early Cretaceous around 136 Ma (Macdonald et al., 2003, Reeves and de Witt, 2000, Brown et al., 1996). The wells under study fall within block 3A, offshore Orange basin, the exploration rights are held by a joint arrangement of PASA, Sasol and BHP Billiton. The focus of the study is centred on reservoir zones encountered in three wells which include AU-1, K-F1 and KH-1, their respective location is listed in Table 1.0

Table 1.0: Names and Locations of wells studied

Wells	Total Depth (m) .	Bottom hole temperature (°C)	Kelly Bushing to Sea level (m)	Coordinates
AU-1	3427	116.7	25m	Latitude $31^{\circ} 38', 50.140''$ S Longitude $16^{\circ} 30', 23.306''$ E
KH-1	4268	140	25m	Latitude $31^{\circ} 02', 20.96''$ S Longitude $15^{\circ} 55', 23.98''$ E
KF-1	3800	120	22m	Latitude $31^{\circ} 16', 28.92''$ S Longitude $16^{\circ} 00', 36.70''$ E

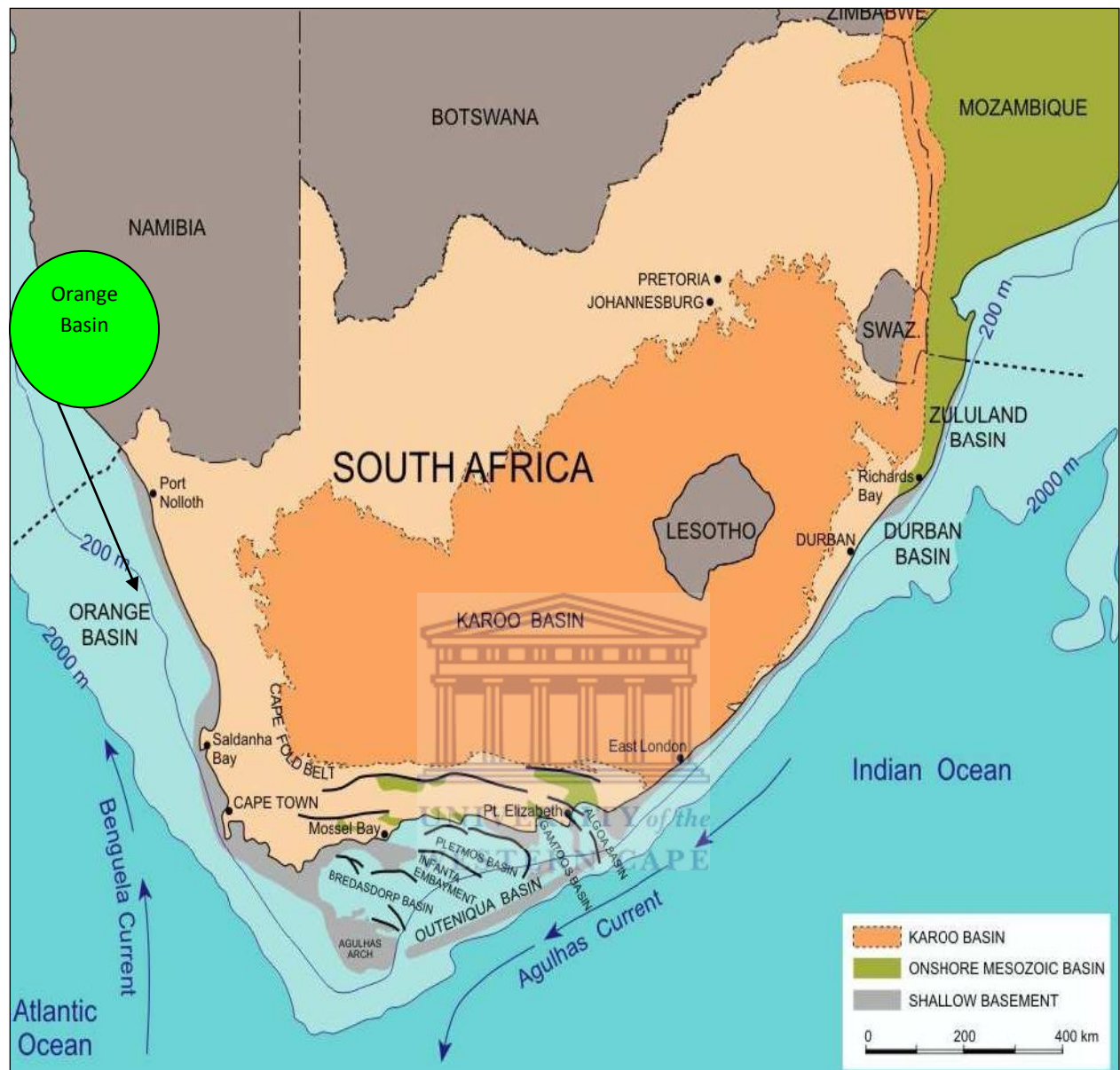


Figure 1.1 Western, eastern and southern offshore zones of South Africa (Petroleum Agency SA brochure 2003)

Table 1.1: List of Samples and Wells studied.

AU-1 well Sample Depth(m)	KF-1 well Sample Depth(m)	KH-1 well Sample Depth(m)
2684.05	3006.25	3066
2684.67	3007.07	3067
2685.39	3007.6	3068.09
2685.84	3008.13	3068.92
2686.51		3069.9
2687.8		3070.89
2688.38		3072
2690.33		3074.42
		3082.25

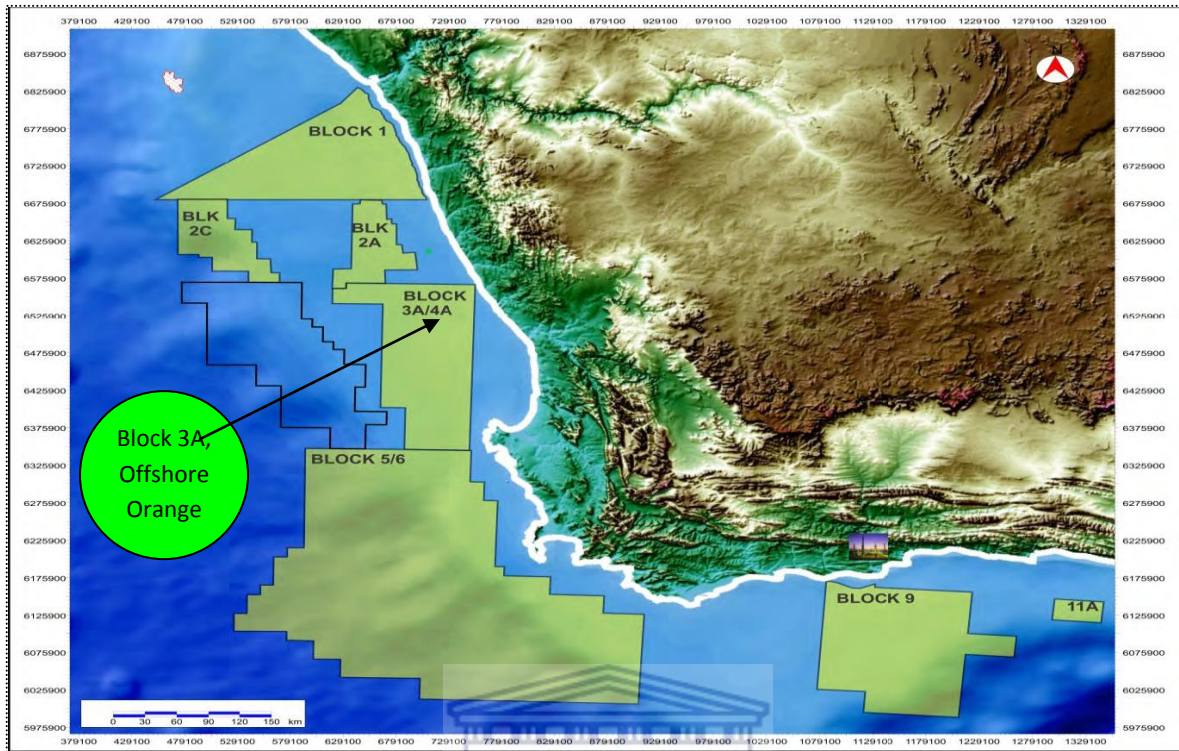


Figure 1.2: Location Map Of block 3A offshore Orange basin, (Petroleum Agency Report, 2008)



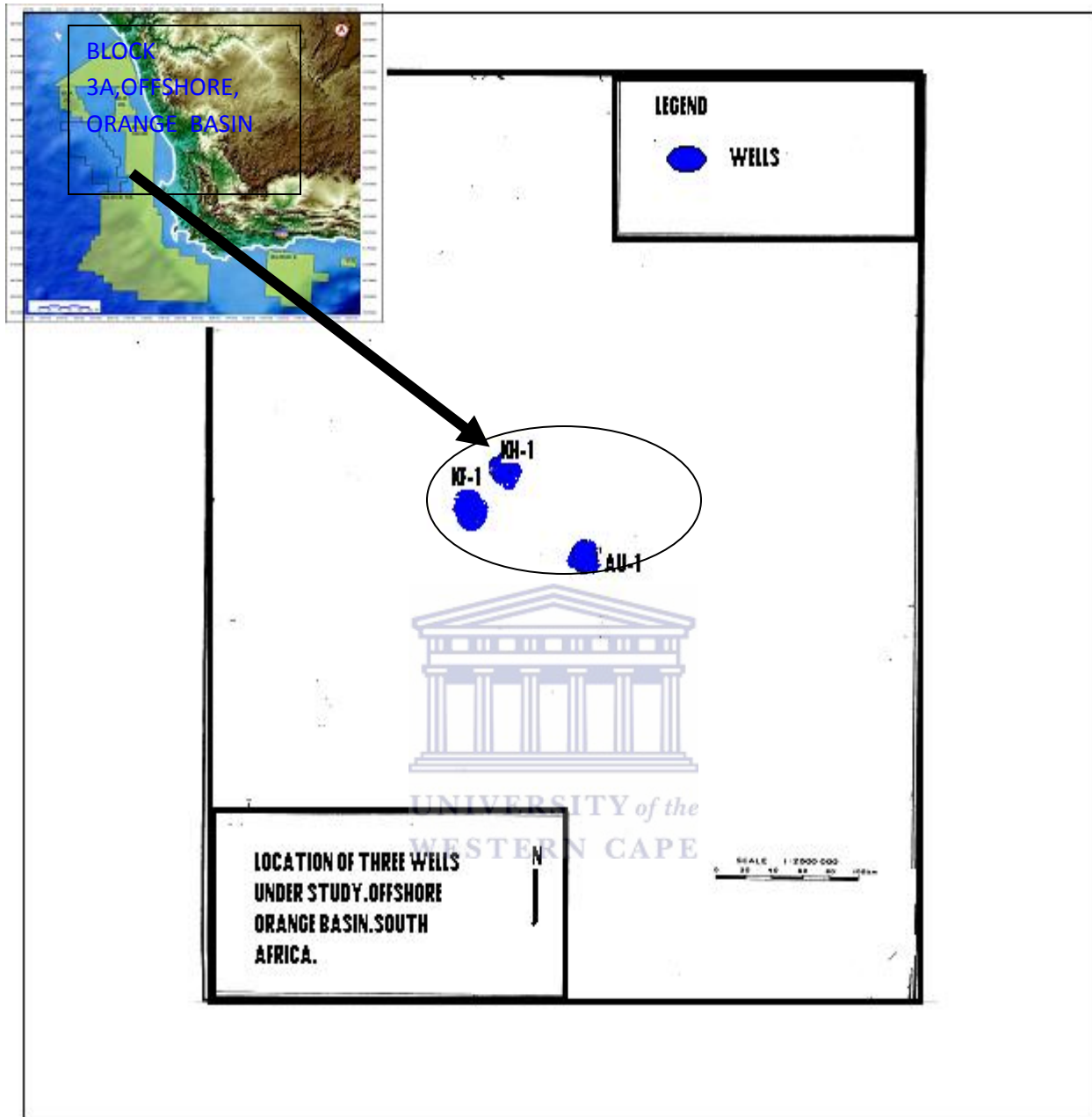


Figure 1.3 Locality map of wells in Block 3A, Offshore, West Coast Orange Basin. (Modified from Geological well report of three wells studied). (PASA Brochure, 2008).

1.5 Previous work on Orange basin

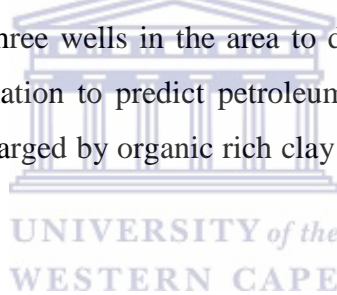
There have been relatively few published articles on the Orange basin which discuss the geology, petroleum systems and the structural features. There is an increasing need for industry professionals and academics alike to continually expand their research aims and scope to delimit factors of economic viability and increase the prospects of hydrocarbon recovery in this basin. Paton et al.,(2007) investigated petroleum systems of the Orange basin using an integrated approach to model the natural gas seepages observed on the seafloor. Observation reveals natural gas seepage at the continental shelf was due to temporal and spatial variations in post rift overburden deposition. The main period of hydrocarbon generation occurred in the late Cretaceous, this was followed by a period of erosion at the end of the Cretaceous, deposition was altered during the breakup of the shelf which allowed more sediments to prograde into the deep basin. The model also explains hydrocarbon generation, -migration and -accumulation as well as the relationship between gas leakage and thermogenic gas migration.

The source rocks identified in the Orange basin include the late Hauterivian- synrift source rock, Barremian to early Aptian source rock units and the source rock unit associated with the global Cenomanian-Turonian anoxic events (Barton et al., 1993). Campher (2009) modelled the maturity of the three source rock units in the Orange basin, and observed that the three source rock units can be linked to the three phases of development of the Orange basin (Pre rift, Synrift and Post rift). The Barremian-Aptian source rock units indicate the source rock unit is over-mature and currently producing gas with potentials for oil in the deeper part of the basin. The model also indicates that the younger Cenomanian- Turonian source rock is not over-mature and is presently in the oil window as inferred from the lower values gotten from vitrinite reflectance.

Hartwig et al., (2010) reported seismic anomalies such as pockmarks, gas chimneys and mud volcanoes associated with gas leakage using 2-D seismic datasets covering exploration blocks from 1 to 4. The gas leakages has been classified in to two main categories: stratigraphically and structurally controlled, the stratigraphically controlled gas seepages occurred above the onlaps and pinch-out of the Albian age sequence, the gas chimneys particularly either reached the

surface or were constrained within the Miocene, or terminate at the Cretaceous-Paleogene unconformity.

The structurally controlled gas chimneys are dominant in the extensional domain west of the present day-shelf break and above the Cretaceous normal faults in the Northern part of the Orange basin; their occurrence is constrained to water depths of less than 400m. Schmidt (2004), shows that the source of hydrocarbon desorbed from near surface sediments in the Orange basin, offshore South Africa is of thermal origin. This was supported by Wilhelms et al., (2001b), who suggested that the depth and origin of Gas chimneys in the Orange basin as well as their relationship to geological features indicates that a biogenic source of gas is unlikely, as microbial activity is considered to be inactive if not completely absent at a temperature greater than 80 degree Celsius. Van der spuy (2007) worked on the prospectivity of the Northern Orange basin and suggested that the Northern Orange basin has proven discovery of huge gas reserves. The study utilized seismic studies of three wells in the area to determine depositional environment and subsequently used the information to predict petroleum plays (rift and drift inclusive) as lacustrine sandstones which are charged by organic rich clay stone as encountered in A-J graben of the Southern Orange basin.



1.6 Reservoir Studies

A clear understanding of reservoir geometry is important in field development planning; such understanding is enhanced by detailed integration of robust seismic, analogs and Petrophysical analysis. Seismic technology has improved over the years from 1D to recently 4D , the continuous improvement is targeted at having a holistic approach to understanding reservoir distribution and associated trapping mechanisms. Reservoirs vary in shape and size and so do their internal properties (porosity and permeability). The reservoir study is narrowed down to the grain scale for detailed understanding of the reservoir's properties, 'lithofacies' was coined to describe physical and chemical characteristics of rocks and include mineralogy, grain size, sedimentary structures, colour and fossil assemblages. Lithofacies are the basic units for the geological description of the reservoirs while the depositional environments under which these reservoirs are formed can be inferred from lithofacies analysis.

UNIVERSITY of the

The lithofacies and different diagenetic events determine the intrinsic properties of the reservoirs and this ultimately determine quality of the reservoirs. Both physical and chemical diagenesis can either enhance the reservoir quality or reduce the quality, thus, a relationship exist between the intrinsic properties (permeability, porosity and saturation) and different diagenetic events that characterise particular reservoirs. Estimating the volume of recoverable hydrocarbons is based on these intrinsic properties of the reservoirs, without these, reservoir evaluation and prospect generation will be seemingly impossible.

Evaluation of a reservoir always requires a multidisciplinary approach utilising geophysics, petrophysics, geology and engineering principles. Geophysical wireline logs are used to determine reservoir properties by estimating porosity, permeability, saturation, NTG (Net to Gross ratio), while geology provides information regarding texture, mineralogical distribution, diagenesis and depositional environment. Application of engineering principles makes use of

information provided by geophysics and geology to strategically do well-placement and decide on production techniques.

As a result of advancement in technology, modern soft wares have made reservoir evaluation less complicated than before; the creation of IP (interactive petrophysics), PETREL, SMT and others have helped geologists and engineers to make reliable assessments of the reservoirs. Reservoir modelling has also improved reservoir studies as it takes into consideration all components of the reservoirs to simulate the behaviour of fluids under different sets of circumstances and also helps in optimisation of hydrocarbon production from reservoirs.



CHAPTER TWO

2.1 Literature Review

The different topics discussed in this section are crucial to achieving the aims and objectives of this research work, these topics include clay minerals, core description, depositional environment, petrophysical properties and diagenetic studies. This review will discuss the origin of clay minerals, the diagenesis and its role in reservoir quality enhancement and reduction. Furthermore an overview of some petrophysical properties will be given and their importance in petroleum reservoir quality assessment will be highlighted.

2.2 Clays and Clay Minerals

Clay and clay minerals are diverse group of hydrous aluminosilicates, strictly classified as having particle diameters of less than 3.9nm (Wentworth, 1922). In addition to aluminium and silica, they may also contain other positive ions of alkali and transition metals. Clays are divided into four main groups which are the kaolinite group, smectite-montmorillonite group, illite group and chlorite group. This particular review will discuss the origin of major authigenic clay minerals, their morphology and their effects on reservoir quality.

2.2.1 Kaolinite Group

Kaolinite was discovered in 1867 in Kao-Ling China and represents a group of minerals with general formula $Al_2 Si_2 O_5 (OH)_4$. The group comprises of members with the same chemistry but different structure (polymorphs) (Grim 1951). The crystal structure is represented with a silicate sheet (Si_2O_5) bonded to an aluminium hydroxide layer ($Al_2 (OH)_4$) called the gibbsite layer. Members of this group include kaolinite, dickite and nacrite (Ruiz Cruz, 1994) the layers are bonded together by weak bonds existing between the silicate and gibbsite layers and occur

generally as booklet shape and vermicules consisting of pseudo hexagonal crystals that grow at the expense of feldspar, micas, acid igneous rocks and mud intraclasts.

Authigenic clay minerals (Figure 2.0) have more damaging effects on the reservoir because they are formed by rock-fluid interactions in tightly packed sediments. Authigenic kaolinites together with some illitic material are the most common clay minerals encountered within the Sandstone reservoirs, (Beaufort et al., 1998). Dickite and nacrite are members of the kaolinite group and have been found to be dominant in crustal rocks where there has been fluid flow (Parnell et al., 2000). Different authors postulated several but similar theories as regards the origin of kaolinite, authigenic kaolinite can precipitate from acidic meteoric fluids in a weathering environment (Estoule –Choux, 1983), from basinal fluids rich in aluminium or from the dissolution of feldspars (MacLuagling et al., 1994). Hydrothermal fluids interaction with rocks has also been identified as a major process of kaolinite formation (Schroeder and Hayes, 1968). It is thus generally suggested that kaolinite is formed from hydrothermal alteration of feldspars and mica group minerals at temperatures of below 120⁰ C and that the mineral is generally not prone to shrinking or swelling regardless of the water content . They often occur as pore filling pseudo hexagonal crystals with booklets and vermicular shapes.

Abundance of kaolinite has also been identified as an indication of unconformities (Tardy, 1971, Emery et al., 1990) .Kaolinite does not form from feldspar only but could also be formed from other minerals, a classical example of such a scenario is in the North Sea where kaolinite in Jurassic Brent sandstones is formed from alteration of muscovite which ultimately caused a reduction in porosity (Bjorlykke, 1984). In certain scenarios, the release of CO₂ from coalification often acidizes the depositional environment which can cause formation of Kaolinite and can modify the porosity and permeability of the reservoirs. Modification of porosity and permeability can occur as a result of meteoric flushing and subsequent dissolution of feldspars and micas which lead to secondary porosity by formation of kaolinite in other sections of the reservoirs. However, since the precipitation of kaolinite reduces porosity, there could be no net gain in porosity values (Bjorlykke, 1983).

The role of an acidic environment in kaolinite precipitation was demonstrated by Ehrenberg (1991), he observed that the precipitation of kaolinite in the sandstones of the Garn formation

(Norwegian continental) shelf occurred at the top and bottom contacts of the formation with adjacent shale boundary as a result of migration of fluids from the adjacent shale. Kaolinite often occurs as pore filling cements, however, the effects on the reservoirs is less pervasive unless it is changed to another form of clay minerals which is more damaging. Grim (1951) noted that kaolinite is less abundant in ancient sediments than in younger sediments and therefore concluded it must have been changed to another form of clay minerals. Identification and separation of allogenic kaolinite from authigenic kaolinite could be challenging, this challenge can be mitigated by the usage of SEM and XRD as detrital kaolinite is fine grained and poorly crystallized when observed on the thin section and Scanning Electron Microscopy (Hancock and Taylor, 1978).

2.2.2 Chlorite Group:

Chlorite is derived from hydrothermal alteration of ferromagnesian mineral rich metamorphic rocks and encompasses a group of minerals characterized by a wide range of chemical and structural variation (Bailey, 1988) and could also be formed from metamorphic rocks with high contents of Fe-Mg-rich silicate minerals such as biotite, garnet, pyroxene and amphibole. Specifically in an alkaline environment with a higher pH value and high iron content and are generally the most common authigenic clay cements in sandstones reservoir, they also serve as a pointer to diagenetic history and the chemistry of the pore waters (Berger et al., 2009).

Different Chlorite group minerals include clinocllore (Mg-rich chlorite), chamosite (Fe-rich), nimite (Ni-rich), and pennantite (Mn-rich) (Bayliss, 1975). Structural formulas of most trioctahedral chlorite may be expressed by four end-member compositions, with sheet thickness of about 14 Å. The structure of the chlorite minerals consists of alternate mica-like layers and brucite-like hydroxide layers, where the unbalanced charge of the mica-like layer is compensated by an excess charge of the hydroxide sheet that is caused by the substitution of trivalent cations for divalent cations. The general formula of chlorite group is given as $(\text{Mg,Fe})_3(\text{Si,Al})_4\text{O}_{10}(\text{OH})_2 \cdot (\text{Mg,Fe})_3(\text{OH})_6$.

Most chlorites are trioctahedral (having a hydroxide sheet surrounded by three divalent cations) and as such they are normally rich in Fe and Mg. Detrital chlorite in sediments reflects its

provenance because they are easily weathered from ferromagnesian minerals-rich parent rocks (Bain, 1977). As a result of this, it is unusual to find abundant chlorite in sediments unless they were deposited in close proximity to the chlorite rich parent rock. Chamley and Weaver, (1989) also suggested that chlorite is largely concentrated and confined to sediments from high latitudes which show little tolerance to weathering, therefore, the abundance of chlorite in sediments can be attributed to its diagenetic formation. The evidence of cooler climate supporting the formation of authigenic chlorite was supported by studies of oceanic sediments from dated cores of the Western Atlantic region which record a general increase in chlorite content from Eocene to the Quaternary (Chamley and Weaver, op.cit). A thin layer of authigenetic chlorite has proven to be very effective in preventing quartz overgrowth; this was evident in Tuscaloosa sandstones of Southern Louisiana (Pitman et al., 1992). Pervasive quartz cementation is one of the major limitations of reservoir quality, and formations of early authigenic chlorite have always preserved the reservoir pore spaces from damage by quartz cementation. The origin of chlorite is complex and is controlled by the source of the material, pore water chemistry, early clay minerals and sealing or opening of the system (Huang et al; 2004). It could develop from the stage of eo-diagenesis to meso-diagenesis and displaces detrital grains (Jinglan et al., 2002). Sun et al., (2008), pointed out that chlorite can precipitate at the early and middle diagenetic stages and such chlorite formed at early diagenetic stage will continue to grow throughout the diagenetic history. The relationship between chlorite cements and reservoir quality has been identified years ago, previous studies have shown that chlorite cements are major causes of anomalous porosity and permeability (Sun et al., 2008), especially in deeper reservoirs sandstones (Bloch et al., 2002).

Aside from the formation of chlorite from fluid-rock interaction in ferromagnesian rich rock, authigenic smectites and kaolinite are also likely to be transformed to chlorite (Grigsby, 2001, Berger et al., 2009). Fe, Si and Al ions released during the dissolution of unstable minerals like lithic fragments and feldspars are sources of chloritization during diagenesis. Fe and Mg ions are sourced from alteration of Fe and Mg rich minerals; examples are biotite, amphibole, feldspar and volcaniclastic rock fragment (VRF) (Klass et al., 1981).

2.2.3 Illite Group

This is a hydrated microscopic muscovite group with the mineral illite being the only common mineral represented. Variable amounts of water molecules as well as potassium ions lie between the silicate-gibbsite- silicate sandwiches. However it is a significant rock forming mineral being a main component of shales and other argillaceous rocks, the general formula is $(K, H) Al_2 (Si, Al) 4O_{10} (OH)_2 \cdot xH_2O$, where x represents the variable amount of water that this group could contain (<http://209.51.193.54/minerals/silicate/clays.htm>) The structure of this group is similar to the montmorillonite group with silicate layers sandwiching a gibbsite-like layer, in an s-g-s stacking sequence. Illite is mostly referred to as hydrated microscopic muscovite and occurs as a dioctahedral mica-like clay mineral common in sedimentary rock especially shales (Pevear, 1999).

Illite is important in hydrocarbon resource studies because it enables the study of the timing of hydrocarbon generation. The breaking up of kerogen to form oil and gas occurs at almost the same temperature as that at which illite is formed (Pevear op.cit). It is difficult to separate the discussion on illite without discussing the smectite and illite mixed layer. The growth of authigenic illite in reservoir sandstones reflects an alkaline environment with raised temperatures, this is expected to develop at deeper burial depth and may be associated with corresponding compaction and dewatering of shale (Muller, 1967). Illite is generally idiomorphic because the crystals precipitate unconstrained from fluid and are present in relatively large pore spaces. Illite could also be formed from the reaction of brines with kaolinite (Maachi et al., 1986), this similar origin is suggested for illite precipitation in the middle Jurassic Brent sand formation in the Northern North sea. (Hancock and Taylor 1978)

The study of illite formation in reservoirs is necessitated due to damage done to the permeability of the reservoirs; illite has also been identified to inhibit quartz cementation but with a lesser capacity compared to chlorite. It exhibits varieties of growth morphology including flakes, fibres

and whiskers. Kaolinite has been found to be replaced by illite on many occasions as it is seen in Permian Rotliegendes of the North Sea (Lanson et al., 2002). Authigenesis of illite in Rotliegendes sandstones reduces the permeability but has little effects on the porosity. There is no recorded authigenic illite of recent age despite abundance of illite in many pore waters of sandstones (Berger et al., 1995), and there are conditions that must be in place for authigenic illite to be precipitated, such as, neutral to alkaline pore fluids, sufficient K, Si₄ and Al₃. Authigenic filamentous illite can severely reduce permeability despite relatively high porosities in sandstones whose effect on rock properties is dependent on the illite's morphology (Cocker, 1986). By combining careful core preservation, critical-point drying, and scanning electron microscopy examination, it can be shown that illite has various morphologies, both natural and artificial, (Rahman et al., 1995).

The petrophysical properties of reservoirs containing illite depend significantly on the technique of core preparation, but commonly, illite collapses upon air drying resulting in high porosity, high permeability and low capillary pressure. Whenever illite gets in contact with fresh water, it gives rise to low porosity, low permeability and high capillary pressure (Rahman et al., op.cit). Illite has also shown high vulnerability to migration, it remains dispersed and is taken with the flowing fluid until the particles are trapped in pore restrictions. Authigenic illite occurs in the pores of many sandstone formations which are known to contain hydrocarbon reservoirs, in particular, the Norphlet formation (Jurassic, Mississippi), Wilcox Formation (Eocene, Texas) and Fort Union Formation (Paleocene, Wyoming) all contain large amounts of authigenic illite (Rahman et al., op. cit). This illite occurs as laths with perfectly developed morphologies; laths have widths of 0.1 to 0.3 microns, thicknesses up to 200 Å, and lengths ranging up to 30 microns. Elemental analyses of the laths reveal Si, Al, and K as major constituents, transmission electron images show that these "hair-like" illites are associated with irregular blob-like cores which have chemistry very similar to that of the laths. The presence of hairy illite in sandstone pores greatly increases micro porosity and pore tortuosity, and decreases the permeability. Illite was found to be the main control on reservoir properties in Sherwood sandstone group of Morecambe field, United Kingdom (Guyen et al., 1980).

2.2.4 Montmorillonite/Smectite Group

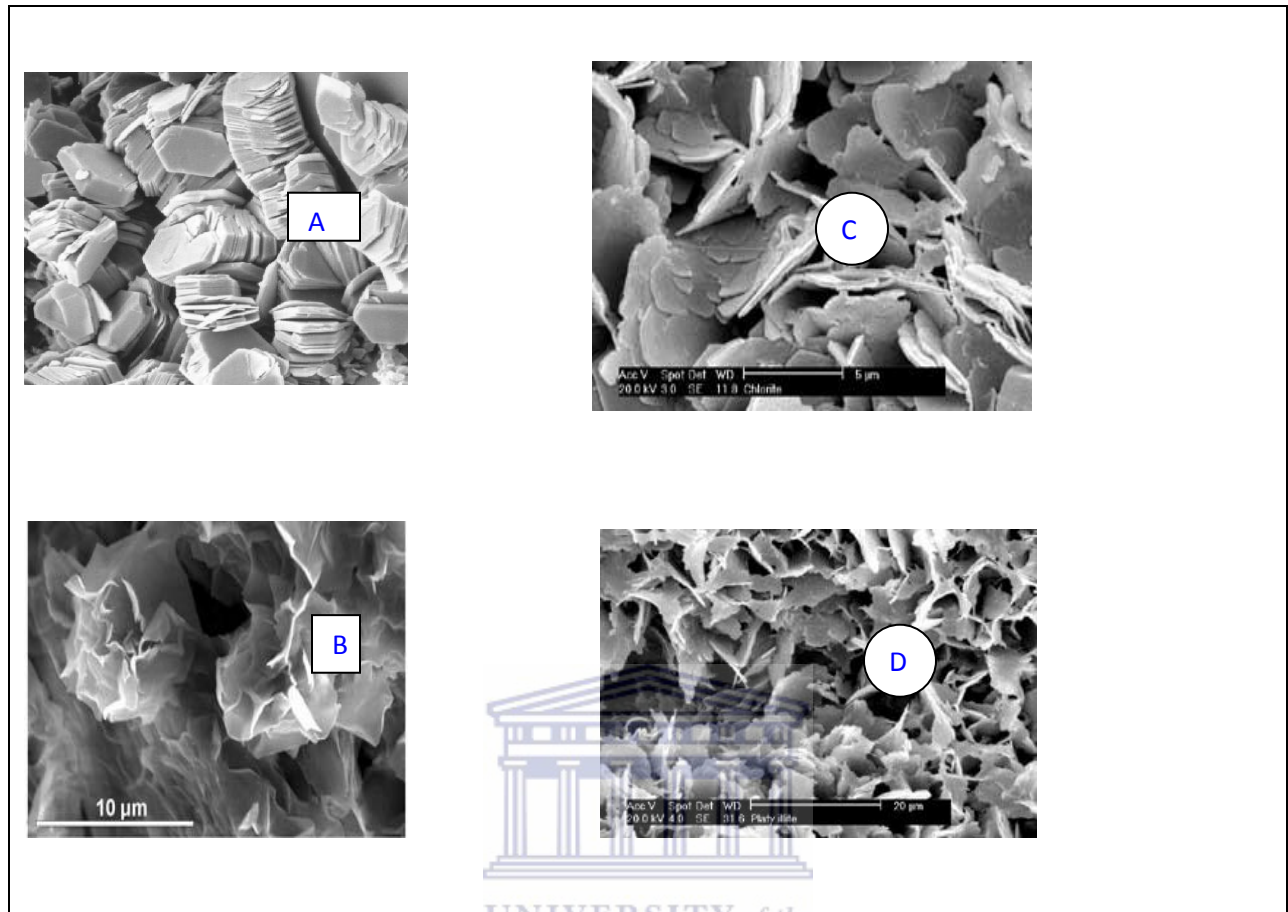
This group is composed of several minerals including talc, vermiculite, sauconite, saponite, nontronite and montmorillonite. They differ mostly in chemical content and the general formula is $(Ca, Na, H) (Al, Mg, Fe, Zn)_2(Si, Al)_4O_{10} (OH)_2 \cdot xH_2O$, where x represents the variable amount of water that members of this group could contain (<http://209.51.193.54/minerals/silicate/clays.htm>). Talc's formula, for example, is $Mg_3Si_4O_{10} (OH)_2$, the gibbsite layers of the kaolinite group can be replaced in this group by a similar layer that is analogous to the oxide brucite ($Mg_2(OH)_4$). The structure of this group is composed of silicate layers sandwiching a gibbsite (or brucite) layer in between, in an s-g-s stacking sequence, the variable amounts of water molecules would lay between the s-g-s sandwiches. (<http://www.galleries.com/minerals/silicate>).

In this review, the study of smectite is limited to the more crystallized authigenic smectite; this has been observed to occur as highly wrinkled, honeycomb-like pore coatings (Wilson and Pittman, 1977). They are formed mostly from alteration of volcanic ash in a mildly alkaline environment (Bilbey et al., 1974; Owen et al., 1989). Often times, smectites are transformed to chlorite and illite in a progressive way, this stage includes a mixed layers smectite/illite or smectite/chlorite progressive transformation with increased abundance ratio. Examples of this have been observed in the North Sea where most smectite occur in the shallowest of the reservoirs and subsequently transformed into other clay minerals at deeper depth (Burley and Macquaker, 1992). Smectites are most often unstable at temperatures greater than $60^{\circ}C$ and tend to convert to illite because of their metastability (Bjorlykke et al 1995, citing Aargard and Helgesson, 1983).

Three different origins of authigenic smectite have been proposed, these include reworking of weathering products in surficial soils and transient sediments deposit, marine alteration of volcanic materials, early diagenetic smectite resulting from different authigenic processes during eo-diagenesis, (Chamley, 1994). Authigenic smectite, specifically nontronite have been formed by hydrothermal influence by mixing and cooling of hydrothermal brines with ocean water and by fixation of K. The most commonly reported authigenic smectite in alkaline lakes are trioctahedral Mg –smectite, including stevensite, hectorite and saponite. Smectite represent about 25% of clay cemented sandstones and are thus a reservoir quality issue (Primmer et al., 1997)

Detrital and authigenic smectite can occur in sandstones (Whitney and Northrop, 1987) and they are a good source of transformation for other diagenetic processes including illitization, quartz cementation and zeolite formation (Boles and Francks, 1979). Smectite is known to have enough clay-bound water which can lead to breakdown of clays and consequently the accumulation of in-situ formation water that can cause over pressuring (Burst, 1969). Smectite have a different pattern of behaviour in sandstones and mudstones because of differentiations in mineralogy, porosity, permeability, water-rock ratios, and oxidation and reduction buffers.

The chemistry of smectite can show either a trioctahedral or dioctahedral arrangement; smectite is dioctahedral if two out of the three octahedral sites are occupied by trivalent cations like Fe^{3+} or Al^{3+} ; otherwise smectite behaves trioctahedrally (Güven, 1988). The dioctahedral minerals include montmorillonite, beidellite and nontronite while trioctahedral includes saponite, hectorite and sauconite. These clay minerals are characterised by properties of unique cation exchange. Smectite have been reported to be major contributors to reservoir damage when in contact with fresh water because of the large surface area exhibited by smectite.(Güven, op.cit).The larger the surface area of clay minerals, the more severe they tend to reduce the permeability of the reservoirs, reservoirs that have a reasonable degree of smectite cements often display poor reservoir quality, the accommodation of bound water which causes smectite to swell always has a damaging effect on the porosity and permeability of reservoirs. Early formation of smectite before fluid migration in any reservoir impedes fluid flow by choking the pore throats due to swelling when it comes in contacts with water.



(A) Thin idiomorphic platelets of kaolinite from Hirschau, South-East, Germany. (B) Montmorillonite showing a rose like texture in Miocene age Arkose, Madrid Basin, Spain (C) Mg-rich chlorite, Rotliegendes Sandstones, Northern Germany (D) Platy Illite from the Rotliegendes Sandstones, Northern Germany.

Source: <http://www.minersoc.org/pages/gallery/claypix>

Figure 2.0: SEM pictures showing different Authigenic Clay minerals in different Basins.

2.3 Core Description:

Cores are usually cut using a special coring bit and are retrieved in a long core barrel. Core barrels can be as long as 9 to 17 m with a hollow drill bit which is attached to the bottom of the drill pipe for the purpose of recovering continuous samples of the formation while the hole is being drilled. Samples obtained are cylindrical cores and can be as long as the core barrel. (Reifenstuhl, 2002).

The description of cores provides basic information including latitude, longitude, water depth, core length and lithological properties including megascopic and smear slides observations. Detailed core descriptions and interpretations include texture, grain size, sorting, sedimentary and biogenic structures, facies, composition, cementation, hydrocarbon occurrence, flow units, significant surfaces and fractures. Core description and interpretation are of crucial importance to regional and field studies because depositional facies, diagenesis, stratigraphy and fracture networks usually control porosity and permeability distributions which ultimately impact on reservoir performances. A basic understanding of the reservoirs dynamic behaviour often comes from integrated core & thin section descriptions and interpretations. Laboratory analysis of core samples is important to reservoir and petrophysical studies as it provides accurate measurement but sometimes damage can be done to the cores if laboratory test procedure, core sampling and handling are incorrectly done (Sinclair and Duguid, 1990). Destructive process which includes plugging do cause partial disintegration of formation and thus significantly increase petrophysical property measurement; this has been identified to cause highly optimistic permeability measurement (Hurst, 1987.)

Laboratory procedures such as drying of the samples may drive off all the water in the clay samples (Sinclair and Duguid, op.cit). Core analysis has often been integrated with other petrographic analysis for qualitative description. Scanning Electron Microscopy, X-ray Diffraction and Energy Dispersive Spectrometry are other sophisticated techniques that have evolved over time to complement core studies and description. Different laboratories use different procedures in core analysis; this always results in discrepancies in results from different laboratories. Porosity measured in dried core plugs using humidity controlled methods has been

noted to be consistently lower than the one measured from oven dried core plugs (Penney and Looi, 1996). Percussion sidewall cores (SWC) are normally obtained when drilled wells have been completed, this is most times necessitated by requests to take more core samples for analysis, and this can be achieved by usage of core barrel which can penetrate different formations regardless of the hardness. Three types of samples are available for description from boreholes; these include ditch cuttings, SWC and the whole core. Ditch cuttings are often used for biostratigraphic study because they are the source of pollen, foraminifera and other palynomorphs which are used for dating. Cores, especially sidewall cores, have been proven to be more reliable than cores obtained while drilling in providing precise assessment of subsurface conditions.



Figure 2. 1: Showing Cores layout <http://hamptonroads.com/node/374>

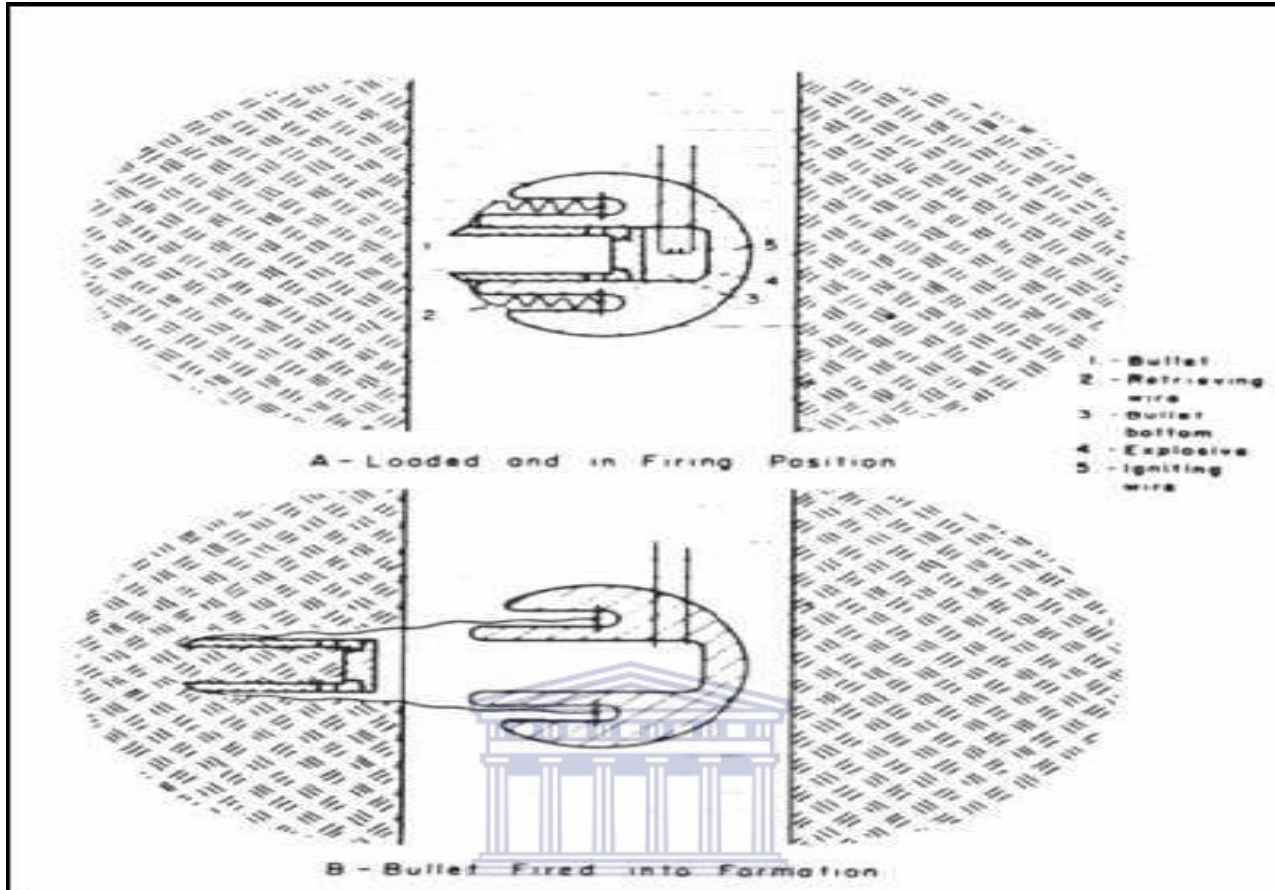


Figure 2.2: Percussion Sidewall-Coring Scheme (after Schlumberger, 1972)

2.4 Depositional Environment:

Each depositional environment possesses distinctive physical, chemical and biological characteristics that allow for specific kinds of deposits. The occurrence and abundance of clay minerals has often times been linked with the depositional environment in which sediments were deposited. Shammari et al., (2011) observed clay coatings are present in all depositional environments observed in Unayzah sandstones, Saudi Arabia .Kaolinite has been observed to be abundant in more mature quartzose and subarkosic sandstones and is the most common clay cement in all depositional environments except for aeolian settings, while illite is common in quartzose /subarkosic sandstones deposited in aeolian and fluvial settings (Kupez et al, 1997).

Smectite is mostly common in deep marine depositional environment. Generally, volcanic ash deposited in a marine environment alters to smectite while the one deposited in non-marine fresh water alters to kaolinite. This process is well documented in coal measure sequences where altered volcanic ash deposits consisting of kaolinite are known as tonseins (Spears & O'Brien, 1995). Diagenetic processes can be controlled by overall chemical, biological and physical processes within the depositional systems, few index minerals have been identified to define a particular depositional environment. Glauconite is often found in deep marine environments, commonly in marine environments that are characterised by alkaline waters and dominated by aqueous sodium and chloride ions with subordinate SO_4^{2-} , Ca^{2+} , Mg^{2+} and with salinity of 35 %. Early and late diagenesis can be strongly influenced by physical and chemical characteristics of the depositional environment

2.5 Petrophysical Properties:

Petrophysical properties are intrinsic properties of reservoirs and form the basis of up scaling in any process of creating a functional reservoir model. Without having to perform routine core analysis to determine petrophysical properties, comprehensive wire line log interpretation can be performed with the industry accepted software to estimate petrophysical properties. Porosity, permeability and saturation are among the petrophysical properties that can be determined from log interpretation, petrophysical properties involve studying of the physical properties of the rock which are related to pore and fluid interaction (Archie, 1950).

The review of some petrophysical properties of reservoirs are discussed below.

2.5.1 Porosity.

This is the measure of the capacity of a rock unit to contain and hold fluids, where the usually occupied by pore space aroil, water and gas. It is also defined as the fraction of bulk rock volume that is filled with void spaces; it can be expressed as a percentage or a fraction by dividing pore volume by total bulk volume of the rock unit. Porosity data can be obtained from direct measurement on core samples or from computation of data obtained by running of wireline tools in the well, the data obtained from cores analysis are often used to calibrate data derived from well logs. The amount of pore spaces which allow transmission of fluids within the rock is

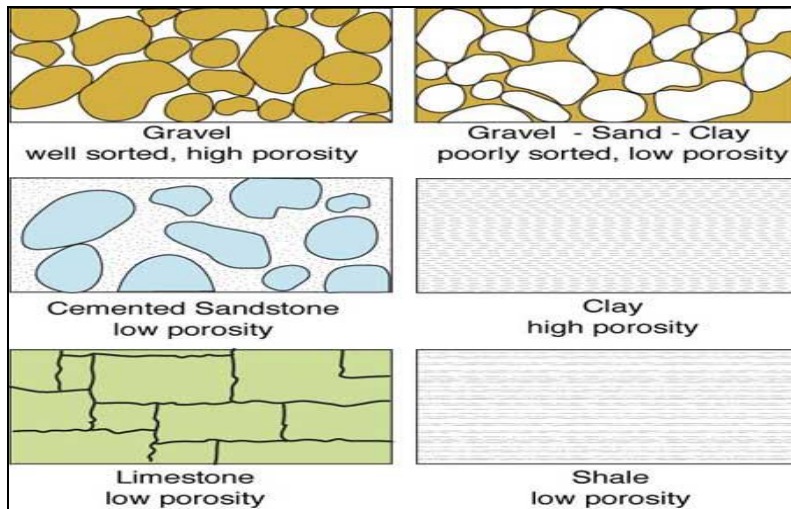
regarded as the effective porosity while total porosity always includes porosity in isolated pores, adsorbed water on grains, or particles surface associated with clays (Levorsen, 1967). Porosity is altered or influenced by some geological factors which include compaction, cementation, leaching, bioturbation, clay coatings and most importantly diagenesis. Effective porosity has been defined by many authors, notably Juhász (1990) and Clavier et al., (1984) defined it as total porosity – volume of dispersed clay in pore spaces of reservoirs expressed as a fraction of the bulk volume:

$$\phi_T = \frac{\rho_{ma} - \rho}{\rho_{ma} - (\rho_{hc} \cdot (1 - S_{xo}) + \rho_{mf} \cdot S_{xo})}$$

where ρ_{ma} is the grain density, ρ is the density log measurement, ρ_{hc} is the in-situ hydrocarbon density (from pressure data or sampling), ρ_{mf} is the mud filtrate density (from correlation charts normally) and S_{xo} is the invaded zone water saturation.

Porosity of a particular rock depends on many factors which include rock types, the arrangement of rock individual grains and the matrix. Based on the classification of wire line logs according to the parameters they can measure, density, sonic and neutron logs have been identified as the tools from which porosity data can be derived. Combination of these logs gives a good indication for lithology and accurate estimates of porosity value.

Porosity can be primary or secondary;. Primary porosity is inter-granular or inter-crystalline and depends on the shape and size and arrangement of the solids; it is common in clastic rocks. Secondary porosity is commonly as a result of dissolution of fissures or cracks and matrix caused by mechanical forces. The key with all of these cements is that we can unravel how and why they were formed, utilizing the wide range of analytical techniques we have at our disposal, and hence be able to predict where reservoir quality will be degraded or preserved within the subsurface geological model. All of the above observations and analyses can be used to create textural, compaction and diagenetic models which can be used to help predict the occurrences, abundance and distribution of pores and pore-filling cements. These models can be used to help constrain and validate petrophysically-derived porosity-permeability models.



<http://www.amiadini.com/NewsletterArchive/110128-NL143/envEnl-143.html>

Figure 2.3: Porosity identification in various rock samples.

2.5.2 Permeability:

This is a measure of the amount of fluid flow within a rock unit in response to an applied pressure gradient; it is the expression of transmissibility of immiscible fluids within the reservoir pore spaces. It exerts an important control on the flow rates and the volume of fluids that can be obtained from the wells, and can be measured through three procedures which are: well testing, wire line tool analysis and laboratory analysis of core samples. Permeability estimated in petroleum-reservoir rocks is commonly expressed in units called millidarcys. Industry accepted mathematical models and software packages have been used to calculate permeability, Carman –Kozeny equation (1968) and Interactive Petrophysics software are two of the many methods of estimating permeability from wireline logs.

There are two measures of permeability which are intrinsic permeability and hydraulic conductivity. While intrinsic permeability is independent of the fluid present in the reservoirs, the hydraulic conductivity is dependent on the properties of the fluid present. Permeability predictions involve the understanding of how various geological factors enhance or reduce fluid flow. Grain size and sorting are the main controls on the reservoir's permeability in unconsolidated sands (Beard and Weyl, 1973). Rocks with coarser grains would have higher

permeability because of the presence of larger pore throats while rocks that are poorly sorted have lower permeability. Different clay mineral cements affect permeability in different ways because they occupy different pore networks within the reservoirs (Stalder, 1973). Pore lining clay minerals have lesser effects on the permeability than pore filling clay cements (Pallatt et al., 1984). However if thick coats of chlorite and illite occur, permeability can be seriously diminished, particularly in fine grained sandstones.

Grain size has also been demonstrated to exert more influence on the permeability of reservoir sands. Reedy and Pepper (1996) demonstrated this in the unconsolidated turbidite reservoir sands of the Gulf of Mexico where a log- linear correlation exists between permeability and grain size of reservoir sands. A poorly sorted sand exhibits low permeability and vice versa.

Total, effective and relative permeability are of interest when fluid dynamics within reservoirs are discussed. Total Permeability is the measure of the transmissibility of a particular fluid within a porous medium when saturated with a single fluid. As absolute permeability hardly exists in reality, estimation of absolute permeability of a core unit is simulated in the laboratory. In contrast, effective permeability is the transmissibility of a single fluid in the presence of other immiscible fluids in the porous medium, it is the ability of a rock unit to transmit a particular fluid amongst other fluids. Relative permeability is the ratio of effective permeability to absolute permeability.

Permeability defined by Darcy's equation is

$$K = Q \mu / A (\Delta P/L),$$

K = Permeability (Darcy)

Q = Flow per unit time (cm/s)

μ = Viscosity of flowing medium (cp)

A = Cross section of rock (cm²)

L = Length of rock (cm)

ΔP = Change in pressure (psi)

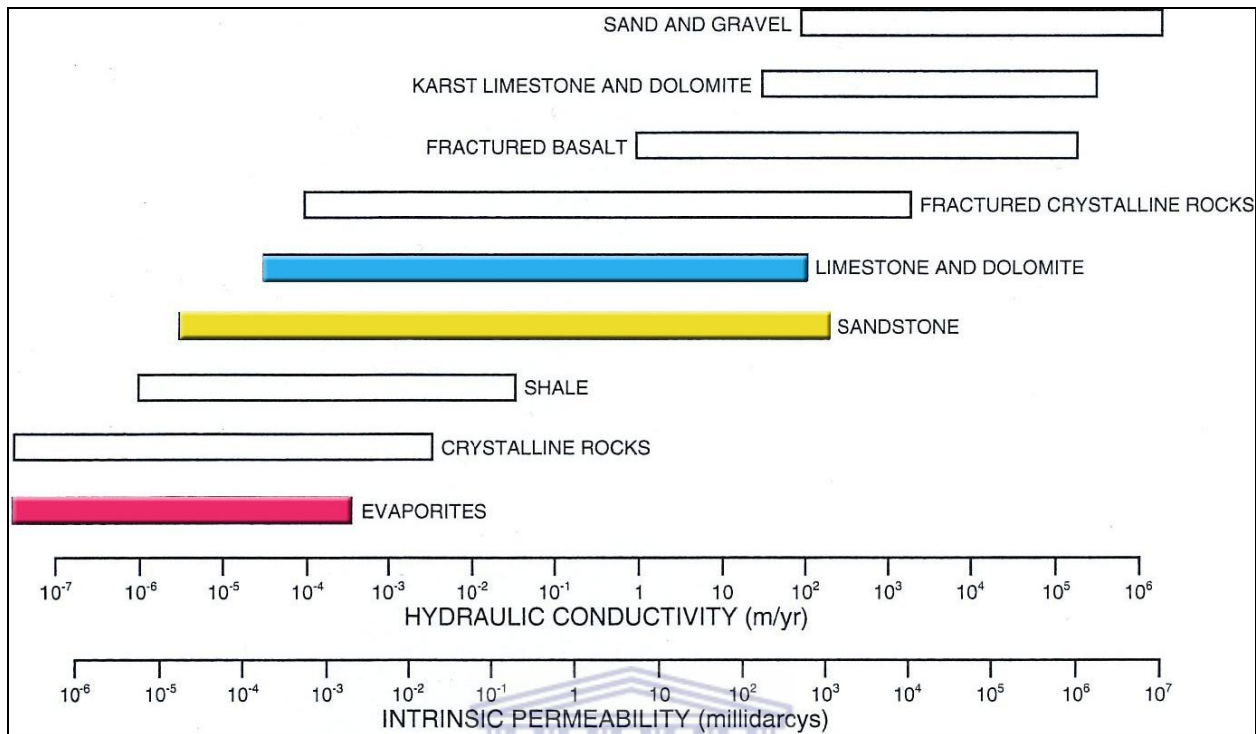
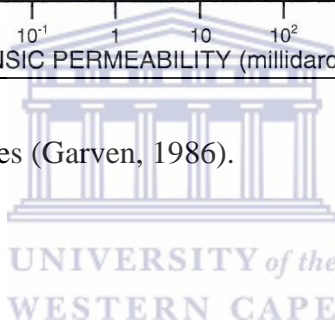


Figure 2.4 Rock permeability ranges (Garven, 1986).

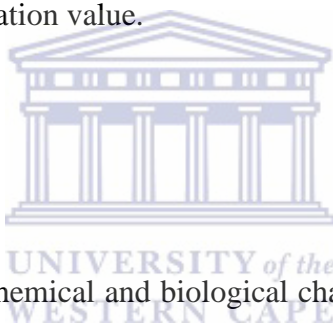


2.5.3 Fluid Saturation

Estimation of saturation values in Petroleum reservoirs is invaluable in petrophysics, it is the ratio of water or hydrocarbon volume to pore volume of the reservoir unit. Additionally, saturation is the percentage of pore volume of a reservoir unit occupied by water or hydrocarbons. Due to immiscibility of water and hydrocarbons because of density contrast, water occupies the pore volume below the hydrocarbon-free level. The migration of hydrocarbons into the pore spaces displaces connate water downward but larger pore spaces are firstly occupied with hydrocarbons because of low capillary pressure needed to displace water in the pore spaces. The knowledge of the position of the oil-water contact helps reservoir geoscientist to plan production techniques that will optimize hydrocarbon recovery. The implication of this is that, once the water saturation is estimated, hydrocarbon saturation value can be estimated. Petroleum reservoir saturation is the summation of water and hydrocarbon saturation, water saturation tends to decrease with increase in height above the free water level where capillary pressure is zero.

The volume of free immobile water that cannot be displaced by hydrocarbon migration is the irreducible water saturation or residual water saturation, (Sirr). Connate water saturation and flushed zone water saturation can be calculated from information supplied by well logs.

Archie (1942) related fluid saturation to the measure of electrical conductivity/ resistivity of the formation and defined the resistivity index (RI) as the ratio of the resistivity of partially water saturated rock R_t to the resistivity of the fully brine saturated rock R_o . The presence of clay cements within the reservoir affects overestimation of fluid saturation values, however, (Waxman and Smith) 1968, proposed a mathematical model that allows the calculation of the formation factor independent of clay conductivity effects (Core Laboratories, 1982). In preparation of drilling fluids, the type of dominant clay minerals is put into consideration because active sites exist on clay surfaces which often cause exchange of ions between drilling fluid and clays. This often alters porosity and fluid saturation value.



2.6 Diagenetic Studies

Diagenesis involves all physical, chemical and biological changes undergone by sediments after its initial deposition and after the sediment is lithified (Bates and Jackson, 1987). The timing of formation and the distribution of diagenetic minerals within a reservoir sequence also influence some of the variations in petrophysical characteristics (Al-Ramadan et al., 2005, Bjorlykke, 1998). It influences the extent of source rock maturity and exerts a major influence in evaluating reservoir potentials of clastic and carbonate reservoir rocks. Diagenesis in sandstones starts with compaction and alteration, followed by pore fill cementation and transformation of mineral phases in more deeply buried sandstones (Wilson and Pittman, 1977). Diagenesis is probably the only singular reason why porosity decreases with depth. Schmidt and Mc Donald (1979) classified diagenesis history into Eodiagenesis, Mesodiagenesis and Telodiagenesis. Eodiagenesis involves diagenetic processes which occur in sediments at surfaces and immediately after deposition at temperature <70 degrees and prior to substantial compaction (Morad et al., 1990), while Mesodiagenesis takes place at deeper depth with substantial compaction at temperatures of about 80 degrees Celsius, and may involve, cementation,

precipitation, dissolution and replacement processes. Telodiagenesis is often due to an uplift process which exposes already buried sediments to hydrothermal flushing of pore waters. Apart from the textural maturity that controls reservoir quality, the significance of clay mineral diagenesis controls on reservoir quality has more implications during drilling, production and well stimulation operations (Imam 1994). Drilling and well completion fluids are designed for the specific variety of clay minerals present in pore spaces (Almon & Davies, 1979). Diagenetic studies have benefited from improvement in imaging and geochemical studies; this aids the quantification of fluid compositions and the historical aspects of the sediments. Clay diagenesis may enhance or inhibit reservoir quality depending on the timing of precipitation and recrystallization; clay authigenesis is controlled by many factors which include initial mineralogy, depositional environment, temperature, pressure dissolutions and biogenic deposits. Detrital composition of sandstones can specifically influence reservoir quality by constraining pathways of both physical and chemical diagenesis (Bloch, 1994). Porewater chemistry plays a major role in controlling the alteration and dissolution of detrital grains including the type of clay mineral formed (Dutta and Suttener, 1986). Clay minerals presence in pore spaces is initiated by cementation processes which ultimately cause lithification of the rock.

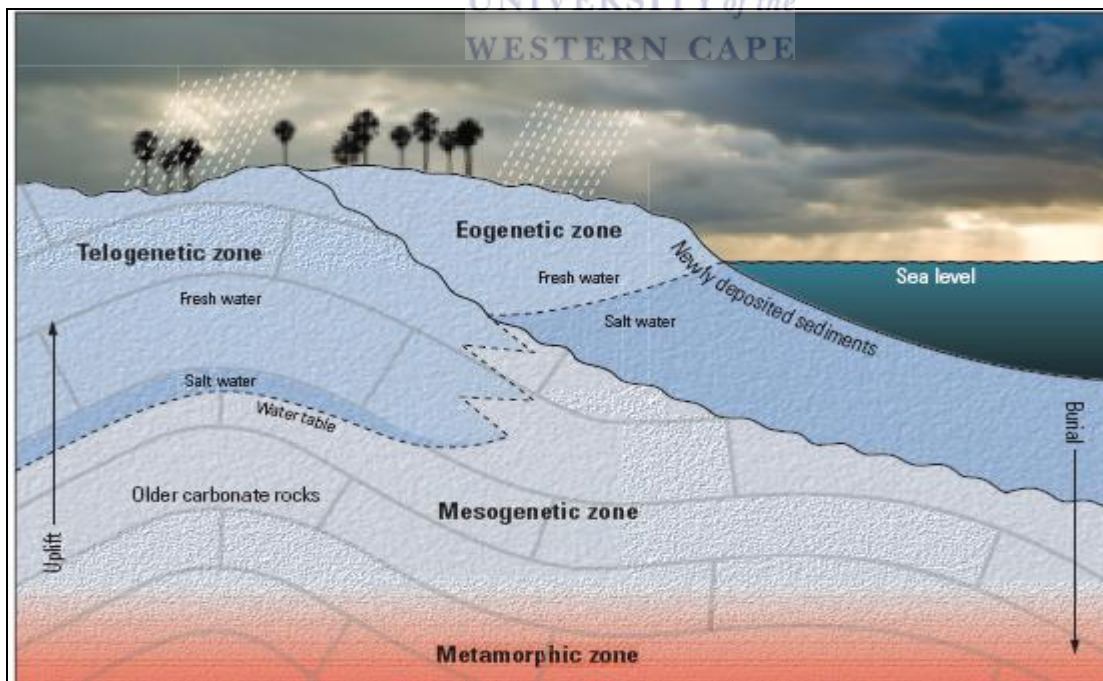


Figure 2.5: Various diagenetic regimes in reservoir rocks. Mazullo (1985)

CHAPTER THREE

3.1 Regional Geology

The Orange basin is situated along the South Atlantic margin and straddles the borders of Namibia and South Africa, it is a divergent passive continental margin (Barton et al.,1993). The tectonic evolution was as a result of the break-up of Gondwanaland, rifting and subsequent drifting apart of South American and African plates in the late Jurassic and early Cretaceous period (figure 3.0) .The break up of Gondwanaland was initiated by extensional forces that started in the early Mesozoic. (Petroleum Agency Brochure, 2006).



Figure 3.0: The rift phase in the Late Jurassic – Lower Valanginian showing the breakup of Africa, Madagascar and Antarctica (modified from Broad, 2004)

This separation divided the South Africa offshore basins into three tectono-stratigraphic zones. The narrow passive margin with protracted rift phase history along the east coast is as a result of separation of Madagascar and Antarctica. Due to limited sediment influx, only the Durban and Zululand basins contain denser sediments. To the S-E, the African plate is bounded by the Agulhas marginal fracture zone (Visser, 1998), a dextral transform margin that formed during the movement of the Falkland Plateau. Movement began in the early Cretaceous at the onset of

drifting and caused the truncation of structural trends such as the Permo-Triassic fold belt on the Jurassic- early Cretaceous graben and half graben complexes of the Outeniqua basin. The western coast of the offshore orange basin is a tensional transverse fractured marginal zone that has undergone local displacement and displays major structural attributes; the columbine-Agulhas arch and adjacent continental margins. The divergent passive Orange basin is characterized by graben structures trending sub parallel to the coast line (Jikelo, 1999).

The basin is highly underexplored with relative ratio of 1 well drilled per 400km square, the sediment supply into the basin was sourced from a river system (Orange river) with a rivaling delta to the north of basin, the sediments are a mix of continental and volcanic sediments (Fatti et al., 1994). Olifant and Berg river systems have also sourced sediments for the Orange basin, but with a major influence in the Southern part of the basin (Brown et al., 1996). Sedimentation probably started in the Kimmeridgian and Tithonian (152-154 ma), the Cretaceous sediments in this basin range from continental in the East to deep marine in the West while the Tertiary succession of sediments mainly comprises of calcareous oozes and chemical sediments with a characteristic deformed thick wedge of sediment due to sediment loading and slope instability (Petroleum agency SA, 2006). Sand deposition was mainly as a result of reworked delta front and marine storm channel bars, as well as wave action. They are generally well sorted ranging in grain size from very fine to medium grained. Dominant occurrence of well laminated and massive, greenish sandstones are a major pointer to the presence of detrital glauconite which serves as an indication of prevailing marine conditions.

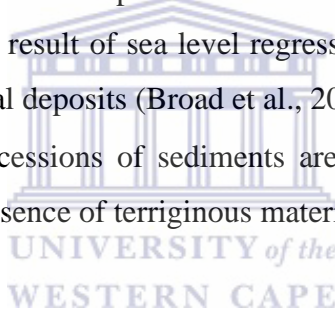
3.2 Tectono-Stratigraphy

The three major tectonic phases that characterize this area are classified into Pre -, Syn- and post-rifts (Gerrard and Smith, 1982). Significant compressional tectonism occurred in the pre rift phase where high grade and low grade metamorphites dominate the southern part and occurrence of granitic and alkaline intrusive dominates the northern part (Broad et al; 2007). The pre-rift rocks are overlain by a succession of Pre-Barremian synrift basic lavas within the central rift sequence and coarse continental clastic, fluvial and lacustrine sediments along with volcanics within the marginal rift basins (Barton et al., 1993). This is in turn overlain by a Barremian to

Aptian succession of Post rift alternating fluvial and marine rocks that are deposited as a result of transgression and regression of sea level (Van der Spuy, 2003).

The sequences of sedimentary succession in the Orange basin are highlighted below;

- Barremian to early Aptian sediments are occasionally interbedded with basaltic lavas together with shale and sandstones of marine origin. Sandstones of Aeolian origin have been intersected in the Namibia portion of Orange basin, (Barton et al., op.cit).
- In the early to middle Aptian, there was extensive deposition of organic shale which may have been due to prevalence of an anoxic environment which was caused by basin margin sag.
- The Albian to Cenomanian time witnessed the deposition of fluvio-deltaic sandstones while the Cenomanian to Turonian period was characterized by aggradational deposits. Progradational deposits as a result of sea level regression were also found but to a lesser extent than the aggradational deposits (Broad et al., 2007).
- The Tertiary to recent successions of sediments are dominantly organic and chemical sediments with minimal presence of terrigenous materials (Barton et al op.cit).



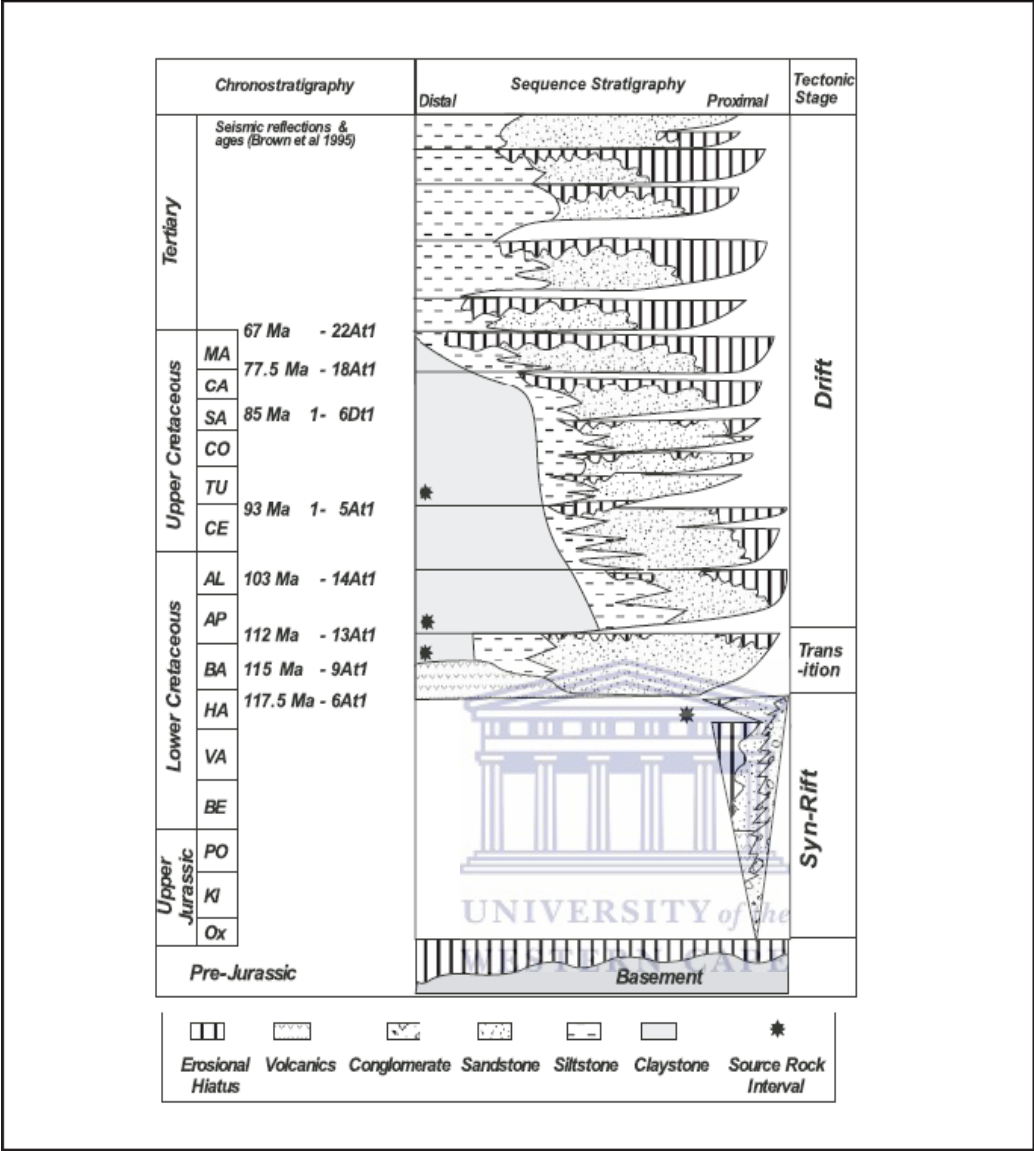


Figure 3.1: Chronostratigraphic and sequence stratigraphic diagram of the Orange Basin (Brown et al., 1996).

3.3 Brief description of Petroleum Systems:

A Petroleum system is defined as the systemic interaction of some geological configurations that could lead to commercial accumulation of hydrocarbons, it is a unifying concept that encompasses all of the disparate elements and processes of petroleum geology (Magoon and Beaumont, 1999). The appropriate timing of generation or formation of these elements is crucial to the accumulation of hydrocarbon in pools. The essential elements of petroleum systems that will be discussed about the Orange basin are source, reservoirs and traps.

3.3.1 Source Rock:

Potential source rocks are dominantly postglacial black shales of late Permian age deposited in lacustrine or low salinity marine environments; these rocks could also act as an effective regional seal. Exploration activities so far in the Orange basin have suggested that there is evidence of active Aptian source rocks and recently Cenomanian and Turonian source facies (Aldrich et al., 2003). The strongest petroleum system is sourced from lower Aptian and Barremian source shales located at the depocentre of the Orange basin (Petroleum agency report 2008). There is occurrence of synrift oil prone Hauterivian shale located within a half graben structure and trapped stratigraphically within lake shoreline sandstones interbedded with shale. An active petroleum system has been speculated to be present within the deep water areas of the basin, as seismic gas chimneys, seismic wipe-out zones, seafloor gas escape features, bottom simulating reflectors, flat and bright spot are all pointers to the likelihood of an active petroleum system (Jikelo, 1999).

3.3.2 Reservoir Rock:

Fluvio deltaic and lacustrine sandstones are the major reservoirs observed within the marginal rift basin while post rift successions of fluvio deltaic to deep marine turbiditic sandstones are also target reservoirs. Sandstones deposited in the late Permian were dominantly volcanoclastic with poor reservoir qualities; Triassic sandstones tend to be more mature (Petroleum agency report, op.cit).

3.3.3 Traps:

Compactional drape anticlines, stratigraphic pinch-out traps and inversion related closures are found within the synrift sequence and can act as major traps. Possible structural traps occur in the earlier sedimentary succession; structural plays have been identified in the deeper waters comprising of roll over-anticlines in the growth fault zone (Van der Spuy, 2003). A large number of possible traps, in the form of channel deposits and basin floor fans were in the basin in the Cretaceous and Tertiary (Roux et al., 2004).

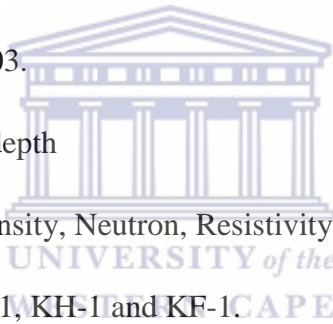


CHAPTER FOUR

4.1 Materials and Methods

This chapter discusses the various materials, approaches and techniques used in this study. The flow chart below shows the stepwise procedures utilized in achieving the results of different analyses carried out for this study. Software packages used in this study are Petrel 2011, IP (interactive petrophysics) and Techlog. Core samples obtained from PASA were used for different analyses while digitized wireline logs, Geological reports of wells to be studied were also collected from the agency. Materials received from PASA are listed below;

1. Petroleum exploration report 2003.
2. Core samples taken at selected depth
3. Digitized wireline logs data (Density, Neutron, Resistivity, Sonic and Gamma ray)
4. Geological reports of wells AU-1, KH-1 and KF-1.



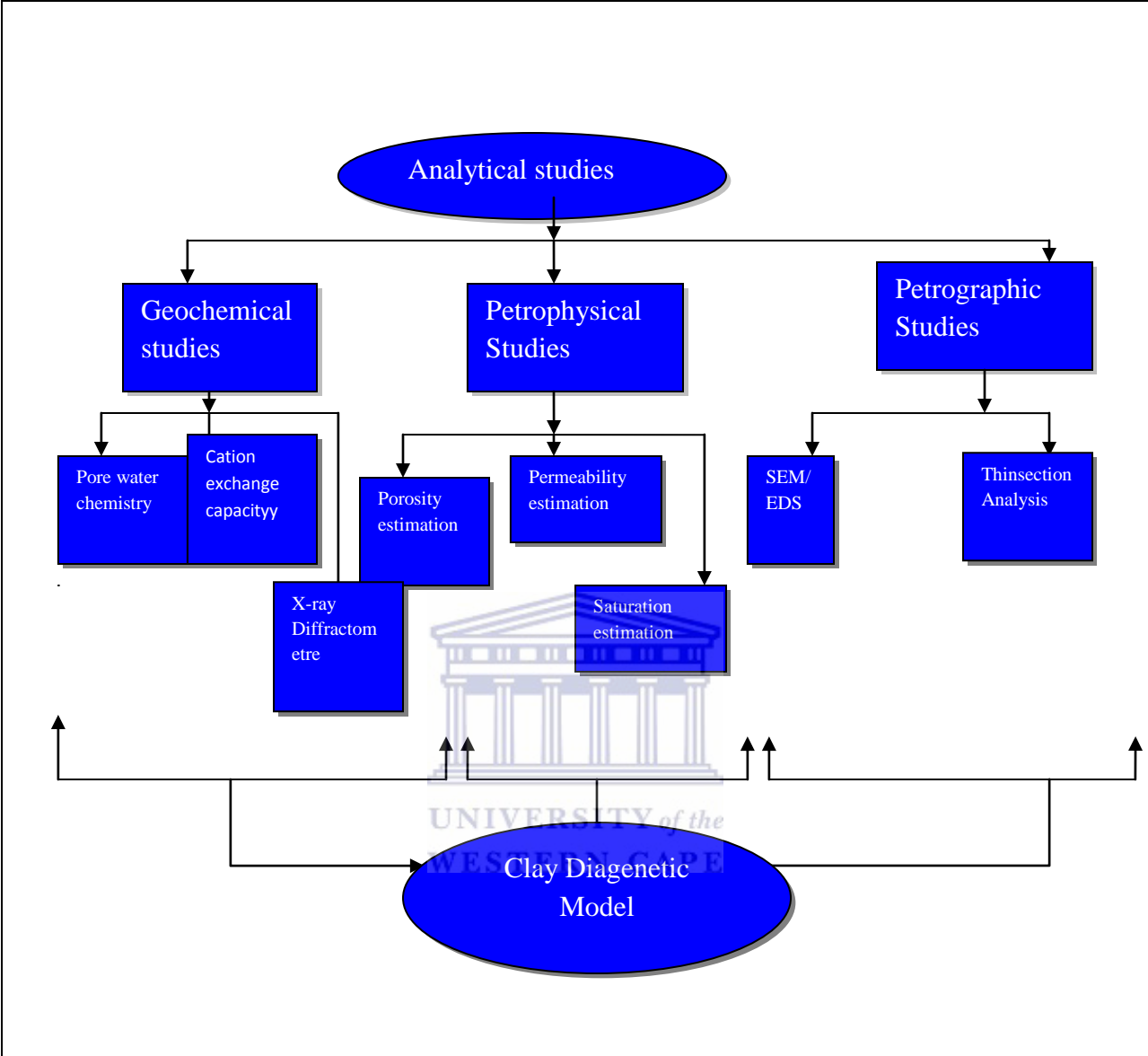


Figure 4.0: Methodology Framework.

Prior to data loading and sample collection, a review of the regional geology has been done to obtain a comprehensive understanding of tectonic evolution, stratigraphy, sedimentary source and quality of the petroleum systems. Core samples have been taken within the cored intervals and at selected depth for the purpose of petrographic and geochemical studies. The sampling position has been determined based on the length of the cores available. Sampled depth intervals would be chosen based on the identification of lithologies from the gamma ray log and length of cores recovered during core description. This was followed by core-log depth match while sample intervals within the reservoir section have been limited for detailed understanding of the

reservoir quality. The core mineralogy has been determined by the whole-core x-ray diffraction for mineralogy identification purposes and this was supported by ED x-ray analysis to know the elemental geochemistry of the core samples. The textural characteristics like grain sizes and shape have been studied with a petrological microscope for thin section slides. SEM has been carried out to confirm observations made from thin sections and determine the type of clay minerals present at specific depths for diagenetic history construction. The prevailing depositional environment conditions contributing to the authigenesis of particular clay minerals have been determined through pore water chemistry analysis, facies description and wireline logs. CEC has been carried out to determine the type of dominant exchangeable cations and to estimate cation exchange capacity per pore volume (Qv) which is a shaliness indicator.

4.1.1 Wireline logs:

Geophysical logging was pioneered by Marcel and Conrad Schlumberger in 1927 with the aim of measuring the electrical properties of a borehole at Merkwiller-Pelchebron in Eastern France (Schlumberger, 1972). Geophysical logging has been applied in all aspect of geology and most importantly petroleum geosciences. It is an invaluable tool used by geologists to confirm the ground truth when calibrated and compared with cores. It offers a unique opportunity in determining the composition, variability and physical properties of rocks around the borehole. The process of wireline logging is done by suspending a sonde from a steel cable or embedding it in a drill string (LWD) - Logging While Drilling. The concept of wireline logging is to measure the radioactive and electrical properties of the borehole with depth, this is usually before casing is done.

Wireline logs may not be direct measures of some petrophysical properties but it can measure some parameters through which petrophysical properties can be derived. Parameters such as resistivity, density and natural gamma radiation are recorded as a function of depth. Wireline logs are classified based on the principles of usage and on the properties they measure, highlighted below.

4.1.1.1 The Classification based on Principles of usage.

1. Resistivity logs: induction log, laterolog and deep resistivity log.
2. Lithology logs: Gamma ray and Spontaneous potential log.
3. Porosity: Density, neutron and sonic log.
4. Auxilliary log: Dipmeter and Caliper logs.

4.1.1.2 The Classification based on Operational Principles.

1. Electrical logs: Spontaneous potential and resistivity logs
2. Nuclear or radioactive logs: Density, Neutron and Gamma ray logs
3. Acoustics logs: Sonic logs

4.1.2 Methods of usage. Five wireline logs will be used in this study in estimating some petrophysical properties of the rocks under consideration. Emphasis is placed on the parameters they measure and how each parameter is used to estimate petrophysical properties.

4.1.2.1 Gamma Ray log:

The GR log is a measure of the natural radioactivity of the rock formations. In sedimentary beds the log normally reflects the shale content of the formations through the measure of Th, K and U components. This is possible because radioactive elements tend to reside in clays and shales. Clean formations usually have a very low level of radioactivity, unless radioactive contaminant such as volcanic ash or granite wash is present or the formation waters contain dissolved radioactive salts. The gamma ray log is useful to detect zonation of reservoir intervals and also to correlate sand bodies. The standard unit for measuring gamma ray value is American Petroleum Institute (API). Scintillation counters attached to a sonde detect and record a natural disintegration from any source in the region close to the borehole. Gamma ray value of less than 45 API indicates clean sand while gamma ray value of 75 API indicates shale with GR values ranging between 45 and 75 API usually regarded as shaly sand. The different GR values always

reflect the radiation intensity of the formation. The relative gamma ray values mentioned above are due to the presence of organic matter and radioactive materials present in the rock samples. The scale range for GR measurement is usually from 0-100 or 0-150. The maximum deflection of gamma ray curve to the left indicates sandstones while the maximum deflection to the right indicates shale. In this study, estimation of the volume clay within the reservoir intervals will be done from the readings made from Gamma ray log.

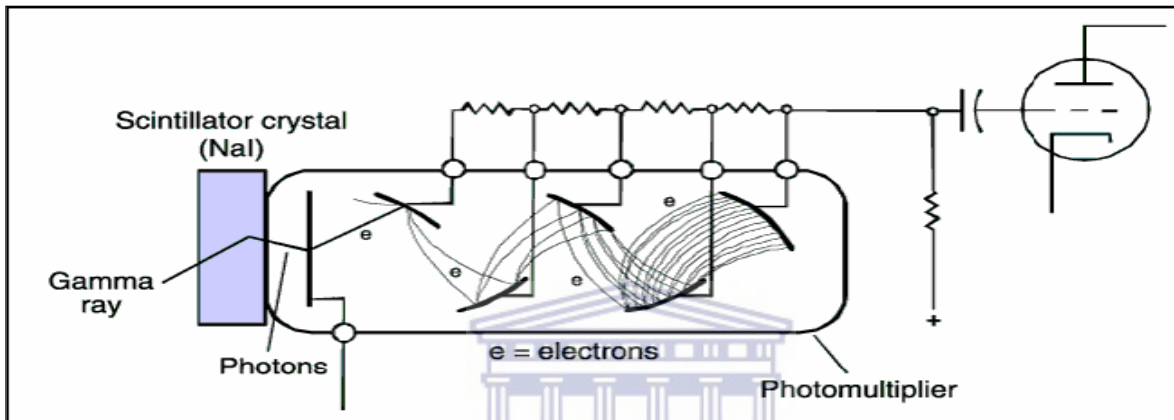


Figure 4.1: Gamma ray tool (after Serra, 1984)

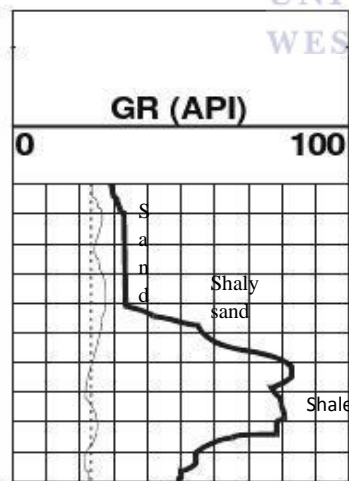


Figure 4.1.1: Typical Gamma ray log response to different lithology. After Schlumberger, (1972)

4.1.2.2 Density Log

This is the measure of the number of low energy gamma rays surrounding the logging tool which is due to the elastic scattering of Gamma rays from the borehole wall and is proportional to the electron density of the rock. When a radioactive material source is applied into the borehole wall, it emits medium-energy gamma rays into the formation. Upon emission of these gamma rays, there is always collision of high velocity particles with electrons in the formation. After each collision, the gamma ray loses some of its energy to the electron, and then continues with diminished energy. This type of interaction is called Compton scattering. The scattered gamma rays from the source reaching the detector at the fixed station are counted as an indication of formation density while the number of Compton scattering collisions is related directly to the electron density of the formation. Consequent upon this, the electron density determines the response of the density tool, the density logging tool measures electron density and photo-electric density.

4.1.2.2.1 Formation Bulk Density

The density log measures bulk density of a formation, which is the overall density of a rock and includes the matrix, pores and fluids enclosed in the pores. Density logs often run in tracks of two or three of log tracks with scale ranging between 2-3 g/cm³ (Rider, 1996).

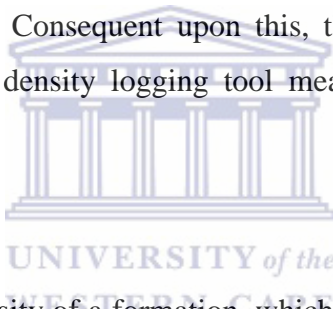
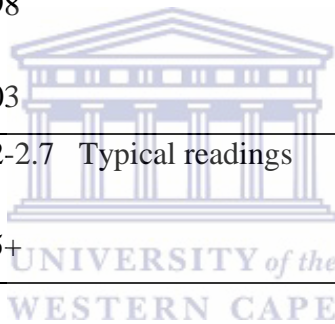


Table 4.0: Density values of various rock samples

Lithology	Density Values
Limestone	2.71
Sandstone	2.65
Dolomite	2.87 Reading in Zero porosity
Anhydrite	2.98
Salt	2.03
Shale	2.2-2.7 Typical readings
Coal	1.5+



4.1.2.3 Neutron Log

This particular log tool measures the hydrogen ion concentration in the reservoir. During neutron logging, geological formations are bombarded with a radioactive source which is always neutron rather than gamma rays. Neutrons are typically emitted by a chemical source such as Plutonium Beryllium (Pu-Be), or produced by electronic neutron generators such as a minitron. Fast neutrons emitted from these sources interact with atoms of similar mass which are hydrogen atoms, because hydrogen atoms are always present in both water and petroleum filled reservoirs. Once the neutrons are slowed down due to collision with hydrogen atoms, they start to scatter elastically and slow down further because they are continuously absorbed into the nuclei of heavier atoms present in the formation. Because of this absorption, they become unstable and tend to lose some energy which makes them emit gamma rays which are recorded by the counter. A suitable detector which is positioned at a certain distance from the source, can measure either

epithermal neutron population, thermal neutron population, or the gamma rays emitted after the absorption.

However there are types of neutron log which are run within the borehole:

4.1.2.3.1 Compensated neutron log: This tool has two detector spacings and is sensitive to slow neutrons, it is used in both cased and open hole and detects thermal neutrons.

4.1.2.3.2 Sidewall Neutron Porosity Log: This is an important tool for measuring the porosity of a reservoir section, it could be run in a cased or open hole, correction must however be made for casing and cement when run in a cased hole (Krygowski, 2003).

Aside from porosity determination, the neutron log tool can also be used for detection of gas bearing zones when combined with the density log as well as for lithology determination when combined with the gamma ray log.

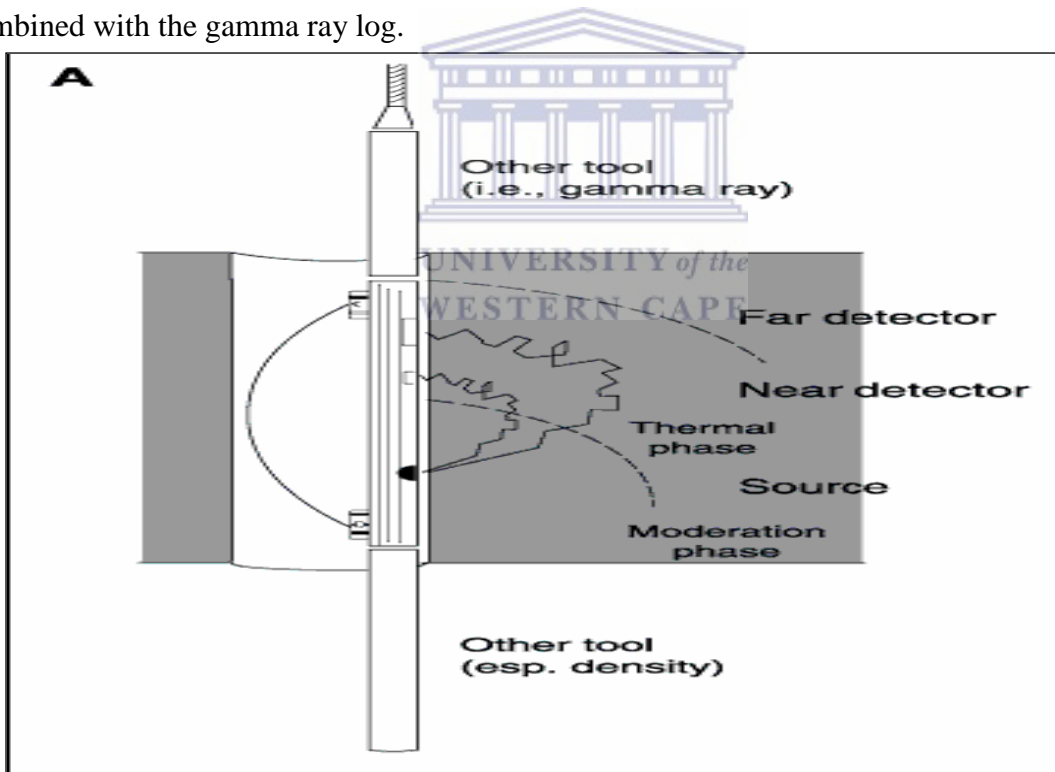


Figure 4.2: Schematic diagram of Compensated neutron tool (after Rider, 1996).

4.1.2.4 Resistivity Logs

This is a method of well logging that works by characterizing rocks and sediments based on their electrical conductivity while resistivity is a fundamental material property which represents how strongly a material opposes the flow of electrical energy. It is also used in formation evaluation during oil and gas well drilling. The resistivity of a well depends on water saturation, pore structure geometry and resistivity of formation water. In these logs, resistivity is measured using electrical conductors to eliminate the resistance of the contact leads. The log must be run in boreholes containing electrically conductive mud or water. Various types of resistivity logs include induction logs, latero- logs and micro resistivity logs

4.1.2.4.1 Induction logs

This is used in measuring the conductivity of an undisturbed formation i.e. a formation that is laterally distant from the borehole. It utilises a high frequency electromagnetic transmitter to induce current into the formation, naturally designed for an 8.5 inches borehole, it can run successfully in a larger hole size performed at 1.5 inches stand off from the borehole wall.

4.1.2.4.2 Laterolog. This tool is applied in undisturbed formations, it can detect over-pressure formations and perform fluid saturation determinations. It makes use of bucking currents or focusing currents to monitor potential difference drops between an electrode and the tool; the drop in the potential of the electrode is a function of the resistivity changes within the formation.

4.1.2.4.3 Micro-Resistivity log: This measures the resistivity of the flushed zone (zone of high mud cake thickness) with high resolution. It measures the resistivity of the invaded zone and does not reflect the true resistivity of the formation.

4.2 Petrophysical Properties Estimation

The following parameters and rock properties will be estimated from integration and interpretation of different log suites. Various accepted industry software package and mathematical models are used for accurate determination of the parameters and properties.

4.2.1 Volume of Shale

This is the measure of the degree of shaliness or clay content within the reservoir interval, the Steiber method is appropriate because it suppresses the abnormal responses exhibited by the gamma ray tool to a small amount of shale.

Using the Steiber equation (1970), Vsh (volume of shale) is calculated as:

$$V_{sh} = IGR/3 - (2IGR)$$

4.2.2 Fluid saturation.

Fluid saturation of hydrocarbon bearing intervals can be estimated from the resistivity logs by combining both a deep resistivity tool and a shallow resistivity tool.

$$S_w = [F^*(R_w / R_t)]^{0.5}$$

Where $F = a/\text{Porosity}^m$, R_w = Resistivity of water, R_t = True resistivity of the formation

The hydrocarbon saturation would be calculated as $S_{hc} = 1 - S_w$

Bulk volume of water (V_b) = $S_w * \text{Porosity}$

$S_{irr} = V_b / \text{effective porosity} / (1 - V_{sh}^2)$. S_{irr} implies the minimum attainable amount of water that can be displaced from the reservoir due to hydrocarbon migration.

When $S_w = S_{irr}$ implies hydrocarbon bearing intervals

$S_w > S_{irr}$ Hydrocarbon production likely

$S_w < S_{i_{irr}}$ Erroneous estimation

4.2.3 Porosity

Because of its high accuracy and minimal borehole effect, the density tool is used in the determination of Porosity,

$$\text{Porosity} = \frac{P_{ma} - P_b}{P_{ma} - P_f}$$

The density tool can give an indication of gas bearing zones in the reservoir when combined with the Neutron log. Porosity from neutron log is thus calculated with the density log, where

$$[0.5 * (\Phi_d^2 + \Phi_{cnl}^2)]^{0.5}$$

Φ_d = Porosity reading from density log.

Φ_{cnl} = Porosity reading from neutron log.

for gas bearing reservoirs while for non-gas bearing reservoirs;

Total porosity = Density porosity + Neutron porosity / 2.

Effective porosity is given as [Total porosity * (1 - V_{sh})] provided V_{sh} is calculated by the Steiber method.

4.2.4 Permeability

Permeability values would be derived by using Coates formula and is measured in milli Darcies

$$K = G \Phi_{eff}^4 \left[\frac{[\Phi_T - (\Phi_{eff} * S_{wir})]}{\Phi_{eff} * S_{wir}} \right]^2$$

The Coates formular for calculating permeability works well in shaly-. sandy formation

Φ_{eff} = Effective porosity

[Φ_T = Total porosity

Sw_{ir} = Irreducible water saturation.

4.3 Wireline logs Loading:

Well logs formatted in Las (Log ASCII Standard) file collected from PASA have been imported into the Interactive Petrophysics workstation and Petrel software; the log signature generated has been compared with the lithology observed on the cores to see any difference, after which a quality check and normalization of curve has been done. If need be, matching of core and log depth has been done based via the Gamma ray log signature and reservoir sections delineated through the integration of different logs displayed. The reservoir has been modeled with Petrel 2011 because of its unique environment of 2D and 3D visualization windows and Microsoft windows based standards of shared earth modelling.

4.4 Core Description:

Materials needed for Core description are

- Measuring Tape
- Hand lens
- Digital camera
- Log sheet
- Sample bags
- Apron
- Water

Cores laid out at the PASA core store were arranged in different boxes and tagged with the name of the specific well. The cores were arranged from bottom to top; this makes the logging of these cores less complex. Quantitative and qualitative information can be gotten from detailed

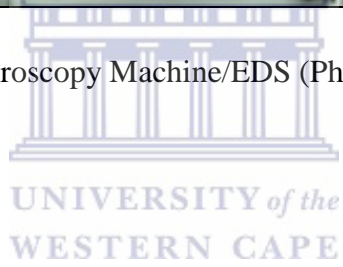
description of cores, broken cores were taken into consideration as to be able to calibrate the total depth of cores with total depth of cores recovered. Cores were cleaned up with a wet apron for better visual observations of rock properties like colour, sedimentary structures, fossil assemblage, grain size and texture. The thickness of each of the cores described was measured and recorded using a measuring tape, grain sizes were viewed with a hand lens which was also used to observe any apparent sedimentary structures. A digital camera was used to capture cores with interesting geological features at different depth, while a grain size standard chart was used to classify the grain sizes.

4.5 Scanning Electron Microscopy/EDS (Energy Dispersive Spectrometry).

SEM utilizes a strong beam of electrons to image a sample by revealing information such as external morphology, chemical composition and crystalline structure. Because of the high resolution and magnification of up to 30,000 times, it was developed as a tool to replace the ordinary light microscope which has limited capacity to image samples. SEM has a larger depth of field which allows a large number of samples to be in focus at one time and produce an image in a 3D arrangement. Applications of SEM include fracture mechanics and structure determination. Because of its versatility, it is used for EDS analysis to determine chemical compositions of samples. This study used a Topcon Leo S440 fitted with EDS, this device measures the energy of X-rays generated by interaction of samples with beam of electrons. Pellets were prepared from samples by mixing with adhesives; the pellets were subsequently inserted into the carbon sputter to allow carbon coating. After this, the pellets were inserted into SEM image /EDS machine analysis. Sample preparation involves mounting on an aluminium stub covered with a carbon adhesive and subsequently coated with silver paste. The whole prepared sample was put in to the SEM and illuminated with electrons which later flow through it.



Figure 4.3: Scanning Electron Microscopy Machine/EDS (Physics Department, UWC)



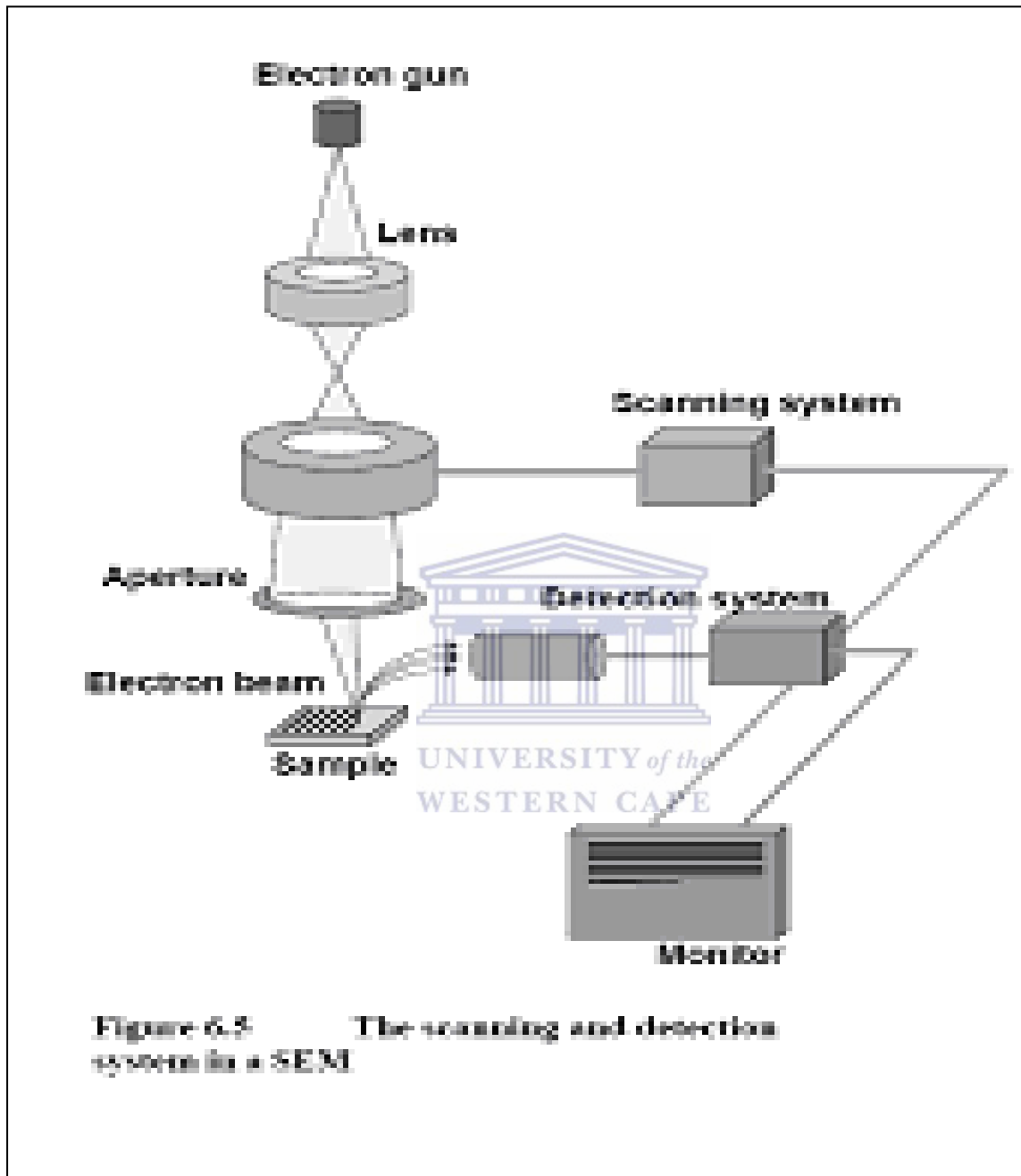
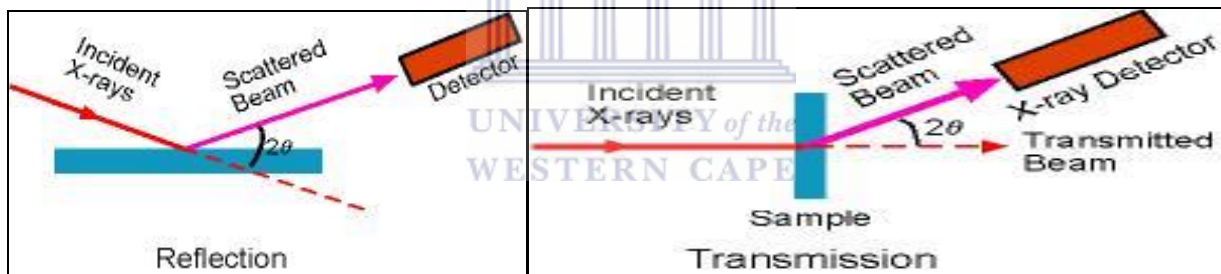


Figure 4.4: Scanning and detection system in scanning electron microscope (Theodor, 2000)

4.6 X-Ray Diffraction (XRD)

This is an electromagnetic radiation which generates photon energies in the range of 100eV to 100KeV. X-rays often penetrate deep into the material or samples to reveal bulk structure. X-rays are generated when a focused electron beam is accelerated across a higher voltage field after which it bombards a stationary or rotating solid object. As beam of electrons collides with the atoms in the primary target and subsequently slows down after collision, it deflects away from the original source because of energy loss and generates a continuous spectrum of X rays (figure 4.5 A). The phase identification of samples taken was done at the Ithemba labs x-ray facility using a Bruker D8 ADVANCED diffractometer. The experimental set up includes a 3 degree divergence slit on the secondary side as well as 3 degrees on the primary side. Samples prepared for analysis were measured from a 2-theta starting point of 10 degrees to 2 -theta stop of 85 degrees with step size value of 0.02 degrees and step time of 0.3 s.



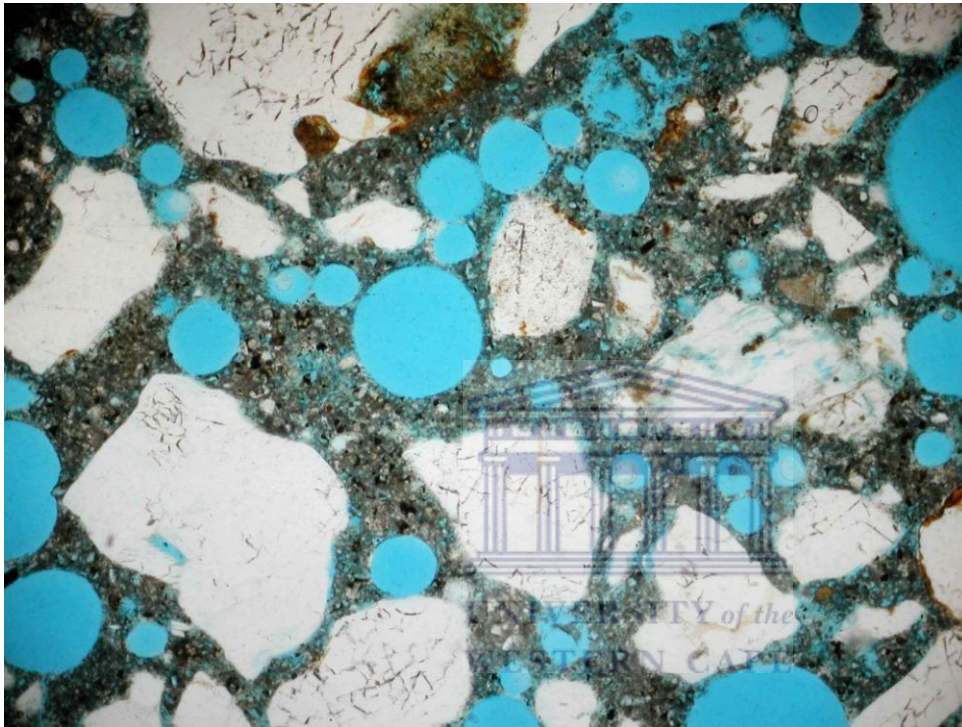
A

Figure 4.5: (A).Concept of diffraction of X-rays.

4.7 Thin sections Analysis

Thin section analysis involves a petrographic description of rock sample, basic properties such as grain size, degree of sorting, mineral abundance and porosity can be estimated from visual observations of thin sections. Preparation of rock samples for thin section analysis was done by impregnating it with epoxy to augment sample cohesion and prevent loss of material during the grinding procedure. Each of the samples were mounted on a frosted glass slide and then cut with a diamond saw to a thickness of approx. 5mm and thinned to a thickness of about 30 microns. It

is an invaluable tool in reconstructing diagenetic history as pore filling or pore lining cements can be identified on the thin sections' photos. Information thus obtained from thin sections was matched with SEM and XRD results to authenticate the observations made. The occurrence of some minerals or authigenic clay cements does not only affect the reservoir but their pattern of distribution does play a major role in influencing reservoir quality.



<http://www.cmc-concrete.com/CMC%20Web%20Photos/airvoids.jpg>

Figure 4.6: Typical thin section photomicrograph

4.8 Cation Exchange Capacity (CEC).

The analyses of cation exchange capacity on rock samples is the measure of the amount of sites on the samples' surfaces that can hold cations by an electrostatic force (Ross, 1946).Crystal surfaces of clay do have exchange sites where ions offer an electrical path through the clay which always result in surface conductance (Bates et al.,1987).These ions do offer themselves for exchange when in contact with saline solution and thus, their capacity is measured by the number of ions that can be exchanged. The usefulness of CEC in agricultural research has been highlighted as CEC serves as an organic matter indicator in soil samples. The importance of CEC for estimation of petrophysical properties of rock samples using different models have been highlighted by many authors (Winsaur and Mc Cardell, 1953, Waxman and Smith, 1968 and Clavier et al., 1984). The Waxman and Smith model is the commonly used model in estimation of Petrophysical properties. CEC studies are crucial in this work because it gives pointers to clay diagenesis as the number and sites of exchangeable cations can be determined easily. Transformation and diagenesis of clay minerals involves the exchange of one cation with another. This exchange does have certain effects on the intrinsic qualities of the reservoirs at specific depth, for example fixation of K^+ in a very alkaline condition enhances the illitization process. The CEC analysis in this study was carried out at BEM laboratory and the procedure involved the crushing of the core samples to a very fine powdered form.

This is followed by weighing off 10 grams from each of the samples and dissolves this using ammonium acetate solution in Erlenmeyer flask. The solution was shaken thoroughly for 16hrs while a 5.5cm Buchner funnel with moistened retentive filter paper fitted with light suction was used to separate the filtrate from the solution. The residue was washed four times with 25M ammonium acetate solution and suction was again fitted to allow slow filtering and the resultant leachate generated was tested for exchangeable cations using inductively coupled Plasma spectroscopy.

Another importance of CEC in clay studies and reservoir quality assessment is the determination of Q_v (shaliness indicator). Q_v is defined as the CEC value per unit volume, is an important parameter in developing a water saturation model.

Table 4.1 CEC values of different Clay minerals. After Worden and Morad (2003)

Clay	CEC (meq/100 g)	Grain Density (g/cc)	Hydrogen Index
Kaolinite	3–15	2.64	0.37
Illite	10–40	2.77	0.09
Montmorillonite	80–150	2.62	0.12
Chlorite	1–30	3.0	0.32

4.9 Porewater Chemistry

Determination of Ec, pH and TDS was made easy because pH meter accounted for these measurements to be taken at a single probe. The pH meter probe was calibrated and always preserved in KCL solution. Using the Eckert method (1988), the crushed core samples of the three wells at selected depth were weighed at 5 grams each and were dissolved with 50ml of ultra-water in a beaker. The beaker solution was centrifuged for ten minutes and allowed to settle for 15 minutes. This was followed by filtration using the suction pump and 50 microns filter paper, a clear filtrate obtained from the filtration was probed for Ec, pH and TDS.

Chapter Five

5.1 Presentation of Results: Core Description, Geophysical logs and Petrophysical properties.

Core description and lithofacies identification are basic fundamental steps in reservoir characterization. The significance of core description is for depth matching with gamma ray logs, depositional environment inference and sedimentary structures determination. Detrital composition of rock samples have been identified to exert a major influence on the reservoir quality as it conditions pathways of both physical and chemical diagenesis (Bloch, 1994). Depth matching of cores with the geophysical wire line logs is important for calibration because the drillers' depth are often different from the logger's depth, also, petrophysical properties estimation can be done by the integration of geophysical wire line logs . Lithological studies; taking into account all visual examinations made on the cores are often used to infer the depositional environment in which the cores were deposited while the type of sedimentary structures observed on a core sample do play a role in influencing the petrophysical properties of the rock units. The results from core description and geophysical logs interpretation will be discussed in this chapter and will be subsequently used to estimate petrophysical properties. The lower Cretaceous sedimentary deposits which are dominantly siliciclastic rock sequences have been grouped into different facies based on the evidence of grain size differences, colour, mineralogy and sedimentary structures. Core photographs were taken at various depths with interesting geological features, a suite of relevant geophysical logs were interpreted and were used to estimate the petrophysical properties.

5.1.1 Core Description

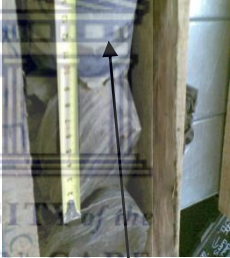

Cores are cylindrical massive rock units obtained during the drilling of wells, by the usage of a core barrel lowered into the well bore. Observations made on cores represent a ground truth of the subsurface formation. Lithological observations and facies identifications are the major information that can be obtained from core description. The total length of cores described from well KF-1, AU-1 and KH-1 are 2.4m, 6m and 18 m respectively. The approach used by Nieto (1998) was used in grouping the rock units into different facies based on their colour, grain size, mineralogy and sedimentary structures. Emphasis was placed on grain sizes as the major justifications for grouping the facies.

5.1.1.1 Core Description of K-F1 Well

Cores were cut at depths of 3006-3009.3m. The cores consist of thinly interbedded to interlaminated highly deformed clay stone, siltstone and sandstones. After calibration with wireline logs, the core-depth shift rule was applied because of discrepancy of 3.1m (Table 5.0 and Figure 5.3) observed between the depth of the cores and log depth, hence the depth cored is corrected and given as 3002.90-3005.93m. Depositional environment may be a low energy environment because of alternating fine and coarse grained sedimentation occurring as an over-bank deposit in a submarine fan channel environment. After careful calibration of cores' depth with gamma ray log as observed on the Interactive Petrophysics software, depth shift correction was applied due to the discrepancy observed in depth of core-log measurements. The total depth described for KF-1 well is from 3002.90-3005.93m, with 90% of the cores recovered. The lithologies range from carbonaceous mudstone to thinly bedded fine-medium grained sandstone, subsequently intercalating with mudstone which later graded into predominantly mudstone. Mud drape and dewatering structures are evident on the cores which serve as a pointer to a high rate of sediment deposition and subsequent liquefaction of soft sediments. This commonly occurs in

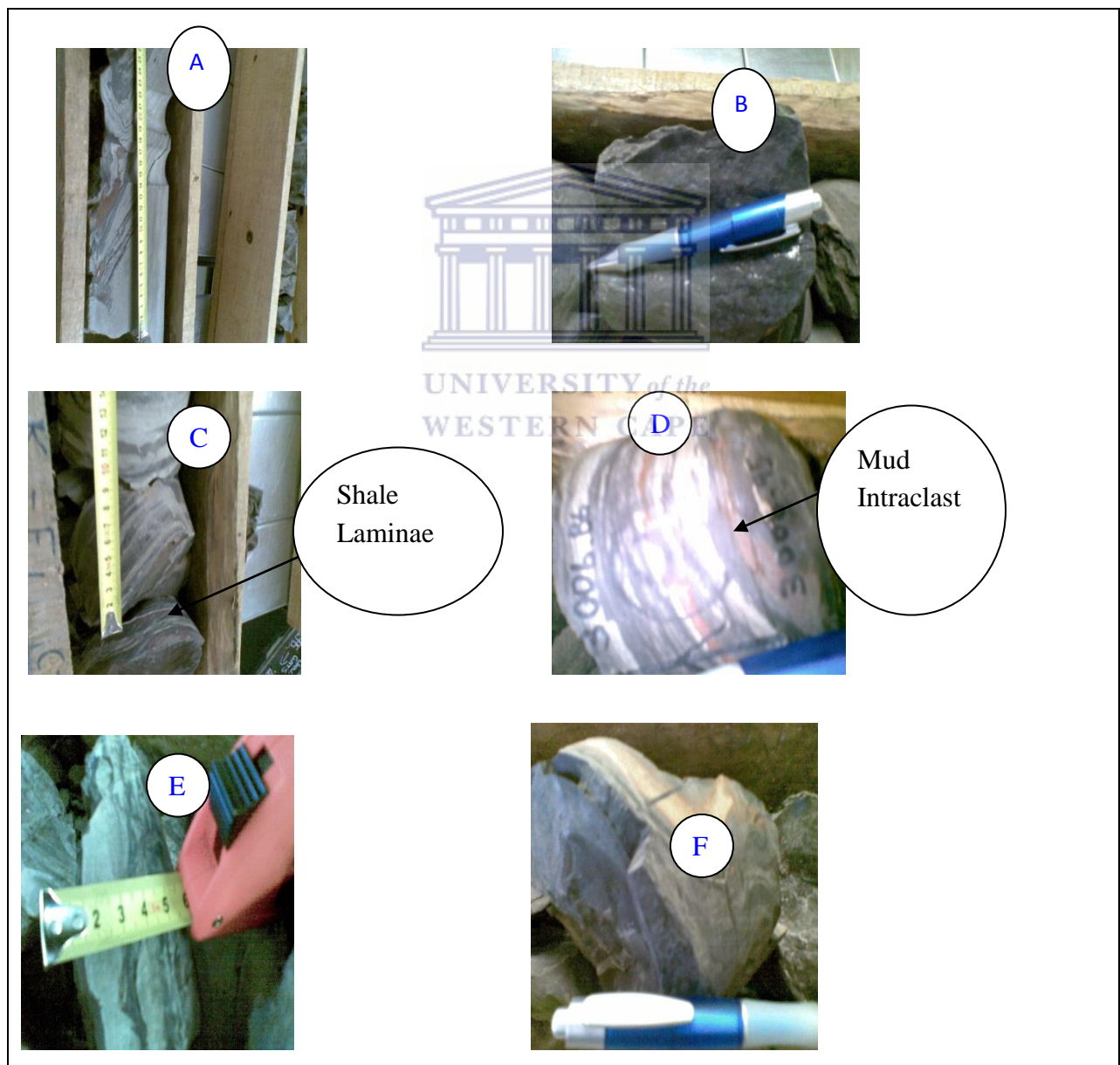
deep water marine environment (Allen, 1984).The reservoir sand interval can be regarded as a thin bed as it is approximately 1.2m.

Table 5.0; Summary of Core description for K-F1 well (Facies Legend below)

DEPTH(M)	DESCRIPTION	SEDIMENTARY STRUCTURE	DEPOSITIONAL ENVIRONMENT
3006-3006.95	Friable carbonaceous laminated mudstone highly ferruginised because of observable reddish brown stains which occur like a band .There is evidence of white shining imprints which suggest shells of invertebrates. Total cores recovered is 0.75m	Mud drape presence  Shale laminae observed at 3006.95m	Low energy sedimentation of fine and coarse material possibly as overbank deposit in a sub-marine fan environment. A1
3006.95-3007.88	Ferruginised carbonaceous mudstone with thin parallel laminae, grading into fine-medium grained, cross laminated sandstones at a depth of 3007.11m. Total core recovered is estimated at 0.78 m.	Dewatering structure and brown clast observed as concretion. 	A1&A2

3007.88-3008.95	Medium grained sandstones intercalating with mudstones and subsequently grading into mudstones which are finely laminated. Total core recovered is 0.78m	Dewatering structure and brown clast inclusion observed.	A2&A1
-----------------	--	--	------------------

Facies Key: Mudstone –A1, Sandstones - A2, Siltstone-A3, Dark Coloured Sandstone -A4, Conglomerate-A5

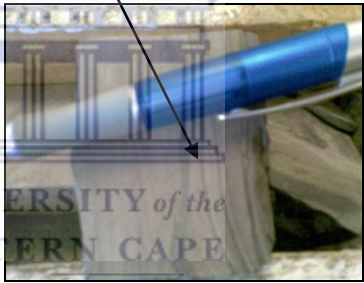



(A) Mud Drape and dewatering structure at depth of 3007.50m (B) Fossilised Mudstone 3008.90m (C) Shale laminae at depth of 3006.95m (D) Mud intraclast at depth of 3006.86m (E) Shale laminae at depth of 3009.5m (F) Water escape structure and Mud intraclast. Figure 5.0: Different core photos at various depth for KF-1 Well.

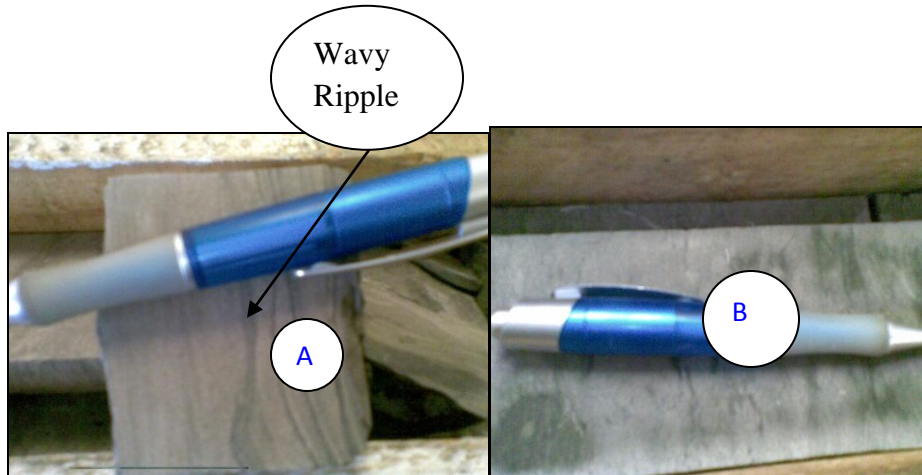
5.1.1.2 Core Description of AU-1 Well

Cores were cut for stratigraphic purposes at depth interval between 2684-2697m. Three lithostratigraphic units observed from the core description include an upper fine-grained sandstone unit grading into a central interbedded sandstone and claystone unit and ending in a lower, predominantly claystone unit. Observations made from core description showed an upper unit of dark-grey, fine to medium grained sandstone grading into siltstone with subsequent intercalations with mudstone at a deeper depth. The sandstone interval within the cores is approximately 6.5m thick, this agrees with the information obtained from the well report. The recovery rate is 100% while core depth agreed with the log depth. The most prominent sedimentary structures observed are current ripple marks and wavy laminations; current ripple marks are associated with the dominance of waves and current superimposition during deposition.

Table 5.1; Summary of Core description for AU-1 well (Facies Legend on Page 62)

DEPTH(m)	DESCRIPTION	SEDIMENTARY STRUCTURE	DEPOSITIONAL ENVIRONMENT
2684-2685.9	Grey coloured, fine-medium grained sandstones. feldspar and muscovite observed under hand lens.	Wavy ripple mark. 	Reworked shallow marine sandstones typical of shelf environment. A2
2685.9-2687.39	Massive, ferruginised sandstone unit grading into Siltstone, colour ranging from dark grey in sandstones to dark in Siltstone. Brown lithic fragment and ferruginised lamina were observed within the siltstone unit	Current ripple marks	A2&A3

2687.39-2688.10	Siltstone intercalation with mudstones, thin parallel laminae observed.	Current ripple marks	A3&A1
2688.10-2689.60	Siltstone grading into friable mudstone with a lot of inclusions brown clasts and lithic fragments. Dark grey sandstone unit observed at 2688.50 -2689.5m		A3&A1
2689.76-2690.92	Intercalation of siltstones and mudstones with evident parallel laminations	Current ripple marks.	A3&A1
2690.92-2693.96	Intercalations of mudstones and siltstones	Wavy ripple laminations.	A3&A1




(A) AU- 1 wavy ripple marks at depth of 2685.39m (B) AU-1 ripple marks at depth of 2689m.

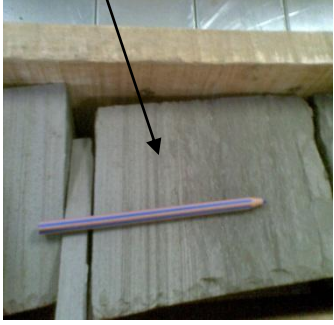
Figure 5.1: Different core photos taken at various depth for A-U1 well.

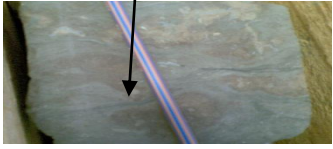
5.1.1.3 Core Description of KH-1 Well

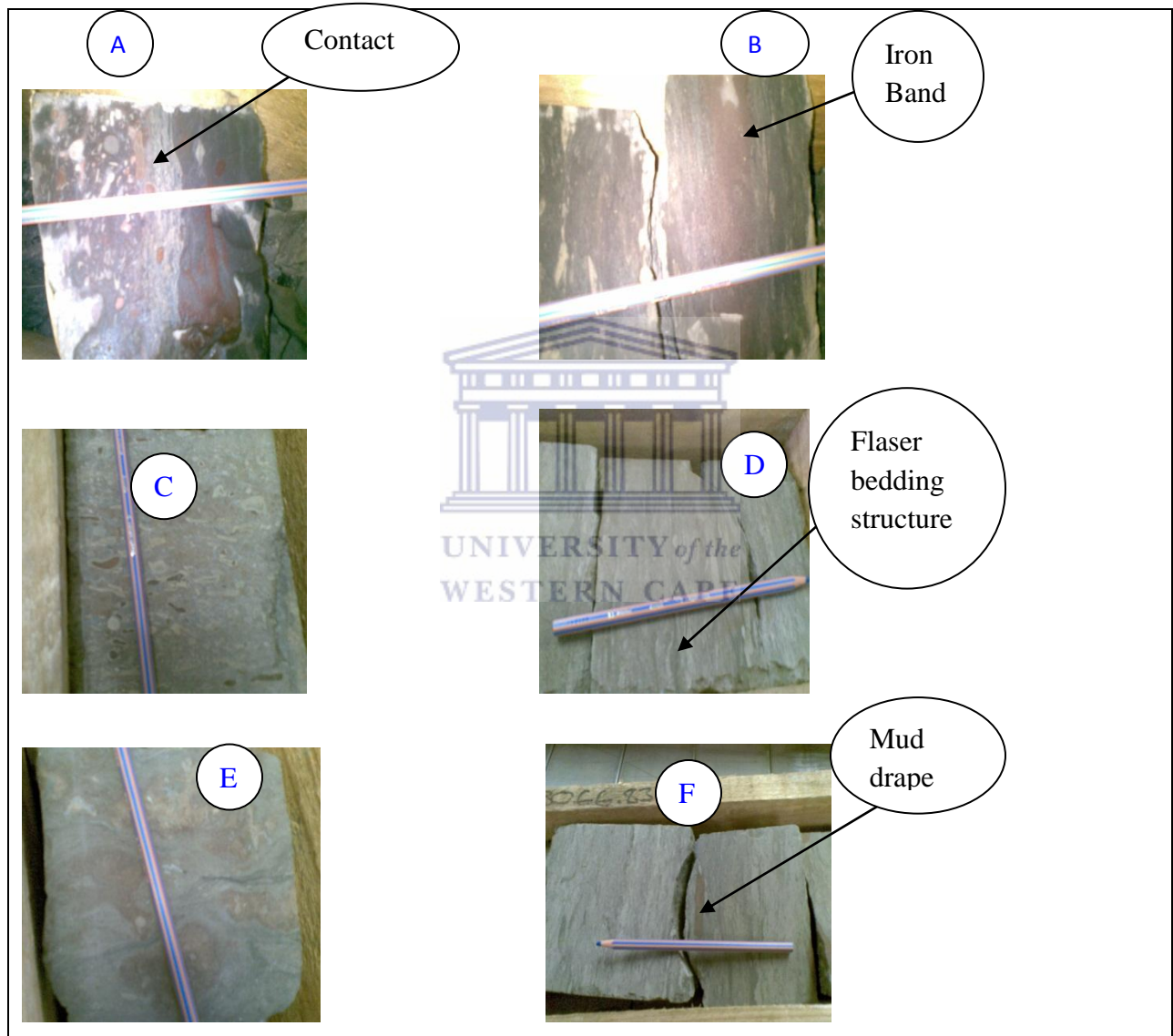
The well was drilled to an estimated depth of 4268m, cores were cut at intervals between 3066-3082m and comprise of an estimated 7m thickness of sandstone unit underlain by a massive claystone unit. Information obtained from the well report suggest the Sandstone unit was deposited as a marine channel sandstone unit. Observations made on the core section show a whole sequence of 7 metres thickness (figure 5.5) comprising of sandstone unit, thinly laminated and highly ferruginised unit which graded into silty sandstone at depth of 3073.5m. There is occurrence of angular to sub-angular lithic fragments at greater depth which may impede porosity and permeability while the presence of mud drape structures signify that the sand body was subjected to extraneous intermittent flows which led to the formation of mud layers infiltrating the sand deposit during quieter or slack flow period (Reineck and Wunderlich,1968).

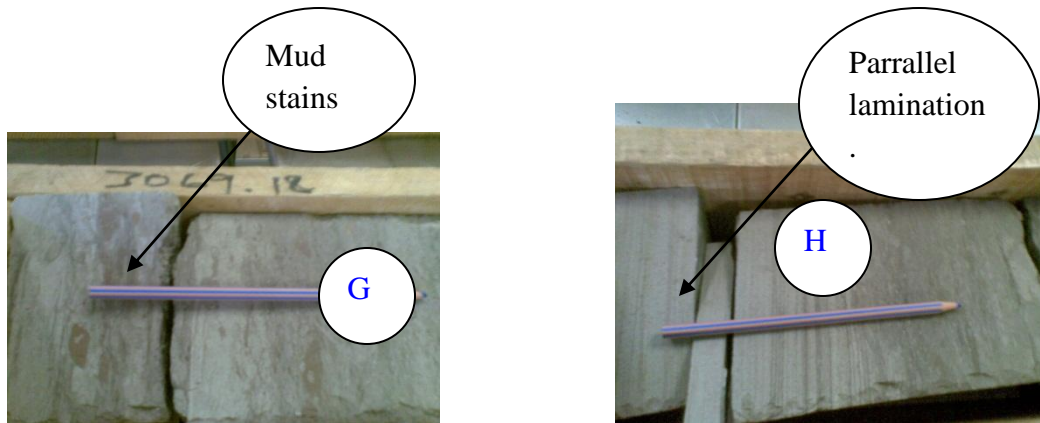
Table 5.2; Summary of Core description for KH-1 well (Facies legend on Page 62)

DEPTH(m)	DESCRIPTION	SEDIMENTARY STRUCTURE	DEPOSITIONAL ENVIROMENT
3066-3066.83	Coarse grained sandstones with lithic fragments presence	Mud drape structure and ripple marks. 	Marine environment, Delta front detached bars.A2
3066.83-3068.22	Grey coloured, medium - coarse grained sandstones, parallel laminated		A2
3068.22-3069.18	Thinly laminated sandstones with mud stains, medium grained and		A2

	dark coloured.		
3069.18-3071.53	Dark stained, medium grained sandstone unit.	Parallel lamination observed. 	A4
3071.53-3072.70	Dark-grey massive sandstone unit with lithic fragments .		A2
3072.70-3073.86	Dark stained , massive sandstone unit grading into siltstone with reddish brown stains occurring like band and follow by subsequent intercalations with siltstone.	Sinuuous Ripple marks	A4&A3
3073.86-3074.85	Silty sandstone changing into conglomeratic sandstones, angular to sub angular lithic fragments with obvious reddish brown band.		A3&A2&A5
3074.85-3075.82	Greywackes/conglomerates abruptly changed into dark coloured, finely laminated but ferruginised mudstones		A5&A1
3078.82-3080.82	Friable, finely laminated mudstone		A1

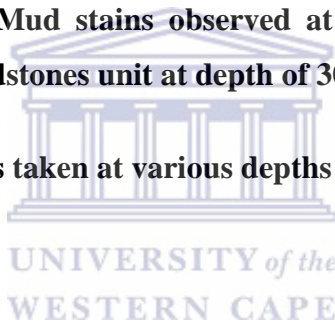
3080.82-3082.08	One metre of cores recovered, mudstones changing into highly ferruginised conglomerate with a lot of pink feldspar.	<p>Wavy lamination</p> 	A1&A5
-----------------	---	---	-------





KH-1 (A) Abrupt change of Conglomeratic Sandstone into Mudstone at depth of 3074.85m (B) Iron band observed on core sample at depth of 3073.2m (C) Lithic rock fragments of pebble sizes embedded within Sandstone unit at depth of 3074.23m.(D)Flaser bedding structure observed at depth of 3071m (E) Conglomeratic Sandstones with rock fragments of angular size and wavy laminations observed at depth of 3081m (F) Mud drape structure observed at depth 3066.5m(G) Mud stains observed at depth of 3069.18m (H) Parallel laminations observed within sandstones unit at depth of 3070m.

Figure 5.2: Different core Photos taken at various depths for K-H1 well.



5.1.2 Geological Interpretation of Wireline Logs

Different suites of logs measure different properties of rocks in the subsurface. Wireline logs have improved formation evaluation studies over the years and have proven to be a good source of information as regards the understanding of subsurface geology. It enables the interpretation of physical properties of rocks or formations geologically, hence wireline logs interpretation would make lesser meaning if not done in relation with geology. The suites of logs used in this work are gamma ray, sonic, resistivity (short and deep) and neutron- density. The accurate interpretation and integration of these logs is crucial to the estimation of formation of petrophysical properties. Depositional environment and lithofacies analysis can also be inferred from the geological interpretation of wireline logs. Gamma ray logs have been consistently used over the years to determine grain size and to know the contributions of various radioactive minerals like Th, K and U isotope series. Both Th and K are associated with clay minerals (Hassan et al., 1976). Estimation of fluid saturation in a reservoir zone can be achieved by the

combination of short and deep resistivity measurements while the combination of neutron and density tools gives porosity value. Using some mathematical model specifically generating a linear regression formula on interactive petrophysics software, can also give permeability values. The conventional core analysis measurement of some of the petrophysical properties correlates in almost a near perfect manner to the values derived from the estimation of these properties from wireline logs for the three wells.

5.1.2.1 Geological Interpretation of Wireline Logs for K-F1 Well.

The interpretation of well KF-1 was preceded by depth match of core with the wireline logs. Core- log depth shift was applied because of discrepancies observed in measurements to a value of 3.1m. The core was cut between a depth of 3002.90-3005.93m (figure 5.3). The first track on the log suite shows the depth intervals in metres, the second track indicates the presence of a porous interval within the reservoir section. Gamma ray log is used for delineation of reservoir and a non-reservoir section, the unit is API (American Petroleum Institute). The resistivity logs combination is for the calculation of fluid saturation while the water saturation output curve is plotted next to resistivity log track (figure 5.3). Phie (effective porosity) comparison track is an output of the sonic log-derived porosity compared to core-derived porosity while the permeability curve and lithology curve with shale base line occupies track 7 and 8 respectively (figure 5.3).

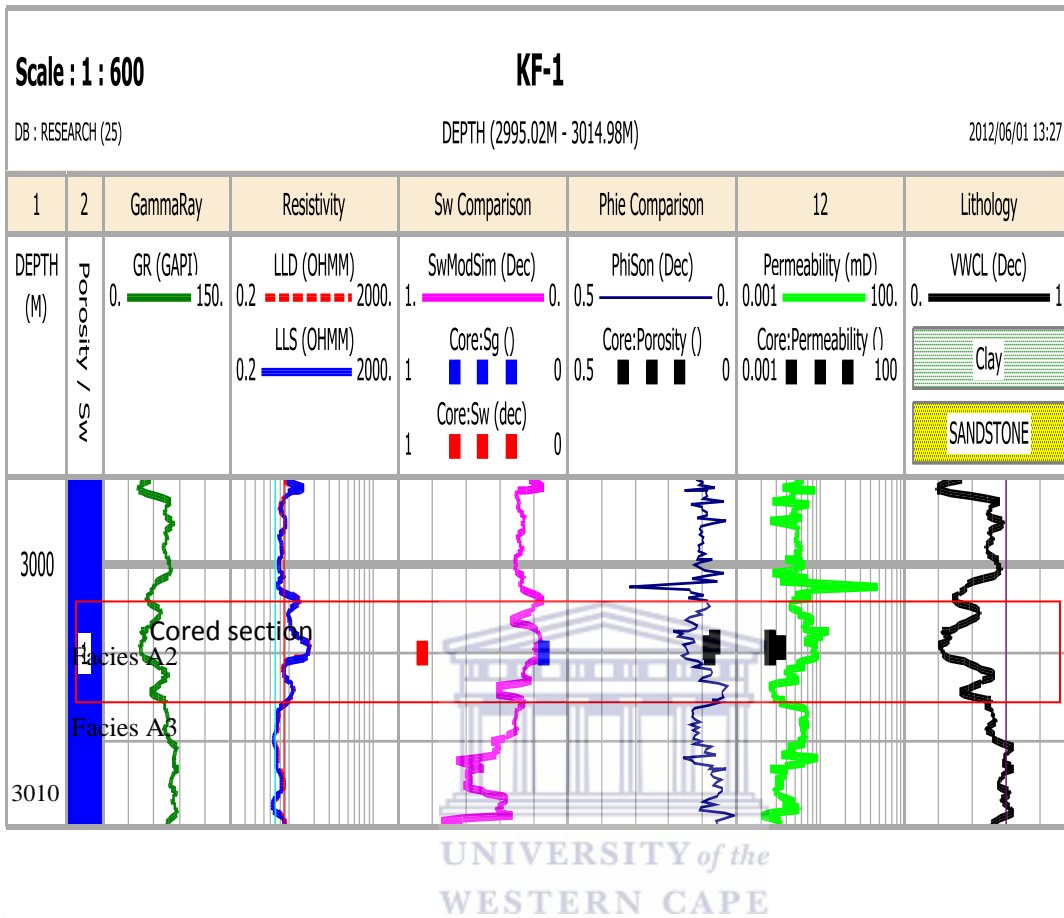


Figure 5.3: Suite of Logs interpreted for KF-1 well

In the reservoir section, the lowest GR value is 45 API for clean sands while for shaly sand the value is around 90 API (figure 5.3). The slightly irregular signature of the gamma ray log suggests minor variations in the grain sizes of the sandstone interval coupled with an alternating transgressive and regressive sequence that accompanies the deposition of the sand and mud rock. This is evident as the log suggest a transition from an initial coarsening upward sequence to a fining upward sequence at around the depth of around 3000m. It is an indication of initial rapid deposition followed by gradual deposition abandonment; the log profile exhibited by KF-1 well is a typical log profile of a marine channel deposits (Rider, 2000). This observation can be justified by the evidence of water escape structures reported in the core description (figure 5.0). Within the cored section (indicated by red line on gamma ray track, figure 5.3), there was evidence of alternating marine transgression and regression sequences that cause erosion and

subsequent deposition of mud rock in the upper contact (Rider, 2000). The short and deep resistivity logs overlap each other and represent relatively low resistivity values at various depths except for the sudden increase observed at depth of 3003.95 m to 3005m. Sudden increase in resistivity value is an indication of the likely presence of hydrocarbon at that depth and this also corresponds to the depth at which clean sand is observed on the gamma ray log. The plot of saturation values of conventional core analysis data on the modified Simandoux (1963) shaly-sand model for water and gas saturation calculation plot confirms that the saturation curve agrees with the average core gas saturation of 14% and water saturation of 86% (figure 5.3). The Simandoux (op.cit) shaly-sand saturation model was used to generate the saturation curve. Careful study of fluid saturation curves shows that the fluid saturation values derived from cores agree with those observed from the logs. The anomalous high water saturation values observed at the basal shale interval might be attributed to the dominant clay mineral making up the shale interval, perhaps because of high surface area of the clays which may also be attributed to the bound water. Because of the unavailability of a neutron log, the sonic log was used for the porosity estimation of the KF-1 well. The porosity value derived from the sonic log (13.6%) is higher than the core-derived porosity (10%) while corresponding values in permeability were observed. Considering the discrepancy of values in sonic log-derived porosity and core-derived porosity, it should be noted that core porosity is often a representation of the ground truth while the usage of only the sonic log to calculate porosity may be inaccurate. The depth of the highest value of the porosity and permeability plots corresponds to the depth (3004.5m) with lowest GR value and the lowest percentage of VCL (20%).

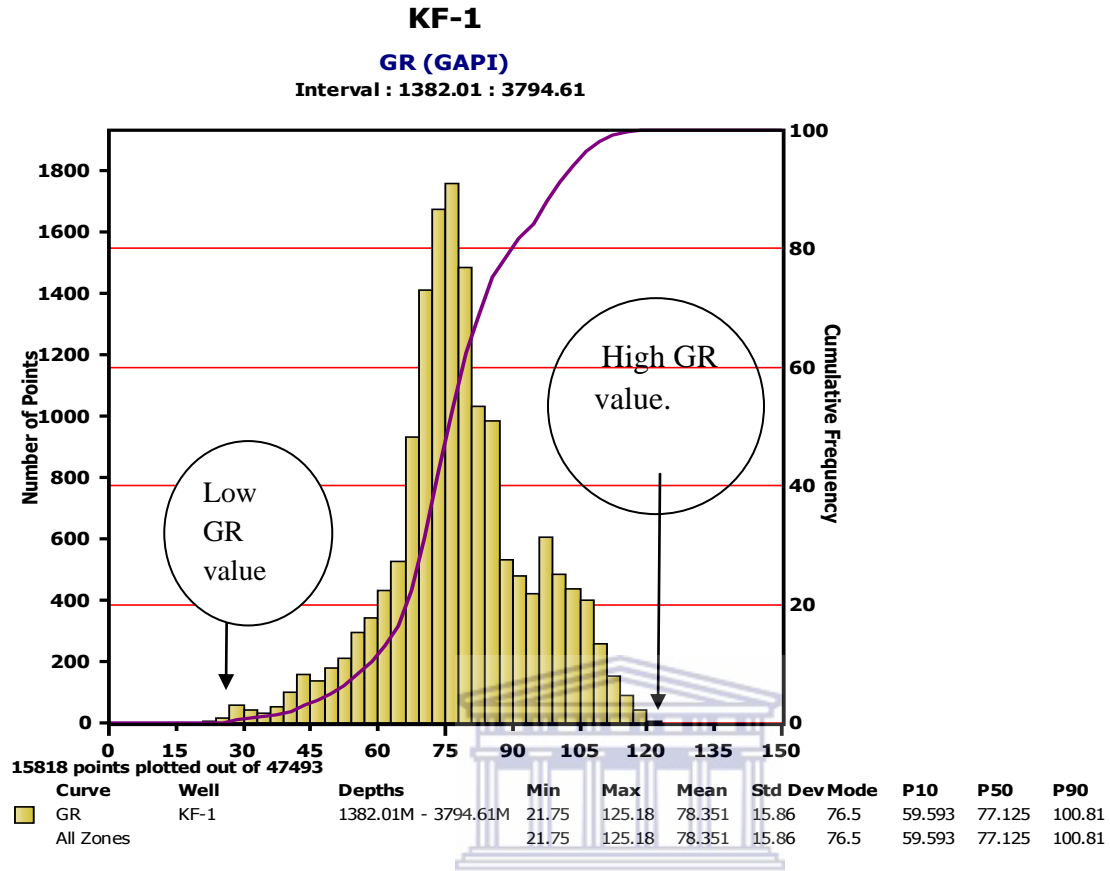


Figure 5.4 :Gamma ray log Histogram for KF-1 well showing values range of clean sands to shale generated from Interactive Petrophysics software.

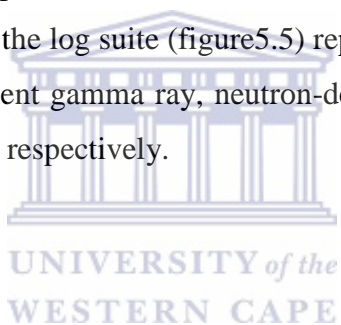
Table 5.3:Petrophysical properties calculated values for KF-1 well from Logs.

KF-1			
Depth (m)	Average porosity (decimal)	Average Permeability (milli darcy)	Average water saturation (decimal)
3006.25	0.098	0.01	0.1

3007.07	0.12	0.02	0.09
3007.6	0.125	0.01	0.1
3008.13	0.093	0.01	0.11

5.1.2.2 Geological Interpretation of Wire line Log K-H1 Well.

Matching of core depth and log depth was done to ascertain any discrepancy in depth, no depth correction was applied. Track 1 on the log suite (figure 5.5) represent the depth profile of the logs while tracks 2,3,4,5,6 and 7 represent gamma ray, neutron-density curve, resistivity logs, water saturation curve and porosity curve respectively.



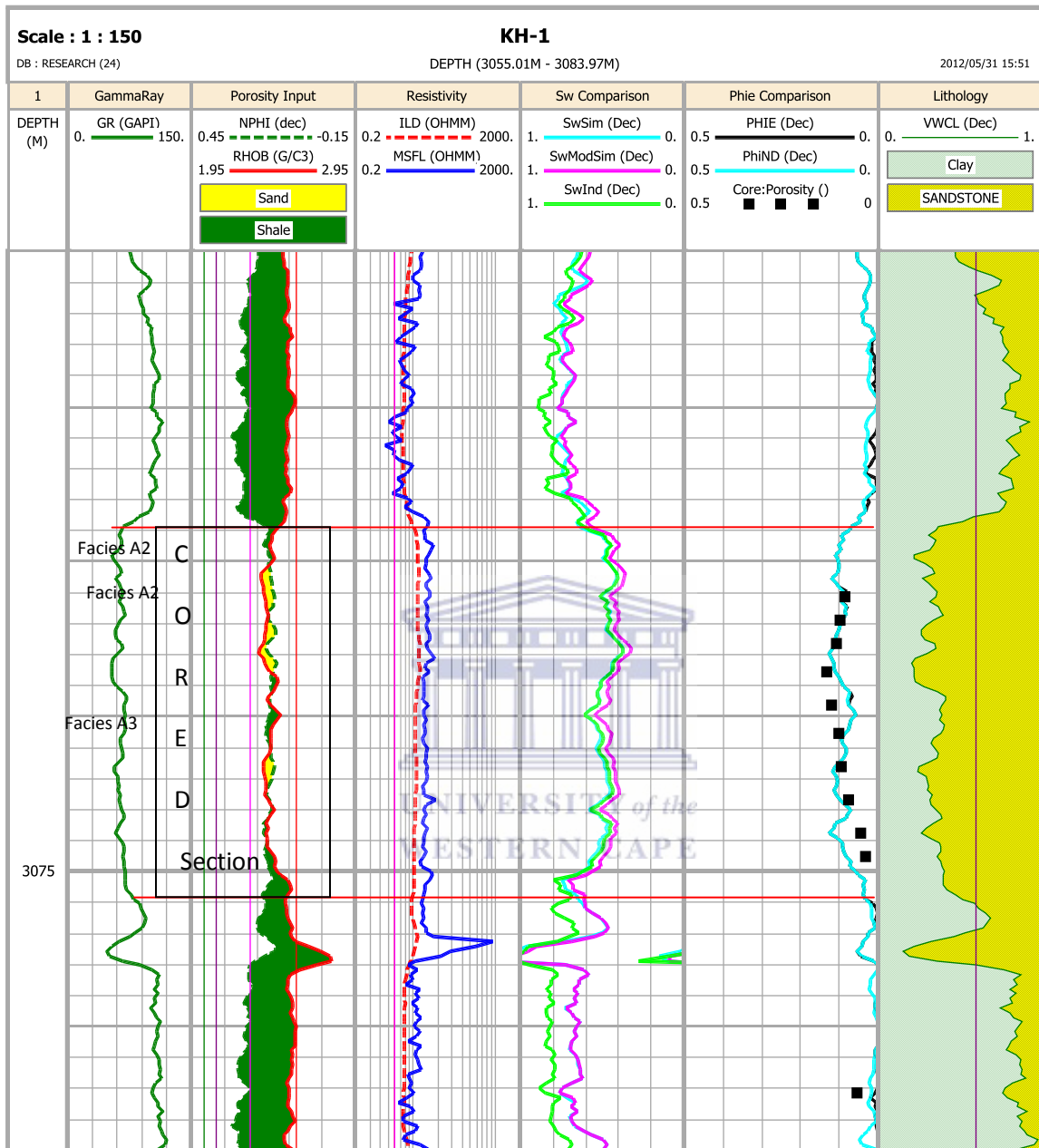


Figure 5.5: Suite of Logs interpreted for Well KH-1 generated from Interactive Petrophysics software.

The sand body is fairly thick (3066-3073m) (see figure5.5, indicated by red horizontal line), the deposition of the sand bodies might be due to vertical accretion which caused sand bars to overlay an initial lower bar facies of shale and siltstones. The log signature is typical for marine sand bars (Delta front detached bars), according to Rider (2000). There was a sharp upper

contact between the sand body and the shale interval while the basal contact shows a gradual change into shale. The lowest GR value is 55 API within the reservoir intervals. Unlike Well KF-1 in which the sonic log was used in calculating porosity, the availability of neutron and density logs enables the calculation of porosity values. The estimation of porosity values was done using the combination of neutron and density log and the subsequent plot showed the overlapping of the conventional core porosity data with the neutron density porosity plot curve. Note that the Neutron-density porosity plot shows more correlation with the conventional core porosity values than the sonic log curve output for the KF-1 well. It appears therefore that estimation of porosity done via neutron and density logs yields more accurate results than those obtained using the sonic log plot. The average porosity within the reservoir section is calculated as 9.9%. Due to unavailability of conventional core fluid saturation data, comparison between core saturation and log saturation models cannot be made. Expectedly, there is an increase in the deep and shallow resistivity values from the upper shaly interval to the reservoir interval; being a more porous interval, a higher resistivity value is expected if the reservoir is not water saturated. The Simandoux (1963) shaly-sand water saturation model indicates an average water saturation of about 50%. From the neutron –density plot, the variance in core porosity plots and log porosity is insignificant (figure 5.5 above). Hence the porosity value from conventional core analysis and log analysis could be used interchangeably. The average volume of clay (VCL) within the reservoir section is less than 30%. It is therefore expected that porosity value fares better than the calculated value. It is assumed that the precipitation of different authigenic cements might have compromised the quality of the reservoir.

Table 5.4: Petrophysical properties calculated values for KH-1 well from Logs.

KH-1			
Depth (m)	Average Porosity (decimal)	Average Permeability (milli -darcy)	Average water saturation (decimal).
3067	0.1	0.04	0.42
3068.09	0.1	0.04	0.4
3068.92	0.12	0.04	0.38
3069.90	0.098	0.04	0.48
3070.89	0.085	0.04	0.58
3072	0.098	0.13	0.5
3074.42	0.1	0.13	0.42
3082.25	0.09	0.15	0.56

5.1.2.3 Geological Interpretation of Wire line Logs for AU-1 Well.

The different curves output of wireline logs for well AU-1 from depth 2679.93-2693.96m is shown in (figure 5.6). Prior to wireline logs loading in the software and subsequent calculation of the petrophysical properties, depth matching of core depth with log was done and no discrepancy was observed. The gamma ray log signature of AU-1 well is similar to that for the KH-1 well, the deposition of the sand bodies might be due to vertical accretion which caused sand bars to overlain an initial lower bar facies of shale and siltstones. The log signature is typical for marine bars (Delta front detached bars), (Rider, 2000). There is a sharp basal contact between the sand body and the shale interval while the upward contact shows a gradual change into shale. The sand body is estimated at about 6.5 metres thick (indicated by thin purple horizontal line in figure 5.6), facies A2 is predominant fine to medium grained sandstone and A3 is siltstone. The average gamma ray value for the reservoir interval is 60 API which is an acceptable value for potential reservoir zone which is not predominant clean sand. The resistivity value is fairly low and there is a run of continuous overlap between deep and shallow resistivity (figure 5.6) .This suggests that the pore spaces of the reservoir are saturated with water. The output curve of the density log was used in estimating the porosity values and appeared to be consistent with porosity and permeability values derived from conventional core analysis data. The average porosity estimated within the reservoir interval is 10% and an average permeability is 0.015Md. The shaly-sand-water saturation model indicates an average water saturation value to be less than 65% within the reservoir zone. The water saturation in the upper shale contact is found to be higher than for the basal shale contact, this can be attributed to the type of dominant clay mineral at different depths within the section. A similar explanation can also be given to variations in water saturation values within the reservoir interval. A clay mineral with higher surface area and Q_v attracts more bound water than clay minerals with lower surface area and low Q_v . Once again, the reliability of petrophysical values estimated from logs is confirmed as the plots of the conventional core data agreed very well with the output curve from the density porosity log, this is evident in figure 5.6. The average volume of clay is estimated to be 32% within the reservoir section.

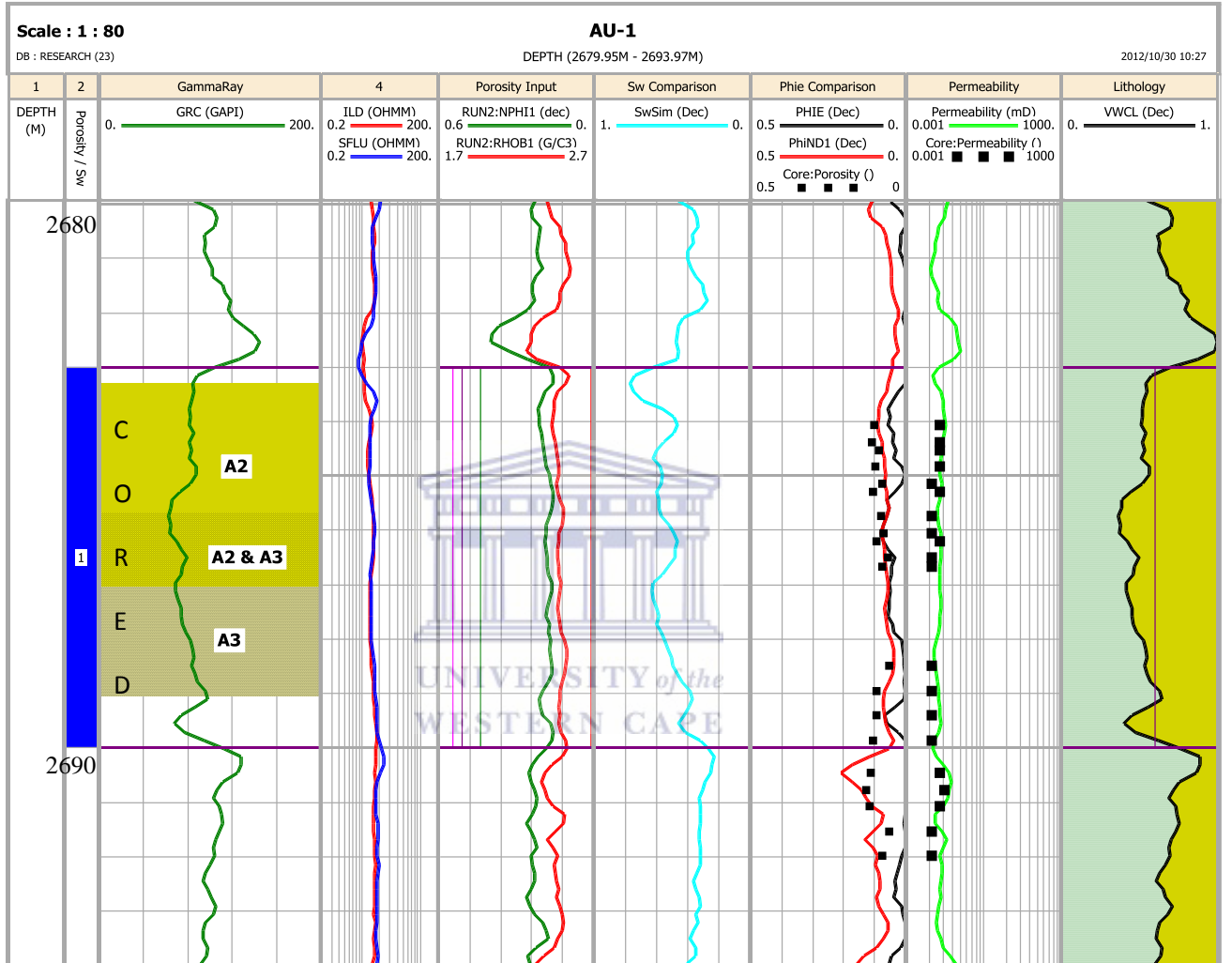
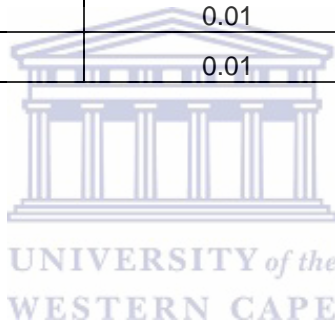


Figure 5.6: Suite of Logs interpreted for AU-1 well generated from Interactive Petrophysics software.

Table 5.5: Petrophysical properties estimation values for AU-1 well.

AU-1

Depth m	Average Porosity (decimal)	Average Permeability (milli darcy)	Average water Saturation(decimal)
2684.05	0.12	0.02	0.5
2684.67	0.11	0.02	0.6
2685.39	0.11	0.02	0.65
2685.84	0.09	0.02	0.68
2686.51	0.1	0.01	0.51
2687.8	0.1	0.02	0.68
2688.38	0.11	0.01	0.45
2690.33	0.09	0.01	0.38



5.1.3 Summary of Core Description and Wire line logs Interpretation

Detrital compositions of rocks always condition a pathway for subsequent diagenesis and may have effect on the values of some petrophysical properties. Calculation of some petrophysical properties values were done through detailed processing and interpretation of wire line logs and later compared with some limited data obtained from conventional core analysis data. The reliability of wire line logs in calculating porosity, permeability and saturation is evident (figure 5.3, 5.5 and 5.6) because of the continuous overlap of core data and the wireline logs output curve.

5.1.3.1 Core Description

The rocks encountered within the K-F1 well were deposited under a low energy environment conditions with alternating fine and coarse grained sedimentation occurring probably as an over bank deposit. Mud drape- and dewatering-structures are prominent on the core , this is a feature of rocks deposited in deep marine environment (Allen, 1984). Lithology ranges from carbonaceous mudstone at 3006m to fine –medium grained sandstones at 3007m and mudstone at 3008.95m.

A-U1 lithology ranges from depth 2684m-2693m and consists of upper fine grained sandstone grading into central interbedded sandstone unit which later grades into mudstone. Current and wavy ripple marks were observed on the rocks which is a characteristic feature of a shallow marine sandstone unit of the shelf environment. The presence of current ripple marks on the cores serves as a confirmation that the sandstone unit may have been deposited under shallow marine conditions. A very massive, parallel laminated but ferruginised sandstone unit was encountered in K-H1 well at a depth of 3066m and this is underlain by a massive clay stone unit. Sedimentary structures observed include dewatering structures and mud drapes. The occurrence of mud layers on the sandstone is evidence that the sand body was subjected to extraneous intermittent flows which allows mud layers to infiltrate the sand body.

5.1.3.2 Wireline Logs

Interactive Petrophysics[®] software (IP) was used to process the well logs datasets and subsequently to calculate some petrophysical properties. Limited conventional core analysis data were loaded on an I.P workstation to output the data points and compare the results with calculated values from the well logs.

In K-F1 well (3006-3008.95m), a 3.1m depth correction was applied because of discrepancy observed in logs and core depth. The Simandoux (op.cit) water saturation model was adopted, water saturation of 86% was obtained from the well report, an average porosity of 10% and permeability in the region of 0.15md. The sonic log derived porosity is calculated to be 13.6% at a depth of 3004.72m, which is more than the core derived porosity of 10% at the same depth. This variance in value suggests that use of the sonic log only is not accurate in calculating porosity values, therefore other porosity logs should be combined and interpreted to obtain more reliable values.

Neutron-Density logs were used to calculate porosity values in the K-H1 well in contrast to the sonic log in the K-F1 well. The average porosity within the K-H1 well reservoir section is 9.9%, the continuous overlap of core data points and log's curve on the neutron –density track (figure 5.5) shows that neutron-density porosity estimation is as accurate as core ; the water saturation is about 50% while the permeability value is significantly low. In the A-U1 well (2684-2693m), the density log was used to calculate porosity values and an average of 10% was estimated, also an average water saturation of 65% was calculated from the logs while an average permeability value of 0.015md was obtained.

It should be noted that the sampled depth of conventional core analysis data is not the same as the sampled depth of cores that were used for this work. This implies that direct comparison of log derived petrophysical properties values with conventional core data values of some specific depth could not be made, average values were calculated however within the reservoir intervals.

The output of the curves for logs and core data values have very close resemblance, as can be observed from figures 5.3, 5.5 and 5.6.

Chapter Six: 6.1. Petrography and Geochemistry

Different petrographic studies were carried out on various rock samples obtained from wells KF-1, A-U1 and K-H1. Unraveling the dominant rock forming minerals in rock samples, understanding the crystal habits and distribution patterns of various allogenic and authigenic minerals are the main essence of undertaking petrographic studies. Textural maturity of sediments can be understood from thin section analysis, while XRD analysis complements observations made on thin section by giving direct information on the type of clay minerals present in rock samples. Scanning Electron Microscopy gives information about the crystal habits displayed by various authigenic cements, and the relative timing of precipitation of clay minerals can also be inferred from careful observations of SEM photomicrographs. Various geochemical analysis carried out are targeted at confirming observations made from petrographic studies and to understand the chemistry of the depositional environment in which the reservoirs were deposited. Pore water chemistry analysis gives information on the electrical conductivity and pH of pore waters, CEC analysis provides information on the dominant clay minerals, exchangeable cations and shaliness indicator while EDS (Energy Dispersive Spectrometry) provides information on the elemental composition of the core samples.

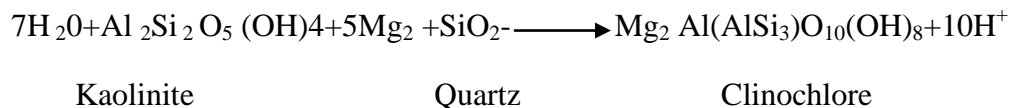
6.1.1 Scanning Electron Microscope Interpretations

The photomicrographs obtained from Scanning electron microscopy of different samples were interpreted with a SEM petrology atlas (Welton, 1984). Various clay minerals observed include montmorillonite, illite, kaolinite, chlorite and some accessories cements like quartz and pyrite.

6.1.1.1 Scanning Electron Microscope Interpretation for AU-1 Well

Results obtained from the analysis shows the occurrence of K-feldspar and pseudo –hexagonal kaolinite postdating quartz cement at depth 2684.05m (figure 6A), quartz cement have completely filled the pore spaces. The formation of kaolinite is apparently due to acidic leaching of K-feldspar or possibly muscovite, the precipitation of authigenic kaolinite and quartz cement

is often common to co-exist in marine environment conditions (Hurst and Irwin,1981) while quartz authigenesis has also been reported to take place in sea water (Mackenzie and Gees,1971).The origin of quartz cement in AU-1 well was probably sourced from silica precipitation due to the dissolution of feldspar by pressure dissolution or sourced from the silica presumably derived internally from the intergranular dissolution of quartz grains in the sandstone (Bloch et al., 2002; Walderhaug, 1994; Walderhaug and Bjorkum, 2003).The occurrence of montmorillonite at depth of 2685.39m (figure 6C) suggest AU-1 has been exposed to meteoric flushing from depositional waters which is slightly alkaline and favours the formation of montmorillonite at the availability of sodium and or calcium ions. The kaolinite also occurs as an euhedral shape as it has been observed globally to occur in marine environment (Kupez et al., 1997), the occurrence of montmorillonite implies that the gibbsite layer of kaolinite is being gradually replaced by a similar brucite layer (Mg (OH) ₄) at depth of 2684.67m (figure 6 B).Thus, mixed layer of kaolinite and montmorillonite is likely at this depth. The fixation of K⁺ must have favoured the easier transformation of kaolinite to montmorillonite, transformation of kaolinite to montmorillonite appears to have completed at 2685.39m (figure 6.C). Chlorite cements also occurs as rims around the pores while pervasive occurrence of quartz cements occurs as pore filling at depth 2686.51m (figure 6D). The quartz crystals shows high deformation which might be due to high pressure and temperature, cleavages of quartz are more pronounced at depth of 2688.3m (figure 6F),the cleavage observed in the quartz might be due to over pressure zone because the presence of montmorillonite has been linked with overpressure zones (Hurst and Irwin,1982). Chloritization of kaolinite and smectite started taking place at depth of 2685.84m (figure 6.0), kaolinite can convert directly to chlorite, specifically magnesium rich chlorite (clinochlore) by reacting with quartz (reaction below). Evidence of chlorite formation was more pronounced at depth of 2686.51m. Chloritization always happens as a smectite-chlorite mixed layer and higher pH values with strong Fe presence (Tian et al., 2008).



Authigenic smectites and kaolinite are all likely to be transformed to chlorite (Grigsby, 2001, Berger et al., 2009) .

6.1.1.2 EDS Interpretation for AU-1 Well.

The results of EDS are presented graphically along side the SEM photos below. This is to enable better comparison of observations made on SEM and EDS and to further probe the progressive alterations or transformation of different clay minerals through the substitution of one ion with the other. The graphical plot of energy (Kev) on y axis and intensity exhibited by different elements on X-axis shows different elements observed from the EDS plot include O, Al, Ca, Na, S, Fe, C, Si, Co, Mg, Ti. The abundance of Si which shows high intensity confirms the siliciclastic nature of Orange basin reservoirs. Fe shows the highest intensity at depth of 2685.39m (figure 6.0 C), this is a further confirmation of the observation made from core description which indicates the core sample from this depth is ferruginised and might also be associated with the presence of iron rich chlorite (chamosite). The occurrence of Mg at depth of 2685.39m (figure 6C) might account for the occurrence of chlorite or montmorillonite. The presence of some elements like Ti and V is a pointer to the presence of illite in AU-1 well.

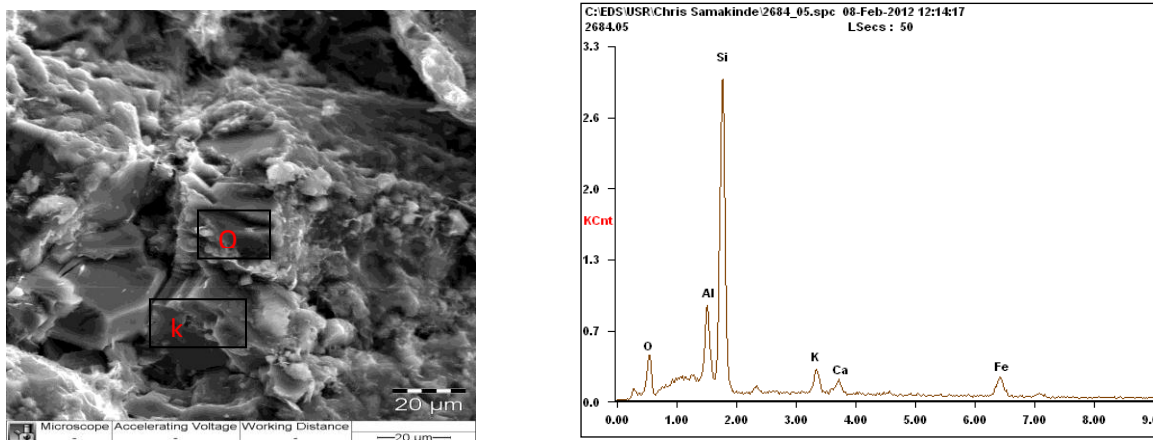


Figure 6A. (2684.05m) ; SEM and EDS from core sample showing quartz and kaolinite.

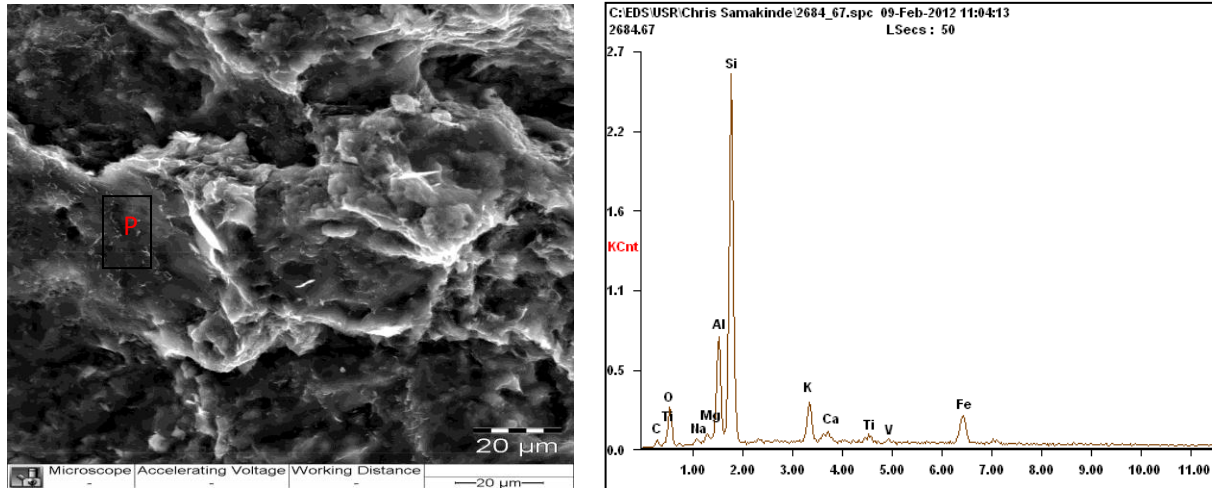


Figure 6B (2684.67m) : SEM and EDS from core sample showing pyrite.

Q-Quartz, P-Pyrite, M-Montmorillonite, C-Chlorite, K-Kaolinite, Po-Pore spaces

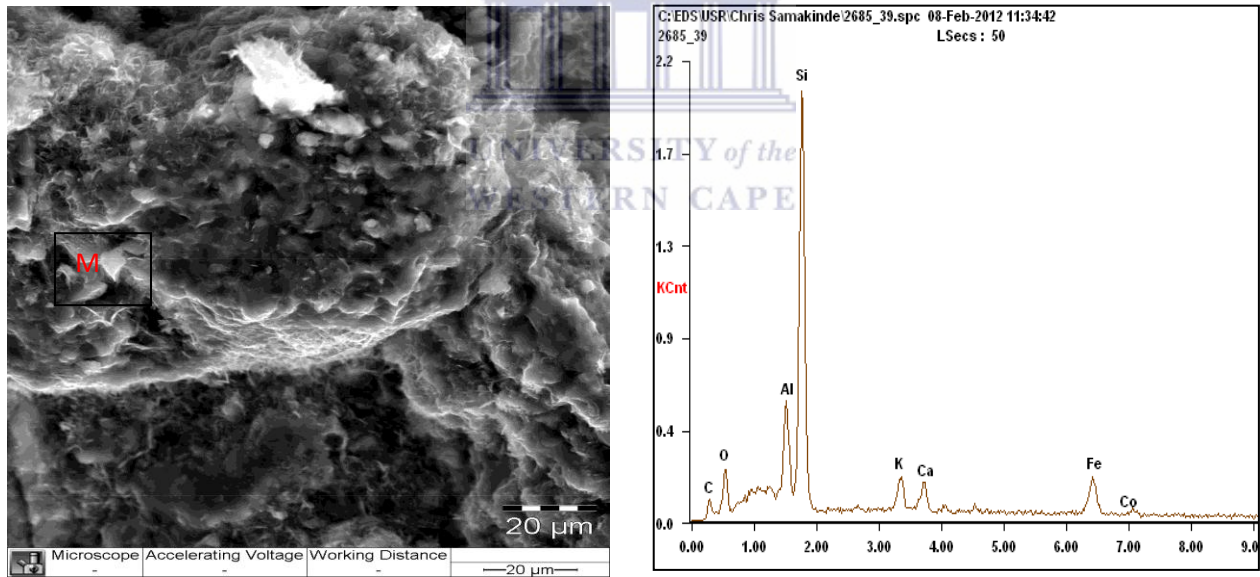


Figure 6C (2685.39m) SEM and EDS from core sample showing montmorillonite.

Q-Quartz, P-Pyrite, M-Montmorillonite, C-Chlorite, K-Kaolinite, Po-Pore spaces

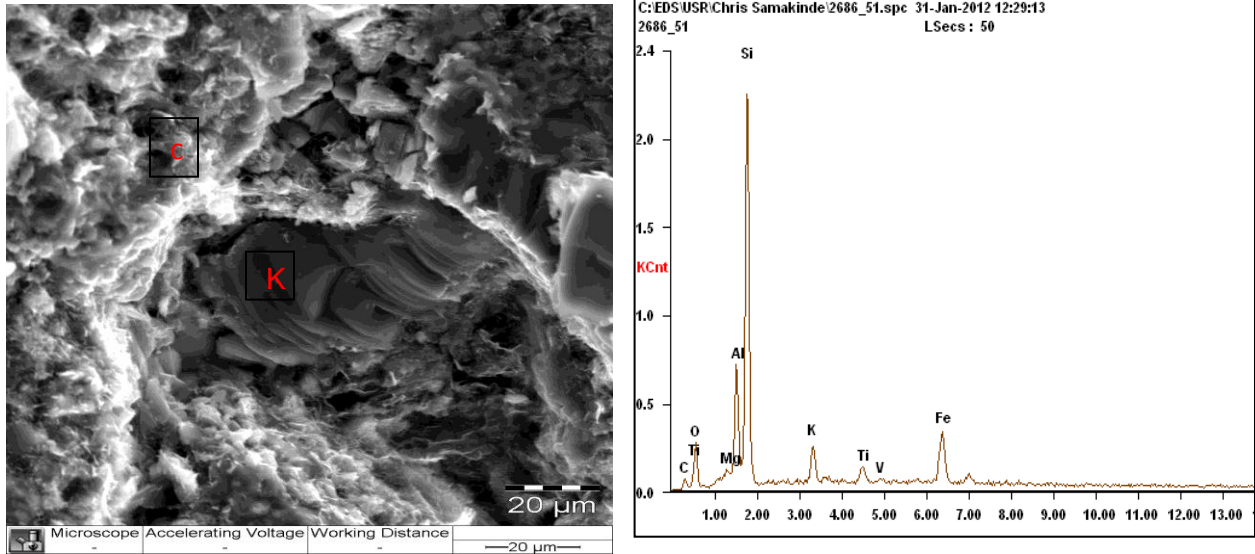


Figure 6D (2686.51m) SEM and EDS from core sample showing kaolinite and chlorite

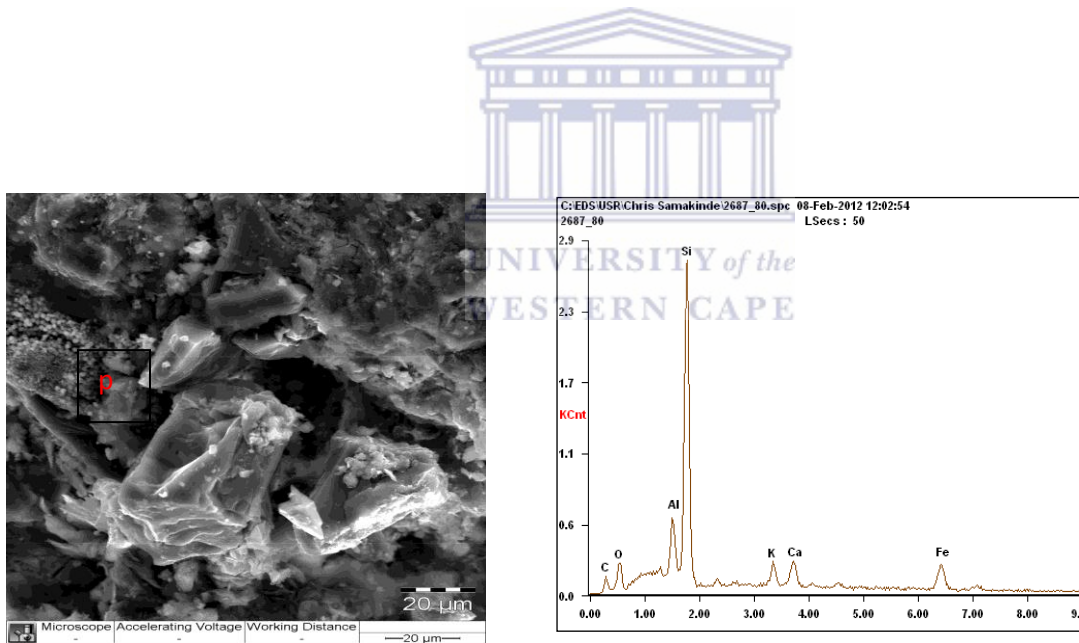


Figure 6E (2687.80m) SEM and EDS from core sample showing pyrite.

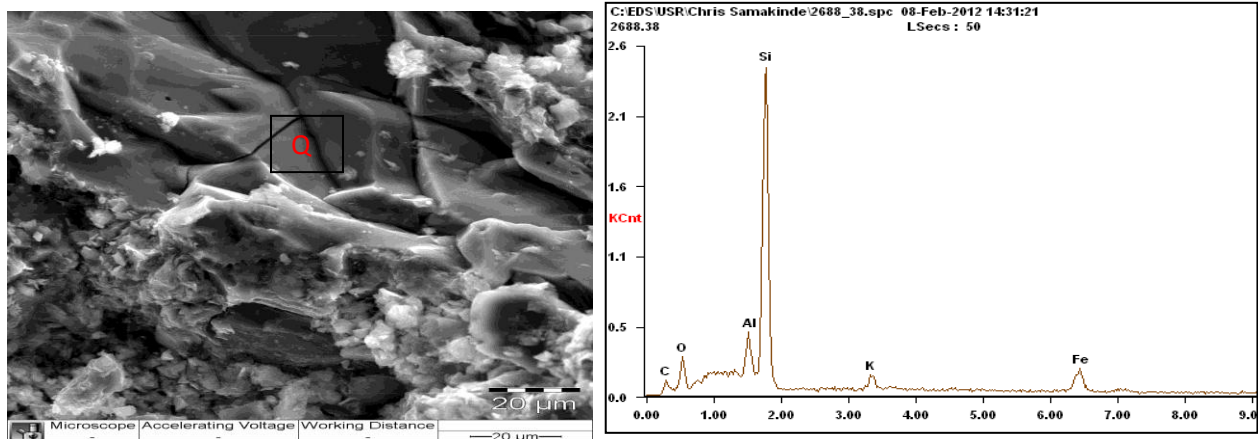


Figure 6F (2688.38): SEM and EDS from sandstone sample showing quartz .

Q-Quartz, P-Pyrite, M-Montmorillonite, C-Chlorite, K-Kaolinite

Figure 6.0 (A-F): Photomicrographs of SEM and EDS of AU-1 well.

6.1.1.3 Scanning Electron Microscopy Interpretation for KF-1 well.

The results obtained from the five samples analysed by means of scanning electron microscopy for well KF-1 show evidence of the abundance of montmorillonite and chlorite coats which occur as rims around the spaces where grains have been plucked out or dissolved at a depth of 3006.25m (figure 6.1A). As mentioned above, the formation of authigenic chlorite is favoured by an alkaline depositional environment or an environment of meteoric waters in the presence of ferromagnesium rich rocks (Berger et al., 2009). From the SEM photos it can be observed that chlorite formation at this depth is authigenic and not detrital. Authigenic chlorite appears more crystallized than detrital chlorite on scanning electron microscope images. Authigenic chlorites occur at every depth in the KF-1 well and are likely to have been formed from a pre-existing clay mineral specifically montmorillonite. At 3007.07m depth (figure 6.1B), chlorites occur as a 'rosette shaped algal bloom' detaching itself from montmorillonite. They have also been observed perpendicular to the grain surfaces, which suggest it is being transformed from the montmorillonite. There are still quartz cements and overgrowth at a depth of 3007.07m present (6.1B). These minerals displayed habits in which major pore spaces were either filled or lined with them. At depth 3007.6m (figure 6.1C) below are differently shaped macropores that have been filled with clay cements.

6.1.1.4 EDS Interpretation for KF-1.

The various intensity peaks observed from EDS graphical plots of energy (KeV) versus intensity show high peaks for Si and Al, there are occurrences of vanadium and nickel which can be a pointer to the presence of the nickel-rich chlorite nimmite. The occurrence of Ti is a suggestion that the sandstone at depths of 3007.60 m and 3008.13 m respectively (Appendix 1) might have been sourced from granitic silicate rocks (Choo et al., 2002) while the presence of ca, c and o could indicates calcite presence. The presence of S at a depth of 3006.25m (figure 6.1A) indicates that the sample composition might have been sourced from volcanic basaltic deposits (Rickwood, 1981). Alternatively it can be explained by a significant occurrence of pyrite. There is iron present in all samples; this is also consistent with the observations made from AU-1 well.

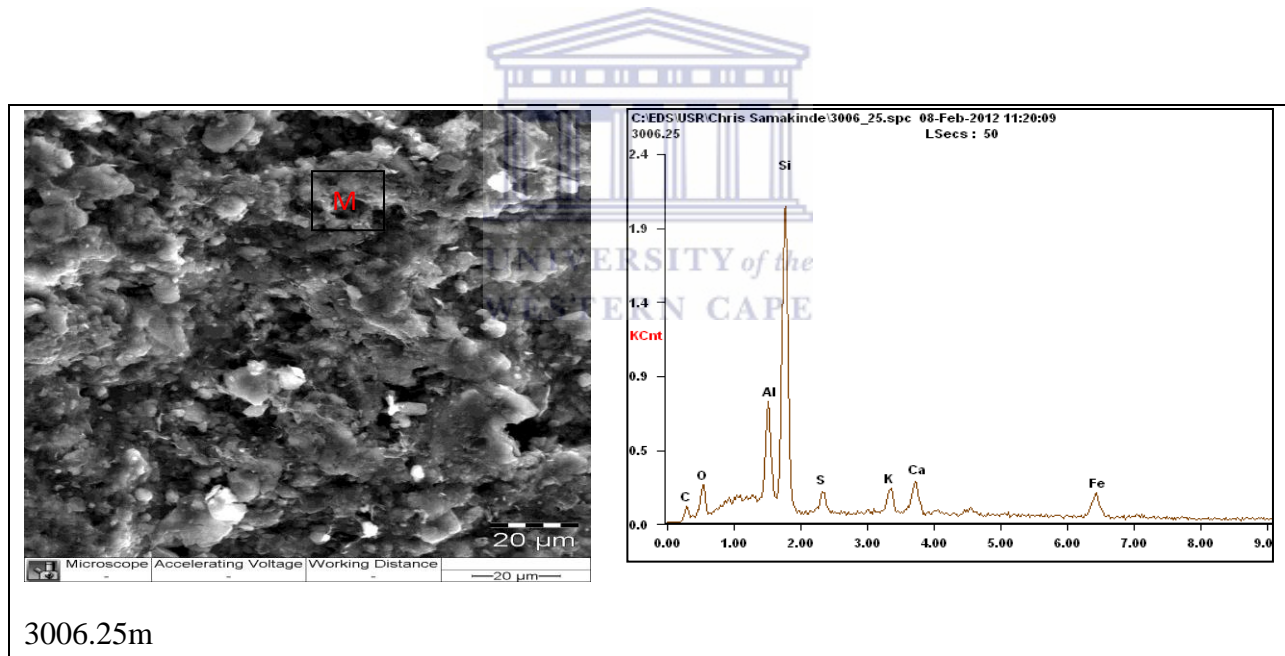


Figure (6.1 A) SEM and EDS from core sample showing montmorillonite.

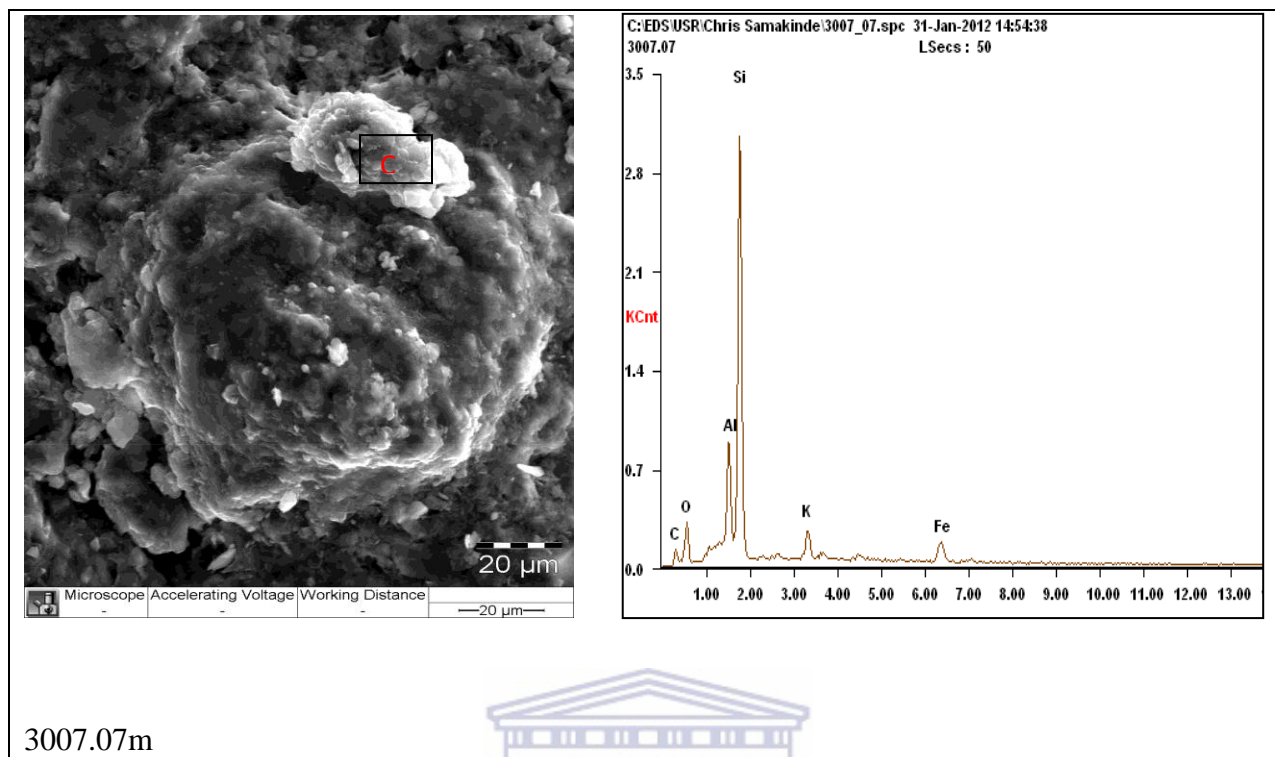


Figure 6.1B SEM and EDS from core sample showing chlorite.

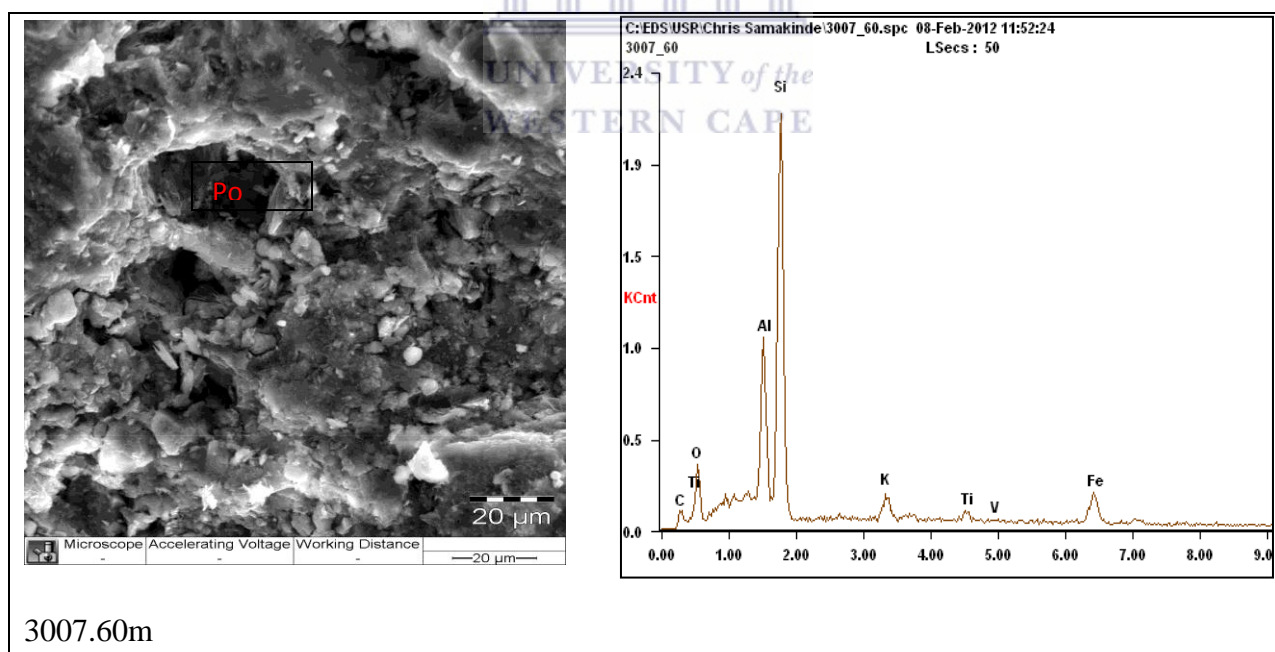


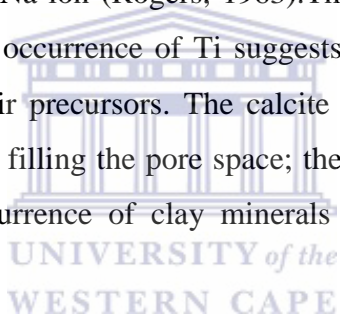
Figure 6.1C

Figure 6.1(A-C): Photomicrographs of SEM and EDS for KF-1 well.

Q-Quartz, P-Pyrite, M-Montmorillonite, C-Chlorite, K-Kaolinite Po-Pore spaces .

6.1.1.6 EDS Interpretation of KH-1 well

The graphical plots obtained from Energy dispersive spectrometry of KH-1 show the occurrence of Al, Si, S, Fe, Na, Mg, Co C with Si showing the highest intensity in all samples analysed within the KH-1 well. The occurrence of S at depths of 3066m and 3067 m (figure 6.2 A and B) respectively indicates the influence of rock materials of volcanic alkaline basalt origin. The occurrence of Na at these depths furthermore suggests a sodium-rich montmorillonite, this may account for the apparent swelling of montmorillonite as observed at these depths. Sodium montmorillonite swells more than calcium rich montmorillonite because the Ca ion is more readily adsorbed compared to the Na ion (Rogers, 1963). The disappearance of S at a depth of 3069.90 m (figure 6.2 C) and the occurrence of Ti suggests that the rocks at this depth might have granitic silicate rocks as their precursors. The calcite at a depth of 3066m (figure 6.2A below) shows an elongated crystal filling the pore space; the presence of the elements found in these samples confirmed the occurrence of clay minerals earlier mentioned from the SEM interpretation above.



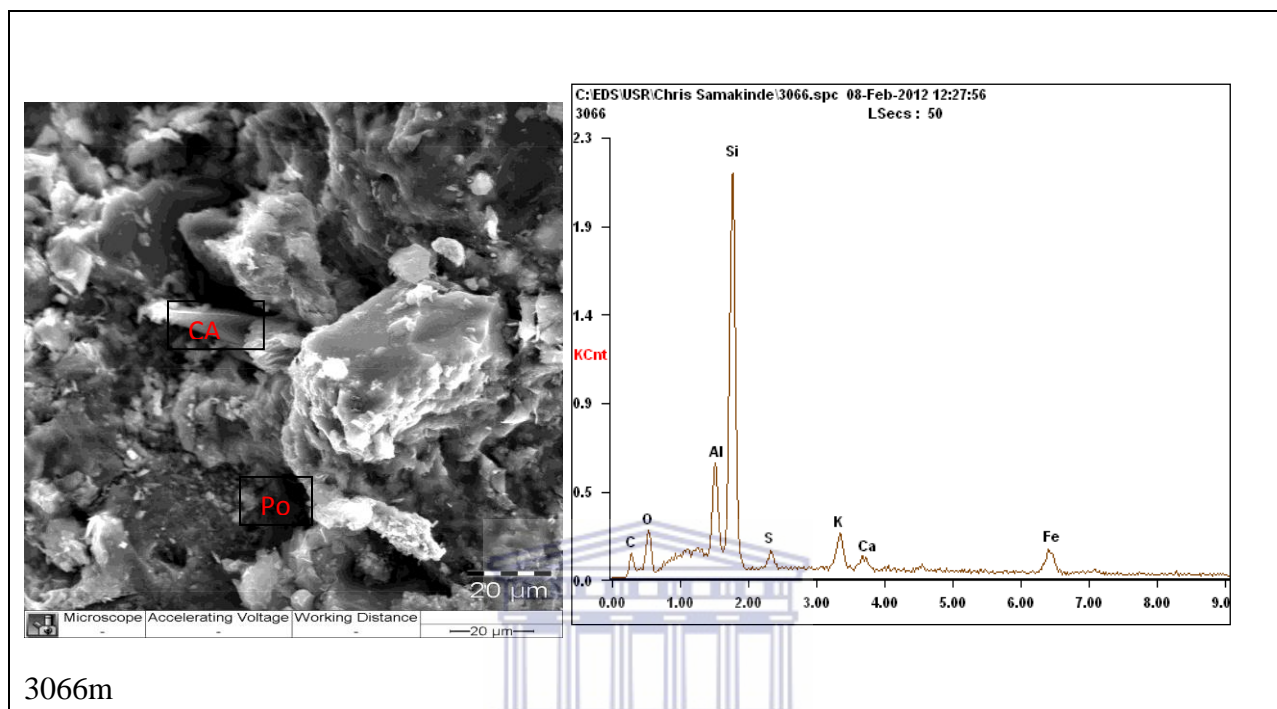


Figure 6.2A: SEM and EDS from core sample showing calcite.

Q-Quartz, P-Pyrite, M-Montmorillonite, C-Chlorite, K-Kaolinite Po-Pore spaces CA-Calcite

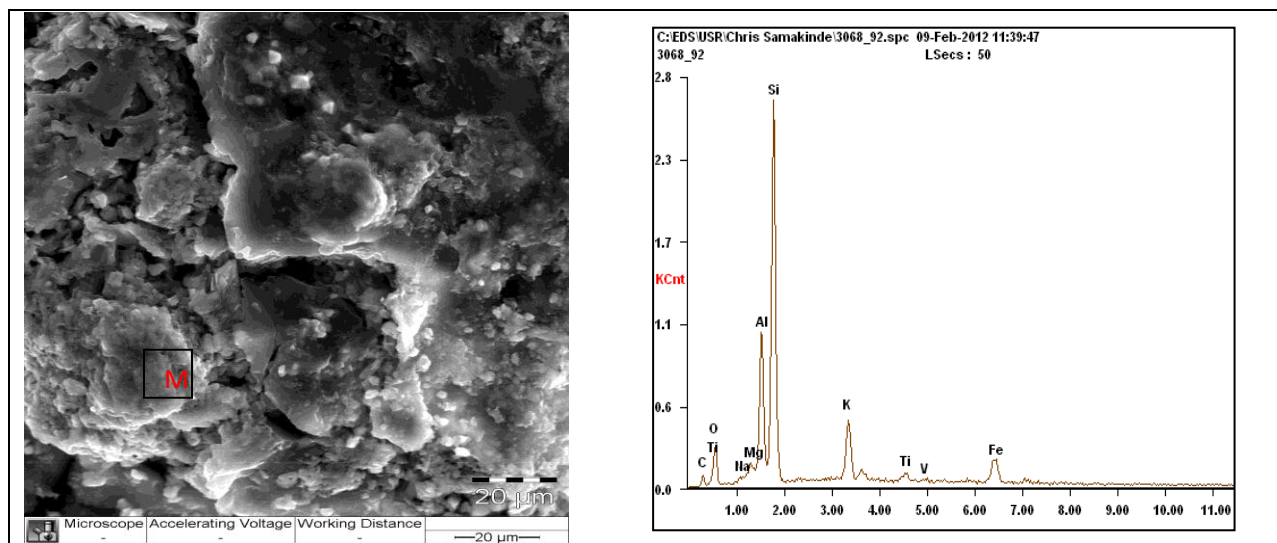


Figure 6.2B (3067m): SEM and EDS from core sample showing Montmorillonite.

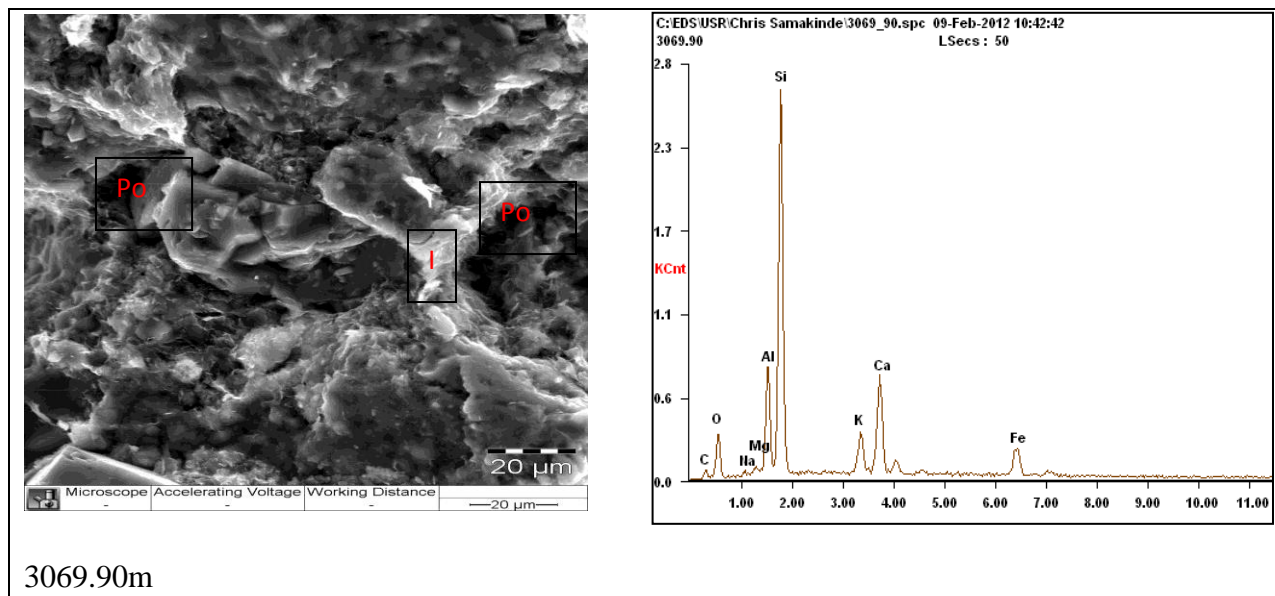


Figure 6.2C: SEM and EDS from core sample showing illite.

Q-Quartz, P-Pyrite, M-Montmorillonite, C-Chlorite, K-Kaolinite, I-Illite, Po-Pore spaces

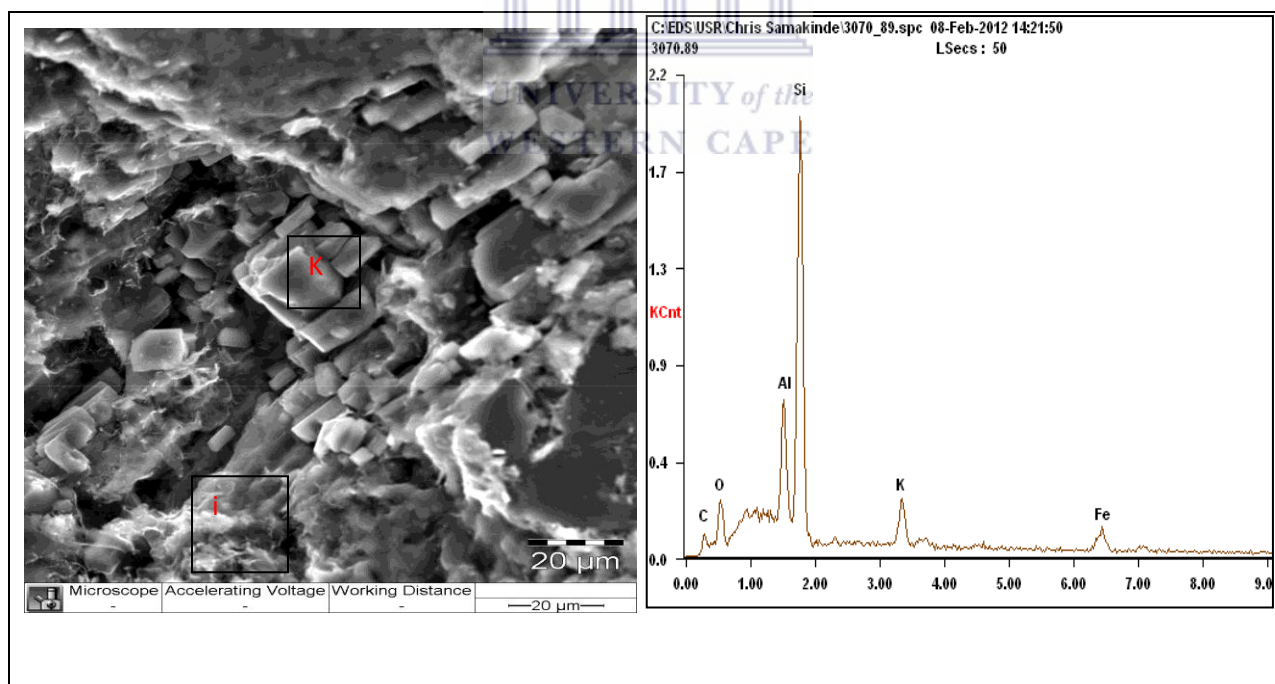


Figure 6.2D

Q-Quartz, P-Pyrite, M-Montmorillonite, C-Chlorite, K-Kaolinite, I-Illite, Po-Pore spaces

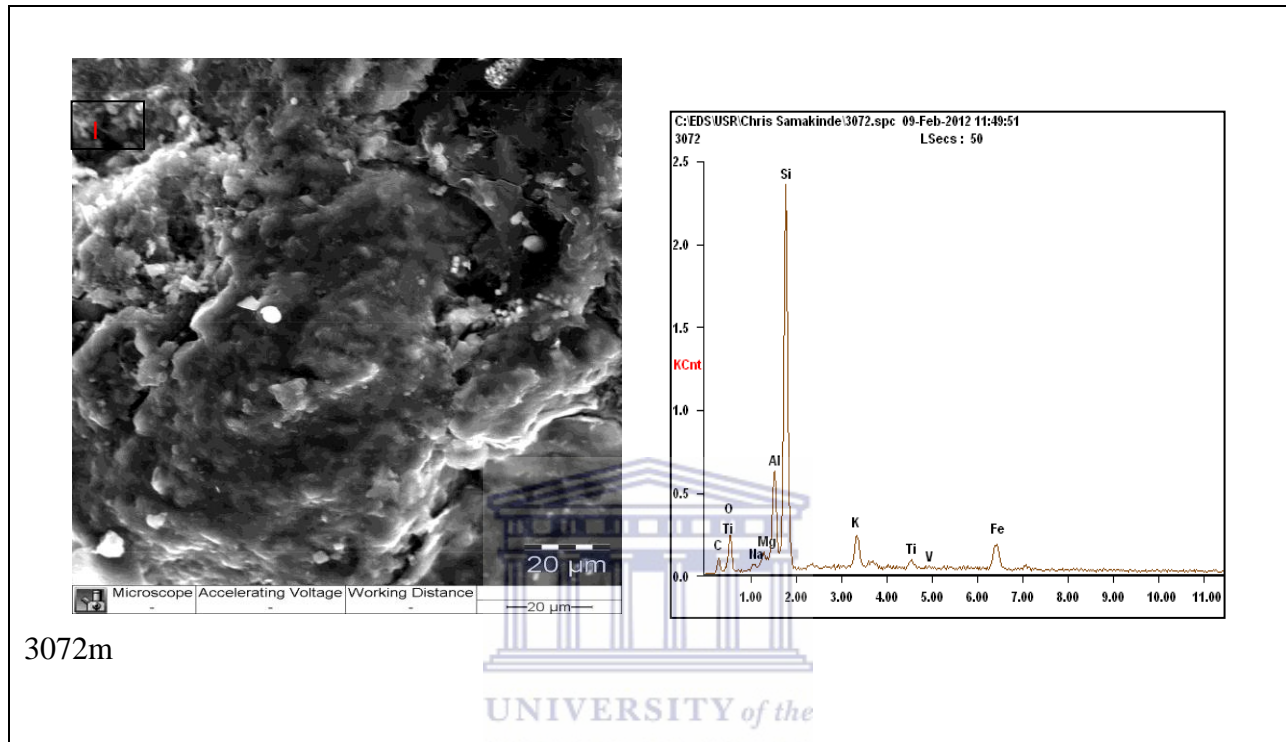


Figure 6.2E

Q-Quartz, P-Pyrite, M-Montmorillonite, C-Chlorite, K-Kaolinite Po-Pore

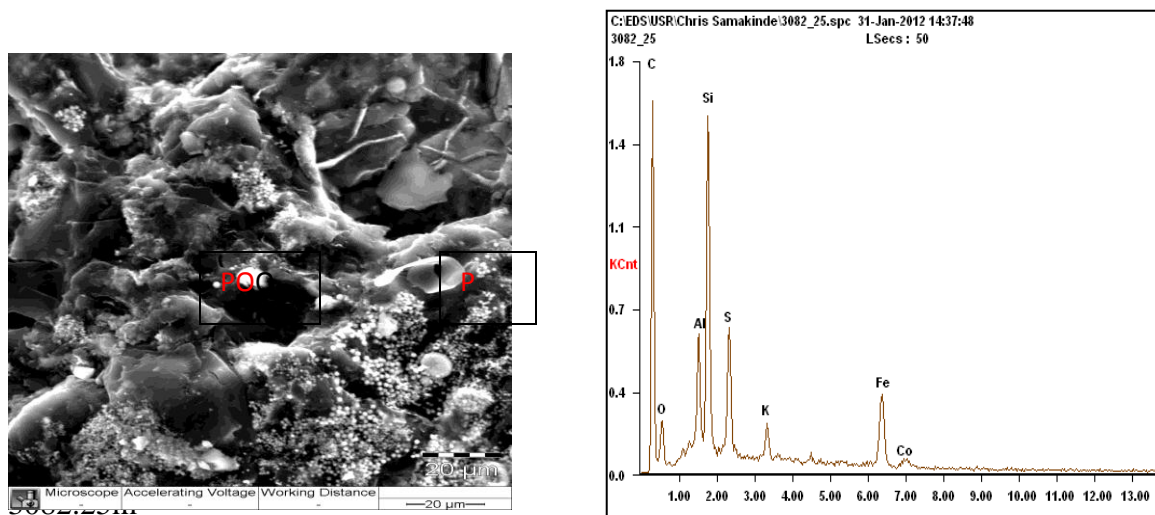


Figure 6.2F: SEM and EDS from core sample showing pyrite.

Figure 6.2(A-F): Photo Micrographs of SEM and EDS for KH-1 well.

Q-Quartz, P-Pyrite, M-Montmorillonite, C-Chlorite-Kaolinite Po-Pore spaces, I-Illite

6.1.1.7 Summary of SEM and EDS analysis

The leaching of K-feldspar or muscovite can account for the consistent presence of kaolinite in AU-1 well. Kaolinite is mostly found to co-exist with quartz cements in a marine environment. The fact that the sand bodies in A-U1 well were deposited under marine conditions confirms the hypothesis as regards the source of kaolinite. There is likely presence of halite or sodium-rich montmorillonite judging from the consistent presence of Na, furthermore the presence of iron rich chlorite is suggested because of the consistent presence of iron from EDS analyses. The source of chlorite does vary but it is considered to have been formed from a precursor mineral in the presence of iron and dominant alkaline pore waters. In the K-F1 well, EDS reveals the presence of Ni in KF-1 well. Nickel is an element often associated with chlorite; nimmite is a form of chlorite that is rich in nickel, consequently the chlorite observed in this well may be nickel-rich. Montmorillonite and calcite are also present in this well. The consistent presence of Ti in the KH-1 well as revealed from EDS could be attributed to illite cement presence. Ti presence in reservoirs could in turn be attributed to the type of parent rock from which the reservoirs were sourced: granitic silicate rich rocks. Montmorillonite as observed from SEM in K-H1 well may be sodium rich because of the apparent swelling observed. Illite was also observed, mostly as a mixed clay mineral with montmorillonite. Sodium-rich montmorillonite swells more than calcium-rich clay minerals do (Rogers 1963), also, quartz cement and kaolinite are present in the reservoirs. Both quartz and kaolinite presence diminishes reservoir quality of siliciclastic sandstones.

6.1.2 XRD Interpretation.

XRD technique was pioneered for usage in studying crystal habits and structures of substances in 1912. It is based on the principle of interference between monochromatic X-rays and a crystalline sample. The technique is widely used in the phase identification of minerals, their compositional information and their nano-scale structures. The core samples taken from three wells KF-1, KH-1 and AU-1 were subjected to XRD analysis at Ithemba labs for qualitative identification of authigenic cements that are present within the lower Cretaceous sandstone of the Orange basin. This is crucial for the understanding of clay minerals diagenesis because clay minerals are difficult to be identified by other means (Ward et al., 2005).

6.1.2.1 XRD Interpretation for AU-1 well.

Pervasive quartz cementation has been identified as a major reservoir problem in the Orange basin. The results obtained from the XRD analysis of AU-1 do not suggest otherwise. The absence of chlorite cements in AU-1 well was however a surprise, previous work on the Orange basin (Opuwari, 2010, Akinlua and Smith 2009 and Adekola, 2010) highlighted the widespread occurrence of iron rich chlorite in the lower Cretaceous Sandstones, of the Offshore Orange basin. Calcite cementation might have been enhanced by highly alkaline pore fluids in the presence of Ca^+ and HCO_3^- . Calcium carbonate detected by XRD might have been sourced from the dissolution of detrital carbonate rock fragments or skeletal marine debris (Dutton, 2008). The occurrence of pyrite suggests that sand bodies in AU-1 well were deposited in an anoxic environment (figure 6.3 A-H). Montmorillonite has the highest compositional percentage among all clay minerals with 2.61%, this is consistent with interpretation made from SEM observations. Muscovite exists in significant quantities too; as illite and muscovite have similar peak angstrom during XRD analysis, the presence of illite could have easily been juxtaposed for muscovite presence. Muscovite can be considered as thermodynamically stable proxy for Illite (Lander et al., 2009). Leaching of feldspar in a slightly acidic condition could be justified because of the presence of kaolinite. The likely presence of HCO_3^- as mentioned above might have supplied hydrogen ions into the pore fluids that favour the formation of kaolinite. Albite (sodic feldspar)

cements presence in reservoir sands is a common phenomenon according to Bjorkum,(1996). Albite can be sourced from the albitization process which includes K-feldspar or plagioclase (Ramseyer et al.,1993).The proportion of calcite cement decreases gradually from a depth of 2684.67m to zero content at a depth of 2686.51m. There was re- precipitation of calcite at a depth of 2687.80m; this contrast might be attributed to the dissolution of detrital carbonate rock at 2684 .67 m in a weak acidic fluid (as seen from pore water ph) and followed by flushing of and transport by meteoric water into other parts of the reservoir section.

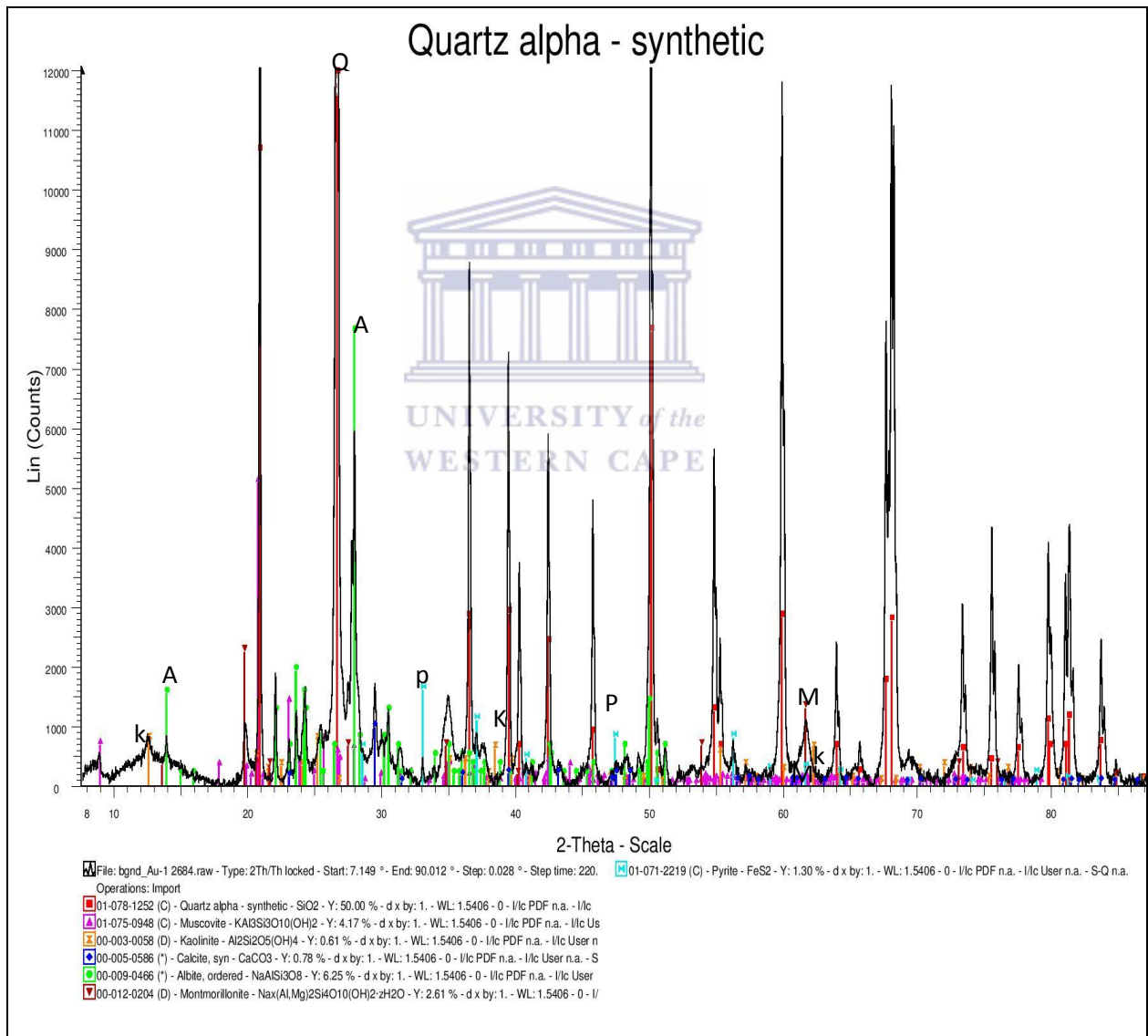


Figure 6.3A (2684.05m) AU-1. **Q-Quartz, P-Pyrite, A-Albite, K-Kaolinite, M-Montmorillonite, Mu-Muscovite, C-Calcite**

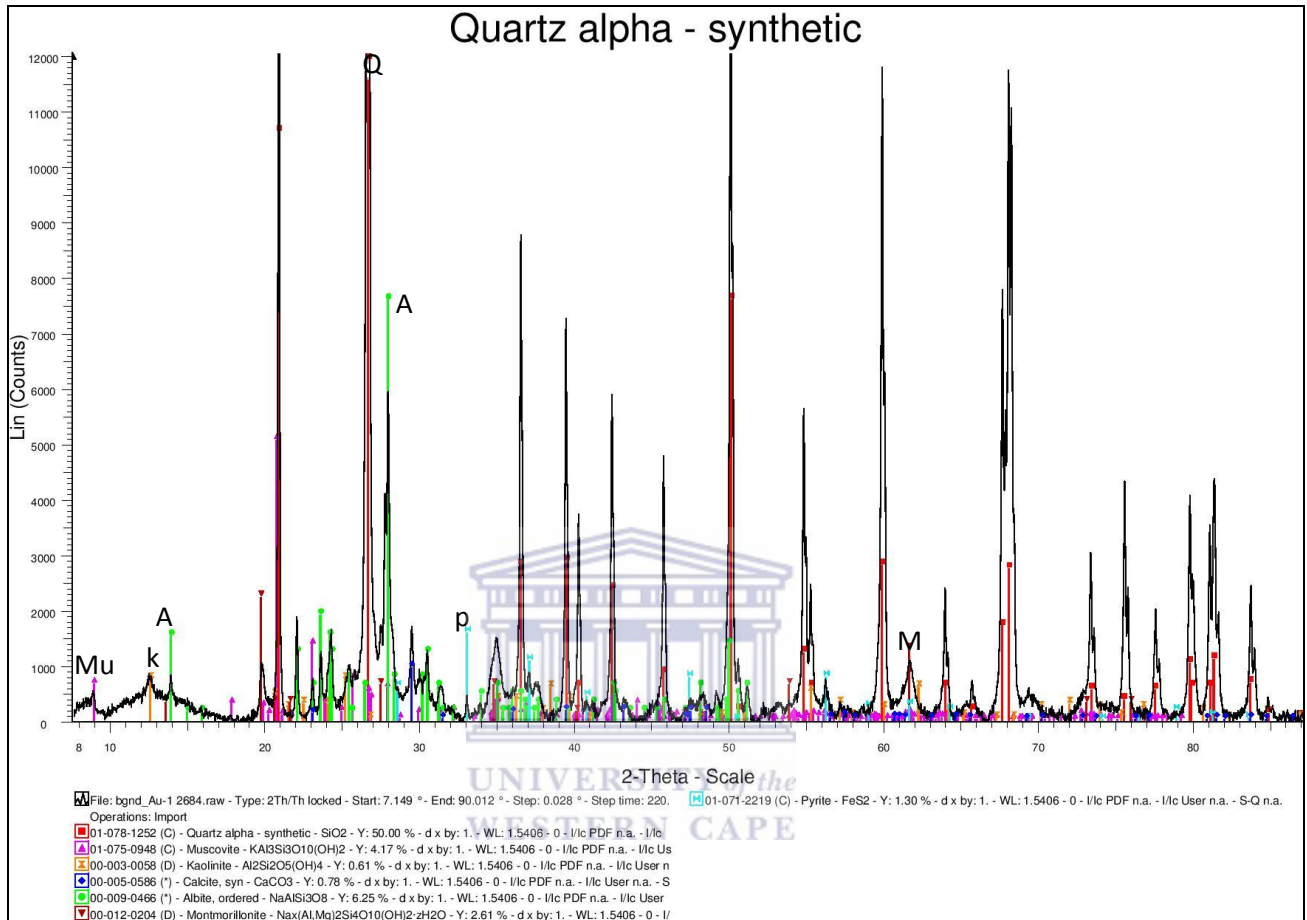


Figure 6.3 B (2684.67m) **Q-Quartz, P-Pyrite, A-Albite, K-Kaolinite, M-Montmorillonite, Mu-Muscovite, C-Calcite**

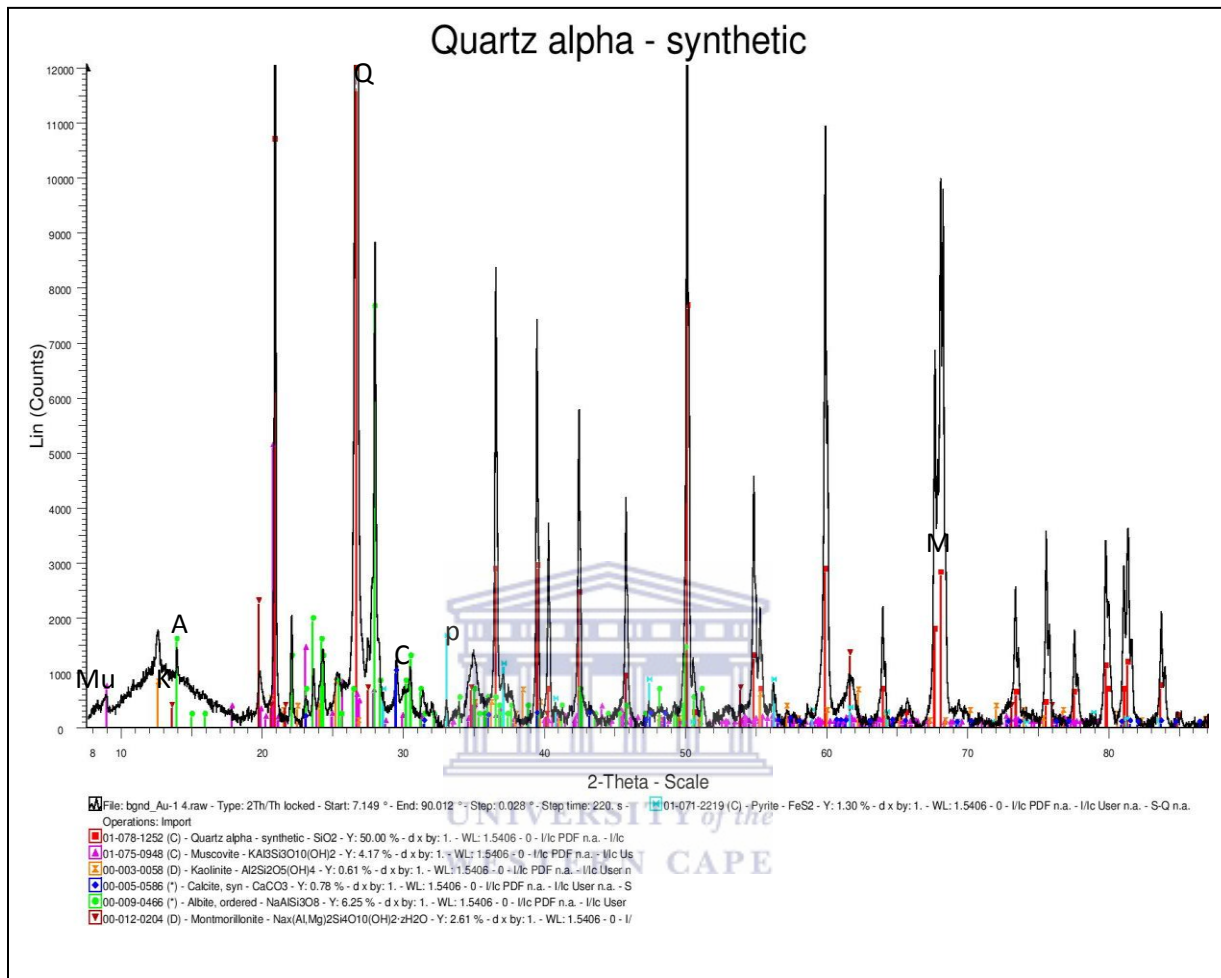


Figure 6.3 C (2685. 39m) **Q-Quartz, P-Pyrite, A-Albite, K-Kaolinite, M-Montmorillonite, Mu-Muscovite, C-Calcite**

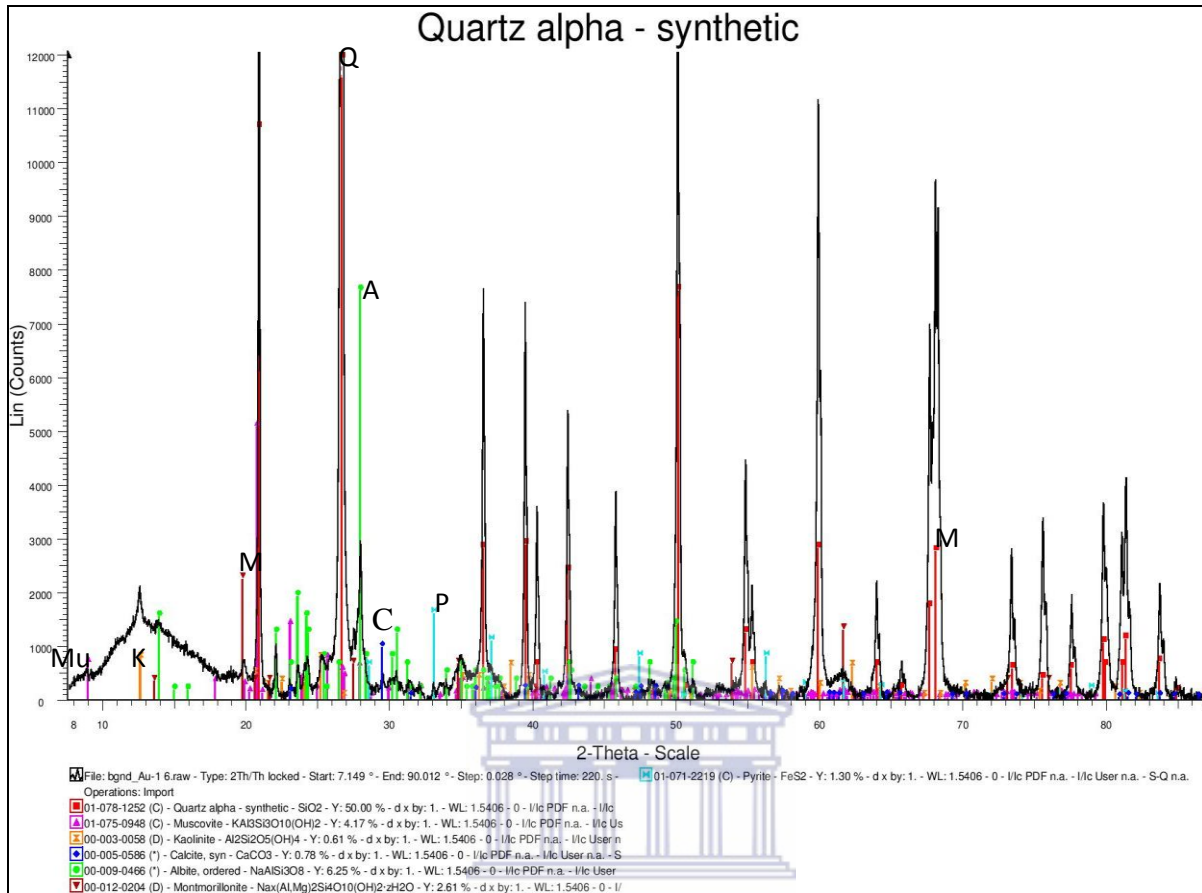


Figure 6.3D (2685.84m) **Q-Quartz, P-Pyrite, A-Albite, K-Kaolinite, M-Montmorillonite, Mu- Muscovite, C-Calcite**

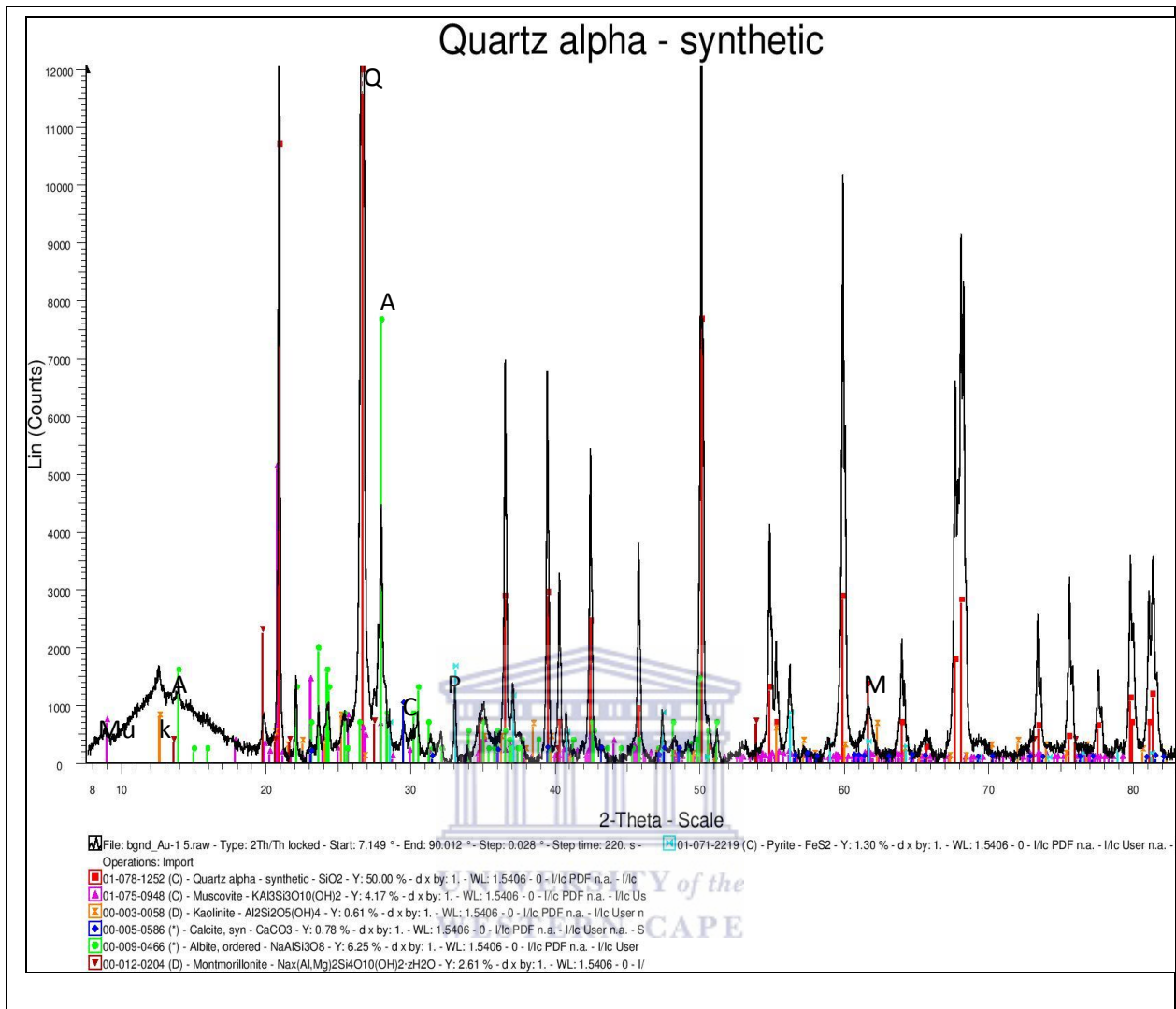


Figure 6.3 E (2686.51m)

Q-Quartz, P-Pyrite, A-Albite, K-Kaolinite, M-Montmorillonite, Mu-Muscovite, C-Calcite

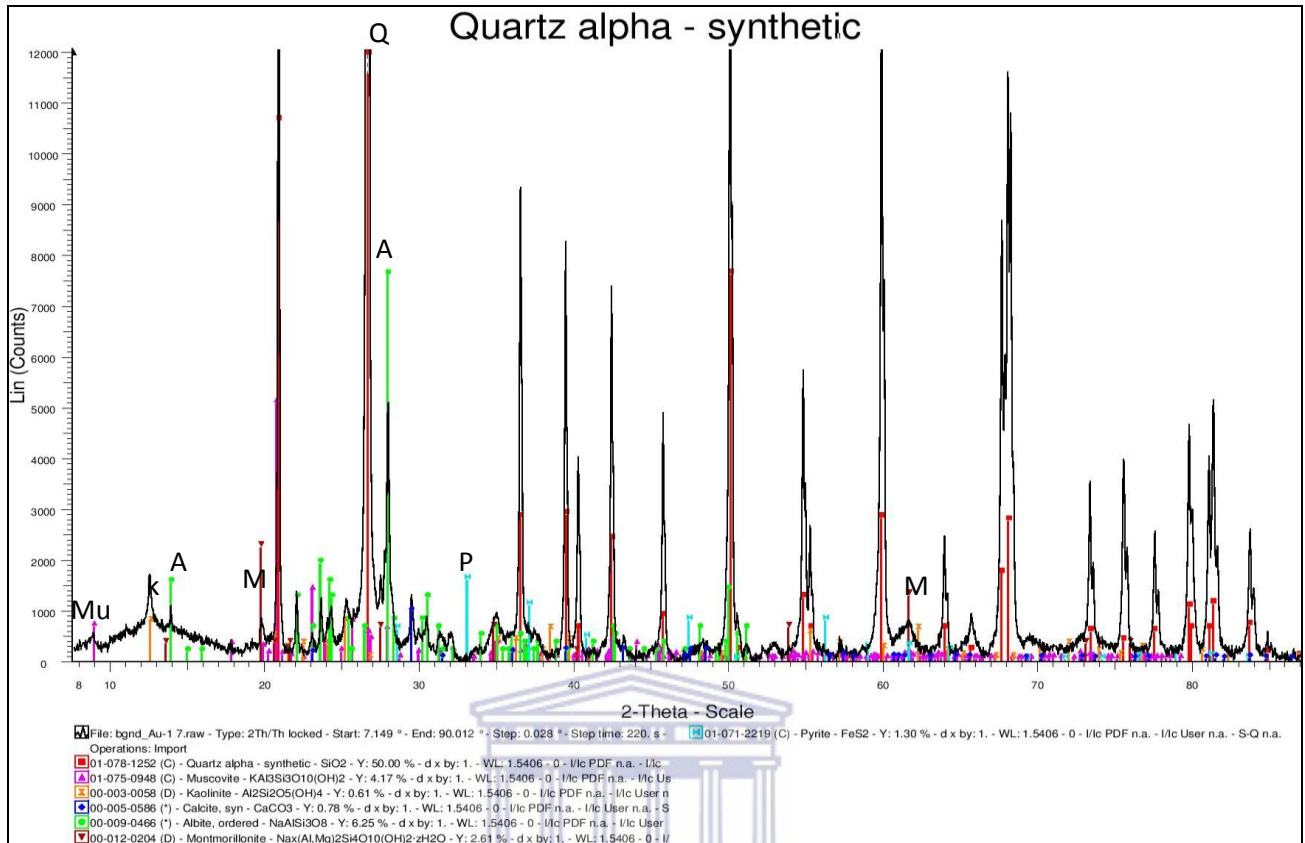


Figure 6.3 F (2687.80m)

UNIVERSITY of the
WESTERN CAPE

Q-Quartz, P-Pyrite, A-Albite, K-Kaolinite, M-Montmorillonite, Mu-Muscovite, C-Calcite

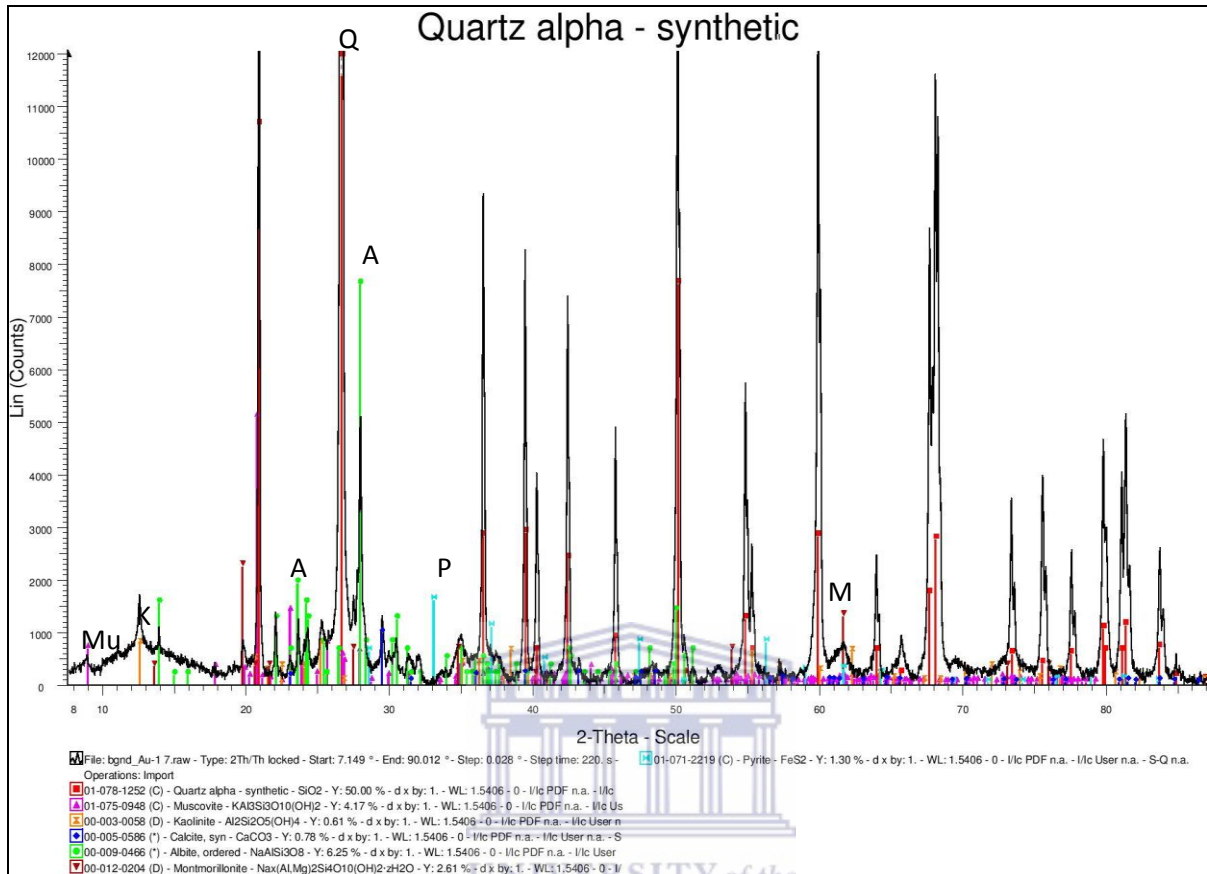


Figure 6.3 G (2688. 38m)

Q-Quartz, P-Pyrite, A-Albite, K-Kaolinite, M-Montmorillonite, Mu-Muscovite, C-Calcite

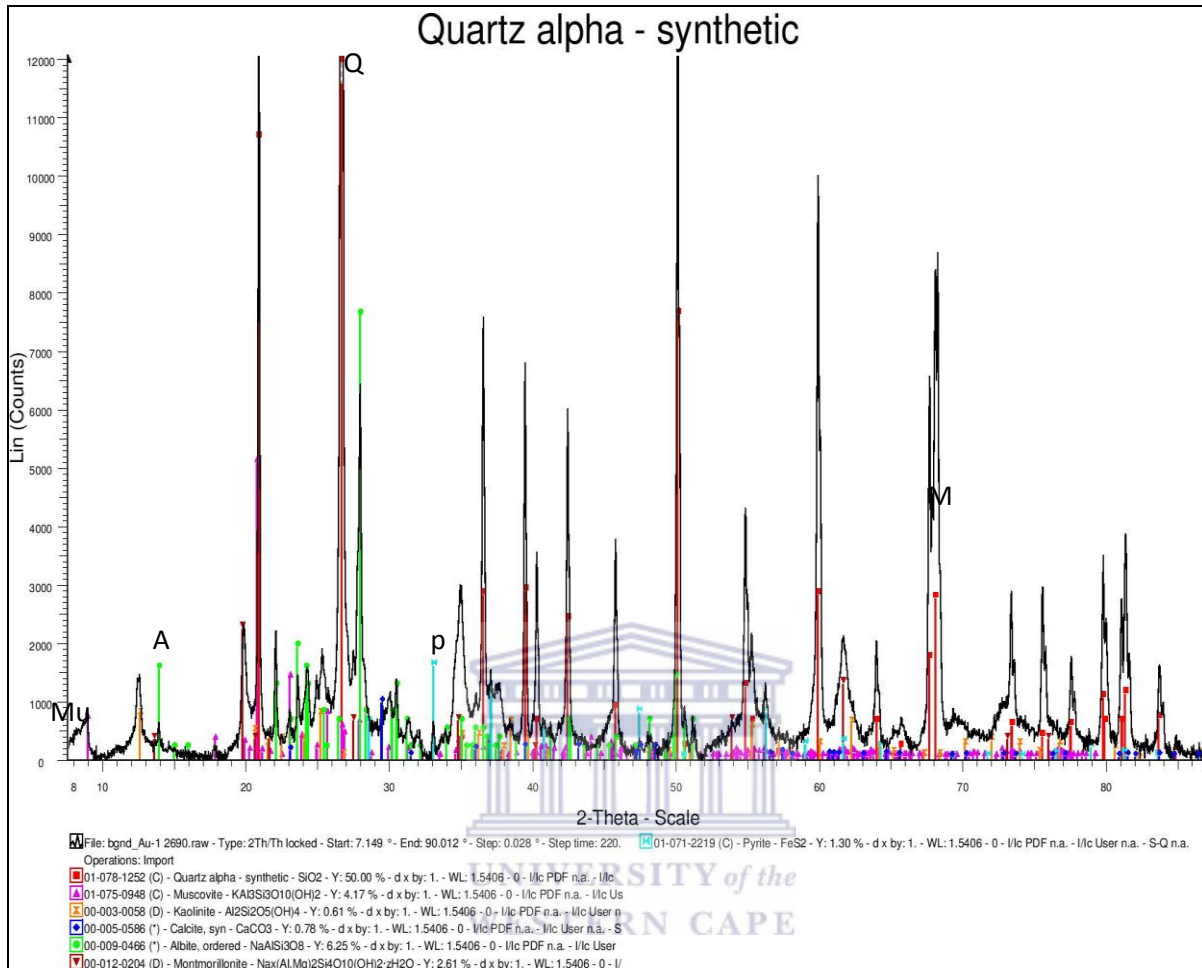
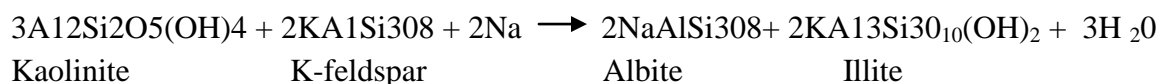


Figure 6.3 H (2690.30m) **Q-Quartz, P-Pyrite, A-Albite, K-Kaolinite, M-Montmorillonite, Mu-Muscovite, C-Calcite**

Figure 6.3(A-H): XRD Photos of AU-1 well

6.1.2.2 XRD Interpretation for KF-1 well

In contrast to the high proportion of calcite cements in well AU-1, XRD analysis of samples from well KF-1 did not suggest a calcite presence (figure 6.4 A-D). In a similar way to the AU-1 well, there is a strong presence of quartz cements in KF-1 which is a sure sign of reservoir problems. The occurrence and the amount of illite precipitation is mostly dependent on the availability of kaolinite, smectite and K-feldspar (Bjorklykke, 1997). Illite precipitation might be linked to initial alteration of micas which can produce kaolinite, siderite, K-Feldspar and smectite as by products (Morad, 1990). Smectite specifically has been identified as a major precursor to the precipitation of illite. The presence of albite could be attributed to the illitization of kaolinite and K-Feldspars in the presence of Na (Bjorklykke, op.cit). The dissolution of smectites and subsequent formation of illite normally takes place at temperatures of 65-75°C or at 85-100°C (Dypvik and Eriksen, 1983). The formation of illite in KF-1 might have been caused by the transformation of montmorillonite considering the geothermal gradient of well KF-1 is 3.5°C/100m according to the Geological well completion report. The Na supply might have been sourced from seawater; this interpretation is supported by the detection of halite as one of the minerals present. The reaction below might also have supported illite and albite formation, as albite and illite may be formed from the reaction between kaolinite and K-feldspar in the presence of sodium. This process is called albitisation in which the sodium ion always acts as the catalyst for the precipitation of albite and other authigenic cements.



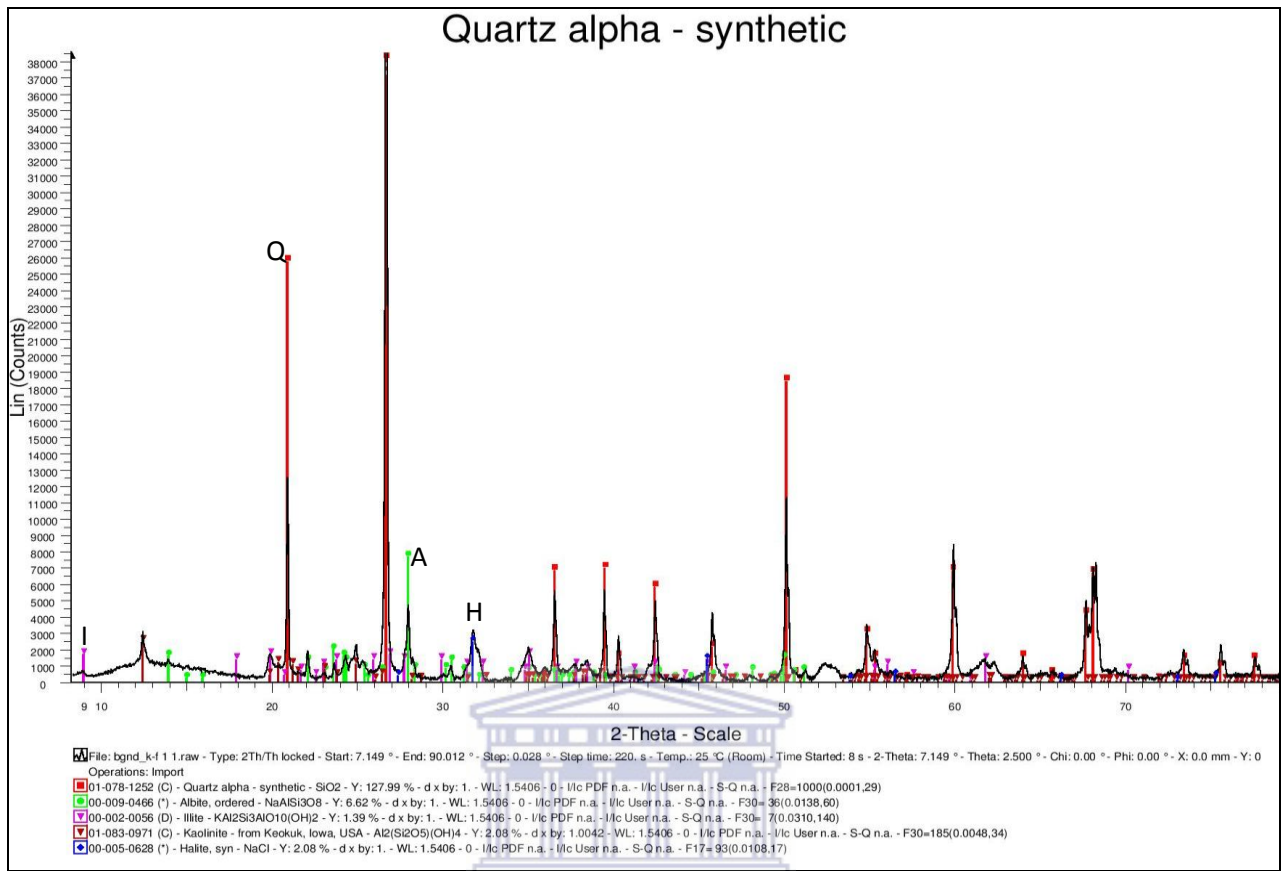


Figure 6.4 A (3006.25m)

Q-Quartz, H-Halite, A-Albite, K-Kaolinite I- Illite

UNIVERSITY of the
WESTERN CAPE

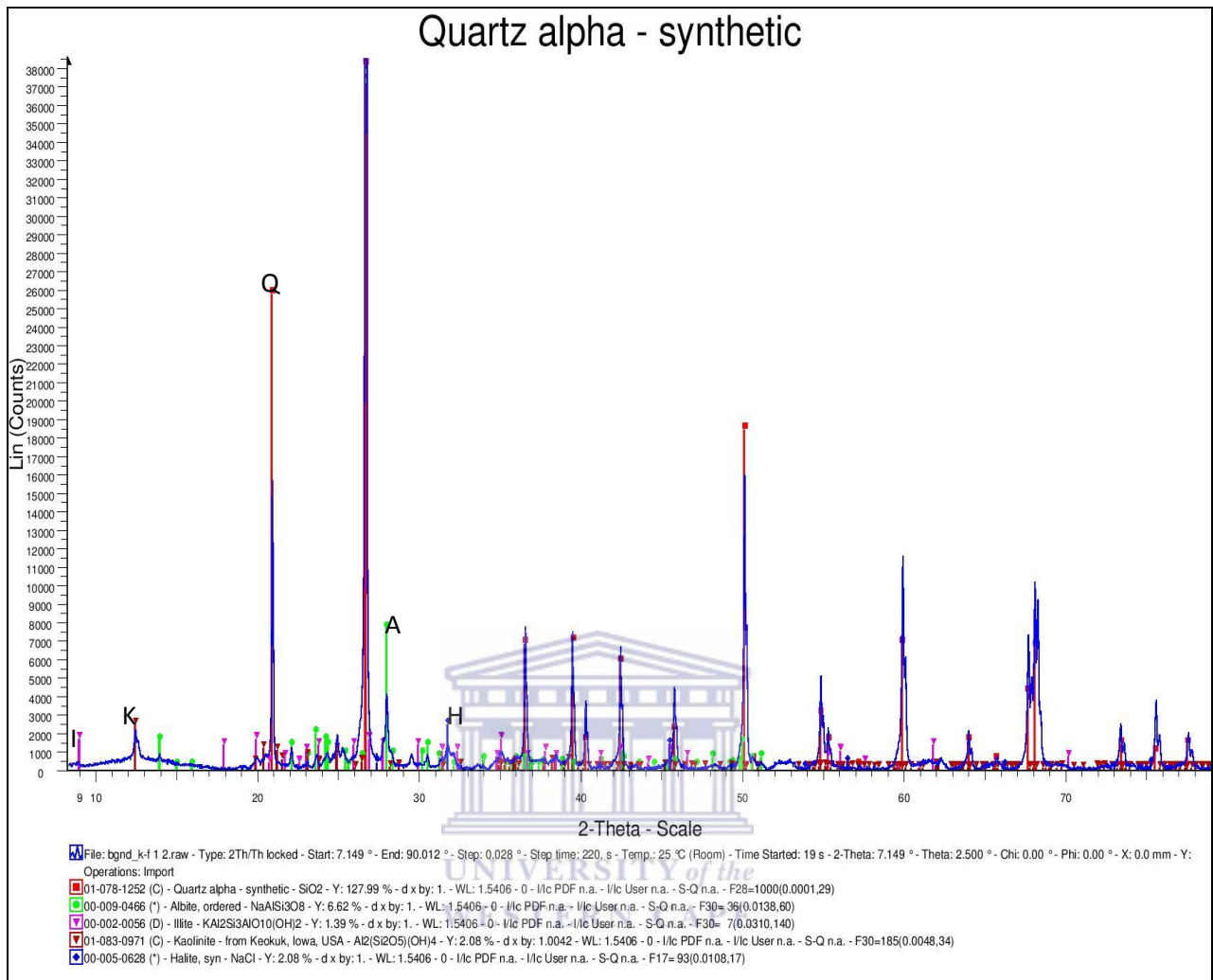


Figure 6.4 B (3007.07 m)

Q-Quartz, H-Halite, A-Albite, K-Kaolinite I- Illite,

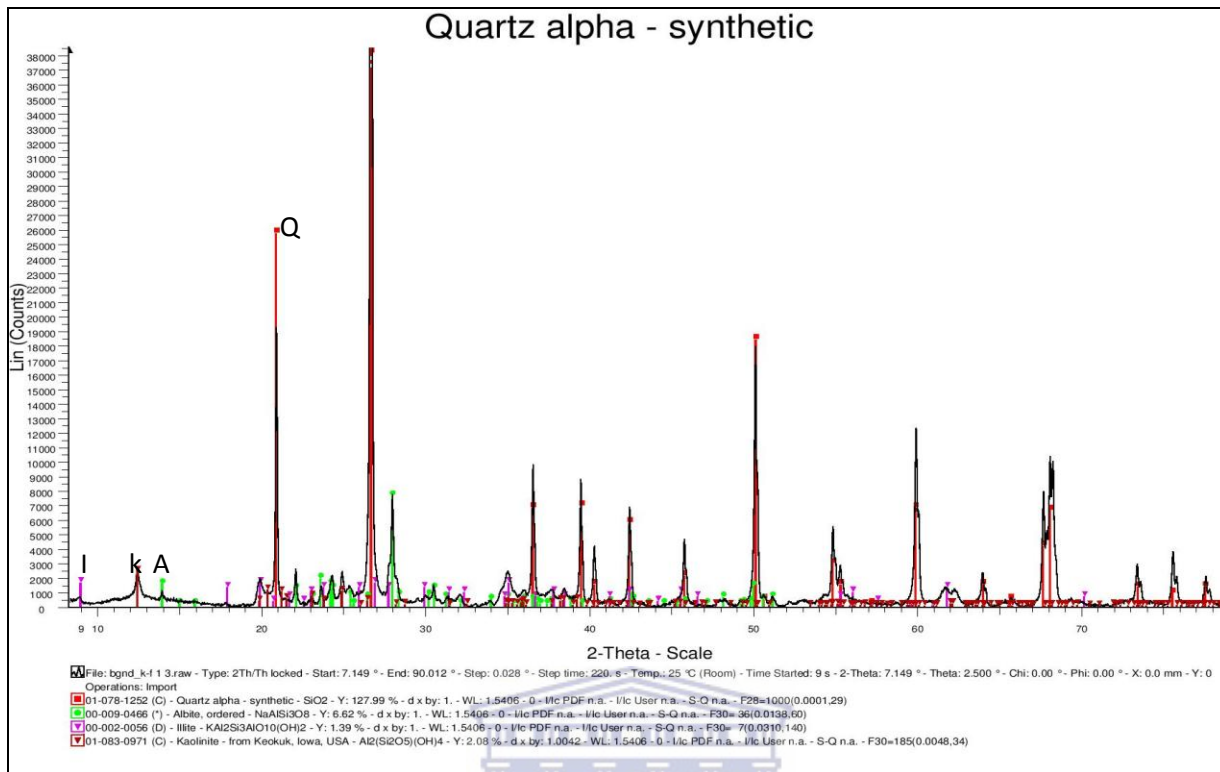


Figure 6.4 C (3007.60m)

Q-Quartz, H-Halite, A-Albite, K-Kaolinite I- Illite

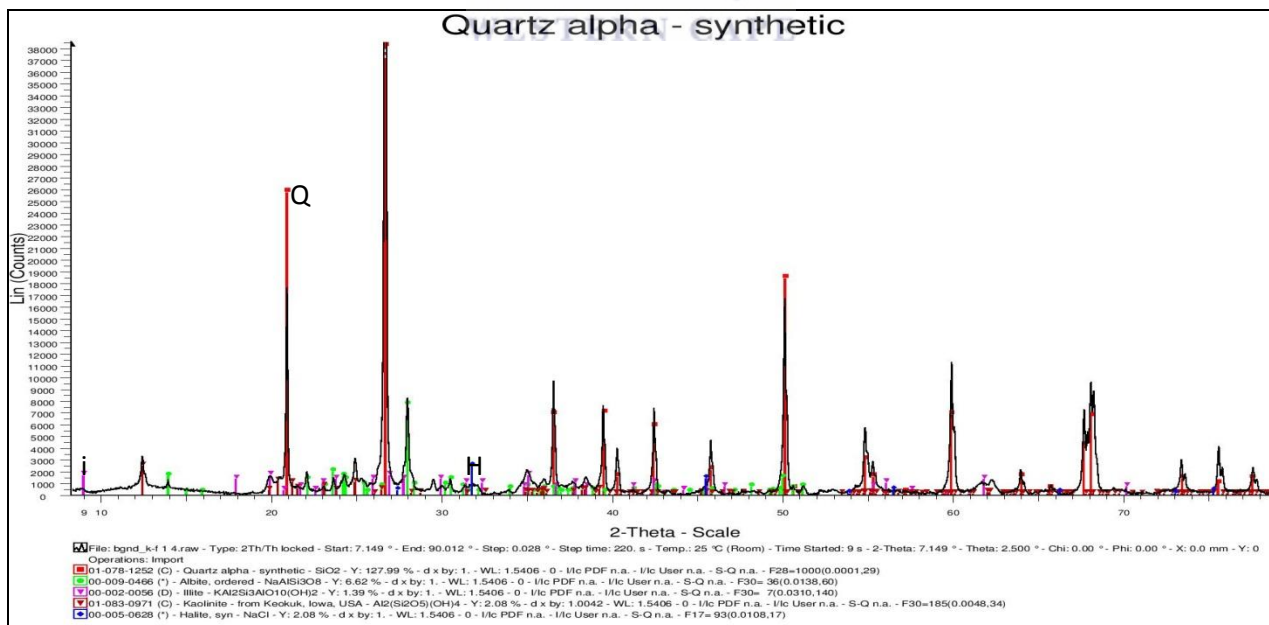
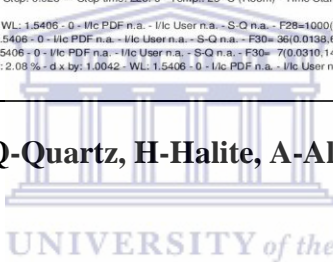


Figure 6.4 D (3008.13m)

Figure 6.4(A-D): XRD Photos of KF-1 well.

6.1.2.3 XRD Interpretation for KH-1 well

Results obtained from analysis of core samples taken from well KH-1 (figure 6.5 A-1) show consistent occurrence of quartz as the dominant cement like it was observed in the other two wells. Quartz cementation is sourced from the dissolution of quartz sand grains that is driven by the chemistry of pore waters. Other potential sources of silica for quartz cementation are numerous and include all documented silicate dissolution reactions in sandstones and shale (Mc Bride, 1989). Unlike Well AU-1, the influence of seawater during the deposition of sand bodies in the well is acknowledged with presence of halite in the core sample, hence the availability of Na ions is inevitable. The presence of illite is assumed to have been formed from a pre existing clay mineral; this assumption favours the explanation as to the origin of albite in KH-1 because illitization of kaolinite with K-Feldspar in the presence Na⁺ might be responsible for the precipitation of albite as it was observed in well KF-1, this observation is confirmed by the interpretation made from SEM analysis of KH-1 well as regards the presence of illite. The dissolution of detrital carbonate as the source of Ca⁺ in pore waters is once again highlighted by (Milliken et al., 1998) whilst the release of carbon too. Calcite cementation in KH-1 was probably due to dissolution of detrital carbonate rock or sourced from shells of aquatic organism in shallow marine settings. The anomalous occurrence of ferroan carbonate cement (siderite) and dolomite at depth 3074.42m suggest that KH-1 well might have been opened to influx of hydrothermal fluids sourced from nearby volcanic activity (Ahmed et al., 2008). Hydrothermal fluids rich in ferromagnesian minerals could have supplied iron and magnesium ions that enabled the precipitation of dolomite and siderite cements in this well.

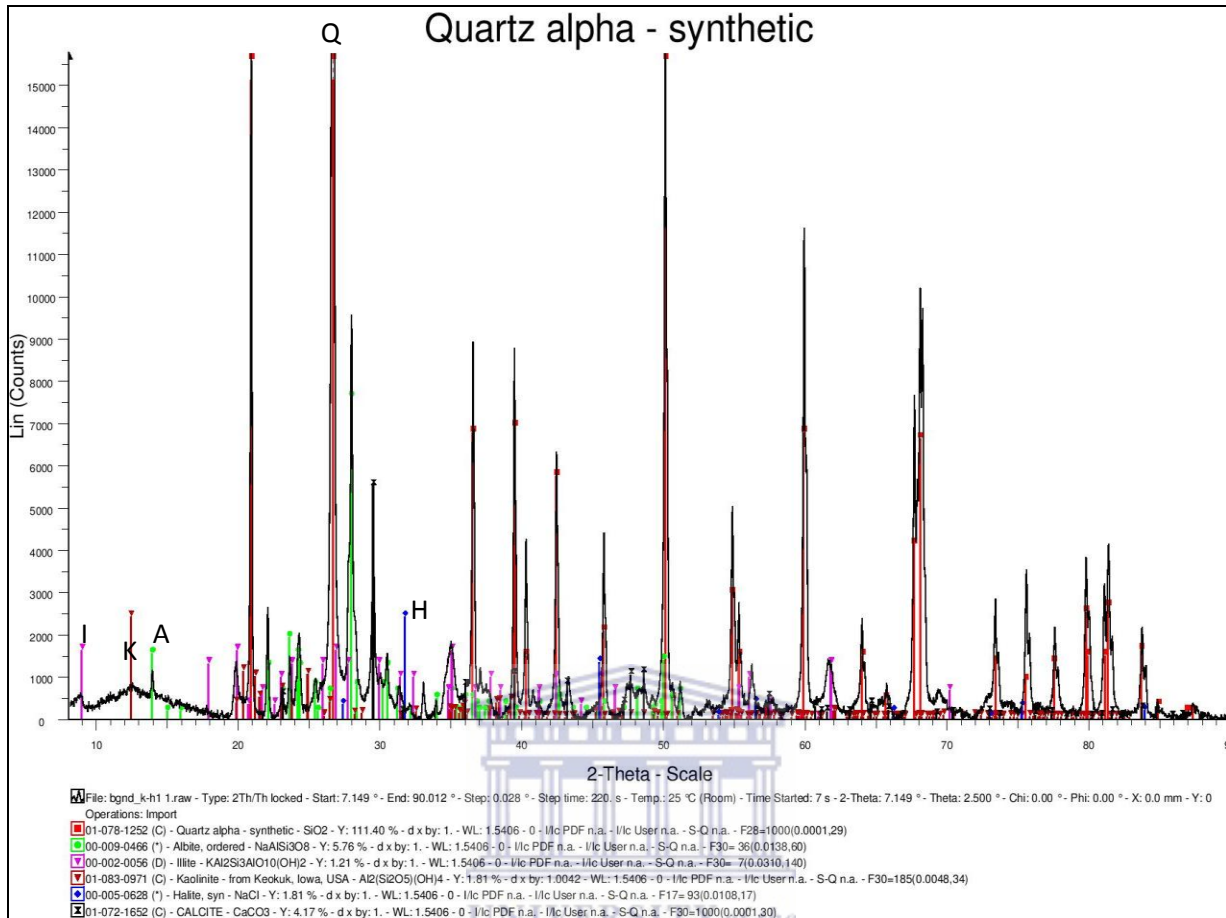
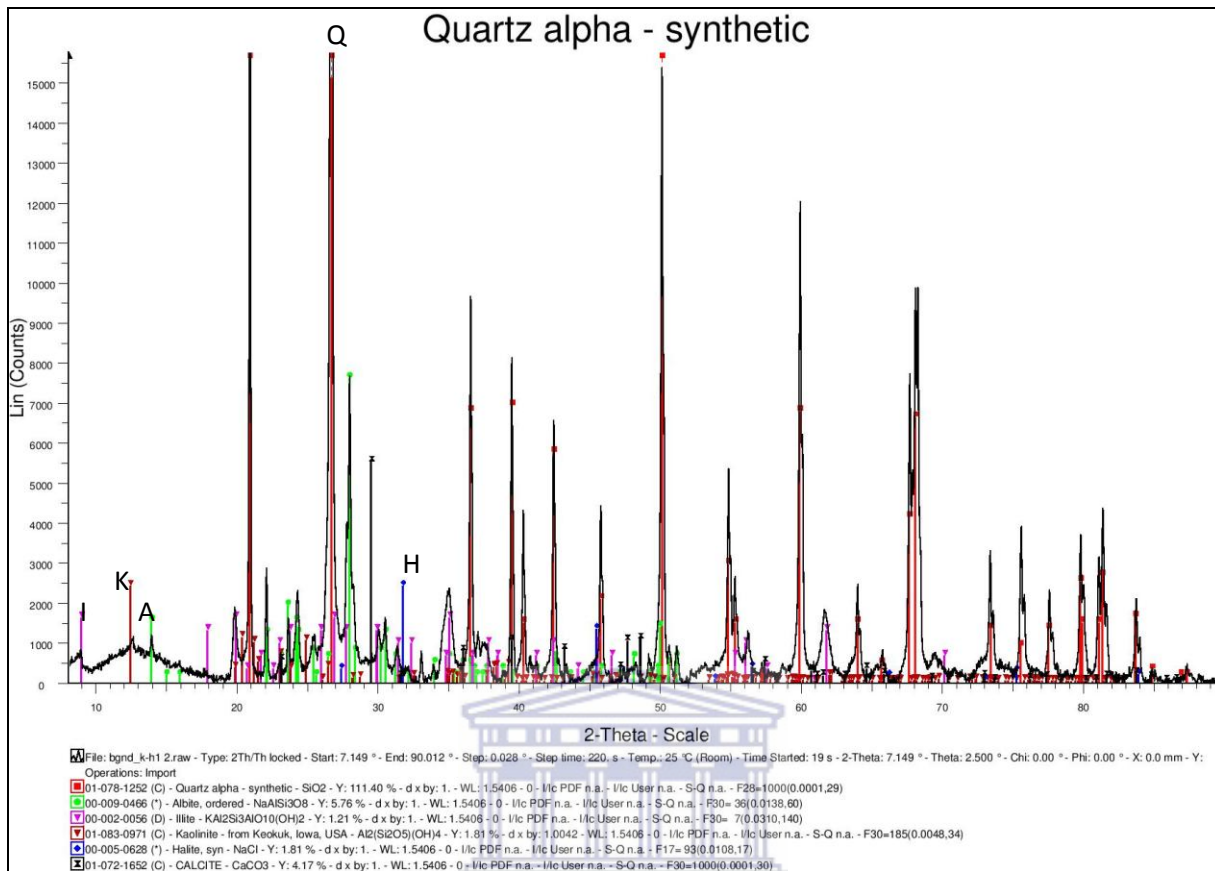


Figure 6.5 A (3066.00m)

Q-Quartz, H-Halite, A-Albite, K-Kaolinite I- Illite



UNIVERSITY of the
WESTERN CAPE

Figure 6.5 B (3067.00m)

Q-Quartz, H-Halite, A-Albite, K-Kaolinite I- Illite

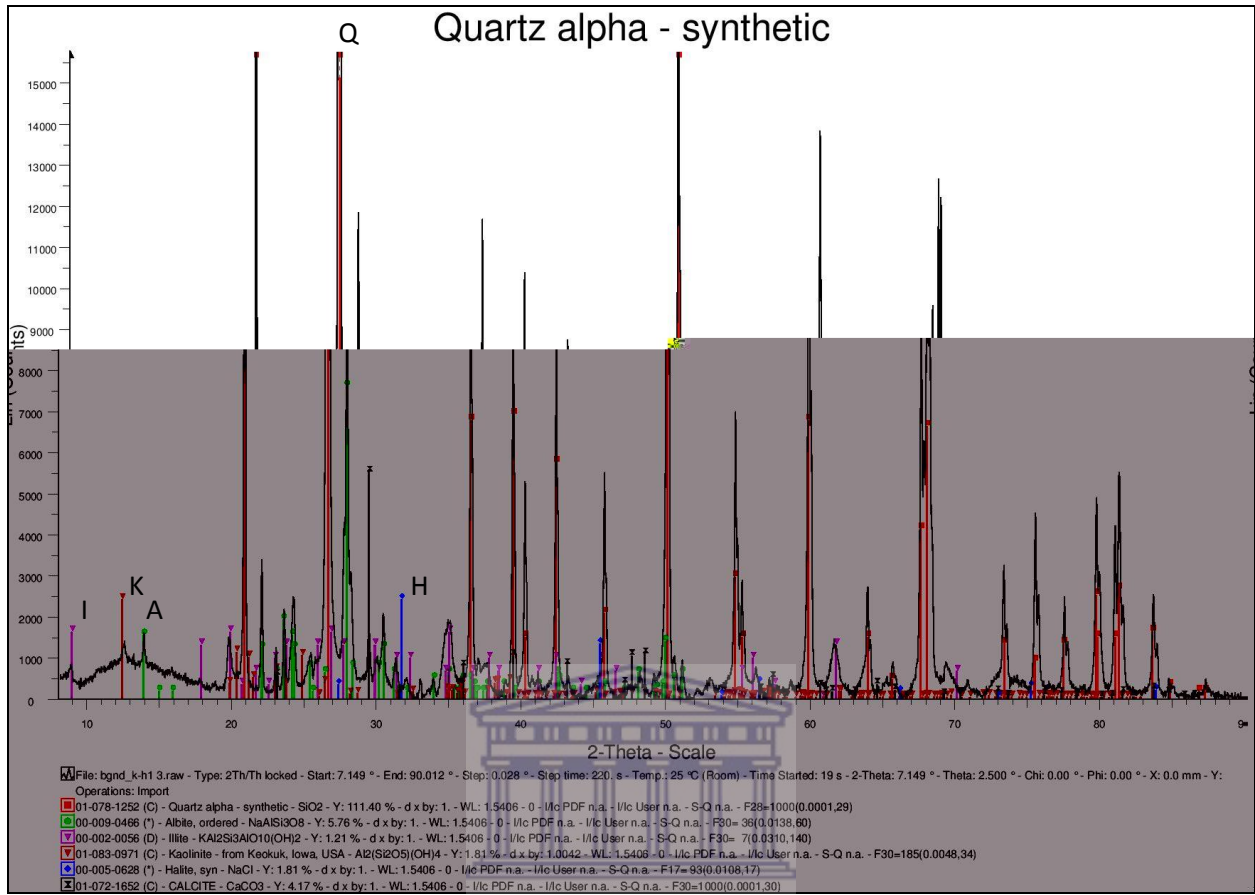


Figure 6.5 C (3068.09m)

Q-Quartz, H-Halite, A-Albite, K-Kaolinite I- Illite

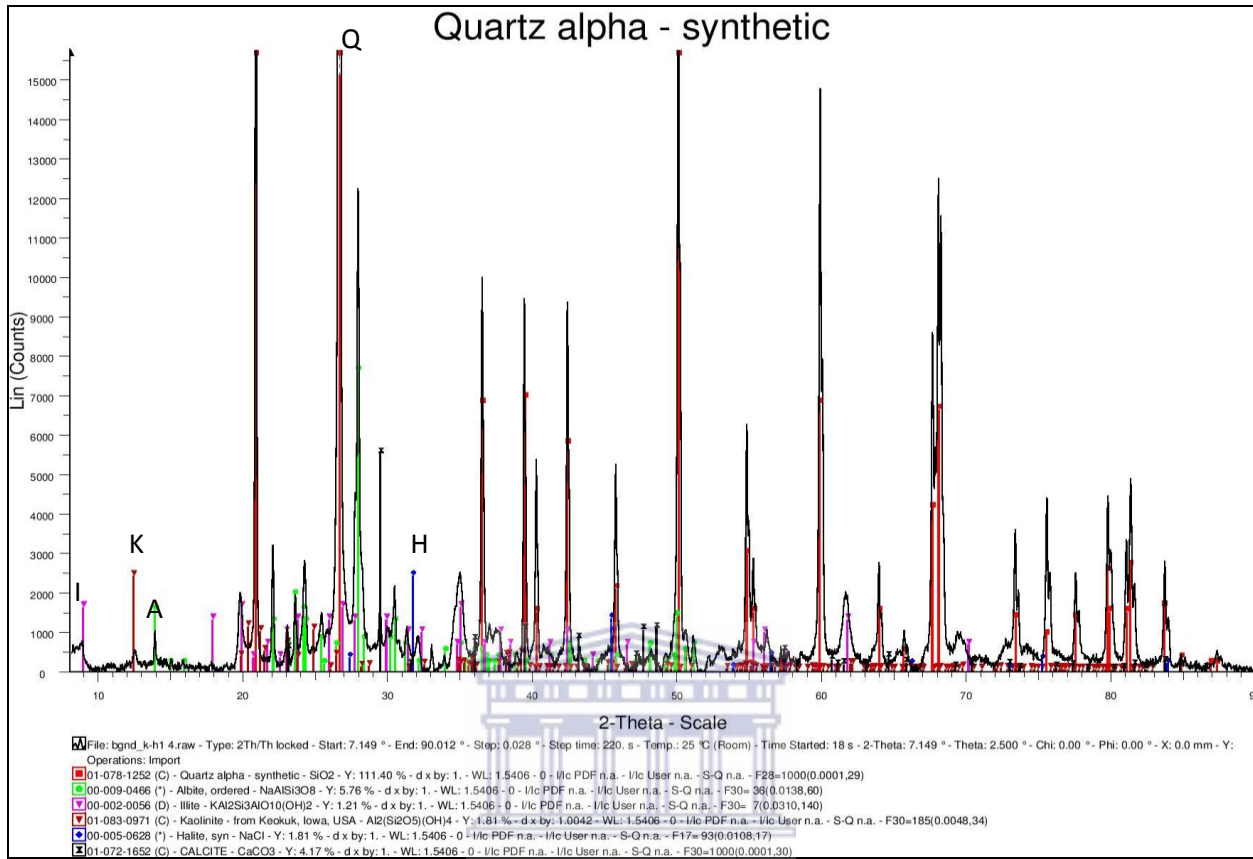


Figure 6.5 D (3068.92m)

Q-Quartz, H-Halite, A-Albite, K-Kaolinite I- Illite

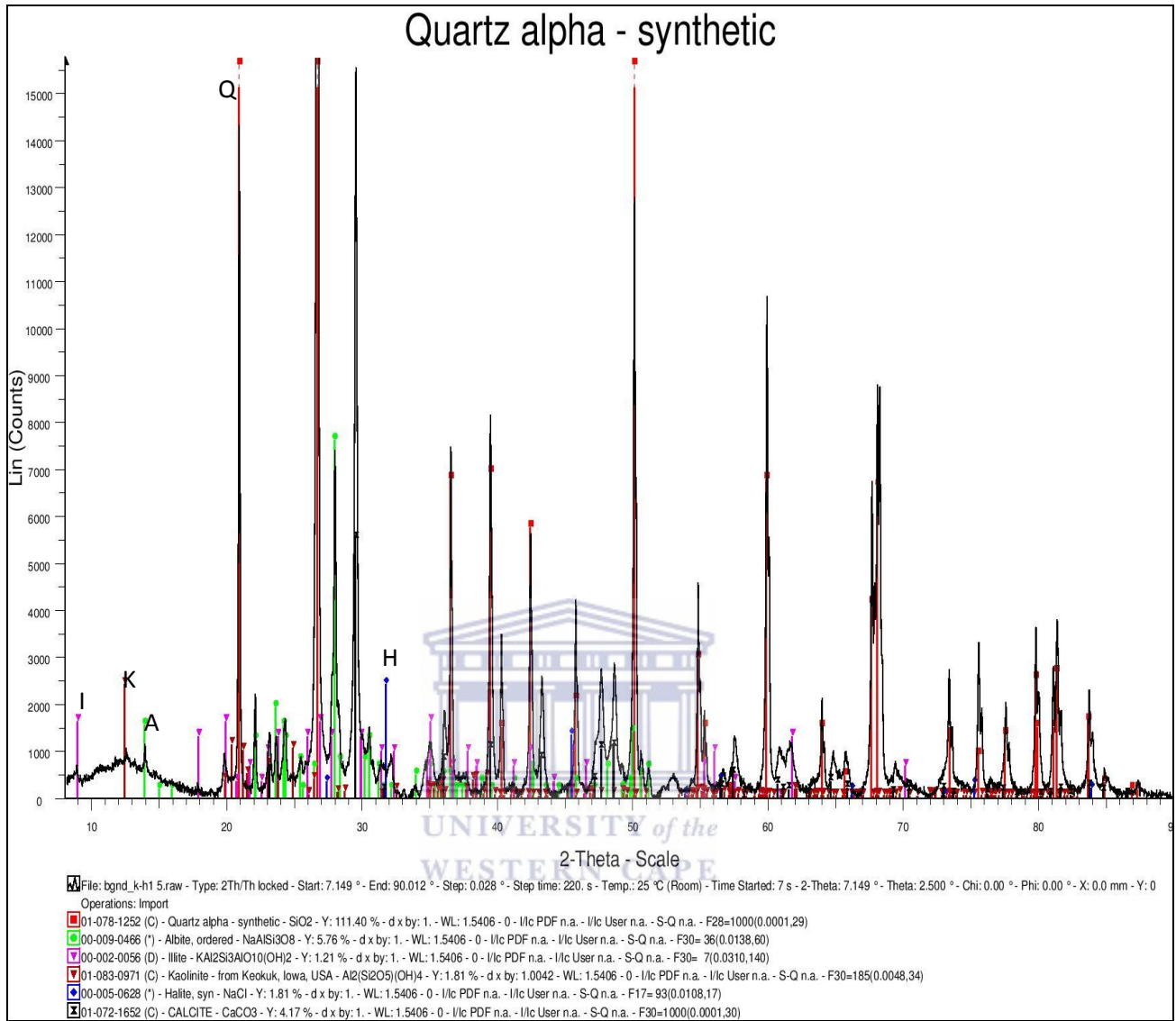


Figure 6.5 E (3069.9m)

Q-Quartz, H-Halite, A-Albite, K-Kaolinite I- Illite

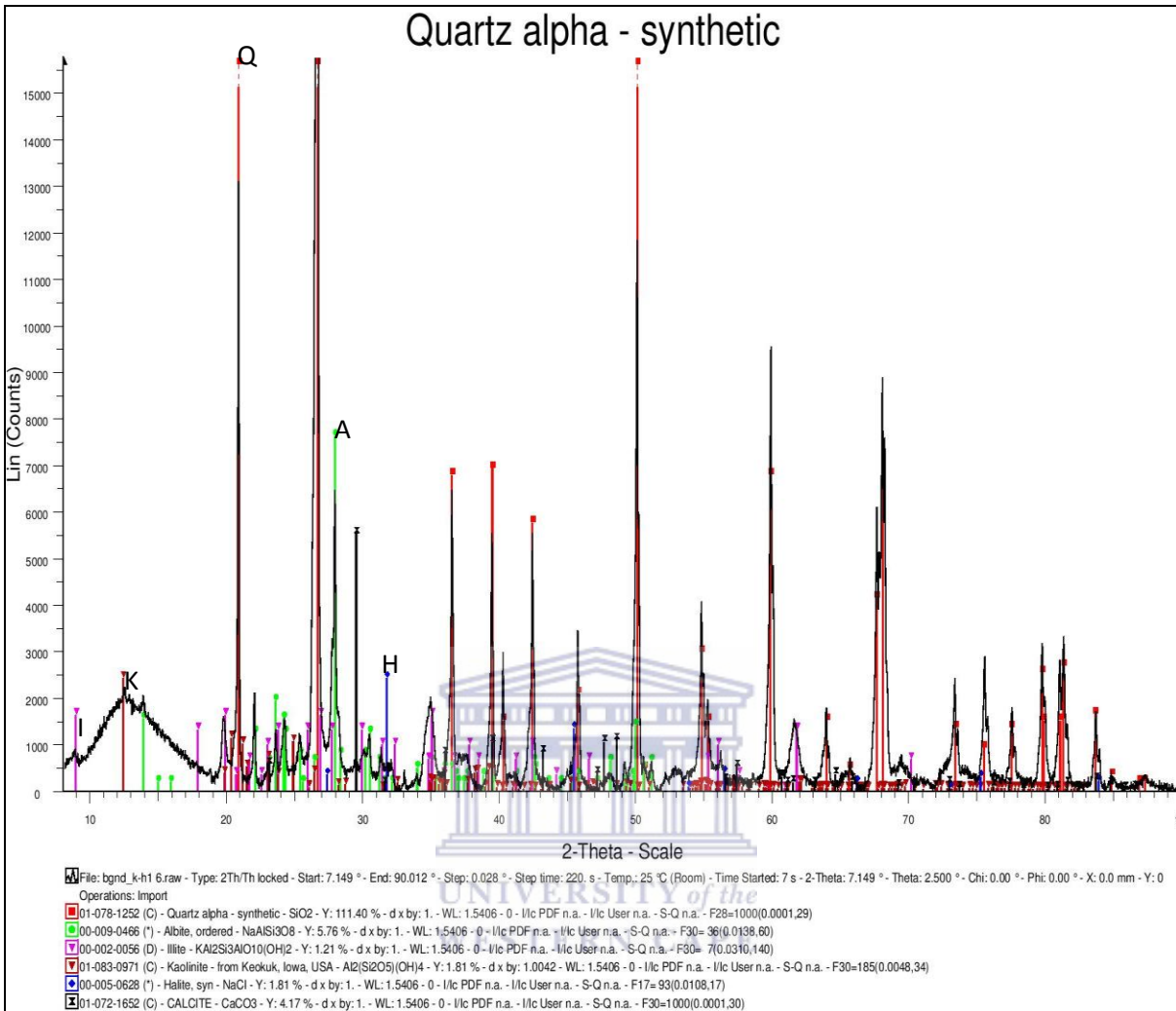


Figure 6.5 F (3070.89m)

Q-Quartz, H-Halite, A-Albite, K-Kaolinite I- Illite

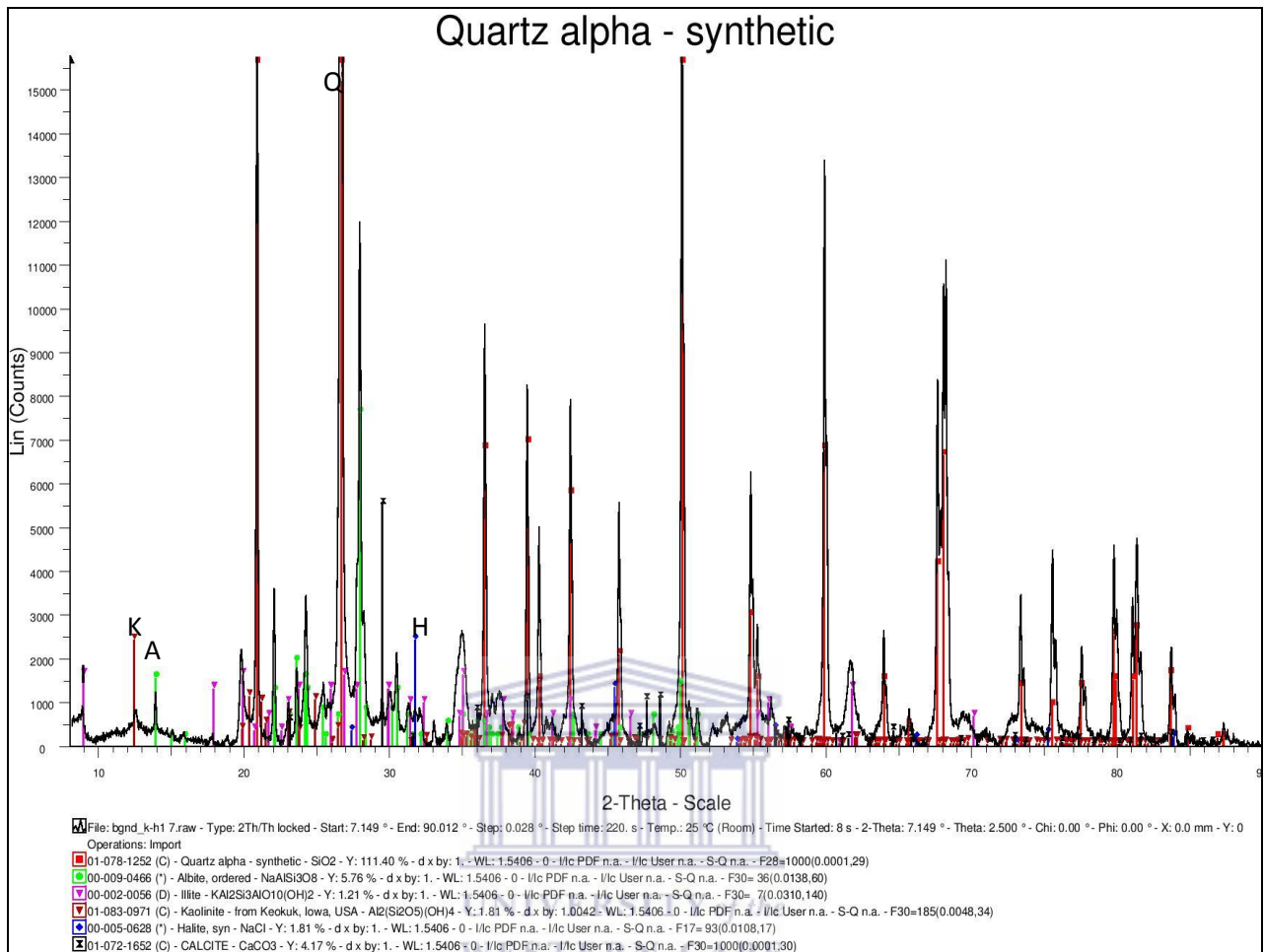


Figure 6.5 G (3072.00m)

Q-Quartz, H-Halite, A-Albite, K-Kaolinite I- Illite

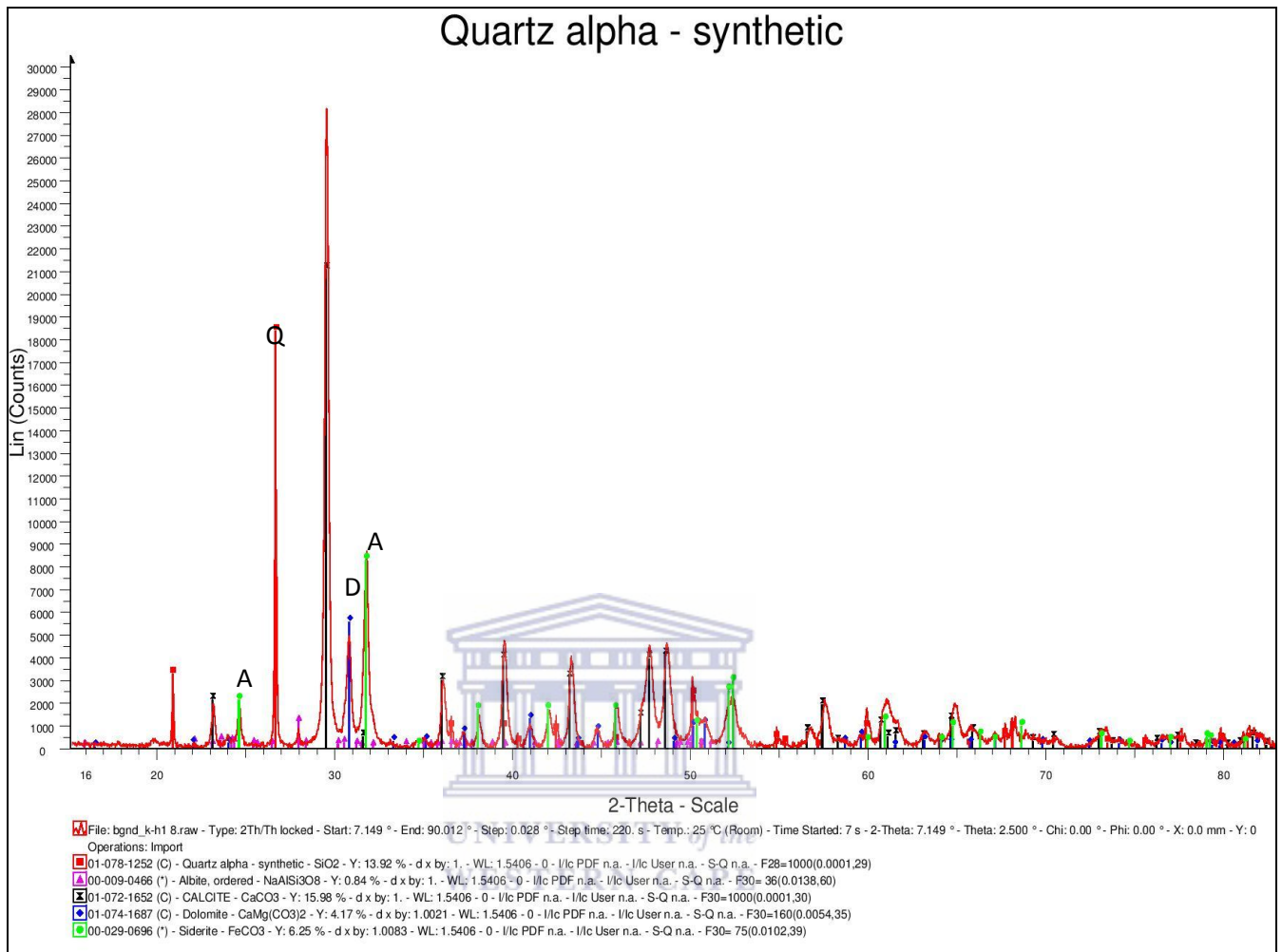


Figure 6.5 H (3074.42 m)

Q-Quartz, H-Halite, A-Albite, K-Kaolinite I- Illite

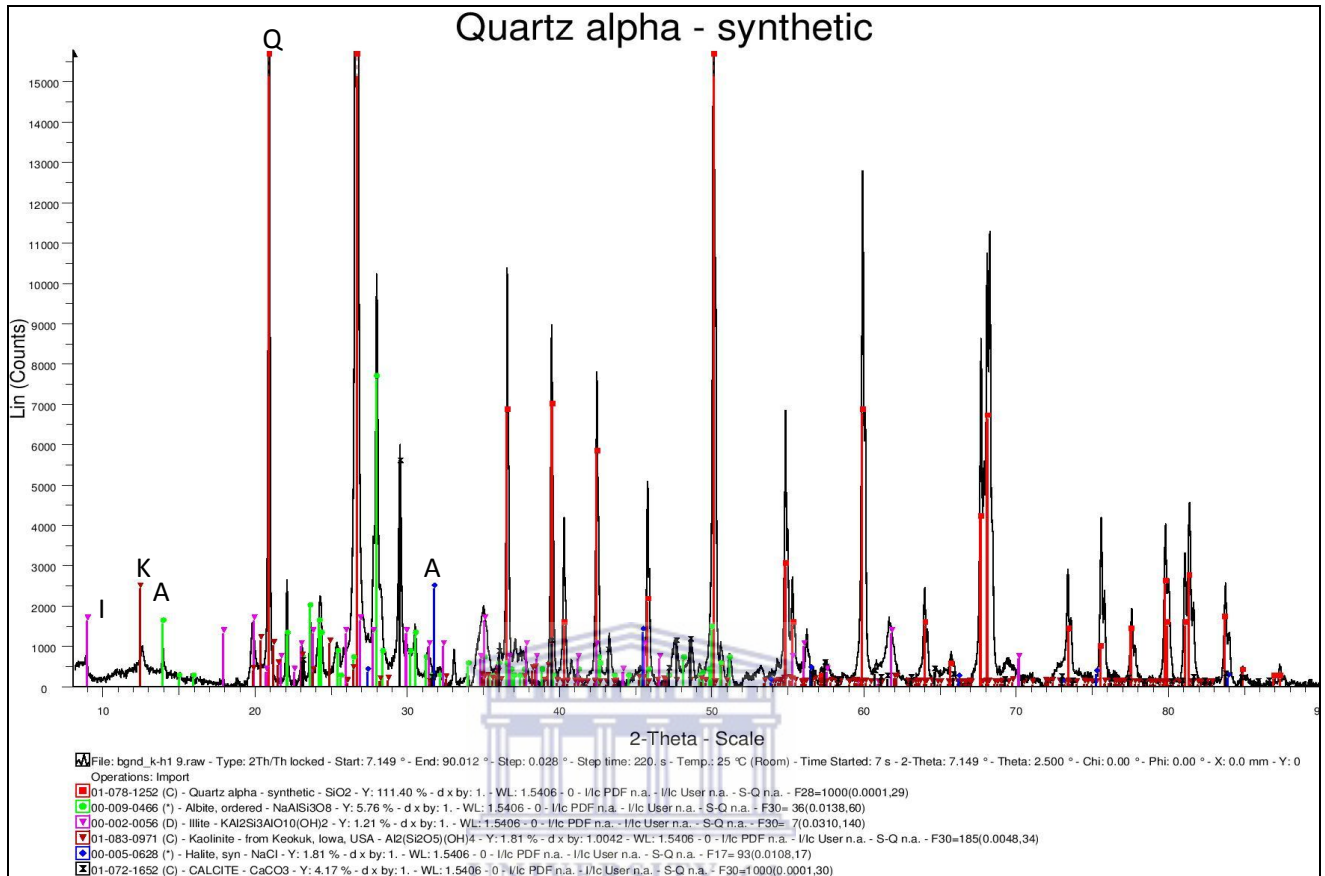


Figure 6.5 I (3082.25 m)

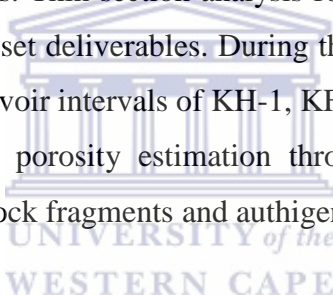
Q-Quartz, H-Halite, A-Albite, K-Kaolinite I- Illite

6.1.2.4 Summary of XRD Interpretation

Calcite cement precipitation is prominent in wells K-H1 and A-U1, its presence confirms the observation made on core description that the reservoir sections encountered in these wells were deposited under shallow marine conditions. The presence of quartz cement and kaolinite is acknowledged in the three wells as expected because they are both known to co-exist in marine environments. Significant quantities of albite are present in the three wells studied but halite is present in wells KF-1 well and K-H1 which explains its formation; the absence of halite in well AU-1 suggests that the concentration of halite may not be significant enough in well AU-1 for detection by XRD, also considering that well A-U1 is at a shallower depth compared to wells K-F1 well and K-H1. There was presence of illite in wells K-F1 and K-H1, while muscovite was detected in well AU-1. Muscovite serves as a precursor to illite formation at deeper depth, therefore, illite may have been formed from muscovite in well KH-1, hence the justification of illite presence in well K-H1. Pyrite presence in well AU-1 suggests a prevailing anoxic environment sometime during deposition. Siderite and dolomite were also detected at depth 3074.42 m in well K-H1, which explains the increase in Mg ions at this depth as observed on the cation exchange plot.

6.1.3 Thin Section Interpretation

Petrographic studies which are mainly thin section interpretation and hand specimen observation of rock samples are often done in conjunction with supplementary analyses like SEM, XRD and core analysis in sedimentary petrology studies. Sedimentary rocks rich in feldspar are often tagged as being mineralogically immature while textural maturity is also determined from the degree of sorting. Porosity estimation is normally done via thin section by impregnation with epoxy blue of the rock samples during thin section preparation, the spaces occupied by the epoxy blue will be visible under the microscope as pore spaces. Microscopic observation of rock samples under crossed polarized light enables the identification minerals, rock fragments, authigenic cements and pore spaces. Thin section analysis for this study was done as part of an integrated approach to achieve the set deliverables. During the preparation of thin sections from rock samples taken within the reservoir intervals of KH-1, KF-1 and AU-1 wells, epoxy blue was not added to the samples, hence porosity estimation through thin section was impossible. However, rock forming minerals, rock fragments and authigenic cements were easily recognized.



6.1.3.1 Thin Section Interpretation AU-1 well.

The observable grain sizes of well AU-1 are angular to sub-rounded in shape. Samples were taken at different depth along the cores (2684.05m, 2684.67m, 2685.39m, 2685.84m, 2686.51m, and 2687.80m). There are obvious quartz grains present in all slides while the green colour as observed at depth 2684.05m (figure 6.6A below) under plain polarised light (PPL) suggests the likelihood of glauconite presence in this well. Glauconite presence is commonly attributed to mica alteration in shallow marine settings under reducing conditions (Odin and Matter, 1981). Information derived from XRD indicates that the presence of calcite is significant in this well, the abundance of calcite confirms that sand bodies in well AU-1 were deposited under shallow marine conditions, calcite cement is very abundant in shallow marine settings because its early precipitation takes place a few centimetres below the sediment-water interface (Bjorlykke,1984).Also, the above statement is buttressed by the presence of pyrite as indicated

by XRD results, pyrite precipitation often takes place in marine environment with prevailing reducing conditions (Sauer et al.,1992). Feldspar content is low in well AU-1, possibly because they might have been altered to clay cements, also none of the minerals observed displays a crystal habit of twinning which is a common attribute of feldspar. Biotite (figure 6.6D) always appears as greenish brown crystal or completely brown when viewed under PPL. There is a dark coloured mineral at a depth of 2686.51m, this opaque mineral, is identified to be pyrite.

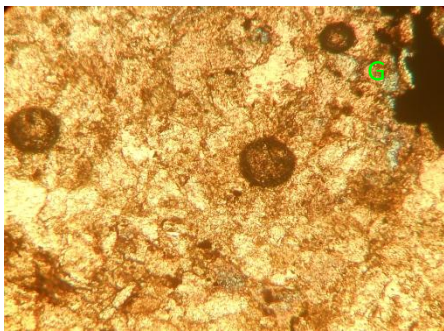


Figure 6.6 A (2684.05m)



Figure 6.6 B (2684.67m)

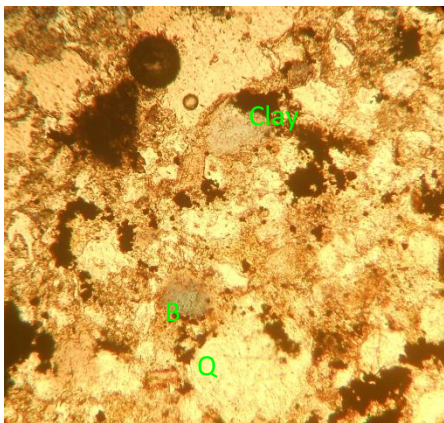


Figure 6.6 C (2685.39m)

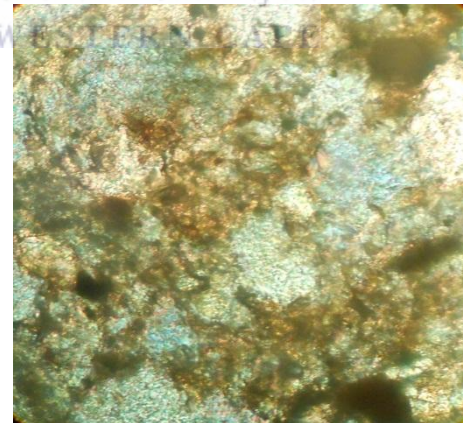


Figure 6.6 D (2685.84m)

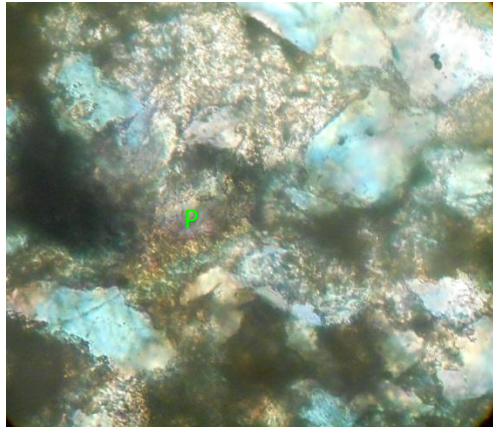


Figure 6.6 E (2686.51m)

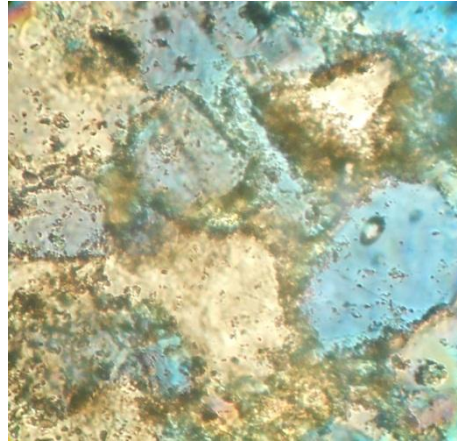


Figure 6.6 F (2687.80m)

P-Pyrite, B-Biotite, Q-Quartz, G-Glaucanite

Figure 6.6 (A-F): Thin section photos of AU-1 well.



6.1.3.2 Thin Section Interpretation of well KF-1.

Four core samples were taken and analyzed for well KF-1 because of limited core availability and lesser reservoir section within the cores cut, samples were taken at depths 3006.25m, 3007.07m, 3007.60m, 3008.13m. There is an abundance of biotite crystals and glauconite at 3007.60m (figure 6.7A) below, the biotite appears brownish green and exhibited platy crystal habit as seen at depth of 3008.13m. This means the biotite crystals may be in the process of conversion to glauconite. Quartz grains appear elongated at depth of 3007.07m: this might be due either to response of quartz grains to overburden pressure and subsurface temperature or because they are sourced from a fluvial environment. The different rock forming minerals observed under PPL are matrix supported as it is seen at depth 3006.25m.

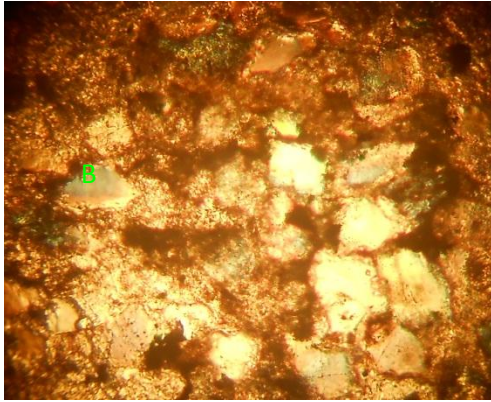


Figure 6.7 A (3006.25m)

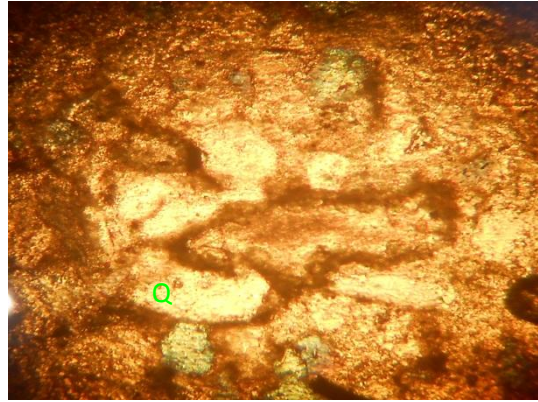


Figure 6.7 B (3007.07m)

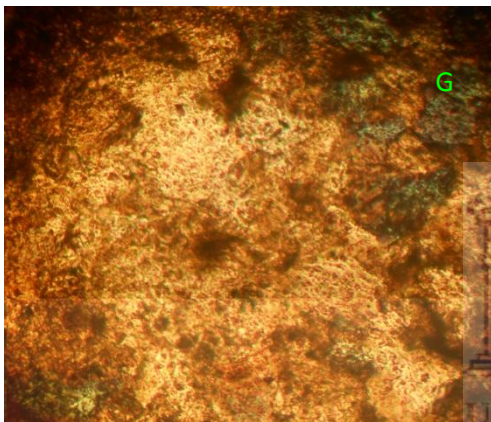


Figure 6.7 C (3007.60m)

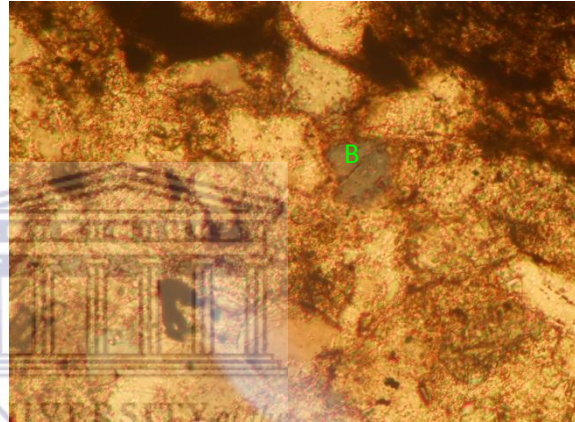


Figure 6.7 D (3008.13m)

Ch-Chlorite, Q-Quartz, B-Biotite, G-Glauconite

Figure 6.7(A-D): Thin section photos of KF-1 well.

6.1.3.3 Thin Section Interpretation of well KH-1.

Thin section photos obtained from KH-1 well are displayed below, the sampled depths are 3066m, 3067m, 3068.09m, 3068.92m, 3069.90m, 3070.89m, 3072m, 3074.42m. Interpretation of samples obtained from this well reveals the dominant presence of quartz grains which are angular to sub angular in shape. There is occurrence of feldspar at depth 3067m (figure 6.8B) but the feldspars look dis-orientated at this particular depth. Chlorite appears to be growing on the surface of quartz grains at a depth of 3068.09m (figure 6.8C). It has been observed that the quartz grains at depth of 3070.89 m are also clay coated. Significant feldspar content was also

confirmed from XRD results of well KH-1. At a depth of 3069.90m, it is suggested that clay cements are significantly present because of consistent brownish colours observed as coatings around the minerals, although, clay cements are difficult to be identified with an optical microscope because they usually appear as amorphous masses of brownish colour (Nichols, 2009). There is evidence of chlorite growing on the surface of quartz grain at a depth of 3072 m, it appears as a coat on the surface of the quartz grain. The growth of chlorite may be attributed to the supply of iron and magnesium in the localized depositional environment pore waters which later favours its precipitation.

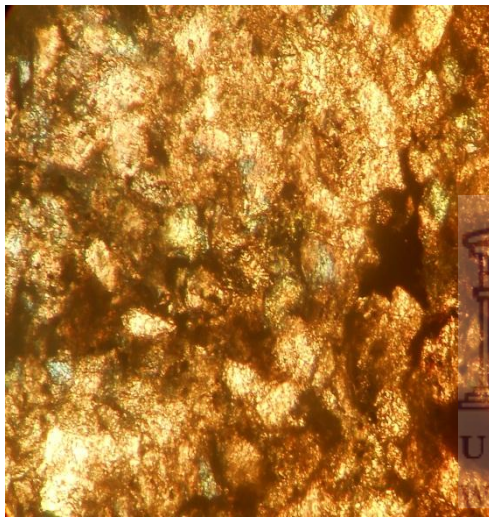


Figure 6.8 A (3066m)

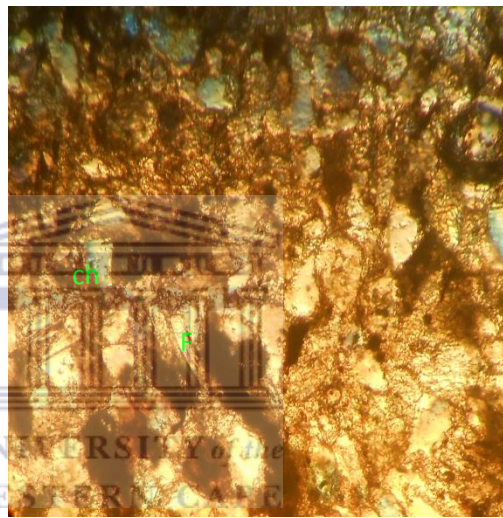


Figure 6.8 B (3067m)

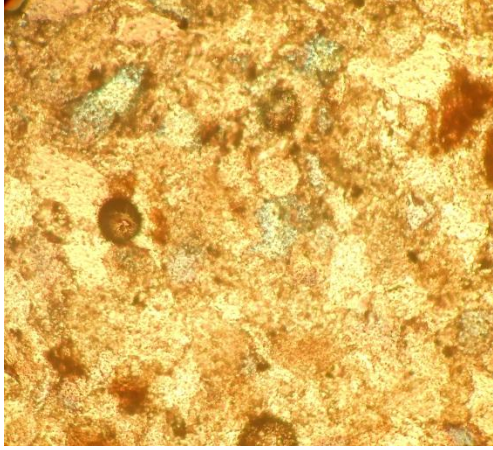


Figure 6.8C (3068.09m)

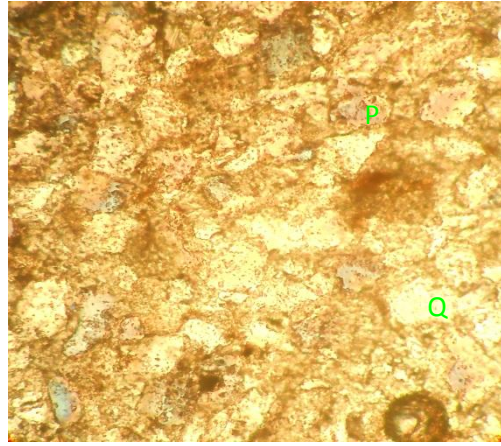


Figure 6.8 D (3068.92m)

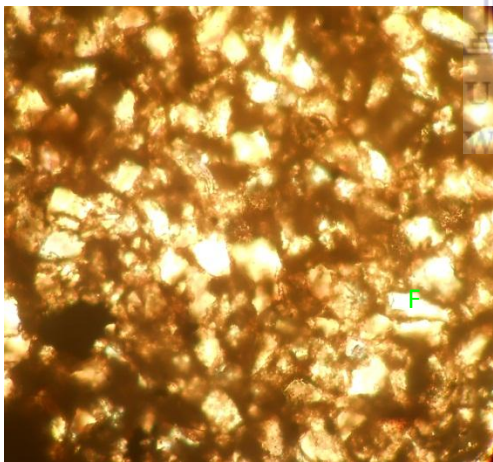


Figure 6.8 E (3069.90m)

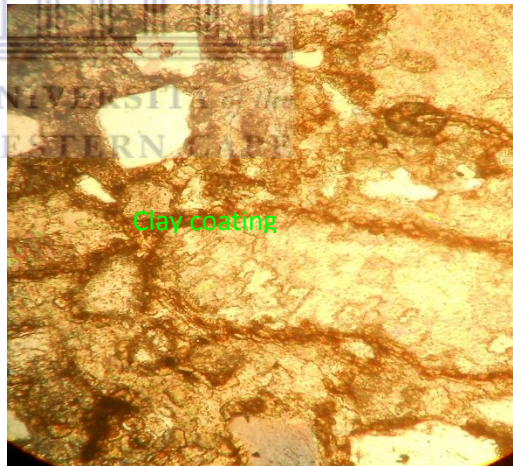


Figure 6.8F (3070.89m)

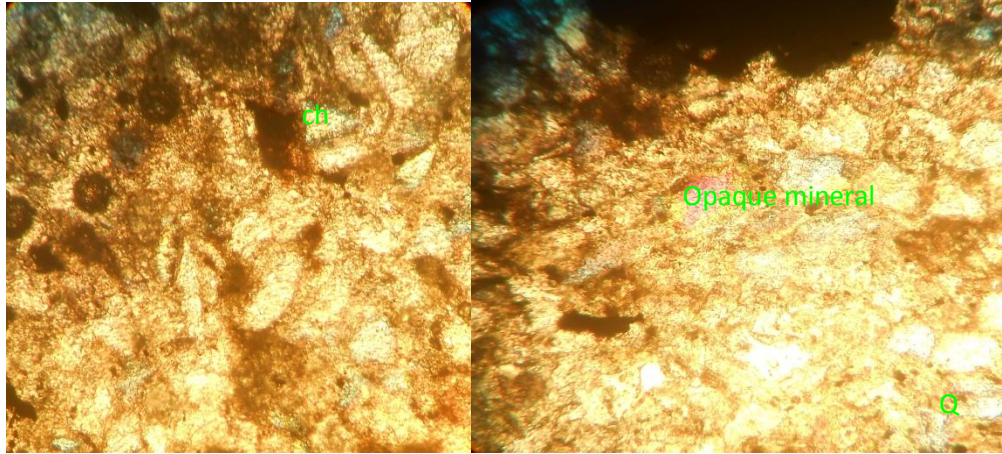


Figure 6.8 G (3072m)

Figure 6.8 H (3074.42m)

P-Pyrite, B-Biotite, Q-Quartz, G-Glaucanite, F-Feldspars, Ch-Chlorite,

Figure 6.8(A-H) : Thin section photos of KH-1 well



6.1.3.4 Summary of Thin Section Interpretation.

Quartz is the dominant mineral observed from the thin sections, they appear elongated at depth 3072m (KH-1 well), the elongation of the quartz grains may be due to response to temperature and pressure in the subsurface. The identification of calcite on thin sections of AU-1 confirms XRD detection of calcite in same well. Pyrite identification on thin sections for well AU-1 also confirms the detection by XRD. Glauconite presence confirms the suggestion of a marine environment as the paleo-environment under which KF-1 reservoirs were deposited. Feldspar was noticed at depth of 3067m in well KH-1 while chlorite was observed to be growing on the surface of a quartz grain in well KH-1 (3072m).

6.1.4 Pore Water Chemistry Interpretation.

Sediment pore water is defined as the water occupying spaces between sediment particles. Pore water can occupy close to 30 -80% of the volume of the sediments, the volume occupied by water being greater for fine grained silty sediment than for sandy sediment (Simpson, et al., 2005). Pore water composition is the main control on diagenetic reactions in sandstones and is usually sourced either from fresh meteoric water which is acidic or sea water which is alkaline (Hurst and Irwin, 1982). Pore water composition is influenced by surface water currents and tides and groundwater upwelling within the subsurface. Pore water samples were taken from wells AU-1, KF-1 and KH-1 core samples through a centrifugation process, which involves the extraction of the chemicals from core samples into ultra-pure water. The result is considered to be pore water samples. This analysis was carried out by observing all laboratory procedures and the results obtained are only vulnerable to insignificant errors; displacement of formation water from pore spaces because of mud filtrate influence. Centrifugation or squeezing is the most useful method of extraction for chemical analyses (Simpson et al., op.cit). An increase from acidic to neutral values favours the precipitation of aluminosilicates and carbonates (Curtis, 1983) while alkaline systems favour carbonate precipitation relative to aluminosilicates and quartz cements (Buyukutku, 2003). Ec (Electrical conductivities) values for various samples taken at intervals were also analyzed. Distribution of differential clay minerals has a great effect on electrical conductivity. In a shaly sand formation, two electrical conductivity paths are created; one due to formation water and the other due to clay conductivity. Ignoring clay conductivity effects often leads to underestimation of hydrocarbon saturation (deWaal, 1989). Ec in pore waters is the measurement of the extent at which dissolved solids in pore water create another conductivity path for electrical current. (It is commonly measured in milli Siemens per meter (mS/m)) while TDS (Total dissolve solid) is the measure of the amount of dissolved solids or dissolved ions in a sample of water. As a result of this, a direct correlation exists between total dissolved solids and electrical conductivity.

6.1.4.1 pH and Ec Interpretation for AU-1 Well.

The pH values obtained from pore water analysis of well AU-1 indicate a range from a slightly acidic medium to a predominant alkaline medium (figure 6.9A below). Values ranged from 6.98-8. The pH values obtained from this well do not support the influence of organic matter maturation within the well, this confirms PASA's geological well completion report on well AU-1 which suggested that there is a lack of a matured source rock within a good migration interval for well AU-1, hence the influence of organic matter on the pH conditions is not expected. The different plots below show values of pH (figure 6.9A) which are slightly extreme at deeper depth, this may signify the solubility of alkali feldspars and the fixation of alkali cations which could be Na^+ , K^+ , Ca^{2+} , or Mg^{2+} ; an indication of alkaline nature of the pore fluid. As mentioned earlier, in a shaly sand formation, two electrical conductivity paths are created; one due to formation water and the other due to clay conductivity. As expected, an increase in pH values corresponds to a decrease in Ec values for well A-U1. The slight reduction in pH value at depth of 2684.67m (figure 6.9A) could be a pointer to the loss of saline bound water by kaolinite which led to a relative increase in acidity and subsequent reduction in pH (Selby and Fateley, 1955). The concentration of dissolved strong cations like Ca, Mg, K, Na, and Al has a significant effects on the value of Ec; they enhance soil Ec in the same way as salinity does (<http://ohioline.osu.edu/aex-fact/0565.html>). As expected, linear correlation between Ec and TDS (Total dissolve solid) exists (figure 6.9 C), also variations of Ec and TDS with depth shows the same trend (figure 6.9 D).

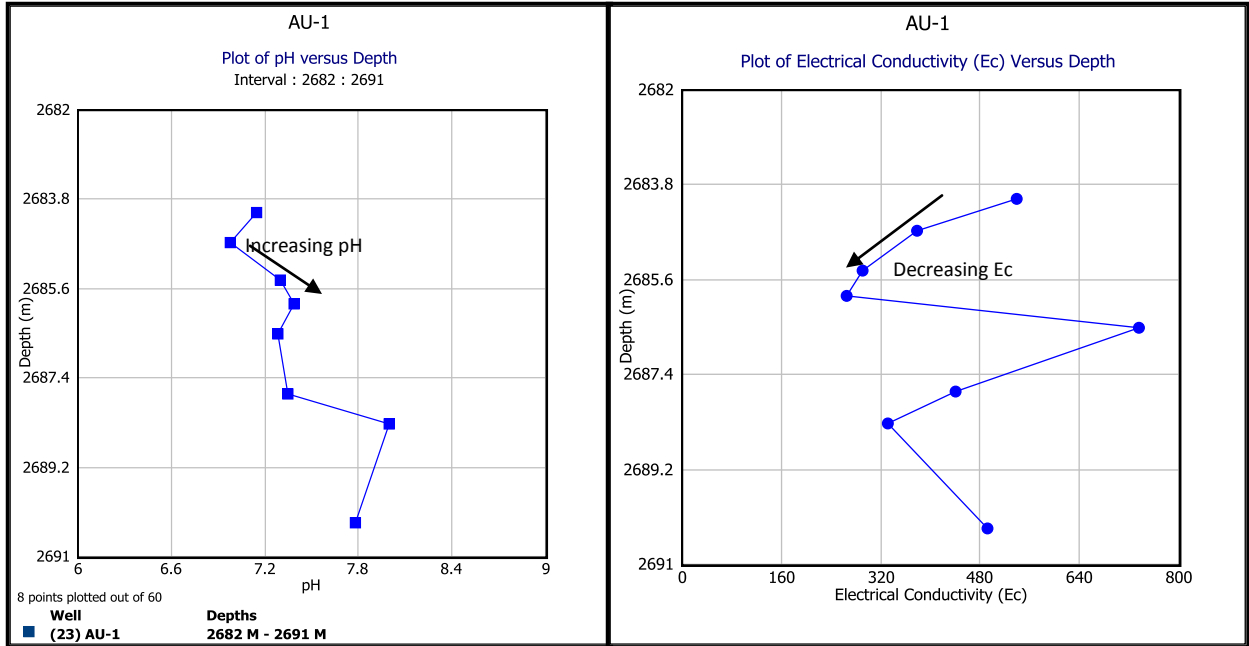


Figure 6.9 A

Figure 6.9 B

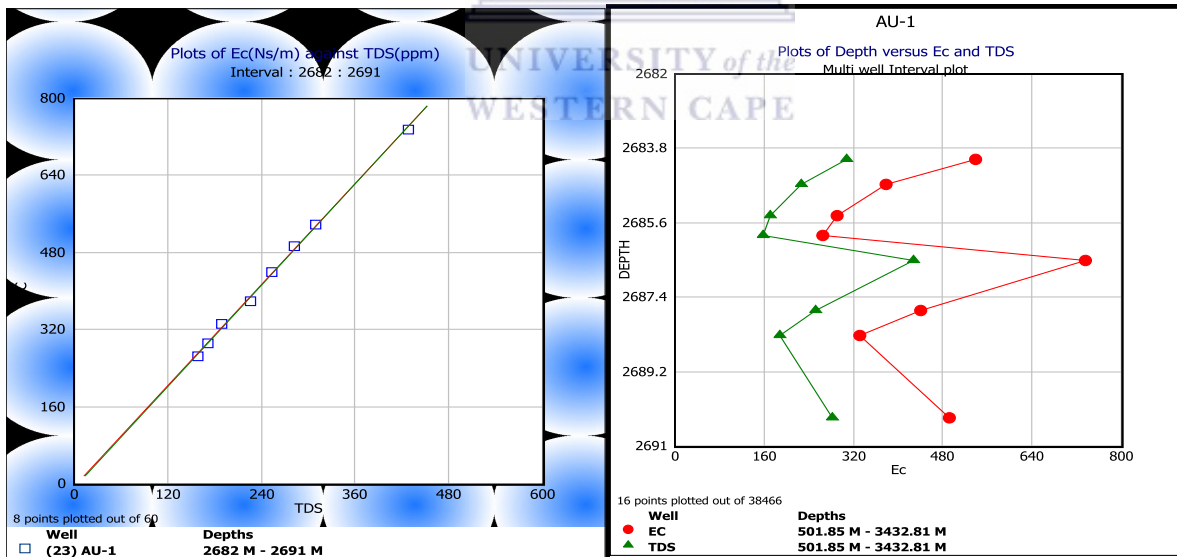


Figure 6.9 C

Figure 6.9 D

Figure 6.9(A-D): Pore water Chemistry plots of AU-1 well

6.1.4.2 pH and Ec Interpretation for KH-1 Well.

Nine pore water samples were extracted from core samples taken from KH-1 and were subsequently subjected to Ec, pH and TDS (Total dissolve solid) analysis after which values obtained were plotted as illustrated below in figure 6.10 A-D. Well KH-1 has a greater thickness of sand bodies intersected within the subsurface when compared to other wells within the block 3A offshore Orange basin according to the PASA geological report. Pore water chemical composition analyses were done for more core samples taken at various depth intervals within the reservoir section. The pH values range from slightly acidic to predominant alkaline, specifically from 6.78-8.34. The highest pH value of 8.34 (figure 6.10) can be attributed to the fixation or dissolution of strong alkali metallic ions in the sediment pore waters or flushing of the reservoirs by hydrothermal a fluid rich in metallic ions. Increase in pH corresponds to an increase in Ec for all depths except for 3068.09m, 3068.92m, 3069.9m and 3070.89m. This anomaly could be explained by the type of dominant clay mineral that are present within the reservoir interval, clay minerals with wider surface area do have higher electrical conductivity and vice-versa (Grim 1951, de Waal, 1989). Generally, it is accepted that when Ec increase, pH should decrease, this is subject to the dominant rock forming minerals of the core samples and thus the lithology. Linear correlation also exists between TDS and EC values which implies that the type and amount of dissolved ions is directly proportional to the electrical conductivity (Ec).

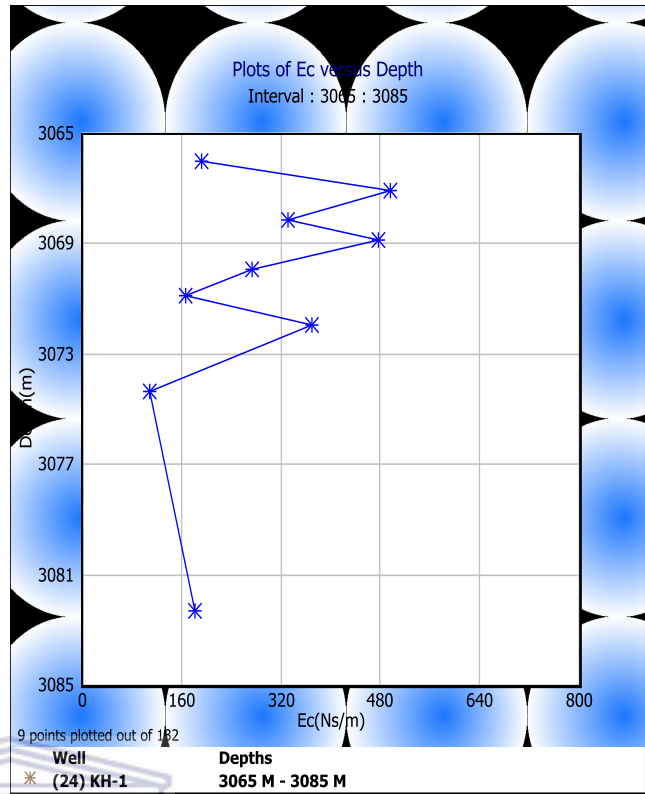
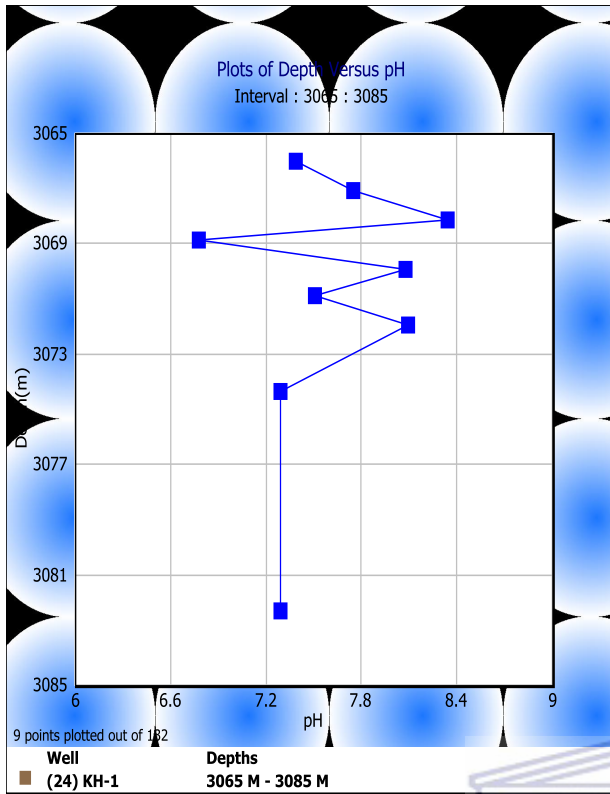


Figure 6.10 A

Figure 6.10 B

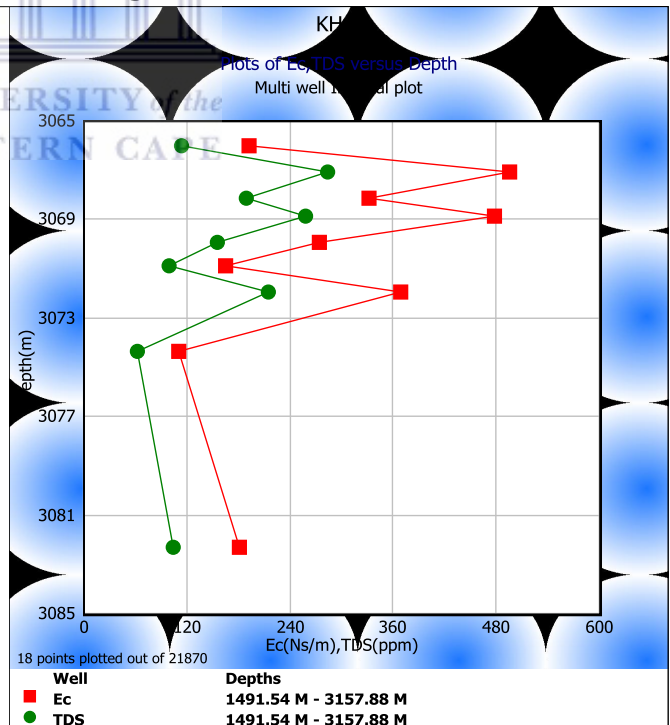
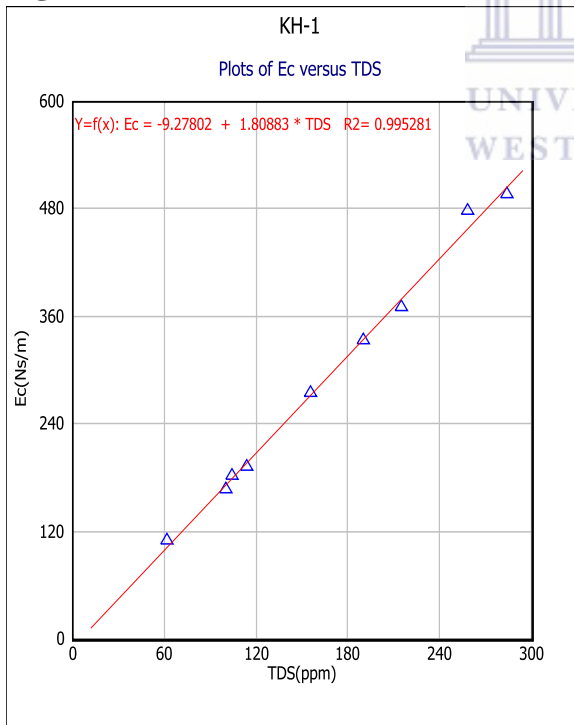


Figure 6.10C

Figure 6.10D

Figure 6.10(A-D): Porewater Chemistry plots of KH-1 well

6.1.4.3 pH and Ec Interpretation for KF-1Well.

Different plots of pore water chemistry for well KF-1 are presented below as figure 6.11(A-D), pH values range from 7.25 to 9.6 which is an alkaline range. An empirical relationship exist between Ec and pH as their corresponding plots against depth show a similar curve signature (Figure 6.11 A and B). As it has been observed in other wells, the regression coefficient value generated from the plots of Ec against pH indicates a linear correlation (figure 6.11C). Also, the data points of electrical conductivity with depth and TDS plot with depth show a similar trend, which is a confirmation to the precision of datasets obtained from the porewater analysis.

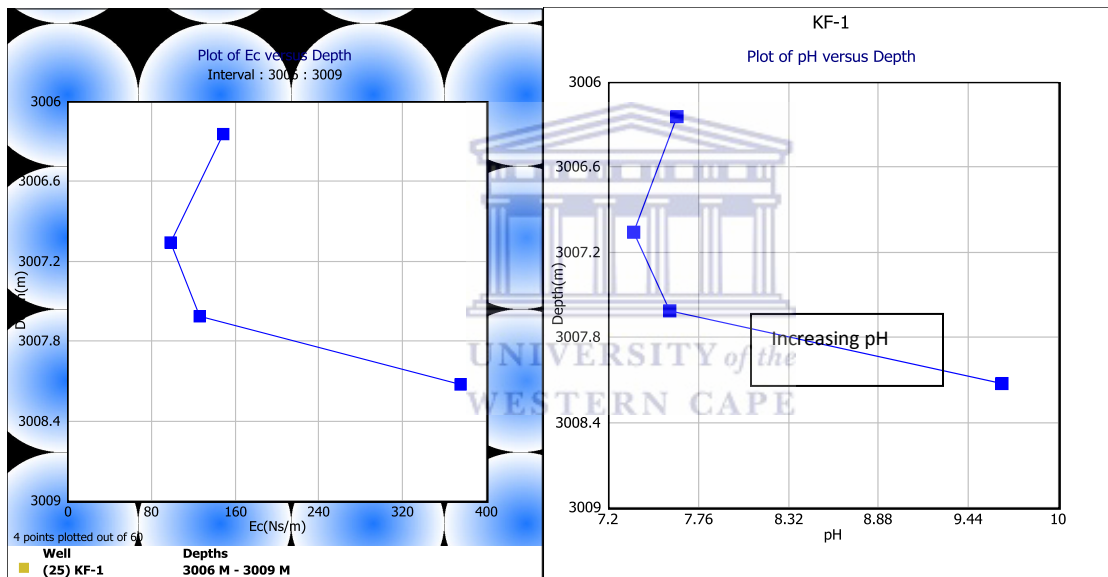


Fig 6.11(A) Plot of Ec versus depth for KF-1 .**Fig 6.11(B)** Plot of pH versus depth for KF-1 well

KF-1

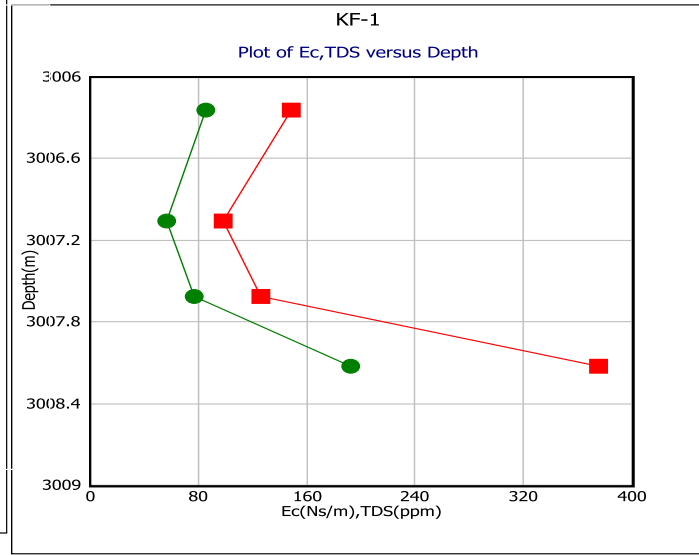
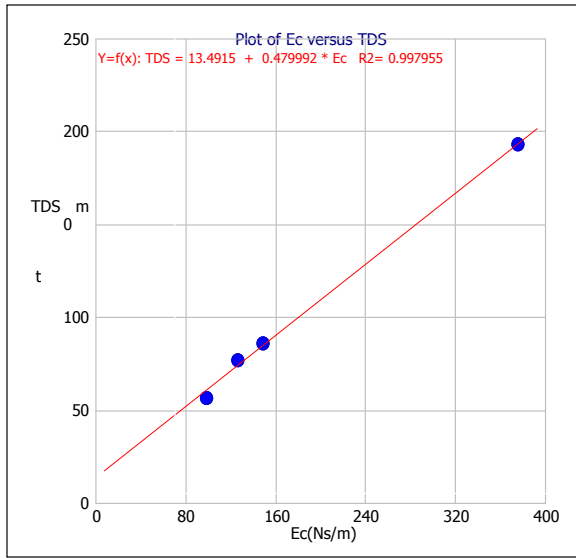


Fig 6.11(C) Plot of Ec versus TDS for KF-1 **Fig 6.11(D)** Plot of Ec,TDS versus depth for KF-1

Figure 6.11(A-D): Pore water Chemistry plots of KF-1 well.



6.1.5 CEC Interpretation for All Wells.

CEC can be defined as the sum of exchangeable cations that can be absorbed at a specific pH on the surface of soil samples. In addition to the potential CEC of clay minerals, organic matter can also significantly affect the CEC of rock samples. For example, the presence of 3-5% organic matter can increase the CEC of rock samples by 20-50% (Gilot, 1987). Clay minerals are generally electrically charged and tend to absorb water by electrostatic forces, the rate of absorption is highly dependent on the exchange capacity of the cations present. It has been observed that the cations exchange capacity of soils rich in kaolinite, halloysite, iron and aluminium oxides is pH dependent (Sawney and Norrish, 1971). The CEC of the clay fraction gives an indication of the nature of clay mineral where only standard analytical data is available. In log interpretation, CEC is proportional to the volume of clay which is also dependent on the activity of the particular type of clay mineral, (Schlumberger, 1972). CEC can be dependent on the total weight of expansible clay minerals present in a rock sample (Ugbo, 2010), this explanation can be given by the proportionality of CEC with surface area and grain charge density (Patchett and Coalman, 1982). Presented in table 6.0 are different CEC ranges for clay minerals.

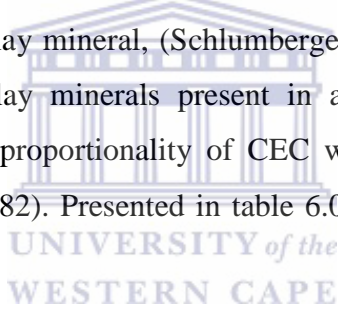


Table 6.0: Table chart of CEC values for different clay minerals. (Patchett and Coalman, op.cit)

Clay Type	CEC meq/g	Neutron Porosity	Average density g/cc	Minor Constituents	Potassium %	Uranium ppm
Montmorillonite	0.8 -1.5	0.24	2.45	Ca, Mg, Fe	0.16	2-5
Illite	0.1 -0.4	0.24	2.65	K, Mg, Fe, Ti	4.5	1.5
Chlorite	0 -0.1	0.51	2.8	Mg, Fe		
Kaolinite	0.03-0.06	0.36	2.65	--	0.42	1.5 -3

Table 6.1 ; Estimated values of CEC for all wells

AU-1		KF-1			KH-1
Depth m	CEC(meq/100g)	Depth (m)	CEC(meq/100g)	Depth (m)	CEC(meq/100g)
2684.05	64.5	3006.25	50.02	3066	52.2
2684.67	54.4	3007.07	14.2	3067	40.5
2685.39	18.7	3007.6	5	3068.09	49.3
2685.84	28.7	3008.13	66.1	3068.92	80.5
2686.51	27			3069.9	39.4
2687.8	64.1			3070.89	82
2688.38	64.7			3072	36
2690.33	38.1			3074.42	7.3
				3082.25	45

6.1.5.1 Cation Exchange Capacity Interpretation of KF-1 well

The CEC measurement was performed on four core samples obtained from well KF-1, the samples were milled into fine powder form and were subjected to the CEC test. The CEC values obtained within well KF-1 range from a lowest value of 5 meq/100g at a depth of 3007.6m to a value of 66.1meq/100g at a depth of 3008.13m (Table 6.3). In well K-F1, a value of 50.02 meq/100g at a depth of 3006.25m indicates the dominance of mixed clay minerals from which a conversion of a clay mineral is being processed, there is suspicion of dominant illite at depth of 3007.07m because of a CEC value of 14.2meq/100g, the illite may have been transformed to montmorillonite at a depth of 3008.13m considering a value of 66.1meq/100g (Table 6.12A). The plot below (figure 6.12A) shows the abundance of calcium ions within well KF-1. Ca

significantly increased from 5 cmol /kg at a depth of 3006.25m to a maximum concentration of 12.5 cmol /kg at a depth of 3007.07m (figure 6.12 A). More calcium ions appeared to have increasingly exchanged for Na, K and Mg at depth 3006.25m which lead to a sudden increase in Ca ions and a corresponding decrease in sodium, magnesium and potassium ions (figure 6.12 A). At a depth of 3007.6m, an increase in concentration of Na, Mg and K corresponds to a decrease in calcium ions concentration. The curves of K and Mg plot almost together, which implies that these cations exist in an almost equal proportion, although with a low concentration value of around 2 cmol /kg (figure 6.12A). With high relative concentration of Ca and Na ions occurring at the exchange sites on the clay surfaces, it is expected that the presence of albite or calcite cement might have been the source of Ca; sodium rich clay (montmorillonite) may also be present at this depth. The occurrence of sodium ion concentration may also be attributed to sea water influence, observations made on XRD confirm this interpretation. The concentration curve of K, Mg and Na follows the same trend while Ca concentration appears opposite. This value suggests the presence of chlorite or illite at the depth of 3007.6m and smectite-illite mixed clays presence within the reservoir at depths of 3006.25m, 3007.05m and 3008.13m(figure 6.12A) (Core Laboratories, 1973). The presence of illite and montmorillonite in well KF-1 is consistent with observations from SEM analysis of the same sample. The presence of organic matter could have significantly increased the value by 20-50% (Gilot, 1987) at this depth, aside from auxiliary cements of calcite that are likely to be present, a strong presence of smectite-illite is also suspected.

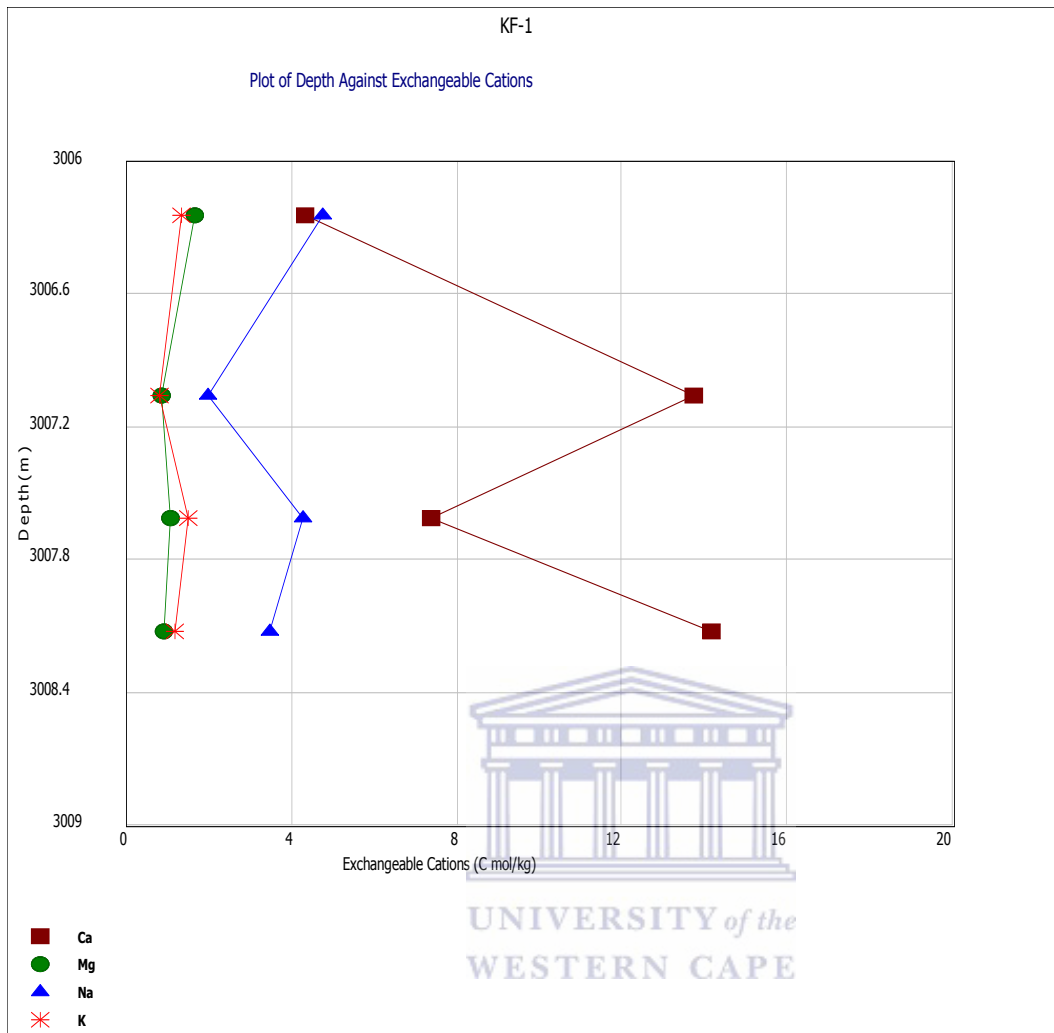


Figure 6.12 A Cations plots of KF-1 well.

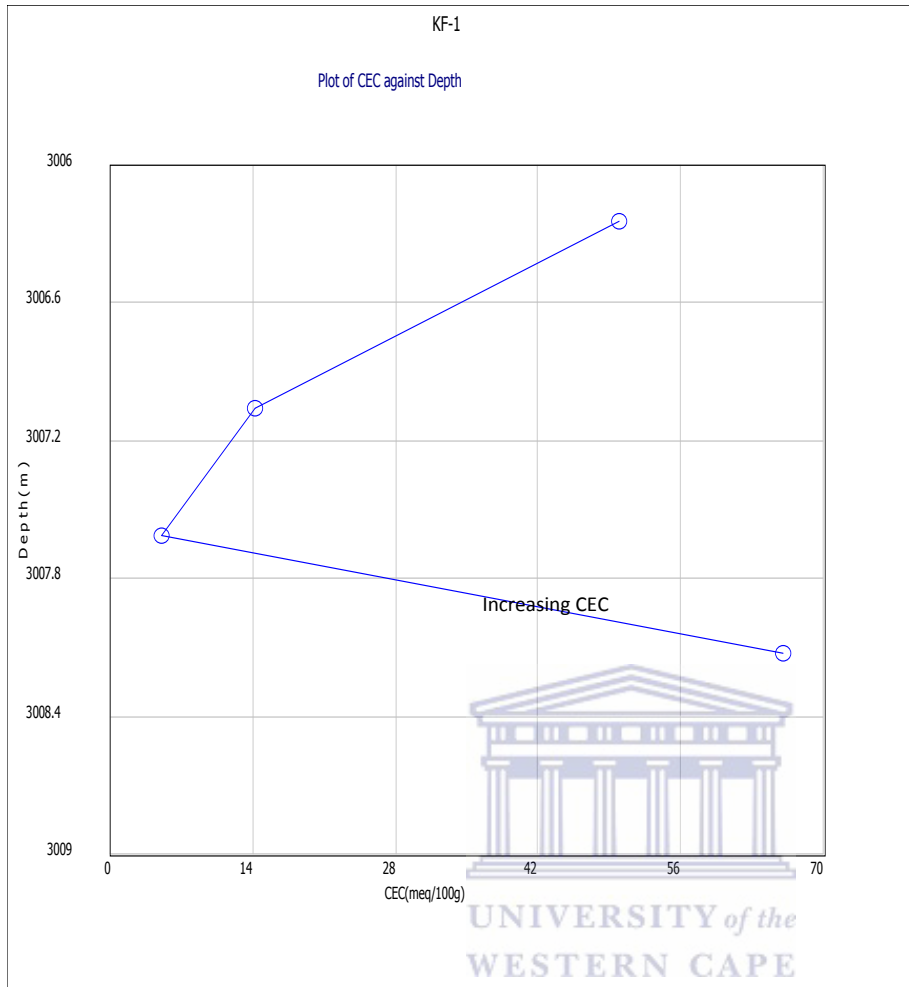


Figure 6.12 B

Figure 6.12(A and B):Cations and Cations exchange plots of KF-1 well.

6.1.5.2 Cation Exchange Capacity Interpretation of AU-1 well.

The relative high concentration of Ca ion also occurs in well AU-1 with a highest estimated value of 19.86 C mol/kg at a depth of 2688.38m to the lowest value of 8 C mol/kg at a depth of 2690.30m. The curve (Figure 6.13 A) below of exchangeable cations indicates that Ca is consistently present with relative higher concentration among all other cations within the well. K increased at a depth of 2686.51m, this could be attributed to the retention of K ions in sandstones following K-Feldspar dissolution (closed system diagenesis) (Fawad et al., 2001). A decrease in K^+ ion concentration from depth 2686.51m to 2688.38m (figure 6.13A) suggests that the potassium retained in sandstone might have been consumed for precipitation of other diagenetic cements (Dutton, 2008). There is almost an equal but increased concentration Mg and K ions from depth 2687.8- 2690.3m (figure 6.13 A), and a corresponding increase in Na ions is noticed between this depth interval; in contrast, a decrease in Ca is noticed within this depth interval. A trend of Ca ion decreases and Na ion increase and vice-versa continues till a depth of 2690.30m where their concentration becomes the same. The reason for this may be due to exchange capacity on montmorillonite surface (as detected by XRD) which always allows Na ion to be substituted for Ca ion and vice versa depending on absorption rate (Rogers, 1963). The CEC values observed at depths of 2684.05 m and 2684.67m are 64.5 meq/100g and 54.4meq/100g respectively (Table 6.0). These values represent mixed layer clay minerals. This assumption is confirmed as K, Mg and Na plots show similar trends at these depths. CEC values of 18.7 meq/100g, 28.7 meq/100g, and 27 meq/100g for depths of 2685.39m, 2685.84m and 2686.51m depict the presence of illite (figure 6.13B). Illitization might have started at depths of 2684.05 m and 2684.67m, probably illitization of montmorillonite. Various clay minerals detected from XRD conform to the observations made from this CEC interpretation.

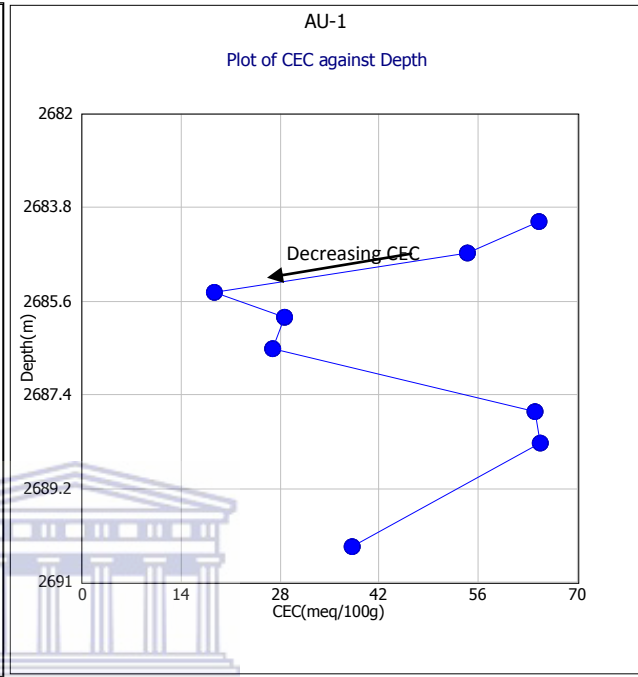
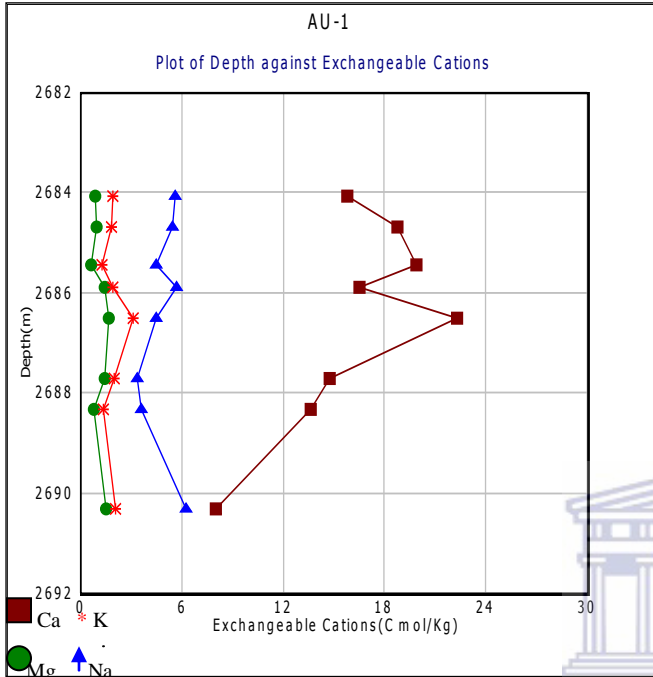


Figure 6.13 A

Figure 6.13 B

Figure 6.13 (A and B): Cations and Cations exchange plot for AU-1 Well

6.1.5.3 Cation exchange capacity interpretation of well KH-1.

Strong presence of Ca ions was once again evident throughout the reservoir interval. Ca has the highest concentration of 19.32 C/mol kg at a depth of 3066m and the lowest concentration of 8.93 C/mol kg at a depth of 3067m (figure 6.14 A). Except at a depth of 3067m, a decrease in Ca ion concentration corresponds to an increase in Na ion concentration at other depths. The concentrations trends of Na, K and Mg appear the same at a depth of 3074.42m with Mg having a higher concentration than Na and K (figure 6.14 A). Mg ion is generally associated with chlorite formation in highly alkaline pore fluids. Having detected the presence of dolomite in well KH-1 at this depth from XRD, it is believed that dolomite might be the source of Mg. Alternatively magnesium can be sourced locally from the alteration of mafic rocks during diagenesis (Uysal et al., 2001b). Na concentration subsequently increased from 1.36 C mol/kg at a depth of 3074.42m to 4.31 C mol/kg at a depth of 3082.25m. Increases in Na ion concentration always corresponds with an increase in CEC values in KH-1 (figure 6.14 A and B). High CEC means significant presence of montmorillonite (Patchett and Coalson, 1982). CEC values range from the lowest value of 7.3 meq/100g at a depth of 3074.42m to a highest value of 82 meq/100g at a depth of 3070.89 m (figure 6.14B). CEC values of 52.2, 40.5 and 49.3 meq/100g for depths 3066m, 3067m and 3068.09m respectively indicate strong presence of illite or chlorite mixed with other clay minerals. The sudden increase of CEC to a value of 80.5 meq/100g indicates the mixed layer may have been dominantly an illite and montmorillonite mixed layer which later transformed into dominant montmorillonite (reversible process) (Stixrude and Peacor, 2002). The fixation of Na from sea water is suspected due to the sudden increment in the values of Na. Illite presence is suspected at a depth of 3074.42 m because of CEC values of 7.3 meq/100g (figure 6.14 B)

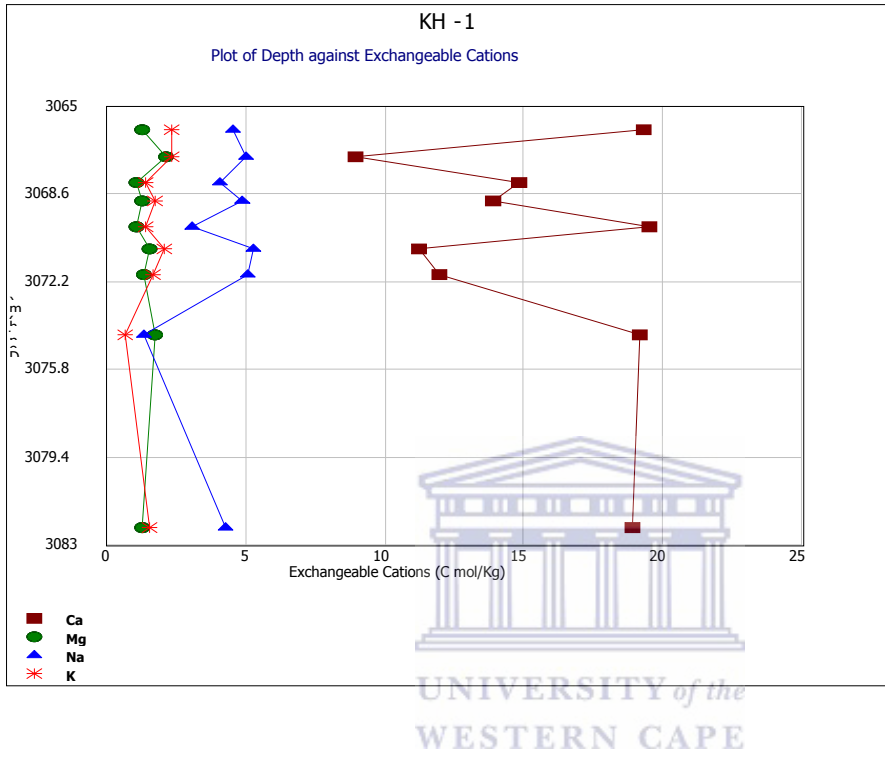
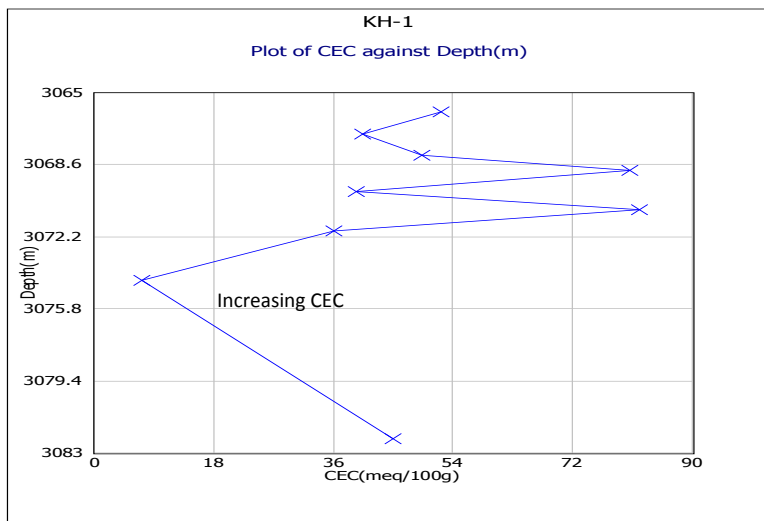


Figure 6.14 (A): Cations plot of KH-1 well



B

Figure 6.14 (B): Cations exchange plot of KH-1 well

Figure 6.14 (A and B). Cations and Cations exchange plot of KH-1 well.

6.1.5.4 Summary of Ph, Ec and CEC Interpretation of All Wells.

Information derived from pore water chemistry analyses and CEC analyses provides an insight into the chemical nature of pore fluids and dominant clay minerals present in the core samples. AU-1 well pore waters show a pH range of 6.98-8 implying dominant alkaline pore fluids. This suggests the presence of strong alkali ions in the pore fluids, the slight acidity observed at 2684.67 m could be linked to the loss of saline bound water by kaolinite which reduces the pH. Values range obtained from CEC analysis indicates dominantly illite and montmorillonite or interstratified illite and montmorillonite while chlorite presence is suspected at depths of 2684.05m and 2684.67m in well AU-1. The cations plots of Mg, Na and K shows a similar trend in contrast to Ca. The cause may have been due to exchanges of other cations for Ca, however, a sudden increase of Ca (figure 6.13) at a depth of 2686.51m may have been due to calcite precipitation which cause increase of Ca abundance. KH-1 alkalinity ranges between 6.78-8.34,

Ec and pH show corresponding trends with depth in the same well except at depths 3068.09m, 3068.92m, 3069.9m and 3070.89m. This may be attributed to the elemental contents of dominant clay minerals present in the core samples, except for depth 3074.42m which has CEC value of 7.3meq/100g (montmorillonite or chlorite), CEC values obtained from other samples in same well indicate illite and montmorillonite mixed clays presence while a sudden increase in Na at a depth of 3070.42 m may be due to albite presence. Well KF-1 has pH values that range between 7.25 and 9.6 which is predominantly alkaline. Calcite, illite and montmorillonite are suspected diagenetic cements.

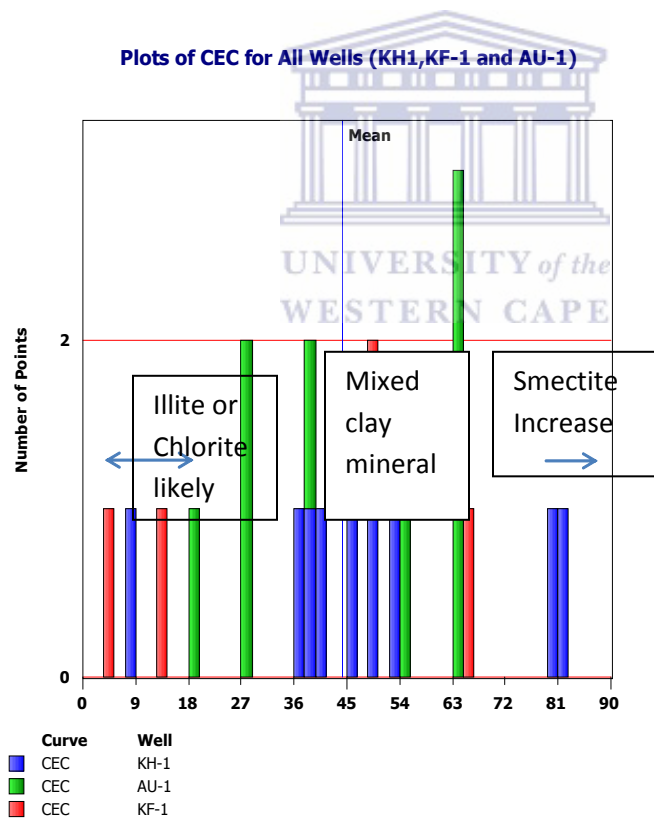


Figure 6.15: Histogram plots of CEC values for the three wells studied

6.1.6 Qv Plots Interpretation

Qv is the cation exchange capacity per pore volume of rock samples and it is mostly used in reservoir characterization as a shaliness indicator of ‘siliciclastic’ reservoir intervals. The higher the Qv value within the reservoir interval, the shalier a reservoir interval is. Qv is normally estimated empirically from Grain density, CEC and Porosity values. The formula relationship is thus established as $Q_v = \text{CEC} \cdot (1 - \Phi) \cdot \text{GD} / (100 - \Phi)$. The importance of Qv in reservoir quality evaluation has been under-emphasized with more focus being on shaliness as a function of the volume of clay. The effects of clay or shale on reservoirs has more to do with the type of clay minerals than the volume of clay, clay minerals with high surface area will indicate more shaliness values than clay minerals with lower surface area.. The plot of Qv against porosity for three wells shows that shaliness is not the major compromise of the reservoir of the quality. In well KF-1 (indicated by purple square spots), the higher the Qv, the lower the porosity values, this probably suggests that clay minerals exert a major influence on the quality of the reservoirs within KF-1 well. Unlike KF-1 reservoirs, reservoirs units within AU-1 and KH-1 wells do not confirm the influence of shaliness as the major compromise of reservoir quality, therefore the influence of clay mineral types exert a major influence on the quality of the reservoirs in KH-1 well (yellow spots; figure 6.16) and AU-1 (blue spots. figure 6.16). Qv plots against porosity for well KH-1 and AU-1 shows an inconsistent trend with depth to underscore the influence of shaliness on the reservoir quality.

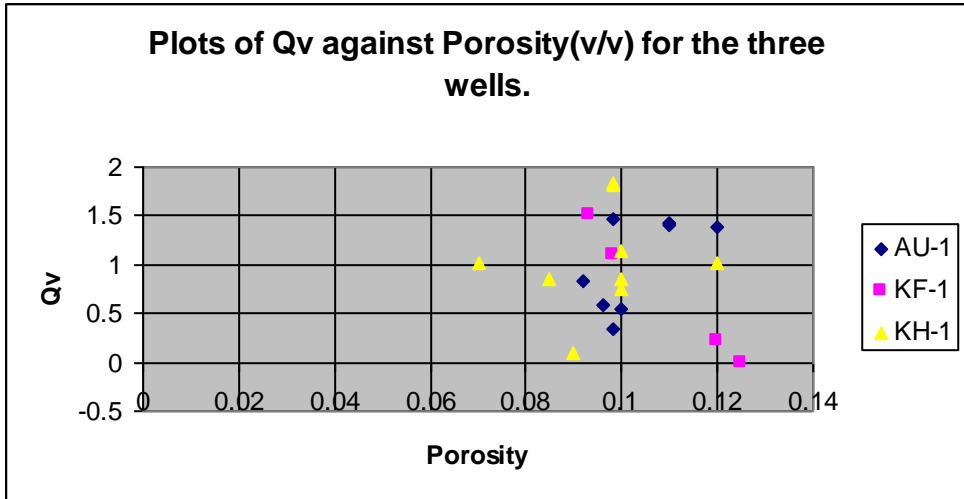


Figure 6.16: Plots of Qv against Porosity for all wells.

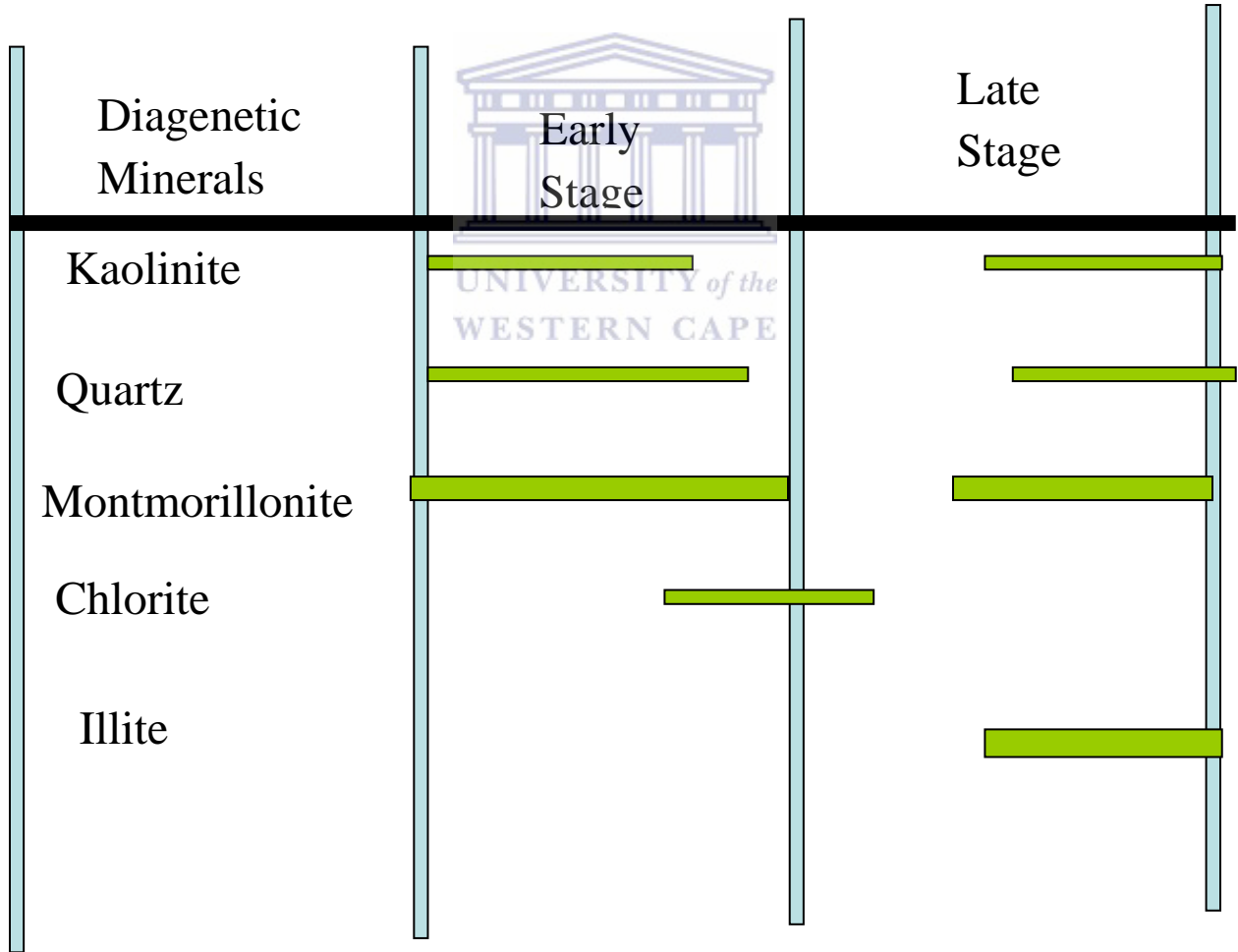
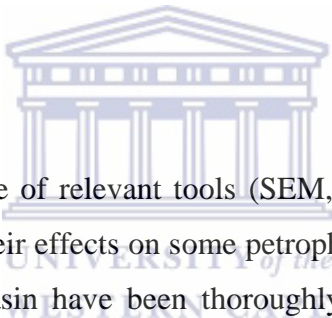


Figure 6.17: Idealized Diagenetic Model of Clay Minerals and some diagenetic cement encountered within Block 3A, Reservoirs, Orange Basin, South Africa

Chapter Seven

7.1 Discussions.



Clay diagenesis study by the usage of relevant tools (SEM,CEC,EDS,XRD ,cores, EC and Ph and wireline logs) to understand their effects on some petrophysical properties of reservoir rocks encountered within the Orange basin have been thoroughly assessed. The assessment results were based on studies made from three wells in block 3A, offshore Orange basin, South Africa. The findings emanating from these assessments are based on cores, logs, geochemical and petrographic studies.

7.2 KF-1 Well.

(A) Core description

Core and lithological description reveals thinly bedded, fine to medium grained sandstones and carbonaceous mudstone predominance, dewatering structures (soft sediment deformation) are prominent in the cores. The rocks encountered within well K-F1 were interpreted to have been deposited under low energy conditions with the alternating fine and coarse grained sedimentation explained as occurring as overbank deposits.

(B) Petrophysical properties

Detailed interpretation of wire line logs reveals an average GR value of 45 API for well KF-1, as well as a hydrocarbon saturation of 14 % and a water saturation of 86%. The Simandoux shaly sand saturation model was used in the estimation of water saturation using the resistivity logs combo. The Simandoux saturation model agrees with values obtained from the conventional core analysis in the well report, hence confirms the reliability of calculating petrophysical properties from wireline logs by the Simandoux model. KF-1 has an average volume of clay of about 20% and an extremely low permeability value in the region of 0.09Md and an average sonic-derived porosity value of about 13.6%. This value (13.6%) is higher than the core porosity value of 10%. Since core analysis always represent the ground truth, it can be concluded that porosity values derived from core analysis is more accurate than the sonic log derived porosity.

(C). Clay mineral Assemblages

In well K-F1, SEM images reveal quartz and kaolinite are consistently present in all samples analyzed; chlorite and montmorillonite presence are also evident. The EDS experiment revealed a consistent presence of Ni unlike AU-1 and KH-1 wells. Nickel is an element often associated with chlorite and Ni-bearing chlorite is called nimmite. Sulphur has been detected which may explain why pyrite is observed in thin section in this well; albite is also present in the sample. XRD confirms the presence of montmorillonite which may also have been converted to illite in the presence of Na and K-feldspar (albitization), hence explains the presence of illite.

(D) Pore water Chemistry and CEC

Well KF-1 has pH values in the range of 7.25-9.6 which is predominantly alkaline. This can explain the presence of calcite, illite and montmorillonite as the major diagenetic cements observed in KF-1 well. Alkaline pore fluids enhance the precipitation of these cements amidst other favourable conditions. CEC analysis also affirms the presence of illite and a mixed layer of montmorillonite and illite because the CEC values range from minimum 5 meq/100g to 66.6 meq/100g. As expected, there is a linear relationship between the TDS (Total Dissolve Solid)

and Ec (Electrical conductivity), this confirms the accuracy of the data obtained from the analysis.

7.3 Well AU-1.

(A) Core description

The sand bodies in well AU-1 consist of dark-grey, fine – medium grained sandstones with an approximate gross thickness of 3.2m; wavy lamination and current ripple marks are prominent throughout the sand body. This is a characteristic feature of a shallow marine sandstone unit of the shelf environment and consequently these sand bodies are interpreted as shallow marine sandstones deposited on the continental shelf.

(B) Petrophysical properties

Well AU-1 reservoir interval has an average of 60 API GR value and an approximate thickness of 3m, an average porosity of 10 %, a VCL of about 32% and an average water saturation of about 65% while permeability is in the region of 0.15Md. From various estimated values of petrophysical properties tabulated below (Table 7.0), it can be inferred that AU-1 and KH-1 reservoirs have a similar quality because of similarities in the values estimated. The major difference is in the water saturation values, which can be attributed to the dominance of montmorillonite in well AU-1 as compared to well KH-1. Montmorillonite has more bound water because of the larger surface area it exhibit.

(C) Clay mineral Assemblages

SEM images reveal the consistent presence of quartz cements throughout the three wells. Kaolinite appears to be postdating quartz cement in well AU-1, while leaching of K-feldspar or muscovite might have accounted for the consistent presence of kaolinite in this well. They (kaolinite and quartz) appear together but with kaolinite appearing just on top of the quartz grains. There is a likely presence of halite or sodium-rich montmorillonite, judging from the consistent presence of Na from EDS results. Furthermore, the presence of iron-rich chlorite is

also possible because of consistent presence of iron as observed from results obtained from EDS (Energy Dispersive Spectrometry).

XRD results reveal that calcite cement precipitation is prominent in well A-U1; its presence confirms the observation made on core descriptions that the reservoir sections encountered in these wells were deposited under shallow marine conditions. The observed presence of quartz cement and kaolinite in the three wells is expected because they are both known to co-exist in a marine environment; illite is absent but muscovite presence is observed. Pyrite presence in AU-1 well suggests a prevailing anoxic environment sometime during deposition. Pyrite identification in the thin sections from well AU-1 also confirms the observation from XRD as to the presence of pyrite.

(D) Pore water Chemistry and CEC

Well AU-1 pore water shows a pH range of 6.98-8 implying predominantly alkaline pore fluids. This suggests the presence of strong alkali ions in the pore fluids, while the slight acidity observed at 2684.67 m could be linked to the loss of saline bound water by kaolinite which reduces the pH. Value ranges obtained from CEC analysis indicate dominant montmorillonite or mixed layer illite and montmorillonite, while chlorite presence is also suspected. The cation plots of Mg, Na and K show a similar trend in contrast to Ca: a sudden increase of Ca at certain depth as observed from cations plot may have been due to calcite precipitation which of course causes an increase in Ca abundance. As expected, there is a linear relationship between the TDS (Total Dissolve Solid) and Ec (Electrical conductivity; this confirms the accuracy of the data obtained from the analyses.

7.4 KH-1 Well

(A) Core description

Well KH-1 has 7m gross thickness of sand, thinly laminated and highly ferruginised; this observation is based on the obvious reddish brown colouration observed during the core

description. Lithologies range from carbonaceous mudstone at 3006m, to fine – medium grained sandstones at 3007m and mudstones at 3008.95m. There is a presence of lithic fragments, mostly angular to sub angular shaped while the sandstone is very massive and parallel laminated. The occurrence of mud layers in the sandstone is evidence that the sand body was subjected to extraneous intermittent flows which allow mud layers to infiltrate the sand body.

(B) Petrophysical properties

Neutron-Density logs were used to calculate porosity values in well K-H1 in contrast to sonic log used in well K-F1. The reservoir interval encountered in well KH-1 is 7m thick and has an average gamma ray log value of 55 API, 8.9% value for average porosity, a volume of clay of less than 30% and a water saturation value of about 50%. The permeability has a total average of 0.15Md. Porosity and permeability may have been compromised by the presence of montmorillonite.



(C) Clay mineral Assemblages

Illite is dominant in KH-1 well samples as observed from the SEM images. The distribution of illite shows a web-like structure which has entangled the pore spaces and is likely to lead to a reduction in fluid flow. Montmorillonite as observed from SEM in well K-H1 may be sodium-rich because of the apparent swelling observed. At depth 3070.89m, illite was observed growing on the surface of montmorillonite. Illite often contains Ti as an elemental composition, thus, the consistent presence of Ti in well KH-1 as revealed from Energy Dispersive Spectrometry (EDS) could be attributed to illite cement presence. XRD affirms all the diagenetic minerals observed on SEM (Scanning Electron Microscopy) images except for the presence of calcite. The presence of albite is also significant because the Na sourced from halite might have favoured the formation of albite.

(D) Pore water Chemistry and CEC

Well KH-1 alkalinity ranges between 6.78-8.34. Ec and pH show a corresponding trend with depth in the same well except at depths 3068.09m, 3068.92m, 3069.9m and 3070.89m. This may be attributed to dissolved cations in the extracted fluid, except at a depth of 3074.42m which has

CEC value of 7.3meq/100g (illite or chlorite). CEC values obtained from other samples in the same well indicate an illite and montmorillonite mixed clay layer presence while a sudden increase in Na at a depth of 3070.42 m may be due to precipitation of albite cement. As expected, there is a linear relationship between the TDS (Total Dissolve Solid) and Ec (Electrical conductivity), this confirms the accuracy of the data obtained from the analyses.

Table 7.0: Table of different Petrophysical properties of Cretaceous Sandstones estimated from Wireline logs processed on Interactive Petrophysics (IP) software.

Wells	Volume of Clay (%)	Porosity (%)	Permeability(Md)	Water Saturation (%)
KF-1	20	13.6	0.09	86
KH-1	30	8.9	0.15	50
AU-1	32	10	0.15	65



7.5 Conclusions

This study has demonstrated that reservoirs encountered in the three wells studied are of similar quality and that specific diagenetic cements are linked to corresponding depositional environments: Calcite presence in wells AU-1 and KH-1 indicates they were deposited in shallow marine conditions, while halite presence confirms the deep marine environment in which KF-1 well was deposited. Glauconite presence, as observed from thin section analysis points to a marine influence in samples analyzed. Aside from dominant quartz cement in all the three wells, calcite, montmorillonite, mixed clays and illite are reservoir challenges and have significantly compromised the quality of the reservoirs. The illite, as inferred from all analyses carried out was formed either from muscovite or transformed from montmorillonite under favourable conditions. The overpressure zone envisaged in the well report of well KF-1 could be linked to the dominant montmorillonite cement presence in this well. Observations made from visual examinations of core samples shows that some section of the reservoir rocks are well sorted and have limited lithic fragments which may reduce porosity and permeability. Therefore, the extremely low petrophysical properties values calculated from wire line logs may have been due

to the precipitation of various diagenetic cements which reduce the porosity and permeability, hence clays and other associated cements exert a major influence on the petrophysical properties calculated. The major clay minerals (illite and montmorillonite) assemblage identified accounts for the low porosity and permeability values obtained from detailed wire line logs analysis of the three wells and usually montmorillonite and illite do have a more devastating effect on reservoir quality than any other type of clay mineral. Based on the integration of all analyses carried out, the most qualitative reservoir zones within the reservoir interval are delineated as 3007.07-3007.6m for well KF-1, 3070.89-3074.42m for well KH-1 and 2684.05-2685.84m for well AU-1. Reservoir qualities of siliciclastic sandstones could improve basinward where depositional and environmental conditions are different and favourable. This may well turn out to be the singular reason why explorers are targeting ultra-deep waters as being done in offshore Niger-Delta and the Gulf of Mexico. It is therefore suggested that the reservoirs in the ultra-deep water of the offshore Orange Basin could be further explored for proven reservoirs with better quality.



REFERENCES

Aagaard, P, and Helgesson, H.C., (1983). Activity/composition relations among silicates and aqueous solutions: II. Chemical and thermodynamic consequences of ideal mixing of atoms on homological sites in montmorillonites, illites, and mixed-layer clays. *Clays Clay Min* 31:207-217

Adekola, S.A., (2010). Integrated Approach to solving Reservoir problems and Evaluations using Sequence Stratigraphy, Geological Structures and diagenesis in Orange basin, South Africa. PhD thesis submitted to the University of the Western Cape. Capetown. South Africa.

Ahmed, I. A. M., Crout, N. M. J., and Young, S. D., (2008). Kinetics of Cd sorption, desorption and fixation by calcite: a long-term radiotracer study. *Geochimica and Cosmochimica Acta*, 72 (6), pp 1498-1512.

Akinlua, A., Smith, R.M., (2009). High Temperature Steam Extraction for the Determination of Aliphatic Hydrocarbon in Petroleum Source Rock. *Chromatographia*, vol. 69, no. 11-12, pp1-7.

Aldrich, J., Zilinski, R., Edman, J., Werner, L., Berge, T., and Corbett, K. (2003). Documentation of a new petroleum system in the South Atlantic. AAPG Annual Convention, Salt Lake City, Abstract A4.

Allen, J.R.L., (1984). Current Ripples; their Relationship to Patterns of Water and Sediment Motion. North-Holland publishing Company, Amsterdam, pp. 433

Almon, W.R., et al., (1981). Formation damage and the crystal chemistry of clays. pp. 81-103 in: *Clays and the Resource Geologist* (F. J. Longstaffe, editor) Min. Soc. Canada, Short Course Handbook 7.

Almon, W.R., and Davies, D.K., (1979). Regional diagenetic trends in the lower Cretaceous Muddy Sandstone, Powder River Basin. pp. 379--400 in: *Aspects of Diagenesis* (P. A. Schoue and P. R. Schluger, editors). SEPM Spec. Publ. 26.

Al-Ramadan, K., Morad, S., Proust, J. N., and Al-Aasm, I., (2005). Distribution of diagenetic alterations in siliciclastic shoreface deposits within a sequence stratigraphic framework: evidence from the Upper Jurassic, Boulonnais, NW France. *Journal of Sedimentary Research*, 75, pp 943-959.

Anjos, S .M .C., De Ros, L. F., and Silva, C. M. A., (2003). Chlorite authigenesis and porosity preservation in Bengal Basin, Bangladesh . *Journal of Asian Earth Sciences*, 35(1): pp 89-100. the upper Cretaceous marine sandstones of the Santos Basin, offshore eastern Brazil [J].

Archie, G.E., (1942). The Electrical resistivity log as an aid in determining some reservoir characteristics. *Transaction of AIME* 146; pp 54

Archie, G.E., (1950). "Introduction to petrophysics of reservoir rocks". *American Association of Petroleum Geologists Bulletin* 34 (5): pp943–961.

Armitage, P.J., Worden, R.H., Faulkner, D.R., Aplin, A.C., Butcher, A.R., and Iffle, J., (2010). Diagenetic and sedimentary controls on porosity in Lower Carboniferous fine grained

lithologies, Krechba field, Algeria; A petrological study of a cap rock to a carbon capture suite
Journal of Marine and Petroleum Geology vol 27, pp 1395-1410.

Bailey, S.W., (1980). Summary of recommendations of AIPEA nomenclature committee on clay minerals. Am. Miner. 65, pp1-7.

Bailey S.W. (1988). Chlorites: structures and crystal chemistry. pp. 347-403 in: Hydrous Phyllosilicates (Exclusive of Micas) (S. W. Bailey, editor). (Reviews in Mineralogy, vol. 19). Mineralogical Society of America, Washington, DC. United States.

Bain D.C., (1977). Geoderma 17, pp19

Barton, K.R., Muntingh, A., and Noble, R.D.P., (1993). Geophysical and Geological Studies Applied to the Hydrocarbon Exploration on the West Coast Margin of South Africa, Extended Abstracts of the third International Congress of the Brazilian Geological Society, Rio De Janeiro, 1993.

Bates, R.E and Jackson, J. A ed. (1987). Glossary of geology, 3rd ed. Alexandria, Virginia, American Geological Institute, pp 65, 123, 262, 432.

Bayliss, P., (1975): Nomenclature of the trioctahedral chlorites. Journal of Can. Miner. Vol 13, pp178-18.

Beard, D.C., and Weyl, P.K., (1973). Influence of Texture on Porosity and Permeability of Unconsolidated Sand AAPG Bulletin, February 1973, v. 57, pp 349-369

Beaufort, D., Cassagnabe`re, A., Petit, S., Lanson, B., Berger G., Lacharpagne J.-C. and Johansen H., (1998) . Kaolinite-to-Dickite conversion series in sandstone reservoirs. Clay Minerals, 33, pp 297 -316.

Berger, A., Gier, S., and Krois, P., (2009). Porosity-preserving chlorite cements in shallow-marine volcanoclastic sandstones: Evidence from Cretaceous sandstones of the Sawan gas field, Pakistan AAPG Bulletin Volume 93, Issue 5, pp 595 – 615

Berger G., Lacharpagne J.-C., Velde B., Beaufort D. and Lanson B. (1997) . Kinetic constraints for mineral reactions in sandstone/ shales sequences and modelling of the effect of the organic diagenesis. *Applied Geochemistry*, vol.12, pp 23- 35.

Berger, G., Lacharpagne J.-C., Velde B., Beaufort D. and Lanson B. (1995) . Mécanisme et contraintes cinétiques des réactions d'illitisation d'argiles sédimentaires, déduits de modélisations d'interaction eau-roche. *Bulletin de Centre de Recherche Exploration et Production*, 19, pp 225-234.

Bilbey, S. A., Kerns, R. L., and Bowman, J. T., (1974). Petrology of the Morrison Formation, Dinosaur Quarry Quadrangle, Utah: Utah Geological and Mineral Survey Special Studies 48, pp 15

Bjørlykke, K., (1998). Clay mineral diagenesis in sedimentary basins, a key to the prediction of rock properties: examples from the North Sea Basin. *Clay Miner.*, 33, pp15-34.

Bjørlykke, K., (1997). Lithological control on fluid flow in sedimentary basins. In B.Jamtveit and B.Yardley (editors). *Fluid flow and transport in rocks-Mechanism and effects*. Chapman and Hall. London in press Carbonate diagenesis in non-marine carbonate foreland sandstones at the western wedge of Alleghanian overthrust belt, Southern Appalachians. In carbonate cementation in sandstones: Distribution patterns and geochemical evolution (ed. S. Morad). *International association of sedimentologists*. Oxford volume 26. pp 87-105

Bjørlykke, K., Aagard, P., and Egerberg K., (1995). Geochemical constraints from formation water analyses from the North Sea and Gulf Coast Basins on quartz, feldspar and illite precipitation in reservoir rocks. *The Geochemistry of Reservoir Geological Society Special publication No. 86*. pp. 33 – 50.

Bjørlykke, K., Nedkvitne, T., Ramm, M., and Saigal G.C., (1992). Diagenetic process in the Brent Group (Middle Jurassic) reservoirs of the North Sea: An overview. pp. 263-287 in: *Geology of the Brent Group* (A.C. Morton, R.S. Haszeldine, M.R. Giles and S. Brown, editors). Special Publication 61. Geological Society, London.

Bjørlykke K., Aagaard P., Dypvik H., Hastings D.S. and Harper A.S. (1986). Diagenesis and reservoir properties of Jurassic sandstones from the Haltenbanken area, offshore Mid-Norway.

pp. 275- 286 in: Habitat of Hydrocarbons on the Norwegian Continental Shelf (A.M. Spencer, editor). Graham & Trotman, London.

Bjorlykke, K., (1984). Formation of secondary porosity: how important is it? [In:] D.A. McDonald & R.C. Surdam (Eds): Clastic Diagenesis. American Association of Petroleum Geologists, Memoir 37, pp 277–286.

Bjorlykke, K., (1983). Diagenic reactions in sandstones. In: Parker, A., Sellwood, B.W. (Eds.), Sediment Diagenesis. Reidel Publishing, Holland, pp. 169–213.

Bjørkum, P. A., (1996). How important is pressure in causing dissolution of quartz in sandstones? Journal of Sedimentary Research, 66, pp. 147–154

Bjørkum, P.A. and Nadeau, P.H., (1998). Temperature controlled porosity/permeability reduction, fluid migration, and petroleum exploration in sedimentary basins. Australian Pet. Prod. & Expl. Assoc. Journal, vol 38, 453-464.

Bloch, S., Lander R. H., and Bonnell, L., (2002). Anomalously high porosity and permeability in deeply buried sandstone reservoirs: Origin and predictability. AAPG Bulletin. 2002. 86(2): 301-328

Bloch, S., (1994) .Effects of detrital minerals composition on reservoir quality, in Wilson, M.D Ed, Reservoir quality assessment and prediction in clastic rocks. Vol 30. Society of economic palaeontologist and mineralogist short course pp 161-182.

Boles J.R., and Francks G.S., (1979). Clay diagenesis in Wilcox sandstones of Southwest Texas: Implications of Smectite diagenesis on sandstone cementation. Journal of Sedimentary Petrology, vol.49, pp55 -70.

Broad, D., (2004). South Africa Activities and Opportunities. An Unpublished Power Point Presentation to Petro China.

Broad, D.S., Jungslager, E.H.A., McLachlan, I.R and Roux, J., (2007). Offshore Mesozoic Basins, Geology of South Africa, pp 553 – 565.

Brown, L.F., Brown, L.F, Jr., Benson, J.M., Brink, G.J., Doherty, S., Jollands, A., Jungslager, E.H.A., Keenan, J.H.G., Muntingh, A and Van Wyk, N.J.S., (1996). Sequence stratigraphy in offshore South Africa divergent basins. An atlas on exploration for cretaceous lowstand traps by SQEKOR (Pty) Ltd. Am. Ass. Petro. Geol. Stud. In Geology. 41, pp 184.

Burley, S.D., Leeson, T.H., and Worden, R.H., (1985). Sandstone Diagenesis: the evolution of sand in sandstone. In sandstone Diagenesis Recent and Ancient, Burley, S.D; and Worden, R.H, (eds) Blackwell Publishing. vol. 4. pp 656.

Burley S.D., & Mac Quaker J.H.S., (1992). Authigenic clays, diagenetic sequences and conceptual diagenetic models in contrasting basin-margin and basin center North Sea Jurassic sandstones and mudstones. Pp. 81 110 in: Origin, Diagenesis and Petrophysics shelf. Clay Minerals, 24, pp 233- 253.

Burst, J.F., (1969). Diagenesis of Gulf coast clayey sediments and its possible relation to petroleum migration. Am. Assoc. of Petroleum. Geol. Bull. 53, pp73-93.

Buyukutku, A.G., (2003). The diagenesis of middle Eocene Sandstones from the Western Thrace Basin, Turkey. Journal of Geological Society of India. Vol.62, pp. 83-90 July 2003

Campher, C., (2009). Geological modeling of the offshore Orange basin, west coast of South Africa. Poster presentation at AAPG International Conference and Exhibition, Rio de Janeiro, Brazil, November 15-18.2009.

Chamley, H. (1994). Clay mineral diagenesis In: Quantitative Diagenesis: Recent Developments and Applications to Reservoir Geology (Ed. By A. Parker and B.W Sellwood), Kluwer Academic Dordrecht pp. pp161-188.

Chamley and Weaver (1989). Introduction to clay sedimentology .Publisher: Springer-Verlag
Language: English ISBN-10: 0387508899 ISBN-13: 978-0387508894

Choo, O.C., Young, S.S., In Seok, K., (2002). Mineralogical evidence for red coloration of sandstones at Chilgok Formation of the Cretaceous Hayang Group, SouthEastern Korea, Geosciences Journal, vol.6, No. 2. pp 141-148.

Chuhan, F.A., Bjørlykke, K., and Lowrey, C., (2001).Closed-System Burial Diagenesis in Reservoir Sandstones Journal of Sedimentary Research; January 2001; v. 71; no. 1; pp 15-26;

Civian, F., (2007) .Reservoir formation damage 2nd edition ISBN-13: 978-0-7506-7738-7.

Clavier, C., Coates, G and Dumanoir, J., (1984) . Theoretical and Experimental bases for the Dual-water Model for interpretation of shaly-sands. SPE Journal, Vol; 24, no 2; pp153-168.

Clavier, C., Huyle, W.R and Meunier, D., (1971). Quantitative Interpretation of T.D.T Logs; Part 1 and 11, Journal of Petroleum Technology, vol.23, No. 6.

Coates, G and Denoo, S., (1981). The producibility answer product. The technical Review Schlumberger, Houston, No.2; pp 55-63.

Cocker, J. (1986). The reservoir properties and diagenesis of the Brent Group: a regional perspective Geological Society, London, Special Publications, 1992, 61: pp 289-327, doi:10.1144/GSL.SP.1992.061.01.16

Core Laboratories (1982). A course in special Core Analysis 5-21, Dallas. United States.

Core Laboratories (1973). A course in the Fundamentals of Core Analysis: Texas core laboratories, Inc; pp 256.

Curtis, C. (1983). Geochemistry of porosity enhancement and reduction in clastic sediments. In : J. Brooks (Ed), Petroleum Geochemistry and Exploration of Europe. Geol. Soc. London. Spec publ., v, 12, pp 113-125.

De Ros, C., (2009). Intergrated Petrographic,Stratigraphic and Statistical Analysis of complex Albian Reservoirs in the Espirito Santos basin, Eastern Brazil. A paper presented at AAPG international conference and exhibition, Rio de Janeiro, Brazil. 2009

De Waal, J. A. (1989). Influence of clay distribution on shaly sand conductivity. SPE Formation Evaluation, 4(3), pp 377-383.

Dutta, P.K. and Suttener I.J. (1986). Alluvial sandstone composition and paleoclimate11.authigenic mineralogy. Journal of sedimentary Petrology 56, pp 346-358.

Dutton, S.P. (2008). Calcite cement in Permian deep water sandstones, Delaware Basin, West Texas. Origin, distribution and the effect of the reservoir properties. AAPG Bulletin, v.92; no. 6, pp 765-787.

Dypvik, H., and Eriksen, D.Ø., (1983). Natural radioactivity of clastic sediments and the contributions of U, Th and K. Journal of Petroleum Geology 5, 409-416

Eckert H., Yesinowski, J.P., Silver, L A., and Stolpe E.M., (1988). Water in silicate glasses: quantitation and structural studies by proton solid echo and magic angle spinning NMR methods The Journal of Physical Chemistry 1988 92 v7, pp 2055-2064

Ehrenberg, S.N., (1991). Kaolinized, potassium-leached zones at the contacts of the Garn Formation, Haltenbanken, mid-Norwegian continental shelf. Marine Petroleum Geology, **8**, 250-269.

Ellis, D.V and Singer, J.M (2007). ‘Clay Quantification’, Well Logging for Earth scientist. 2007

Emery, D., Myers, K.J., and Young, R., (1990). Ancient subaerial exposure and freshwater leaching in sandstones. Geology 18, pp1178–1181.

Esteoule –Choux., (1983). Kaolinitic Weathering profiles in Brittany: genesis and economic importance In: WILSON RCL (ed) Residual Deposits: surface related weathering process and materials. Geological society of London special publications, vol 11, pp33-38

Fatti, J.L., Vail, P.J., Smith, G.C., Strauss, P.J. and Levitt, P.R., (1994) . Detection of gas in sandstone reservoirs using AVO analysis: A 3-D seismic case history using the Geostack technique: Geophysics, 59, pp1362-1376

Fawad, A., Chuhan, L., Bjorlykke, K., and Lowrey, C., (2001). Closed-System Burial Diagenesis in Reservoir Sandstones: Examples from the Garn Formation at Haltenbanken Area, Offshore Mid-Norway doi: 10.1306/041100710015 Journal of Sedimentary Research January 2001 v. 71 no. 1 pp 15-26

Folk, R.L. (1980). The Petrology of Sedimentary Rocks. Austin, Texas, Hemphill Publishing Company. 182 pp. ISBN 0-914696-14-9 .Sedimentology and Stratigraphy [Gary Nichols] on Amazon.com. *FREE* ... Publication Date: May 26, 2009 | ISBN-10: 1405135921 | ISBN-13: 978-1405135924

Garven, G., (1986). The role of regional fluid flow in the genesis of the Pine Point deposits, western Canada sedimentary basin. *Economical geology*, vol 81, no 4, pp 1015

Gerrard, I. and Smith G.C., (1982). Post-Paleozoic Succession and Structure of the Southwestern African Continental Margin, *Studies in Continental Margin Geology*, AAPG memoir 34, pp 49 – 74.

Gilot, J.E., (1987). Clay in Engineering Geology. *Developments in Geotechnical Engineering*, 41 Elsevier, Amsterdam pp 468

Greensmith, J.T. (1989). *Petrology of the Sedimentary Rocks* 7th edition Unwin Hijman Ltd.China

Grigsby J. D., (2001). Origin and growth mechanism of authigenic chlorite in sandstones of the lower Vicksburg Formation, South Texas. *Journal of Sedimentary Research*. Vol. 71(1): pp 27-36

Grim, R. E., (1951). The depositional environment of red and green shales: *J. Sed. Petrology*, v. 21, pp 226-232.

Guven, N., (1988). Smectites. In: Bailey W (ed) *Hydrous phyllosilicates (exclusive of micas)*. *Rev Mineral* 19:497–559.

Guven, N., Hower, W. F., and Davies, D. K., (1980). Nature of authigenic illites in sandstone reservoirs: *Journal of Sedimentary Petrology*, v. 50, pp 761–766.

Hancock N.J., and Taylor A.M., (1978). Clay mineral diagenesis and oil migration in the Middle Jurassic Brent sand formation. *Journal of the Geological Society of London*, 135, pp 69-72.

Hassan, M., Hossi, A., and Combaz, A., (1976). Fundamentals of the differential gamma ray log Interpretation technique. SPWLA 17th Ann. Symp., Paper 1976-H, pp: 1-18.

Hartwig, A., Boyd, D., Kuhlmann, G., Adams, S., Anka, Z., di Primio, R. and Albrecht, T. (2010). Characterization of Hydrocarbon Generation and Migration Dynamics Based on Seismic Interpretation and Basin Modeling: an Integrated Study of the Orange Basin, South Africa. AAPG International Conference and Exhibition (Calgary, Canada 2010).

Huang, H., Bowler, B. F. J., Oldenburg, T. B. P., Larter, S. R., (2004). The effect of biodegradation on polycyclic aromatic hydrocarbons in reservoir oils from the Liaohe basin, NE China. *Org. Geochem.*, 35(11-12), pp 1619–1634

Hurst, A., (1987). Problem of reservoir characterization in some North Sea sandstone reservoirs solved by the application of Micro scale geological data. *North Sea Oil and Gas reservoirs*, Graham and Trotman; pp153.

Hurst, A. and Archer, J.S., (1986). Reservoir description: an overview of the role of geology and clay mineralogy. *Clay Miner.* 21, pp791-811

Hurst, A. and Buller, A.T., (1984). Dish structures in some Paleocene deep-sea sandstone (Norwegian Sector, North Sea): origin of the dish-forming clays and their effect on reservoir quality. *J. Sedim. Petrol.* 54, pp 1206-1211

Hurst, A. and Irwin, H., (1982). Geological modelling of clay diagenesis in sandstones. *Clay Miner.* 17, pp 5-22.

Imam, M., (1994). Stratigraphic evolution and geochemistry of the Neogene Surma Group, Surma Basin, Sylhet, Bangladesh. Imam MB (1994) X-Ray Diffraction Study on Neogene Shales from Patharia Anticline, Eastern Bangladesh, with emphasis on Smectite clay Dehydration and Implications. *J Geol Soc India* 44: pp547–561.

Jikelo, A.N., (2000). Petroleum Prospectivity of deepwater orange Basin, South Africa
Petroleum Agency S.A, Parow ,South Africa.

Jikelo, A.N. (1999). Oil and Gas potentials of the South African offshore basins. J Afr. Earth Sci, GSA 11, abstracts 33. (PRI 49).

Jinglan, L., Morad, S. and Zhang X., (2002). Reconstruction of the diagenesis of the fluvial-lacustrine-deltaic sandstones and its influence on the reservoir quality evolution—Evidence from Jurassic and Triassic sandstones, Yanchang Oil Field, Ordos Basin. Sciences in China (Series D), 45(7): 616~634

Juhasz, I., (1990). Core Analysis: Opportunities and challenges in the 1990s: European core analysis Symposium; 1-15.

Juhasz, I., (1981). Normalized Qv- the key to shaly sand evaluation using the Waxman-smith's equation in the absence of core data. Transaction of SPWLA 22nd Annual logging Symposium, pp 1-36.

Jun, P., Jinku, L., Yan, W., and Jianfeng, L.,(2009). Origin and controlling factors of chlorite coatings—an example from the reservoir of T3x Group of the Baojie area, Sichuan Basin, China Scientific Research Department, Southwest Petroleum University, Chengdu, Sichuan 610500.

Krygowski, D.A., (2003). Guide to petrophysical Interpretation. Austin Texas USA). Petroleum Prospectivity of the Deepwater Orange Basin, South Africa .Petroleum Agency, Parrow. South Africa.

Kulhlamm G., Paton D., di Primio, Van der spuy D. and Horsfield B., (2007). Petroleum system modeling at a passive continental margin setting, Orange Basin (SouthAfrica). Jahrestagung der Afrikagruppe deutscher Geowissenschaftler (Potsdam).

Kupez, J., Gluyas, J. and Bloch, S., (1997). Reservoir Quality Prediction in Sandstones and Carbonates, Volume 69 of AAPG Memoir series ISBN0891813497, 9780891813491.

Landers, M., Gilkes, R. J., and Wells, M. A. (2009). Rapid dehydroxylation of nickeliferous goethite in lateritic nickel ore: X-ray diffraction and TEM investigation. Clays and Clay Minerals, 57(6), pp751-770.

Lanson, B., Beaufort, D., Berger, G., Bauer, A., Cassagnabè, A. and Meumier, A., (2002) : Authigenic kaolin and illitic minerals during burial diagenesis of sandstones: A review. *J. Clay and Clay minerals*, 37, pp 1-22

Levorsen, A.I., (1967). *Geology of Petroleum*, 2nd Edition; W.H Freeman and Co; San Francisco, United States.

Li, H. J., Wu, T. R., and Wu, B., (2004). Distribution and controlling factors of high quality clastic deeply buried reservoirs in China. *Geological Science and Technology Information*. 2004. 23(4): 76-82 (in Chinese).

Maachi, et al., (1986). Diagenetic controls on reservoir quality in Permian Rotliegende sandstones, Jupiter Fields area, southern North Sea. *Geological Society, London, Special Publications*, 1997, 123:105-122, doi:10.1144/GSL.SP.1997.123.01.07

Macdonald, D., Gomez-Perez, I., Franzese, J., Spalletti, L., Lawver, L., Gahangan, L., Dalziel, I., Thomas, C., Trewin, N., Hole, M. and Paton, D., (2003). Mesozoic break up of SW Gondwana: implications for regional hydrocarbon potential of southern South Atlantic Marine. *Petroleum Geology* vol 20, pp 287-308

Mackenzie, F. T. and Gees, R., (1971). Quartz: Synthesis at earth-surface conditions. *Science*, 173, pp 533-535.

MacLuagling, O.M., Haszeldine, R.S., Fallick, A.E., and Rogers G., (1994). The case of the missing clay, aluminium loss and secondary porosity. South Brae oilfield. Northsea. *Clay minerals journal* Vol 29, pp 651-663.

Magoon, L. B., and Beaumont, E. A., (1999). Petroleum systems, in *Exploring for oil and gas traps* edited by E. A. BEAUMONT and N. H. FOSTER: Tulsa, Oklahoma, USA, American Association of Petroleum Geologists, *Treatise of Petroleum Geology*, pp. 59–92.

Mazullo, S.J., (1985). Pennsylvanian facies-diagenetic reservoir, Lower Strawn formation, Seminole South –east Field, Midland basin, West Texas. In P.O.Roehl and P.W Choquette (Editors), *Carbonate Petroleum reservoirs*, Springer Verlag, New york pp 227-238

Mc Bride, E.F., (1989). Quartz cementation in sandstones; a review. *Earth sci. Rev.* 26. pp 69-112

Morad, S., Al-Aasm, I.S., Ramseyer, K., Marfil, R., and Aldahan, A.A., (1990). Diagenesis of carbonate cements in Permo-Triassic sandstones from the Iberian Range, Spain: evidence from chemical composition and stable isotopes. *Sedimentary Geology* 67, pp 281– 295.

Muller, G., (1967). Diagenesis in argillaceous sediments In: G .Larsen and G.V. Chilingar (Editors).*Diagenesis in sediments.* Elsevier, Amsterdam pp.127-177

Nadeau, P.H., and Bain, D.C., (1986). Composition of Some Smectites and Diagenetic Illitic Clays and Implications for their Origin. *Clays and Clay Minerals*, v. 34, no.4, p. 455-464.

Nadeau, P.H., Wilson, M.J., McHardy, W.J., and Tait, J.M. (1984). Interstratified Clays as Fundamental Particles. *Science, New Series*, v. 225, no. 4665, pp 823-925.

Nichols (2009). *Sedimentology and Stratigraphy* ISSN 9781405193795_4_002 Final Proof page 20.

Nieto, Rojas N (1998). Caracterización geológica y petrofísica del yacimiento K2 en los campos Apiay, Suria y Libertad. *ECOPETROL*, Internal reporte.

Nyberg, O., Lien, K., Lingberg, P.A. and Smistad, J.K., (1978). Mineral composition, an aid classical log analysis used Jurassic sandstones of the Northern Sea: *SPWLA 19th Annual Logging Symposium*; 1- 35.

Odin, G.S. and Matter, A., (1981). De glauconiarum origine. *Sedimentology*, In: Banerjee, S; Jeevankumar, S. and Eriksson, P.G. Mg-rich Ferric illite in marine transgressive and highstand system tracts: Example for Paleoproterozoic Semri Group, central India. *Precambrian Research* 162 (2008), pp 212-226.

Odin, G. S., (1990). Clay mineral formation at the continent-ocean boundary: the verdine facies. *Clay Minerals*. 25(4): 477-483

Opuwari, M., (2010). Petrophysical Evaluation of the Albian age Gas bearing Sandstone Reservoirs of the O-M Field, Orange Basin, South Africa. A thesis Submitted in Partial

fulfilment of the requirement for the degree of Philosophae Doctor (PhD) in the Faculty of Science, Earth Sciences Department, University of the Western Cape, Bellville, South Africa.

Owen, D. E., Turner-Peterson, C. E., and Fishman, N. S., (1989). X-ray diffraction studies of the <0.5 mm fraction from the Brushy Basin Member of the Upper Jurassic Morrison Formation, Colorado Plateau: U.S. Geological Survey Bulletin 1808-G, pp 1-25.

Pallatt, N., Wilson, J., and McHardy, B., (1984): The relationship between permeability and the morphology of diagenetic illite in reservoir rocks, J. Pet. Technol., 36, 2225–2227, 1984.

PASA. (2003a&b): Exploration Opportunities in the Deepwater Orange Basin, off the West Coast of South Africa. Petroleum Agency of South Africa. www.petroleumagency.com

Parnell, J., Watt, G., Chen, H., Wycherley, H., Boyce, A., Elmore, D., Blumstein, R., Engel, M., and Green, P., (2004). Kaolin polytype evidence for a hot-fluid pulse along Caledonian thrusts during rifting of the European Margin Doi: 10.1180/0026461046830195 Mineralogical Magazine v. 68 no. 3 pp 419-432

Parnell, J., Baroni, J. and Boyce, A., (2000): Controls on kaolinite and dickite distribution, Highland Boundary Fault Zone, Scotland and Northern Ireland doi: 10.1144/jgs.157.3.635 Journal of the Geological Society of London v. 157 no. 3 pp 635-640.

Paton, D.A., Van der Spuy, D., di Primio, R. and Horsfield, B., (2008). Tectonically induced adjustment of passive-margin accommodation space; influence on the hydrocarbon potential of the Orange Basin, South Africa. American Association of Petroleum Geologists Bulletin, v.92. No.5. pp 589-609.

Paton, D.A., di Primio, R., Kuhlmann, G., van der Spuy, D. and Horsfield, B., (2007). Insights into the petroleum system evolution of the Southern Orange Basin South Africa. South African Journal of Geology; vol. 110; no 2-3; pp 261-274

Patchett, J.G. and Coalson, E.B., (1982). The determination of porosity in sandstone and shaly sandstone, part 2, SPWLA 23rd Annual Logging Symposium; pp 36.

Penney, R. K., and Looi, S.Y., (1996). Understanding Effective and Total Porosity: the Key to Optimising Mineralogical Evaluations: APPEA Journal, v. 36, p. 284-292.

Petro SA Report, (2003). Ibhubesi field Geological Evaluation Orange Basin, Block 2 South Africa.

Petroleum Agency SA Report (2004/005/006/007). Petroleum Exploration Information and Opportunities: Petroleum Agency Brochure.

Pevear, D.R., (1999). Illite and Hydrocarbon Exploration. Proceedings of the National Academy of Sciences of the United state, v. 96, p. 3440-3446.

Pe- Piper, G., and Weir-Murphy, S., (2008). Early diagenesis of inner-shelf phosphorite and iron-silicate minerals, Lower Cretaceous of the Orpheus graben, southeastern Canada: Implications for the origin of chlorite rims. AAPG Bulletin. 2008. 92(9): pp1153-1168

Pittman, E.D., Larese, R.E., and Heald, M.T., (1992). Clay coats: Occurrence and relevance to preservation of porosity in sandstones. In D.W. Houseknecht, & E. D. Pittman (Eds.), Origin, diagenesis, and petrophysics of clay minerals in sandstones (pp. 241–264). SEPM Special Publication 47, Society of Economic Paleontologists and Mineralogists.

Pittman, E. D., Larese, R. E., and Heald, M. T., (1992). Clay Coats: Occurrence and Relevance to Preservation of Porosity in Sandstones. America: SEPM Special Publication. 1992. 47: pp 241-255

Primmer, T.J., Cade, C.A., Evans, J., Gluyas, J.G., Hopkins, M.S., Oxitoby, N.H., Smalley,P.C., Warren, E.A. and Worden, R.H., (1997). Global patterns in sandstones diagenesis: their application to reservoir quality prediction for petroleum exploration. American Association of Petroleum Geologists Memoir 69, pp 61-77.

Rahman, S.S., Rahman, M.M. and Khan, F.A., (1995). Response of low-permeability, illitic sandstone to drilling and completion "fluids. J. Pet. Sci. Eng. 12 (4), pp 309–322

Ramseyer K.L., Diamond, W., and Boles J.R, (1993). Authigenic K-NH₄-Feldspar in sandstones .A fingerprint of the diagenesis of organic matter. Journal of sedimentary petrology v.63, pp 1092-1099.

Reeves, C., and de Wit, M., (2000). Making ends meet in Gondwana: retracing the transforms of the Indian Ocean and reconnecting continental shear zones. *Terra Nova*, vol 12, 272-280

Reedy, G.K., and Pepper, C.F., (1996). Analysis of finely laminated deep marine turbidites: Integration of core and log data yields a novel interpretation model, *SocPetrol. Engr. Ann. Tech. Conf. And Exhibit*, Colo. p. 119-127.

Reifenstuhl, R.R., (2002). Reservoir characterization pilot study: Porosity permeability, petrography, and facies analysis of 75 Upper Cretaceous to Mississippian age outcrop samples, east-central Brooks Range foothills and North Slope, Alaska, in *Abstracts with programs, American Association of Petroleum Geologists Annual Meeting*, v. 11, p. A146

Reineck, H.E., and Singh, I. B., (1973). *Depositional Sedimentary Environments. With Reference to Terrigenous Clastics.* Springer, Berlin, pp. 439

Reineck, H.E. and Wunderlich, F. (1968). "Classification and Origin of Flaser and Lenticular Bedding". *Sedimentology* Vol.11 (1-2): 99-104. doi:10.1111/j.1365-3091.1968.tb00843.x

Rickwood, P.C., (1981). The largest crystals. *American Mineralogist*. vol. 66, pp 885-907.

Rider, M., (1996). *The Geological Interpretation of Well Logs: Caithness*, Whittles Publishing, pp. 280.

Rider, M.H., (1996). *The geological interpretation of well logs.* Petroleum Exploration consultant Rider-French consultant Ltd Cambridge and Sutherland. Halsted press, a division of John Wiley and Sons, New York.

Rider, M.H., (1996). *The Geological interpretation of well logs.* Petroleum Exploration Consultant, Rider-French Consulting Ltd. Halsted press, a division of John Wiley and Sons, New York.

Rider, M.H., (2000). *Geological interpretation of Well Logs (Rider-French consulting Ltd.* Sutherland.

Rogers, W.F., (1963). *The Composition and Properties of Oil Well Drilling Fluids.* Gulf Publishing Co., Houston.

Ross, C.S., (1946). Sauconite- a clay mineral of the montmorillonite group ameri. Mineralogical assoc. v.31.pp 411-424

Roux , J., Van der Spuy, D. and Singh, V.(2004). Deepwater drilling on the way off South Africa. Offshore February 2004 .Petroleum Agency South Africa, Parrow, Capetown. South Africa.

Ruiz Cruz, M.D. (1994). Diagenetic development of clay and related minerals. J. Clay Miner., 29, pp 93-104.

Sauer, R., Seifert, P., Wessely, G., (1992). Guidebook to excursions in the Vienna Basin and the adjacent Alpine-Carpathian thrustbelt in Austria. Mitteilungen der Österreichischen Geologischen Gesell 85, pp1–264

Sawney, B.L., and Norrish, K., (1971). pH dependent cations exchange capacity: Minerals and soils of tropical regions. Soil Sci. vol.112: 213-215.

Schlumberger, (1972). The essentials of log interpretation, practice, Schlumberger Ltd, Paris, France.

Schmidt, V., and Mc Donald D.A., (1979) .Texture and recognition of secondary porosity in sandstones Soc. Econ. Palaeontology Mineral Spec. publ no 26.in press.

Schmidt, S., (2004). The Petroleum Potential of the Passive Continental Margin of South-Western Africa – A Basin Modelling Study. Unpublished PhD dissertation, Fakultät für Georessourcen und Materialtechnik der Rheinisch-Westfälischen Technischen Hochschule Aachen, Germany, pp 182

Schroeder and Hayes (1968). Dickite and Kaolinite in pennsylvanian limestones in Southern Kansas. Clays and clay minerals vol.16, pp 41-49

Selby, J., and Fateley, W. G., (1955). Products of clay mineral decomposition as related to phosphate fixation: SoilSci. Vol.80, pp 109-120

Serra, O., (1984). Fundamentals of Well Log Interpretation (Vol. 1): The Acquisition of Logging Data: Dev. Pet. Sci., 15A: Amsterdam (Elsevier).

Shammari, M., Francks, S. and Soliman, O. (2011). Depositional and Facies Controls on Infiltrated/Inherited Clay Coatings: Unayzah Sandstones, Saudi Arabia: AAPG Annual Conference and Exhibition: Making the Next Giant Leap in Geosciences.

Simandoux, P., (1963). Dielectric Measurements on Porous Media: Application to measurement of water saturation. Study of the behaviour of argillaceous formation. SPWLA, Houston, vol; 97-124.

Simpson, S.L., Bateley, G. E., Charlton, A.A., Stauber, J.L., King, C.K., Chapman J.C., Hyne, R.V., Gale, S.A., Roach, A.C., and Maher, W.A., (2005): Handbook for sediment quality assessment (CSIRO: Bangor, NSW).

Sinclair, G. G. and Duguid, S. J., (1990). “Laboratory Induced Damage - A Review of the Problem”. First SCA Euro- pean Core Analysis Symp., London, UK, Gordon and Breach Science Publishers

Spears, D.A., and O'Brien, P.J. (1995): The formation of sapphirine and orthopyroxene during overprinting of Mariánské Lázně Complex eclogites. Zentralblatt für Geologie und Paläontologie, Teil I, 827-836.

Stalder, P., (1973). Influence of crystallographic habit and aggregate structure of authigenic clay minerals on sandstone permeability. Geologie en miljnbouwvol 52(4) pp 217-220.

Stixrude, L and Peacor, D. (2002): First-principles study of illite–smectite and implications for clay mineral systems. J. Nature 420, pp165-168 (14 November 2002) |doi: 10.1038/nature01155; Received 21 May 2002; Accepted 19 September 2002

Sun, Z. L., Huang, S. J., Zhang, Y. X., et al., (2008): Origin and diagenesis of authigenic chlorite within the sandstone reservoirs of Xujiahe Formation, Sichuan Basin, China. Acta Sedimentologica Sinica.. 26(3): pp 459-467 (in Chinese).

Tardy, Y., (1971). Characterization of the principal weathering types by the geochemistry of waters from some European and African crystalline massifs. Chemical Geology 7, 253271

Theodor, W.F., (2000). Petrophysical properties from small rock samples using image analysis techniques, ISBN 90-9014-338-6.

Thompson, A., (1979). Preservation of porosity in the deep woodbine /Tuscaloosa trend, Louisiana. Trans gulf coast association. Geol. society, 30, pp 196-403.

Tian, J. F., Chen, Z. L., Fan, Y. F. (2008). The occurrence, growth mechanism and distribution of authigenic chlorite in sandstone. Bulletin of Mineralogy, Petrology and Geochemistry. . 27(2): pp 200-205 (in Chinese)

Ugbo, J., (2010). Direct Estimation of an equivalent shaliness parameter using resistivity and spectroscopy logs: A Total Illite/Expansible Clay Approach. A Dissertation Submitted to the School of Biological, Earth and Environmental Sciences, University of New South Wales, Sydney, Australia In partial fulfillment of the requirement for the degree of Doctor of Philosophy (PhD) in Applied Geology

Uysal, I.T., Golding, S.D. and Thiede, D.S., (2001a). K–Ar and Rb–Sr dating of authigenic illite–smectite in Late Permian coal measures, Queensland, Australia: implication for thermal history. Chem Geol 171: pp 195–211

Uysal, I.T., Golding, S.D., Glikson, A.Y., Mory, J. and Glikson, M., (2001b). K–Ar evidence from illitic clays of a Late Devonian age for the 120 km-diameter Woodleigh impact structure, Southern Carnarvon Basin, Western Australia. Earth Planet Sci Lett 92: pp281–289

Van Der Spuy, D., (2007). Prospectivity of Northern Orange basin, offshore South Africa Petroleum agency SA .Parrow. South Africa.

Van der Spuy, D., (2002). What of the synrift? Graben plays in the Orange Basin, South Africa. First annual International symposium . Poster 7.PESGB, London.

Van Der Spuy, D., (2003). Aptian source rocks in some South African Cretaceous basins. Geological Society of London Special Publications, v. 207. pp 185-202.

Velde, B., (1985). Clay minerals, a physico-chemical explanation of their occurrence. Developments in Sedimentology 4, Elsevier, New York, pp 427

Visser, D. J. L., (1998). The geotectonic evolution of South Africa and offshore areas: Explanation of structure map, scale 1:1000 000. Council for Geoscience. Pretoria.

Walderhaug, O., (1994). Temperature of quartz cementation in Jurassic sandstones from the Norwegian continental shelf-evidence from fluid inclusions. *Journal of Sedimentary Research*, A64, pp. 311-323.

Walderhaug, O. and Bjorkum, P.A., (2003). The effect of stylolite spacing on quartz cementation in the Lower Jurassic Sto Formation, southern Barents Sea. *Journal of sedimentary Research*, 73, pp. 146-156

Ward, C.R., Nunt-jaruwong, S. and Swanson, J., (2005). Use of mineralogical analysis in geotechnical assessment of rock strata for coal mining. *International Journal of Coal Geology* 64, pp. 156–171.

Waxman, M.H., and Smith L.J (1968). Electrical conductivities in oil bearing shaly-sands. *Journal of Petroleum Technology*; pp107.

Weaver, C.E., (1989): Clays, muds, and shales. *Developments in Sedimentology* 44, Elsevier, Amsterdam, pp 819.

Welton, J.E., (1984). SEM Petrology Atlas: AAPG Methods in Exploration Series, no 4, pp 237

Wentworth, C.K (1922) "A scale of grade and class terms for clastic sediments", *J. Geology* V. 30, pp 377-392

Whitney, E. and Northrop, R (1987). Role of Water in the Smectite-to-Illite Reaction *Journal Clays and Clay Minerals* - Vol. 38, no. 4, pp. 343-350,

Wilson, M.D., and Pittman E.D., (1977). Authigenic clays in sandstones: recognition and influence on reservoir and paleoenvironmental analysis. *J. sedim. Petrol.*, vol 47: pp 3-31.

Wilson, H. H., (1977). "Frozen-In" Hydrocarbon Accumulations or Diagenetic Traps *Exploration Targets, Amer. Assoc. Petrol Geol. Bull.*,vol 61, pp 483-491.

Wilhelms, A., Larter, S. R., Head, I., Farrimond, P., di Primio, R., and Zwach, C. (2001b). Biodegradation of oil in uplifted basins prevented by deep-burial sterilization: *Nature*, v. 411, pp 1034-1037

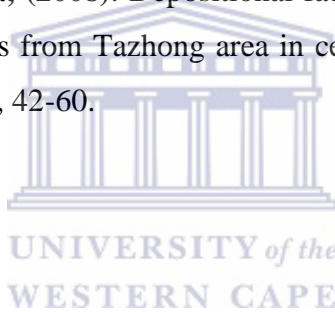
Winsauer, W.O. and McCardell , W.M., (1953). Ionic double layer conductivity in reservoir rocks. Transactions of AIME, vol 198, p.129

Worden, R. H., Morad, S., (2003). Clay mineral cements in sandstones. Special publication of the International Association of Sedimentologists; no. 34 Blackwell publishing

Worthington, P. F., (2003). Effect of Clay Content upon Some Physical Properties of Sandstone Reservoirs DOI: 10.1002/9781444304336.ch10 Copyright © 2003 International Association of Sedimentologists.

Worthington, P.F., (2008). The Application of Cut-Offs in Integrated Reservoir Studies. SPE Reservoir Evaluation and Engineering (SPE 95428).

Zhang, J., Qin, L. and Zhang, Z., (2008). Depositional facies, diagenesis and their impact on the reservoir of Silurian sandstones from Tazhong area in central Tarim Basin, Western China. Journal of Asian Earth Sciences 33, 42-60.



Related Websites

<http://www.minersoc.org/pages/gallery/claypix>

<http://www.hamptonroads.com/node/374>

http://www.ptslabs.com/oilfield_services/petrographic_analysis.php?sec=o

<http://209.51.193.54/minerals/sillicate/clays.htm>

<http://ohioline.osu.edu/aex-fact/0565.html>.



UNIVERSITY *of the*
WESTERN CAPE